EVALUATION OF 1-D AND 2-D HYDRAULIC MODELS FOR DESIGNING AND ASSESSING FULLSPAN STREAM CROSSINGS

By

Alyssa Sachiko Virgil

A Thesis Presented to

The Faculty of Humboldt State University

In Partial Fulfillment of the Requirements for the Degree

Master of Science in Environmental Systems: Environmental Resources Engineering

Committee Membership

Dr. Margaret Lang, Committee Chair

Dr. Eileen Cashman, Committee Member

Michael Love, Committee Member

Dr. Margaret Lang, Program Graduate Coordinator

December 2020

ABSTRACT

EVALUATION OF 1-D AND 2-D HYDRAULIC MODELS FOR DESIGNING AND ASSESSING FULLSPAN STREAM CROSSINGS

Alyssa Virgil

This project compared design decisions and hydraulic analyses of full-span stream crossings using one- and two-dimensional (1-D and 2-D) hydraulic models. The project was initiated by the California Department of Transportation's interest in moving from 1-D to 2-D hydraulic modeling and by the Federal Highways Administration's support for adopting SRH-2D (Sedimentation and River Hydraulics-2D developed by the US Bureau of Reclamation) in Aquaveo, LLC's Surface-water Modeling System as their standard design model. Two-dimensional hydraulic models calculate more detailed water depths and velocities than 1-D models, which can better identify fish passage conditions, areas of potential scour or deposition, and aquatic organism habitat characteristics.

The project evaluated two recently constructed full-span (channel spanning) crossings that were designed based on HEC-RAS 1-D model analysis and constructed in 2017. The 1-D hydraulic models were not available for either of the projects, so the 1-D model results within the final project reports were used for comparison with 2-D model results completed for this project. Little Mill Creek crossing is a bridge with five rock weirs installed in the channel below located in Del Norte County, California. North Fork Ryan Creek is located in Mendocino County and is a box culvert with inlet and outlet

headwalls and rock weirs installed both upstream and downstream of the crossing. The sites were re-surveyed in 2019 and 2020, and current conditions were modeled using SRH-2D. Current site conditions and 2-D model depth and velocity results were used to identify design elements that may have been designed differently using a 2-D model analysis in an effort to inform future full-span crossing design processes.

Using local 2-D model velocities for bank rock slope protection or riprap (RSP) sizing and abutment scour calculations resulted in differences in RSP size recommendations and abutment scour depth estimations. For Little Mill Creek Bridge, the RSP was estimated to be currently undersized, while at North Fork Ryan Creek crossing the RSP was oversized compared to the 2-D analysis based calculations. The local velocities and water depths available from 2-D model results provide greater spatial detail of the estimated forces experienced at the banks and abutments and account for local turbulence.

In terms of practicality, model efficiency and computing power continue to increase, making 2-D modeling more accessible. Computer processing time was found to increase linearly with the number of mesh elements so model run times are not likely to limit 2-D modeling for stream crossing sites. Sites with expansive floodplains could experience longer run times if detailed results, and therefore more mesh elements, are needed on the floodplain.

ACKNOWLEDGEMENTS

I would like to acknowledge all the inspiring people that I was able to meet because of this graduate program and thesis project. I appreciate the many opportunities I received during my time in the Environmental Resources Engineering program.

I want to thank Margaret Lang who has guided me through this process with nothing but patience and support. I have learned so much from Margaret and I will think back on the multiple projects we have worked on together with gratitude and good memories.

I also want to thank Eileen Cashman for being part of my committee and for your thoughtfulness and care. I also appreciate your technical knowledge and support in steering this thesis into a more approachable document.

Also, I want to thank Mike Love for both his knowledge out in the field and guidance on analysis in this thesis. It was great to work with you and I appreciated all of your insight, which helped enormously in the analysis.

I also want to thank the entire field crew including Tony Llanos, Marcie Jimenez, Tyler Caseltine, David Rivera, and Chris Fabbri. My thesis project would not have existed without the work done by this field crew. I had a great time working with you all.

Thank you to our contacts at Caltrans who helped in gathering information for this project and for setting up training on the use of the SRH-2D model. I would like to especially thank Kristine Pepper who helped in gathering project information, Bruce Swanger who set up our SRH-2D training, and Melinda Molnar who leads the larger

project this thesis is linked to. I would also like to thank Scott Hogan from FHWA for his help in setting up SRH-2D and the training and guidance he provided.

I would also like to thank my family, whose support means everything to me. I would not be where I am today without them and I cannot thank them enough for the love and support they continuously show me.

Lastly, I want to thank Zack Ramsey who has been by my side for essentially my entire academic career and will be for years to come. Thank you for supporting my endeavors and my seemingly unrelenting desire to fill my schedule, while also looking out for my well-being. And thank you for rooting me on in the many phases of finishing this project.

TABLE OF CONTENTS

LIST OF TABLES

LIST OF FIGURES

LIST OF APPENDICES

ABBREVIATIONS AND ACRONYMS

AOP	Aquatic organism passage
Backing Class No. 1	RSP Class used by Caltrans (50^{th} percentile weight: 75 lb)
BLDR	Boulder
Caltrans	California Department of Transportation
CDFW	California Department of Fish and Wildlife
cfs	Cubic feet per second
DS	Downstream
fps	Feet per second
HEC-RAS	Hydrologic Engineering Center's River Analysis System
lb	Pound
NMFS	National Marine Fisheries Service
OHWM	Ordinary high water mark
psf	Pounds per square foot
RCB	Reinforced Concrete Box (culvert type)
RSP	Rock Slope Protection (riprap)
SRH-2D	Sedimentation and River Hydraulics 2-D
US	Upstream
WSE	Water Surface Elevation
XS	Cross-section

INTRODUCTION

The design and implementation of stream crossings have a significant effect on stream hydraulics and the continuity of stream processes. Full-span stream crossings are meant to remove some of the main challenges of stream crossings, such as maintaining habitat continuity, fish passage, sediment transport, flow conveyance, and bank stability. The design of full-span stream crossings is based on determination of the stream's bankfull width, which is the wetted channel width during the channel-forming flow (approximately a 1.5- to 2-year return period flow). The crossing must completely span this distance to eliminate flow restrictions and interference at bankfull and lower flows. Currently, the design for most of these structures is simulated using a one-dimensional (1-D) hydraulic model which outputs water depths longitudinally through the project reach and average velocities at cross-sections. The most common 1-D model, HEC-RAS, also does not fully simulate the hydraulic conditions within culverts or beneath bridge elements. A two-dimensional (2-D) hydraulic model has the potential to provide additional, design-relevant results including local depth-averaged velocity magnitudes and directions, and locations of eddy formation.

Two-dimensional hydraulic modeling can identify locations that form eddies with the potential to cause erosion and possibly lead to bank and structural instabilities. The formation of eddies at the base of structures is a common cause of structure failure, and the ability of 2-D models to capture the characteristics of these eddies is important to the stability analysis of the crossing design. Additionally, eddies can cause flow to be

concentrated over a smaller flow width, leading to locally higher velocities that would not be predicted by a 1-D hydraulic model. Velocities in a 2-D model can be extracted for specific locations, providing greater hydraulic detail at the banks, at stabilizing structures such as rock weirs, and at interfaces between structures and the natural channel.

The objective of this thesis is to identify the additional information attained from 2-D hydraulic modeling results compared to 1-D hydraulic model results for the design of two full-span stream crossings. This research serves as a case study examining two full-span stream crossing sites designed by the California Department of Transportation (Caltrans) that used 1-D hydraulic models for their design. The results from the 2-D hydraulic analysis of these sites is used to determine the benefits to the design and the understanding of the crossing performance gained from using a 2-D model. The two stream crossing sites are on Little Mill Creek and North Fork Ryan Creek in Northern California (Figure 1). Little Mill Creek bridge and North Fork Ryan Creek crossing were built in 2016 (one weir adjusted in 2017) and 2017, respectively. The two sites are under Caltrans jurisdiction and the data used for this thesis was collected as part of an on-going Caltrans-funded study. The sites were modeled in 2-D, using the Sedimentation and River Hydraulics 2-D (SRH-2D) model created at the U.S. Bureau of Reclamation by Dr. Yong Lai. The SRH-2D model is run through Surface-water Modeling System (SMS) software developed by Aquaveo, LLC.

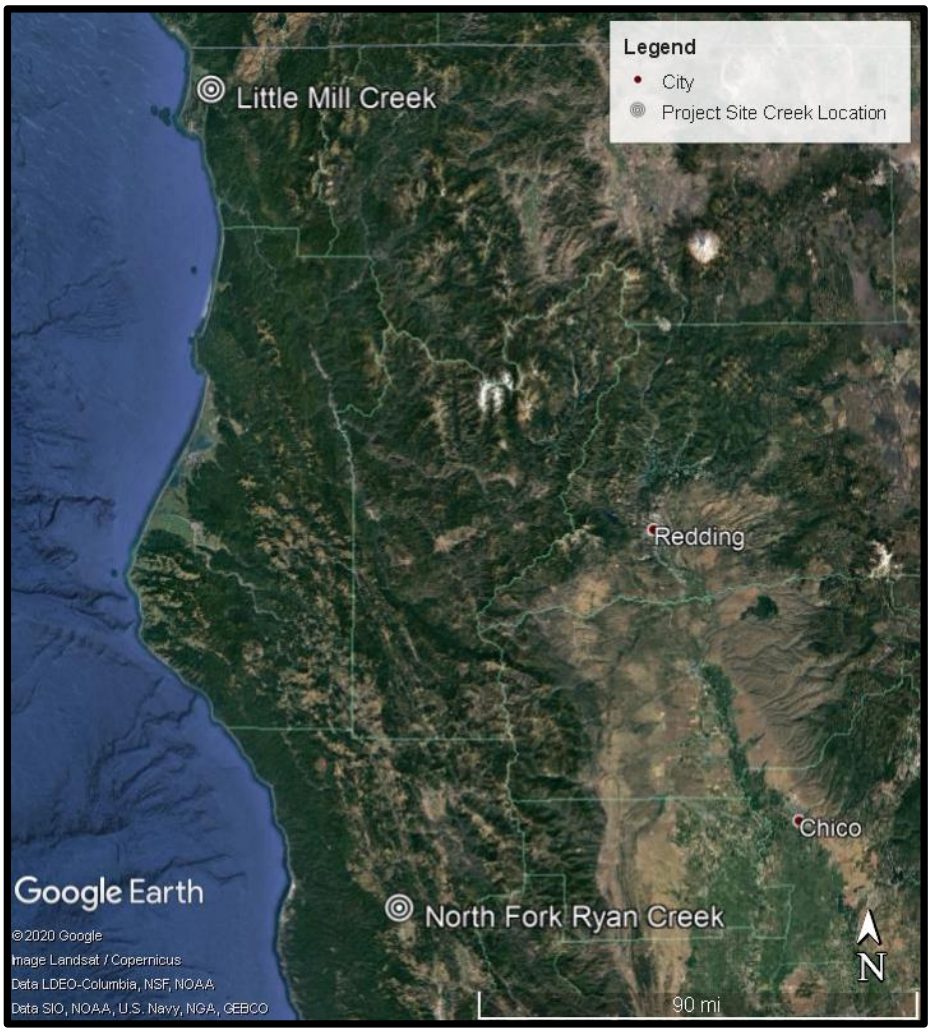

Figure 1. Location map of Little Mill Creek (Del Norte County) and North Fork Ryan Creek (Mendocino County) (Google Earth 2020).

Originally, the plan for this project was to compare the results of the 2-D hydraulic models to those of the 1-D models developed by Caltrans, but the 1-D models and their detailed results were not available. The design reports and basic conclusions from the 1-D models used for the design of the two study sites were available and these were used for comparisons. The 2-D flow characteristics are identified from the results of

the 2-D model simulations, and the final conclusions drawn from the 1-D and 2-D analysis results are compared. This analysis assumes that current conditions are similar enough to designed conditions to achieve an accurate comparison of design recommendations from the 1-D models created from the original design and the 2-D models created with the current conditions. The practicality of implementing 2-D hydraulic models in stream crossing design analysis is also explored in this thesis, examining terrain survey density, model setup, and model simulation run time.

This thesis includes a literature review on the current state of full-span stream crossing design, analysis, and implementation. Followed by the methodology used for all analyses, from data collection to hydraulic modeling. The results are presented and then conclusions are drawn for the two case study sites.

LITERATURE REVIEW

This literature review summarizes the current knowledge of design practices and performance of full-span stream crossings from the published literature of state and federal agencies and researchers. An introduction to full-span stream crossings and their characteristics compared to alternative crossing designs is followed by a description of current design standards and criteria within state and federal agencies. The standards and criteria presented highlight those used in the Pacific Northwest because of its geomorphic and hydrologic similarity to much of California and the similar species of concern. Methodologies for analyzing the designs and performance of full-span stream crossings in site-specific conditions are identified, and descriptions of the most common software tools used in design and performance assessment are presented. The focus of this thesis project is to evaluate the analyses and designs resulting from modeling stream crossings in 1-D compared to 2-D hydraulic models. The understanding and observations of full-span stream crossing performance are summarized from the limited existing studies that evaluated completed full-span stream crossings and developed monitoring procedures needed to assess their performance.

Introduction to Full-Span Stream Crossings

A stream crossing is a structure that allows for transportation over a stream, often constructed for roads. Stream crossings were historically designed with less regard of

stream features, resulting in fish passage obstructions and sediment scour or deposition compromising the stability of the stream crossing (Cenderelli et al., 2011). Stream crossing design processes have continually been updated to incorporate new knowledge of the environmental processes that occur within and around streams. One of the newest additions to prospective stream crossing design is full-span stream crossings.

A full-span stream crossing is defined as a crossing that fully spans the stream channel width with some factor of safety. Full-span crossings can be designed and constructed to have mobile or immobile beds, or incorporate grade control structures such as concrete or rock weirs to provide fish passage. Thus, full-span crossing designs can vary, from crossings without substrate to culverts embedded into the substrate to bridges, while still providing acceptable hydraulic performance and flow conveyance (Furniss et al., 1998; TRB, 2017). Determination of the full-span crossing width varies between states and agencies (compared in further detail in Table 1).

Stream simulation crossings are a subset of full-span crossings, designed to promote full continuity in stream channel processes and passage for all aquatic organisms (CDFW, 2009b; NMFS, 2001; USFS Stream Simulation Working Group, 2008). Stream simulation crossings are designed to match the geomorphology in an adjacent or nearby reference stream reach. Both crossing types have widths equal to or greater than a stream channel width criterion, typically bankfull channel width. However, unlike stream simulation designs, full-span crossings may not be designed with a mobile channel bed or a channel slope that matches a reference reach in the adjacent stream channel. The reference reach is a design requirement for stream simulation crossings that may not be

possible for all full-span crossings due to site specific constraints. In situations where stream simulation designs are not possible, a stable crossing bed, typically constructed of immobile rock in the form of a geomorphically-based roughened channel or boulder weirs, is preferred for passage of fish and aquatic organisms and conveyance of debris and sediment. For example, some full-span crossings require channel grade control to protect upstream infrastructure and habitat from channel incision (Castro & Beavers, 2016). Designs with these features have been adopted by the Federal Highways Administration (FHWA) and are described in their HEC-26 design manual, "*Culvert Design for Aquatic Organism Passage*" (Kilgore et al., 2010). The US Forest Service's design manual, "*Stream Simulation: An Ecological Approach to Providing Passage for Aquatic Organisms at Road-Stream Crossings*", describes stream simulation designs that focus on mobile beds which mimic the reference reach morphology (USFS Stream Simulation Working Group, 2008).

Benefits of full-span stream crossings

Full-span crossings provide a variety of benefits, but they are most often installed to provide fish and aquatic organism passage. Additional benefits of full-span crossings include flood flow conveyance, effective debris passage, and stream continuity, including hydraulics, sediment transport, and habitat. Full-span stream crossings are often beneficial for complex culvert locations to address slope breaks, maintain channel gradients, and protect adjacent infrastructure.

Fish passage

Stream crossings can create a variety fish passage barriers including (CDFW, 2009a, 2009b; NMFS, 2001; USFS Stream Simulation Working Group, 2008):

- crossing widths smaller than the natural channel width constrict flow, create high velocities within the crossing, and produce localized scour and deposition at outlets and inlets, respectively
- crossings without a diverse stream bed substrate or roughened surface can have shallow water depths creating depth barriers for passage
- crossings requiring hydraulic elements (e.g. baffles or weirs) can develop excess turbulence or jump heights that exceed the ability of some species
- protruding culvert inlets can promote local fill scour, sediment deposition, debris accumulation and excessive inlet velocities
- crossings with perched outlets create jump barriers
- crossings spanning less than bankfull width can impair upstream and downstream habitat by promoting sediment aggradation or degradation and bank instability.

Full-span stream crossings can potentially mitigate these conditions by providing a continuous streambed.

Technical fishways and other alternative hydraulic designs can provide fish passage, but have the potential to create other problems. In this case, technical fishways are designs such as the Denil Fishpass, vertical slot, and pool and weir. These fishways are designed to produce hydraulic conditions that meet the needs of a target fish species and life stage. Technical fishways are often designed for fish species that have high

economic value or long distance migrations (anadromous fish) (Silva et al., 2017). This focus on anadromous fish or other 'high-value' fish has led to bias in successful design of fishways away from resident species and has led to some fishways being 'highly selective' in terms of the species of fish that can pass (McLaughlin et al., 2012; Silva et al., 2017). Technical fishways can also create complex hydraulic conditions, like turbulence, that require evaluation for fish passage and other design criteria like depth, velocity, fish fatigue, and temperature over its full operating range (USFWS, 2019). Although technical fishways are a relatively small capital cost compared to the whole of water development schemes, if they do not work as designed to, or if large-scale ecosystem services are severely compromised, the ecosystem experiences a substantial long-term cost to its natural capital (Silva et al., 2017). Full-span stream crossing structures, on the other hand, are less likely to be more species selective or create more challenging passage conditions than the natural stream channel. However, some design elements, such as the addition of weirs in a full span stream crossing, could be problematic. Evidence suggests that weirs may reduce fish community diversity and create an uneven distribution of populations upstream and downstream of the weirs (Poulet, 2007). Facilitation of fish passage is a major reason to implement full-span stream crossings, but other benefits are also realized and described in the following sections.

Flood flow and debris passage

The resiliency of stream crossing designs will be increasingly prioritized to prepare for the expected effects of climate change, including an increase in extreme event

magnitudes and frequencies. A 2017 Transportation Research Board Webinar on "*Fundamentals of Resilient and Sustainable Buried Structures*" identified resiliency in road-stream crossings as accommodating natural stream widths and having a 100-year design life (TRB, 2017). Resiliency is broadly described as the ability to recover and can specifically be applied to stream crossings as the ability to withstand extreme events. It has been documented that full-span crossings have the potential to withstand extreme events. Gillespie et al. (2014) compared the performance of stream simulation culverts in the upper White River in the Green Mountain National Forest (GMNF) of Vermont to adjacent local town crossings following Hurricane Irene in August 2011. The flooding caused in this region by Hurricane Irene was estimated to be a 500-year event. Stream simulation sites, in the upper White River watershed within the GMNF in Vermont, were found to have a headwater-to-depth ratio for the 100-year design flood between 0.5 and 0.7 (meaning that 30 to 50 percent of the structure's overall height was designed to be above the 100-year water level at the inlet), which would allow them to pass flows and debris greater than the 100-year event (Gillespie et al., 2014). In the Upper White River watershed, three of four stream crossings that failed were hydraulic designs with crossing width to bankfull width ratios less than 0.52. The fourth crossing was a bridge located on an alluvial fan with a span greater than bankfull width, but woody debris plugged the bridge. In adjacent towns, over 70 crossings were damaged or completely lost and all spanned less than bankfull width (Gillespie et al., 2014). In another example, eight stream simulation crossings installed in Oregon's Siuslaw National Forest in 2003 have survived floods between the 20 to 25-year recurrence intervals. Similarly, in Alaska's Tongass

National Forest, 93 stream simulation crossings have survived floods up to the 25 to 50-year recurrence interval without major failure and maintained fish passage in 98 percent of sites (Gillespie et al., 2014). Additionally, stream simulation crossings in Washington Department of Natural Resources forestland did not experience total crossing failures with recorded floods prior to the study period (Barnard et al., 2014). Modeling results in the Barnard et al. (2014) study determined the culvert velocity during the 100-year flow was similar to the reference reach for the fifty studied culverts. The slope ratio (ratio between the bed slope inside the culvert and bed slope in the adjacent channel) of these culverts did not change with time from installation or in response to periodic high flow events (Barnard et al., 2014).

Stream crossings have generally been designed to pass the 100-year return period flow with the headwater depth not exceeding the crossing height (NMFS, 2001), but for many locations the water flow itself does not cause the majority of stream crossing failures. This is especially true in many Pacific Northwest and coastal California watersheds which are forested with steep topography. Studies have found that sediment and debris are the most common failure mechanisms for stream crossings, with small woody debris often initializing the accumulations (Furniss et al., 1998). Debris and sediment carried by high flows can accumulate at crossing inlets and are often the driving force for crossing damage or failure at flows lower than the design flood flows (Cafferata et al., 2017; Furniss et al., 1998). The unaccounted effect of debris and sediment make it difficult to predict crossing failure with hydraulic modeling (Cafferata et al., 2017; Furniss et al., 1998). In the upper White River watershed, 70 percent of costs from the

damage of GMNF stream crossings by Hurricane Irene conditions was estimated to have occurred because of debris plugging (Gillespie et al., 2014). Of the damaged stream crossings, three of four that failed were hydraulic designs with crossing width less than 52 percent of bankfull width (Gillespie et al., 2014). The added width and smaller headwater-to-depth ratios of full-span stream crossings can significantly improve passage of debris, like wood and large sediment loads (Furniss et al., 1998; Gillespie et al., 2014).

Stream crossing alignment with stream approach is also important to reduce the hazard of collecting woody debris at the stream crossing inlet (Caltrans et al., 2007; Flanagan, 2005). Dynamic channel beds and banks, can also provide unimpeded passage of water and sediment during a greater variety of flow conditions (Gillespie et al., 2014). The resiliency of the stream crossing structures increases with the passage of debris, reducing the area of force placed on the structure and the potential for backwatering effects of increased water depths and turbulence (eddies) (Furniss et al., 1998).

Hydraulics and sediment transport

Like with fish passage and flood resiliency, new research and knowledge has led to improvements in stream crossing hydraulic and geomorphic analysis. Hydraulic capacity has historically guided stream crossing design, but more recently stream crossing design analysis has grown to include in-channel hydraulics and sediment transport. Full-span crossings focus on hydraulics in terms of water depth and velocity, while also addressing concerns about scour and destabilization. Subsets of full-span designs, like stream simulation, rely on the duplication of adjacent reach geometry, substrate, and formations within the crossing to create similar hydraulics and sediment

transport. Specific to stream simulation full-span crossings, the bed material that may be washed away by flood events would be replenished by sediment transport from upstream (Barnard et al., 2013a; USFS Stream Simulation Working Group, 2008). The colluvium, bank material, and key instream pieces are considered more permanent, so those that are designed for the stream crossing site would be designed to be permanent as well (CDFW, 2009b). Other full-span designs attempt to place controls on the hydraulics, by manipulating geometry and substrate to create similar hydraulic conditions. In this way, even standard crossing installations without substrate can be made into full-span designs, to provide additional hydraulic performance and maintenance benefits (Furniss et al., 1998; TRB, 2017).

Direct observations of streams can provide insight into channel hydraulics and sediment transport. Differences in sediment particle size distribution on the bed are assumed to indicate differences in hydraulic conditions. Timm et al. (2017) observed that stream simulation crossings transported sediment downstream more effectively than other fish passage designs. These observations were in low gradient systems that could be influenced by slight variations in bed slope. A study by Barnard et al. 2014 surveyed 50 stream simulation culverts in Washington State ranging in age from 1 to 13 years since construction, spanning from 2.4 to 7.3 meters, slopes up to 14 percent, and lengths of 12 to 46 meters (Barnard et al., 2014). Barnard et al. (2014) observed that sediment size and gradation were similar between stream simulation culverts and reference reaches in Washington State. The average channel velocities modeled at the 2-year return period flow, approximately bankfull flow, were also found to be comparable in the stream

simulation culvert and the reference reach. Additionally, bed material found in stream simulation crossings was not significantly coarser or finer over time or during high flows (Barnard et al., 2014). Full-span stream crossings often allow for channel hydraulics and sediment transport to continue through the stream crossing, which in turn allows for a continuous habitat and aquatic organism passage conditions. However, complexity of the streambed inside stream crossings does not often occur, likely because of isolation from large wood debris, bank vegetation, and bank sediment inputs (Barnard et al., 2014).

Some full-span crossings require channel grade control to protect upstream infrastructure and habitat from channel incision (Castro & Beavers, 2016). In this case, a stable crossing bed, typically constructed of immobile rock in the form of a geomorphically-based roughened channel or boulder weirs, is preferred for passage of fish and aquatic organisms and conveyance of debris and sediment (Kilgore et al., 2010; USFS Stream Simulation Working Group, 2008). The stability of design elements or crossing structures may also need to be protected from higher shear stresses or larger return period flow through energy breaks, like rock slope protection (RSP).

Habitat continuity and non-aquatic organism passage

Another potential benefit of full-span crossings is wildlife and non-fish aquatic organism passage. Both aquatic and non-aquatic animals move along or in stream channels as part of large-scale migrations or daily movements to feed and seek shelter (USFS Stream Simulation Working Group, 2008). Non-aquatic species often move along stream banks, so a stream crossing that lacks bank continuity at lower flows can result in more animals crossing the roadway, increasing their chances of encountering vehicles. Aquatic and

semi-aquatic species, like amphibians, may move upstream or downstream during specific times of day in search of food. Some organisms are not capable of jumping like some fish species, so a vertical barrier could limit their habitat even more extensively (USFS Stream Simulation Working Group, 2008). Organism movement is important for maintaining the population resilience and diversity in the species' gene pool, making regional populations more resistant to local habitat or population losses (USFS Stream Simulation Working Group, 2008). Barriers to organism movement are observed in other stream crossing designs, like technical fishways and other strictly hydraulic designs.

Difficulties of full-span stream crossings

Those working on design and application of full-span stream crossings face some challenges, with relatively higher initial capital costs than other smaller stream crossings and the unpredictable effects of climate change. However, climate change will affect all stream crossings designs, not only full-span stream crossings.

Initial cost

The main challenge faced by full-span stream crossings is the initial capital cost because the crossings span a larger width and require extra design features, like streambed material, grade control, or structural foundations. Christiansen et al. (2014) analyzed the net fiscal and social benefits of replacing a conventional culvert with a stream simulation design for 495 culverts in the Green Bay tributaries of Wisconsin. The net fiscal benefit calculated accounted for initial cost, maintenance, improved lifespan/reduced failure, and flood damage repair. The net fiscal benefit is a lifetime cost

for the crossing structure and does not account for possible differences in length of lifespans for a conventional culvert compared to a stream simulation crossing, rather it is accounted for in the net social benefit. The social benefits accounted for habitat restoration, fish passage, water quality, and reduced road user cost due to failure or repair closures. Their results were that on average replacing a conventional culvert with a stream simulation crossing yielded a net fiscal benefit of -$4,500 and net social benefit of $7,800. However, approximately 44 percent of crossings replaced with a stream simulation design yielded positive net fiscal benefits and 77 percent yielded positive net social benefits (Christiansen et al., 2014). Additionally, the cost of installing and then replacing a crossing that is a barrier to fish passage often exceeds the higher initial cost of installing a full-span stream crossing (Barnard et al., 2013a).

Climate change

The two sites studied in this project are located in California, so climate change estimates for California were explored. The projected changes in overall wintertime precipitation in California due to climate change are uncertain with some studies predicting an increase (Duffy et al., 2006; Kim, 2005; Maurer, 2007; Mote & Salathé, 2010; Pierce et al., 2013) and some a decrease (Cayan et al., 2008; Hayhoe et al., 2004). The uncertainty comes from complex topography and the location of California between mid-to-high latitude regions where increases in overall precipitation are expected and subtropic regions where decreases in precipitation are expected (Neelin et al., 2013). The extent of extreme rainfall events cannot be observed in annual mean precipitation values, as seasonal variation cancels the extreme dry and wet periods out over the course of a

year. The conclusion agreed upon about California precipitation patterns into the future, is that California will experience more extreme seasonal variation in precipitation, with wetter winter months and drier spring and summer months (Cayan et al., 2008; Gershunov et al., 2019; Kim, 2005; Mote & Salathé, 2010; Pierce et al., 2013).

Atmospheric rivers will play a significant role in the increase and intensification of extreme precipitation events. An atmospheric river is a long, narrow band of moist air moving through the atmosphere and those experienced in the U.S. typically form over the North Pacific Ocean (NOAA, 2020). Atmospheric rivers deliver intense bursts of water vapor along the West Coast: roughly 30 to 50% of annual precipitation in west coast states is delivered in a few atmospheric river events (NOAA, 2020). A study by Gershunov et al. (2019) tested sixteen global climate models for accuracy in modeling historic atmospheric river behavior and the contribution of daily precipitation events to annual precipitation in Western North America. The five most accurate models produced consistent changes in future behavior of atmospheric rivers, showing reliability in predictions for the Western North America region. The model projections predict increasing year-to-year variability in annual precipitation, particularly over California, where predictions of change in annual precipitation are uncertain. The study found that in three representative river basins along the West Coast, increase in extreme precipitation events is almost entirely an effect of atmospheric rivers (Gershunov et al., 2019). An additional study found that significant precipitation increases along the California coast are associated with an eastward extension of the region impacted by the Pacific jet stream, which forms atmospheric rivers (Neelin et al., 2013). A study done by Dettinger

(2011) using a seven-model ensemble found that extremes in atmospheric rivers change significantly, while average statistics do not. The number of years with many atmospheric river events increase (but average number of atmospheric river storms per year remains about the same), the maximum storm intensities of atmospheric rivers increase (but average intensity remain about the same), and atmospheric river storm temperatures increase. Additionally, the peak season for atmospheric river events is projected to lengthen. The patterns found in this study, identify the potential for more frequent and more intense extreme flow events in California under projected climate change (Dettinger, 2011). A study by Ralph et al. (2013) also found that a model of California's Russian River predicts that storms that form during AR conditions and higher soil moisture conditions produce a six times greater peak streamflow and more than seven times the storm-total runoff. The study highlights the importance of monitoring for AR conditions and pre-storm moisture conditions in forecasting streamflow and runoff (Ralph et al., 2013).

With the potential for extreme events to occur more often than their current recurrence interval might suggest, all stream crossing designs may need to be increasingly 'oversized' to improve their resiliency. In terms of full-span crossing design, oversized would be designed based on a wider bankfull width and greater flow rates. Washington State Department of Fish and Wildlife recently evaluated the possible changes in bankfull stream widths given projected changes to stream flow during two time periods, 2030-2059 and 2070-2099 (Wilhere et al., 2016). The study assumed that the initial response of channels to increased stream flow is widening; however, it should

be noted that other potential geomorphic responses, such as channel incision, are also possible. It was found that about 80% of the area studied is projected to experience an increase in bankfull discharge over both time periods, which would consequently create an increase in bankfull width. This study recommends analysis of projected bankfull and 100-year flows over a crossing's complete design life and conducting a cost-benefit analysis of designing crossings to accommodate the bankfull width for current versus future projected flows (Wilhere et al., 2016).

Applicability of full-span stream crossings

The states with conditions and criteria most similar and applicable to northern California are Oregon, Washington, Alaska and British Columbia because of their similar stream characteristics, hydrology, and species of concern. The National Marine Fisheries Service (NMFS) typically works with state agencies to keep crossing design criteria consistent with federal guidelines and is an important regulatory agency due to the presence of anadromous species in California waters. The agencies have varying preferences for stream crossing type, but, in general, the crossing design preferences are (1) bridge; (2) geomorphic design; (3) hydraulic design. Geomorphic designs may include stream simulation, full-span, or low-slope culverts (summarized for state and federal agencies in

APPENDIX D). Most bridge and geomorphic design crossings are also full span crossings.

Design Standards and Criteria

Design standards for stream crossings differ with the design type and the site location. Stream crossing designs can be generally classified as either geomorphic or hydraulic. Full-span stream crossings can incorporate elements of both categories depending on the site conditions and limitations. Most full-span stream crossings will have geomorphic design features, such as a natural sediment bottom, to complement the bankfull width. However, some designs may require structural elements to maintain a stable streambed and the channel gradient to provide for fish passage and protect adjacent property and infrastructure. These design elements can include baffles and concrete or rock weirs that maintain a pool and weir structure with resting pools in steeper crossings. State design guidelines recommend and try to limit these hydraulic designs to crossing retrofits in both California and Washington (Barnard et al., 2013a; CDFW, 2009b; NMFS, 2001).

The minimum design standard of a full-span stream crossing is a crossing width greater than or equal to bankfull width. Many guidelines also include a factor of safety such as the crossing width must be 1.2 times the bankfull width (Caltrans et al., 2007; CDFW, 2009b). In addition to the width criteria, full-span stream crossings are generally required to provide hydraulic capacity and passage of debris during the 100-year

recurrence interval design flow with a headwater-to-depth ratio of less than 0.8, but typically between 0.5 and 0.7 for the 100-year return period flow (Gillespie et al., 2014). This height requirement allows sufficient space between the soffit (bottom surface) of the crossing's opening and the 100-year water level to accommodate both flow water and debris (Gillespie et al., 2014). Determining the crossing size is often an iterative process with width or height controlling the size. Despite differences in state and agency design guidelines, the general consensus is that guidelines are presented not as a strict step-by-step design procedure but rather as a guide for identifying a site-specific solution that addresses each stream crossing location's unique characteristics (Barnard et al., 2013a; Bates & Kirn, 2009; University of New Hampshire, 2009).

Differences in the design criteria for full-span stream crossings are apparent when comparing design standards between states, and even separate agencies within the same state. In California, full-span crossings are generally used whenever economically possible, and are required when ecological connectivity and aquatic organism passage (AOP) are primary concerns (CDFW, 2009b; NMFS, 2001). Stream simulation culvert designs are generally used in Washington when bankfull width is between 10 and 15 feet, while stream simulation is still used in other full-span structures like bridges that can be substantially wider (Barnard et al., 2013a). In California there is no lower limit on stream widths for stream simulation designs but there is a 6-foot minimum crossing width regardless of a stream's bankfull width (Caltrans et al., 2007; CDFW, 2009b; NMFS, 2001).

Standard design features

The standard design features of full-span stream crossings for California, Oregon, and Washington are outlined below. A more detailed and expansive set of design standards from additional state and federal agencies are included in

APPENDIX D.

Crossing geometry (width, slope, length)

Full-span designs rely on an accurate measurement of bankfull width and there are multiple sources to guide measuring bankfull width (Barnard et al., 2013a; CDFW, 2009a; Harrelson et al., 1994; USFS Stream Simulation Working Group, 2008). Bankfull width, as defined by CDFW, is the width when the channel flows full and a further increase in depth results in a rapid increase in width as flow spreads across the floodplain (CDFW, 2009a). In Barnard et al. (2013a), bankfull width is the stage when water just begins to overflow into the active floodplain. For streams with no floodplain, it is the width of a stream or river at the dominant channel forming flow with a recurrence interval in the 1 to 2 year range (Barnard et al., 2013a).

Some designs reference the 'active channel width', or the "portion of channel receiving sufficient and frequent enough flows to maintain cleanly scoured substrate", which is different than bankfull width in most cases (CDFW, 2009a). Active channel width for Washington design guidelines, is defined as the "geomorphic expression describing a stream's recent discharges" that have been actively working on the channel, and are often identified by slope changes along the stream banks or changes in vegetation (Barnard et al., 2013a).

Sizing of full span crossings are generally defined as a function of the bankfull width. The full-span crossing designs have width criteria of around 1.25 times the bankfull width or 1.5 times the active channel width. Design criteria also include limits on the crossing slope and the crossing length, and the site-specific stream channel slope

where the design type is applicable. Table 1 summarizes the crossing width criteria used along the Pacific West Coast.

Table 1. California Department of Transportation (Caltrans) and California Department of Fish and Wildlife (CDFW) criteria for full-span or similar crossing designs, including type, width, stream slope, crossing slope, and crossing length.

CA Agency	Design Approach	Crossing Width	Stream Slope	Slope in Crossing	Crossing Length
Caltrans[1] (2009 update) / NMFS[2]	Active Channel (NMFS)	1.5x active channel width	<=3%	0%	<= 100 ft
Caltrans[1] / CDFW[3]	Low Slope	1.25x bankfull width	<=1%	Stream slope	<= 75 ft
Caltrans[1]	Stream Simulation	> bankfull width; 6 ft minimum	<=6%, most cases	Reference reach slope	
CDFW[3]	Stream Simulation	>= bankfull width; 6 ft minimum	<=6%	Stream slope, <6%	Any, recommended for >100 ft

[1] (Caltrans et al., 2007)
[2] (NMFS, 2001)
[3] (CDFW, 2009b)

Crossing bed (embedment and bed material)

Most full-span crossing designs include bed material that is similar to adjacent stream reaches, but there are conditions where a stabilized bed is necessary for keeping bed material in the culvert and creating resting areas for fish passage (Table 2). If the crossing uses a closed-bottom structure, there are criteria for the depth of substrate embedment needed to minimize the possibility of losing the crossing bed to erosion.

These criteria are typically defined as an embedded percentage of the structure height with typical values ranging from 20 – 50% (Caltrans et al., 2007; CDFW, 2009b).

Table 2. California Department of Transportation (Caltrans) and California Department of Fish and Wildlife (CDFW) streambed criteria for full-span or similar crossing designs, including design type, crossing substrate, and crossing embedment.

Agency	Design Approach	Crossing Substrate Material	Crossing Embedment
Caltrans[1] (2009 update) / NMFS[2]	Active channel	natural recruitment	<= 40% upstream, 20-40% downstream
Caltrans[1] / CDFW[3]	Low slope	natural recruitment (L<50 ft) or backfill w/ native (L: 50-75 ft)	20-40% throughout
Caltrans[1]	Stream simulation (updated 2014)	similar to reference reach	Circular culvert embedded 30-50% of culvert height
CDFW[3]	Stream simulation	Streambed with equivalent bed mobility as the reference reach (same D84 mobility)	minimum bed thickness is 1.5 times the largest immobile particle diameter, but embedded at least 20% of the culvert height

[1] (Caltrans et al., 2007)
[2] (NMFS, 2001)
[3] (CDFW, 2009b)

Scenarios where full-span crossings may not be feasible

The designation of a design type does not guarantee the proper hydraulics, sediment transport, and aquatic organism passage. The hydraulic and sediment transport through the stream crossing will depend on the site-specific conditions, and how the structure was designed and analyzed. Flow hydraulics and sediment transport can be interrupted by any poorly functioning stream crossing. Full-span stream crossings attempt to reduce design flaws (erosion, debris collection, etc.) introduced by hydraulic designs, by spanning the bankfull width and allowing a greater flow capacity; however, they are not applicable in all scenarios.

Full-span crossings, by definition, span greater than bankfull width, so the applicability of full-span crossings will change with the cost of spanning the bankfull width. Additionally, stream simulation in full-span stream crossings may be limited by excess floodplain flow that would be forced into a bankfull width crossing.

Stream simulation designs have limitations to the natural features the stream crossing design can simulate (Caltrans et al., 2007, Chp. 5). Natural channel features, like woody debris, bank vegetation, and channel processes, like channel migration, are not often duplicated within stream crossings. However, features like embedded wood and exposed bedrock can be simulated using larger grain materials to provide areas of bed or bank stability up to a design flow (Caltrans et al., 2007). Stream simulation crossings are generally only feasible in geomorphically stable channels (USFS, 2008), and not applicable to channels experiencing incision or widening (Caltrans et al., 2007). The slope of the stream crossings should not differ from the natural channel, so it becomes

difficult to simulate an adjacent reach if channel incision has lowered the downstream channel compared to upstream of the crossing.

Design Methodologies

The design process used in the available Caltrans reports is outlined in the diagram below (Figure 2). HEC-RAS 1-D and 2-D are currently used for hydraulic analyses. Caltrans is attempting to implement 2-D hydraulic modeling with SRH-2D within SMS software.

Design analysis software and supplemental tools

Numerous modeling and analysis tools are necessary for understanding and designing for the hydraulics, sediment transport, resilience, and fish passage at stream crossings.

For many conditions, a standard procedure and workflow is defined, but site characteristics are often unique so additional modeling or calculations may also be required. The design/analysis process is also often iterative, moving between design and analysis, before the design is finalized. This section describes the basic hydraulic models used for analysis and design of all sites as well as supplemental tools that assist in intermediary calculations needed for design. For both the necessary and supplemental design tools, this section describes their application, limitations, and data needs.

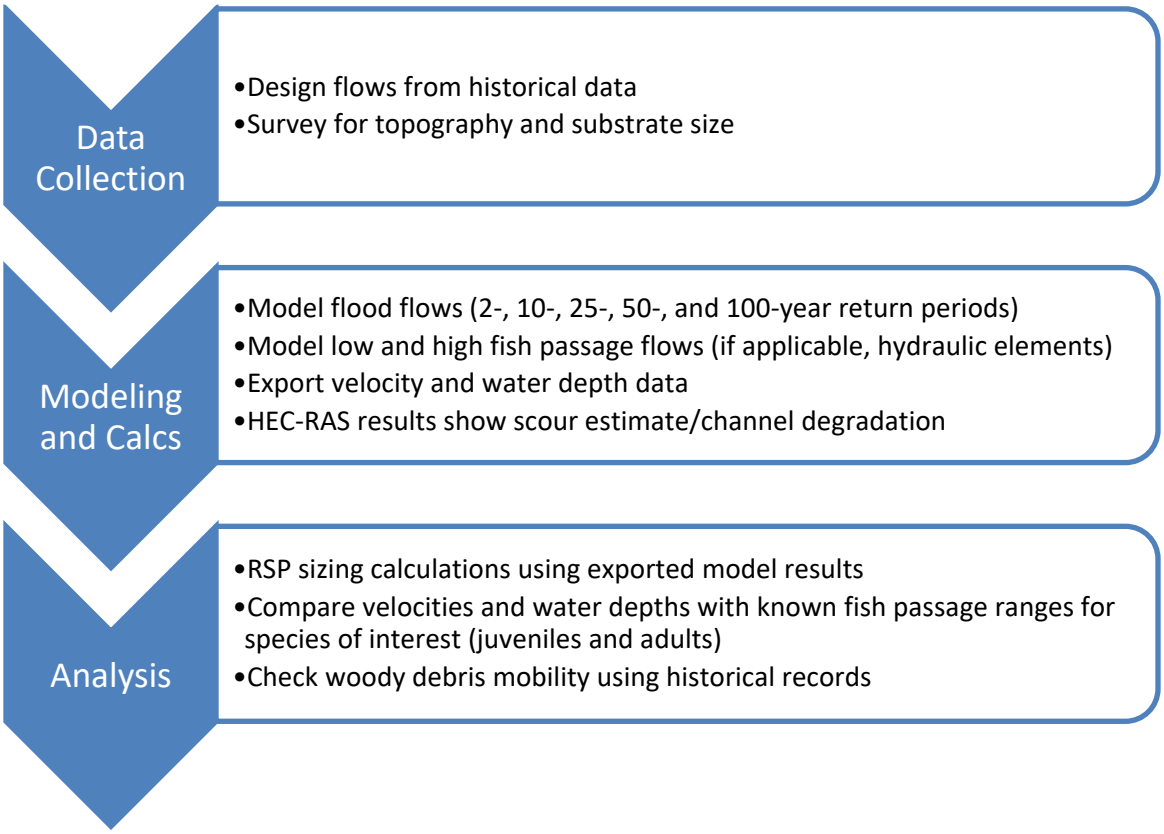

Figure 2. Design process used in available Caltrans reports for full-span crossing sites. Modeling fish passage flows is only done for hydraulic elements like geomorphic roughened channels and rock weirs.

Hydraulic modeling software

Hydraulic models are used to analyze the hydraulics, sediment transport, and flood resiliency of road-stream crossing designs. The most common software used are: HEC-RAS 1D and 2D, and SRH-2D (Brunner & CEIWR-HEC, 2016a; Lai, 2008). Use of SRH-2D by departments of transportation is encouraged and supported by the FHWA, especially for use at crossings where aquatic organism passage is required.

One-dimensional models simulate water in the longitudinal direction, the principal direction of flow. The simulated velocity and depths are the average values over

the entire channel cross-section. One-dimensional models have simpler inputs and are more computationally efficient. However, one-dimensional models cannot account for structures that do not span the full channel width and do not provide detail for complex flow patterns such as areas of concentrated or split flow.

Two-dimensional models simulate velocity in the longitudinal and transverse directions, while assuming a depth-averaged velocity in the vertical direction. The models account for velocity and depth variation across the channel. The additional hydraulic detail provided by the 2D model is important for conditions such as multi-opening crossings, flow around bridge piers and footings, flow around channel bends or islands, braided channels, and skewed or angled crossings.

Previous research comparing 1-D and 2-D hydraulic models has found that there remains a place for the use of 1-D hydraulic models because of the significantly shorter computer run time (Deal et al., 2017). One-dimensional modeling can provide adequate information for sites where horizontal flow characteristics (cross-sectional flow variability and eddies) are not substantial or serve as a preliminary check on design, but there is more information that can be obtained by 2-D hydraulic modeling.

HEC-RAS 1D and 2D

HEC-RAS, the Hydrologic Engineering Center (HEC) River Analysis System (RAS), was developed and is maintained by the Institute for Water Resources of the U.S. Army Corps of Engineers. This software is free and one of the most common hydraulic modeling tools for these applications. The current version of the software is version 5.0 released in 2015. HEC-RAS can simulate steady or unsteady flow hydraulics in one- and

two- dimensions. The software also includes options for analyzing bed mobility/sediment transport, water temperature, and contaminant transport.

HEC-RAS can simulate channel networks, dendritic systems, or single reaches under subcritical, supercritical, and mixed flow regimes. The effects of infrastructure, channel modification and other obstructions such as bridges, culverts, diversions and tide gates can be accounted for in the computations (Brunner & CEIWR-HEC, 2016a). Steady flow analysis is used to calculate the water surface profiles and hydraulic conditions for various design flows of interest (e.g. flood flow, fish passage flows). Unsteady flow analysis can simulate one-dimensional and two-dimensional unsteady flow through channel networks by routing user specified hydrographs through the defined channel system (Brunner & CEIWR-HEC, 2016a).

The one-dimensional version of HEC-RAS can also be used to analyze sediment transport and channel bed evolution through scour and deposition. Sediment transport and mobile bed analysis use bed grain size fraction and sediment loading entering the reach to simulate scour and deposition as well as hydraulic sorting and armoring. HEC-RAS is designed to simulate long-term trends for scour and deposition within the stream channel that might result from changes in the frequency and duration of flow, sediment load or modifying the channel geometry (Brunner & CEIWR-HEC, 2016a).

For many design applications, both the one-dimensional and two-dimensional versions of HEC-RAS are used. One-dimensional simulations are initially developed to aid in calibrating the 2D analysis and the results are used to identify locations where 2D hydraulics are important such as flow concentration along outer channel bends and

around structures. Moving from a 1D to a 2D hydraulic analysis is especially important regions of rapidly changing flow direction, detailed channel and floodplain simulations and analysis of structures.

SRH-2D

SRH-2D (Sedimentation and River Hydraulics – 2D River Flow Modeling) is a hydraulic model developed by the U.S. Bureau of Reclamation's Dr. Yong Lai. The software solves two-dimensional depth-averaged dynamic wave equations (the St. Venant equations) using a finite-volume numerical method over a flexible mesh (Lai, 2008). SRH-2D model compares and analyzes sediment transport data, hydraulic data, and floodway delineations (Lai, 2008). Third-party graphical user interfaces (GUI), such as SMS, TECPLOT, and ArcGIS, allow for further visualization of the outputs of the model. SRH-2D is useful for designs with significant lateral effects, such as in-stream structures, through bends, multiple channels, and complex floodplains (Aquaveo, 2018).

Required input into the hydraulic model includes: topography/bathymetry data (survey, Lidar, or raster DEM), the associated coordinate system, roughness data, boundary conditions, and flow data (Brunner & CEIWR-HEC, 2016b). For 2-D modeling, the topographic data needs to capture changes in slope, so that the interpolation between survey points is accurate. The methods for surveying the sites in this project are further described in the Methodology section. Depending on the specified boundary conditions, flow discharge or water surface elevation must be input for the boundaries in the forms of constant, time series, or rating curve (Lai 2008, Chapter 4). Water surface elevation is required at exit/outlet boundaries if the flow is subcritical. The

steady state simulation model can be run using a DRY bed setup, which does not require initial water surface elevations. The resulting water surface elevations from the steady state simulation are then used as the initial conditions from the transient simulation (Lai 2008, Chapter 4). For the sediment transport analysis, additional data is required: bed surface and subsurface sample to determine particle size distribution, sediment transport data of suspended and bed loads over a range of flows, samples of floodplain materials, and erodibility testing of floodplain material (Aquaveo, 2020).

SRH-2D provides additional hydraulic information compared to a comparable 1-D model because the velocities, water depths, and shear stress are calculated for each element in the 2-D mesh grid. Changes in velocity and water depth laterally across the stream, from bank to bank, give a more accurate representation of conditions at the banks and at structures. In 2-D hydraulic models, eddies are visible and the erosion potential at the banks can be estimated. Additionally, SRH-2D can simulate pressure flow that could occur at stream crossings, which is useful when modeling extreme event flows. SRH-2D also provides additional information on sediment mobility and transport compared to HEC-RAS, with a two-dimensional sediment transport analysis (Brunner & CEIWR-HEC, 2016b; Lai, 2008). In this project, model outputs from SRH-2D are compared to outputs from one-dimensional models in HEC-RAS.

SMS with Riverine package

SMS (Surface-water Modeling System) is a graphical user interface (GUI) that links SRH-2D to external hydraulic models, including HEC-RAS (Aquaveo, 2018). The benefit of using the SMS GUI is the ease of importing data and the data visualization for

the model outputs. The software allows the user to import numerous file types: raster images, topography, elevation/bathymetry data, ArcGIS shapefiles, CAD files, and delimited text files and spreadsheets (Aquaveo, 2018). SRH-2D is often used in combination with HDS 5 and 7 technical manuals (explained in the following section), and SMS integrates HDS 5 through the FHWA HY-8 addition (Aquaveo, 2020; Schall et al., 2012; Zevenbergen et al., 2012).

Supplemental design and analysis tools

In addition to 1-D and 2-D hydraulic modeling, a range of more specialized methods are needed for crossing design. These supplemental tools are used to develop input parameters for the hydraulic models and provide more detailed analysis of different site characteristics such as detailed culvert barrel hydraulics, fish passage conditions or perform geomorphic analyses to inform understanding of channel stability. The tools discussed here include only those that are public domain and are commonly used by departments of transportation or other government agencies.

HDS 5 and HDS 7 technical manuals

The HDS 5 (Hydraulic Design of Highway Culverts, Third Edition) technical manual is a compilation of the software available, updated culvert design standards, and new information for aquatic organism passage, culvert assessment, and culvert repair and rehabilitation (Schall et al., 2012).

The HDS 7 (Hydraulic Design of Safe Bridges) technical manual is a comprehensive and detailed summary of the information necessary for designing and

assessing bridges (Zevenbergen et al., 2012). The manual presents procedures for bridge hydraulic analysis, unsteady flow analysis, and analysis on scour countermeasures.

FHWA HY-8

The HY-8 Culvert Hydraulic Analysis program is FHWA's primary tool for 1-D analysis of culvert hydraulics. This software is used to determine the culvert geometry, size, and material for a particular crossing, using input data of design discharges, tailwater channel geometry, a roadway cross-section, and an embankment template (Aquaveo, 2020; Schall et al., 2012). The current software version 7.6 calculates the headwater depth and a water surface profile through the culvert barrel for design discharges or other discharges of interest. HY-8 is included in SMS software to model culverts and other pressure flow sections in 2-D models (Aquaveo, 2020).

FHWA Hydraulic Toolbox

The Federal Highway Administration (FHWA) Hydraulic Toolbox is a set of calculators that performs common hydrologic and hydraulic analyses and design computations for: Rational Method hydrology, channels, weirs, bridge scour, riprap countermeasures, sediment gradations, and culvert assessments (Bergendahl & Arneson, 2014). The FHWA Hydraulic Toolbox can save multiple hydraulic calculations together, analyze multiple scenarios, and create documentation for the output (Bergendahl & Arneson, 2014).

USFS FishXing

The U.S. Forest Service (USFS) FishXing software was developed to assist in assessing and designing culverts for fish passage (USFS, 2012). The most current version

(version 3) calculates 1D culvert hydraulics similar to HY-8 and includes a fish swimming performance database for a variety of species. The swimming capabilities of target fish species are compared to the culvert hydraulics at selected fish passage design flows to evaluate whether passage would be possible under the predicted conditions. The output includes water surface profile and detailed water depths through the culvert, water velocities through the culvert barrel, and identifies the cause and location of factors limiting fish passage (USFS, 2012).

The FishXing software has been widely used as an assessment tool to identify fish passage barriers and to assist in prioritizing sites for replacement or modification (USFS, 2012). The FishXing software is recognized and recommended in many stream crossing design manuals (e.g. Barnard et al., 2013; Bates & Kirn, 2009; Caltrans et al., 2007; Hotchkiss & Frei, 2007; NMFS, 2001).

USFS Stream Simulation Design spreadsheet

The USFS has developed a Stream Simulation Design spreadsheet for support of the stream simulation approach (USFS Stream Simulation Working Group, 2008). The spreadsheet's worksheets include calculations for particle size distribution and Manning's roughness (n). The particle size distribution tool takes pebble count data and arranges it into a particle distribution, while also calculating the particle sizes at key percentiles (50^{th}, 85^{th}, 90^{th}). The Manning's roughness calculator accounts for bank roughness, cross-sectional area variations, obstructions, vegetation, and meander to produce a final Manning's roughness. This tool is useful in estimating many of the inputs needed for other analysis tools and developing site hydraulic models.

USFS Stream Channel Flow Resistance Coefficient computation tool

The USFS Stream Channel Flow Resistance Coefficient Computation Tool (hereafter referred to as 'Resistance Coefficient Tool') was developed by Steven Yochum for the USFS National Stream and Aquatic Ecology Center (2018). The resistance coefficient tool assists in selecting flow resistance coefficients for stream channels, such as the Manning's roughness coefficient (n) and Darcy-Weisbach friction factor (f). The user inputs characteristics of bed and bank grain material, bedforms, streambank and cross-section variability, sinuosity, vegetation, large instream wood, and other obstructions. The software outputs multiple estimates of Manning's n and Darcy-Weisbach f. Nine quantitative methods are applied within the software for redundancy (Yochum, 2018).

Scour depth equations

The NCHRP (National Cooperative Highway Research Program) developed scour equations for analyzing a variety of abutment types and conditions (Ettema et al., 2010). The abutment scour equations are based on equations for contraction scour with an additional factor to account for the abutment type, flow distribution, and sediment transport conditions. There are two contraction scour equations included in Section 8.6.3 of '*Evaluating Scour at Bridges, 5th Edition*': one for live-bed and one for clear-water (Arneson et al., 2012). The live-bed equation assumes that the abutment experiences a majority of the scour-inducing forces from the sediment transported in the main channel. The clear-water equation assumes that the abutment experiences a majority of scour inducing forces from the turbulence of flow on the floodplain moving around the

abutment (Arneson et al., 2012). The factor value is determined from the type of abutment (spill-through or wingwall), contraction scour type (live-bed or clear-water), and the ratio of unit discharge in the constricted flow opening to unit discharge in the upstream channel.

Geomorphic design elements equations

Geomorphic design elements include streambed material and stream bank material and protection. Streambeds are designed to be mobile or stable based on specific flows, while stream banks are designed for stability.

Determining streambed material for within crossing

There are two design concepts for sizing streambed material: producing a mobile bed that is replenished by sediment transport from upstream and/or producing a stable bed by oversizing material (Caltrans et al., 2007; Kilgore et al., 2010). Naturally occurring streambed mobility generally changes with channel type (Caltrans et al., 2007), so it is helpful to study a reference reach when designing for streambed mobility. The substrate for stream crossing bed material designed for mobility can be made from a combination of grain sizes to produce an equivalent substrate to a reference reach streambed; however, if the stream crossing geometry and hydraulics differ from the reference reach, the difference must be accounted for in the design streambed's specifications, and a stable, permanent bed may be more reliable for design (Caltrans et al., 2007). Sometimes a mobile bed design will have an underlying stable sub-floor. The alluvial (mobile) elements should be designed to mimic the reference reach, by matching the flow for incipient motion of the substrate inside the culvert to the flow causing

incipient motion in the reference reach. Various sediment entrainment calculations (unit discharge, average shear stress, or critical velocity) can be used to estimate the flows for incipient motion in the crossing and the reference channel (Caltrans et al., 2007). The Bathurst Critical Unit Discharge and the Modified Shields methods are recommended by U.S. Forest Service and CA Fish and Wildlife (Caltrans et al., 2007; CDFW, 2009b; Kilgore et al., 2010; USFS Stream Simulation Working Group, 2008). The colluvium, bank material, and key instream pieces are considered more permanent. Stability of colluvium, bank material, and key pieces should be analyzed with similar sediment entrainment equations to the 100-year flow (CDFW, 2009b).

Guidance for stream simulation bed material sizing can be found in Section 5.5.5 'Bed Material Sizing' of the Caltrans Fish Passage Design for Road Crossings guidelines (Caltrans et al., 2007).

RSP and rock sizing for construction of stream banks (6.3.8.3 Bates et al 2009)

Rock slope protection (RSP) is made up of riprap, which is angular quarry stone. RSP for banks is recommended when lateral bank erosion may undermine an existing structure and erosion potential is significant (Barnard et al., 2013a; Caltrans et al., 2007). The ideal solution would be for the stream crossing to span the entire active floodplain, to allow for natural lateral channel movement and bank erosion; however, if this is not economically feasible, lateral bank erosion must be identified and halted to protect infrastructure (Barnard et al., 2013a). Lateral bank erosion can be identified in the field or through aerial photography (Caltrans et al., 2007; Lagasse et al., 2012). Bank protection design should refer to the California Bank and Shore Rock Slope Protection Design

document (Caltrans et al., 2007; Racin et al., 2000). But current designs must use the new Caltrans standard RSP sizes, which are a modified version of the Hydraulic Engineering Circular (HEC) 23 RSP sizes (Caltrans, 2020; Craggs, 2016). Caltrans made this decision to establish consistency between federal and state projects and manuals (Craggs, 2016). The updated Caltrans standard RSP sizes are identified by Class and the total range of weights is from 4 lbs to 12 tons, rather than 1 lb to 16 tons in the old standards (Caltrans, 2020; Racin et al., 2000). Caltrans is also testing combinations of RSP and vegetation to provide a broader working solution, but for now designs are developed specific to the stream crossing site (Caltrans et al., 2007).

Lateral bank erosion can be caused by meander bends, in-stream structures, or hardening of portions of the stream bank. Deposition of sediment from backwatering or eddies can increase lateral shifting of stream channels and can deepen meander bends (Barnard et al., 2013a). Many stream systems meander across a floodplain over a longer time period than monitoring shows, so viewing historical imagery and comparing to current conditions can provide insight, as well as looking for signs in the landscape, such as meander scars (Barnard et al., 2013a; Caltrans et al., 2007). Additional resources provide methodology for predicting channel migration (A Framework for Delineating Channel Migration Zones by Rapp and Abbe (2003) and the Handbook for Predicting Stream Meander Migration by Lagasse and Spitz et al. (2004)), but a qualified expert should be consulted. Lateral instability can also be a consequence of a misaligned stream crossing, but a misaligned stream crossing can also result in lateral movements of the stream (Caltrans et al., 2007; USFS Stream Simulation Working Group, 2008).

The design analyses described above are used to evaluate a stream crossing's effectiveness and robustness in response to various stream flow conditions. The analysis provides the necessary insight into design characteristics like flow capacity and structural stability of the bed, banks, and structure. The design analyses are used in this project to evaluate the performance of two current stream crossing designs using 2-D hydraulic model results and to compare the predicted performance to design analyses completed for the current stream crossings, using previously completed 1-D hydraulic model results.

METHODS

The methodology for this project begins with collecting topographic survey data at the full-span stream crossing sites. The topographic data was then used to create a model surface in Sedimentation and River Hydraulics 2-D (SRH-2D) (see the Literature Review for more information on SRH-2D) (Lai, 2008). The model outputs 2-D results for water depths, velocity vectors, and shear stress. The results are interpreted for flow capacity, erosion/scour potential, and high flow fish passage. The interpretations and design conclusions from these results are compared to design decisions made for the current structures based on 1-D hydraulic modeling results. HEC-RAS 1-D models were used in Caltrans' design analyses for the current installed structures. The 1-D hydraulic models were not available for either of the projects, so the 1-D model results summarized within the final project reports were used for comparison with 2-D model results from this project analysis. A sensitivity analysis was completed for the Manning's roughness values used for the model surfaces.

Site Backgrounds

For this project, two full-span stream crossing sites in Northern California were chosen for evaluation: (1) Little Mill Creek in Del Norte County (DN197, Postmile 6.15) and (2) North Fork Ryan Creek in Mendocino County (MEN101, Postmile 52.36). The sites are both under Caltrans jurisdiction and cross under state highways. The two stream crossings are completed fish passage remediation locations, as tracked in the California

Fish Passage Assessment Database (CalFish & Caltrans, 2020). The watershed characteristics and full-span designs vary between each stream crossing and are described below.

Little Mill Creek

Little Mill Creek is a tributary to the Smith River with a drainage area of 3.96 square miles and a mean annual precipitation of 90.49 inches (obtained from the Oregon Climate Service) based on the previous 2016 Little Mill Creek hydraulic analysis (Caltrans, 2016). The current mean annual precipitation generated by USGS Streamstats is 93.7 inches (USGS, 2020). Little Mill Creek bridge is located roughly one hundred feet from the creek's confluence with the Smith River. This Little Mill Creek confluence with the Smith River is approximately 4,500 feet upstream of the US 101 Smith River Bridge (the Dr. Ernest M. Fine Memorial Bridge), where USGS river gage station no. 11532650 is located (stream gage name: SMITH R NR FORT DICK CA). The target species for fish passage through this crossing is Northern CA Coast Coho (threatened) (CalFish & Caltrans, 2020). Fish passage through this stream crossing has been determined 'remediated', but the fish response is unconfirmed (CalFish & Caltrans, 2020). On Little Mill Creek, roughly one mile upstream of Little Mill Creek Bridge a cascade has been identified as a natural total barrier that creates the upstream limit of fish passage (CalFish & Caltrans, 2020)(Figure 3).

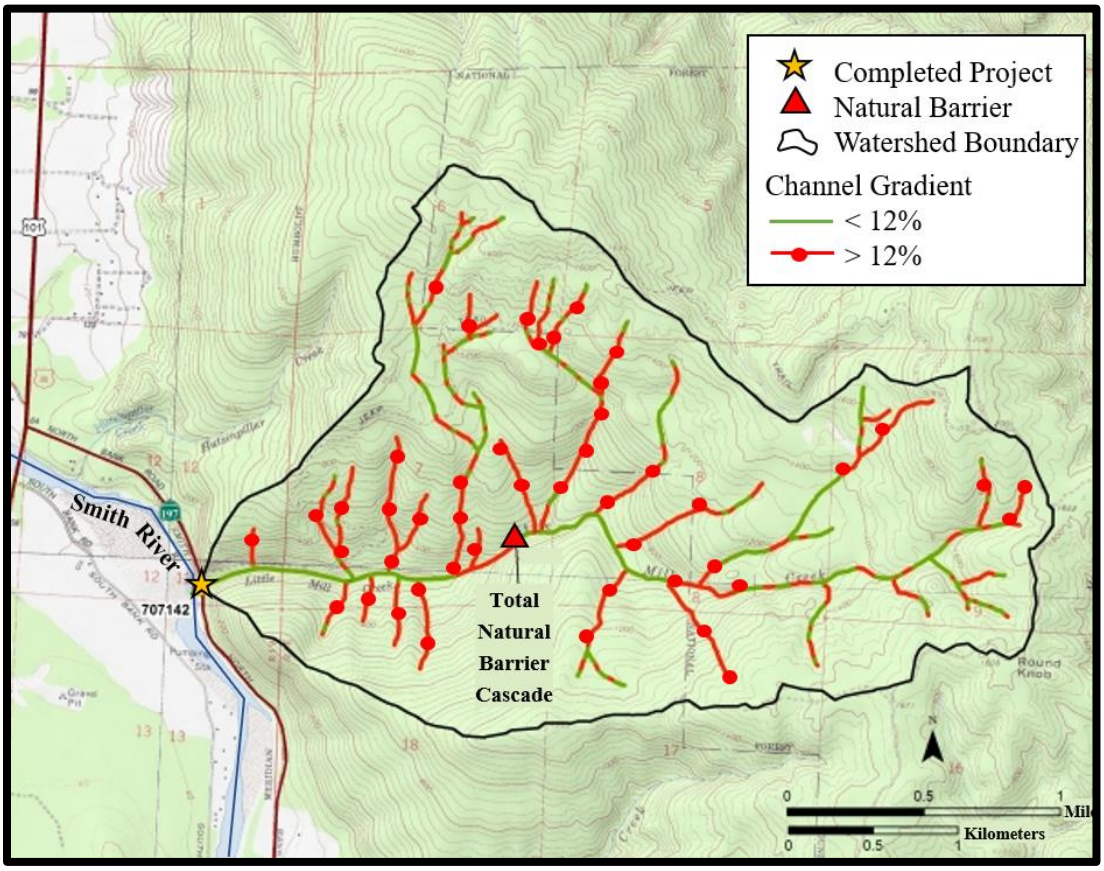

Figure 3. Little Mill Creek site map showing project location relative to natural barriers and watershed boundary. Little Mill Creek project is located at a latitude of 41.8731684 and longitude of -124.1239698 degrees. Stream gradient is also identified (adapted from CalFish and Caltrans 2020). Images of Little Mill Creek Bridge can be found in APPENDIX A.

Little Mill Creek bridge was built as an emergency construction project to repair a sinkhole in State Highway 197 (Caltrans, 2016). The project replaced a damaged 14-ft diameter structural steel plate pipe (SSPP) culvert with a 90-foot long and 34-foot wide single span bridge (Caltrans, 2016)(see Figure 4 and Figure 6). The bridge abutments are built on spread footings and the bank slopes under the crossing are 1.5H:1V. The new bridge was designed with consideration of the coincident flow events for Little Mill

Creek and the Smith River, to account for increased water elevations at the stream crossing due to backwatering of the Little Mill Creek channel from the Smith River (Caltrans, 2016).

Figure 4. Photo on the left taken by Humboldt State University on 8/5/2002 before fish passage remediation. Photo on the right taken by CDFW on 11/30/2016 after remediation showing the new highway 197 bridge over Little Mill Creek in Del Norte County. Both photos were taken downstream looking upstream (adopted from CDFW BIOSViewer updated as of 2020).

The designed profile of the crossing includes four weir structures (Figure 5) (see full profile in APPENDIX E). The bridge deck (56.5 feet) is 24.5 feet above the installed channel proposed grade line (32.0 feet). The Smith River water surface elevations control the water surface elevations at Little Mill Creek bridge during the 25-year and 100-year Smith River flow events (Caltrans, 2016). The minimum soffit elevation of the bridge is 47.78 feet, based on water surface elevation of the 100-year Smith River event (47-foot water surface elevation). The resulting freeboard estimate was 5.78 feet, based on the 25-year Smith River event (42-foot water surface elevation).

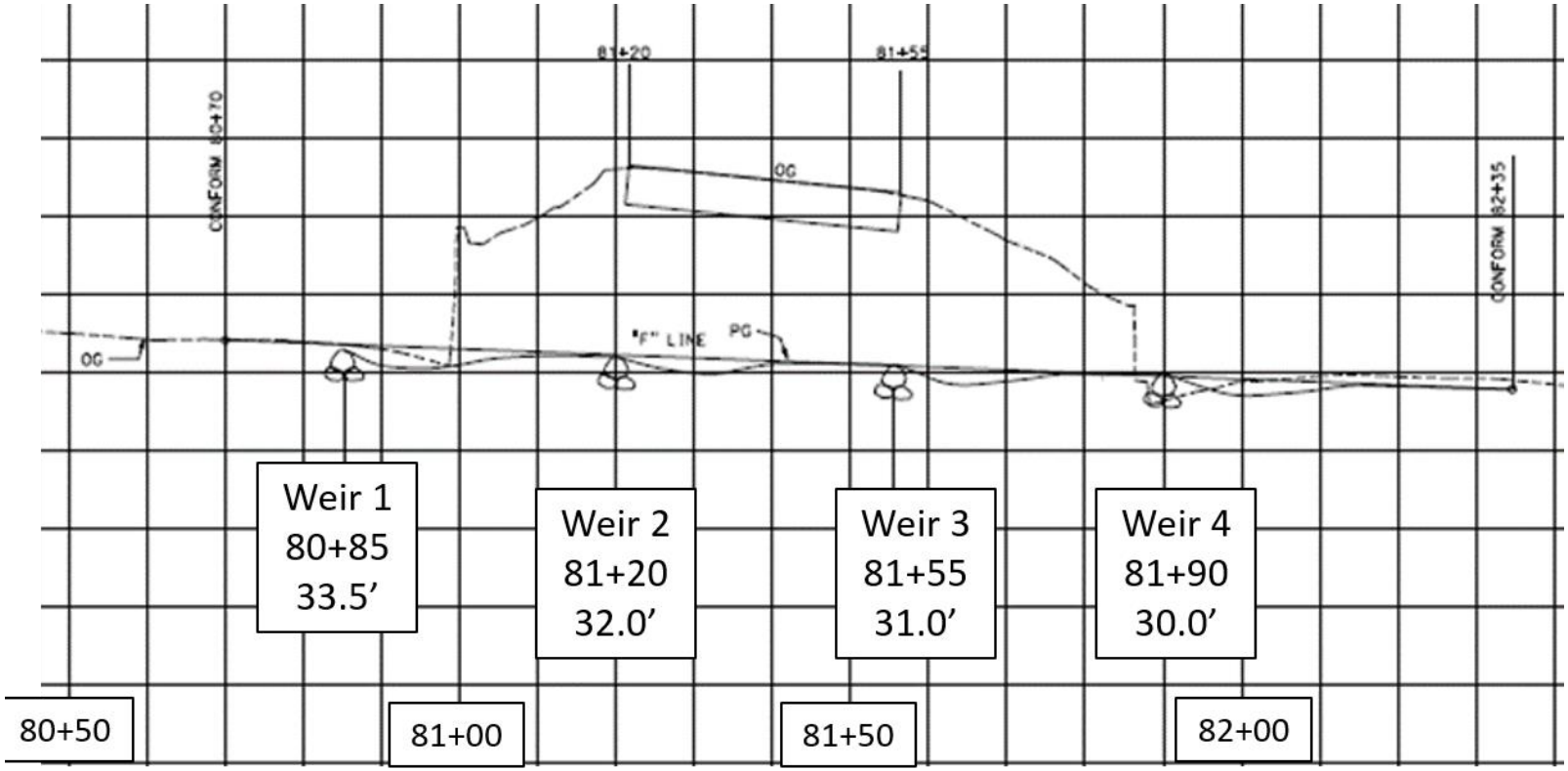

Figure 5. Design drawing profile plot of Little Mill Creek. Plot shows longitudinal profile, rock weirs, and crossing structure (adopted designed profile plot received from Caltrans).

Woody debris is present and mobile at high flows in Little Mill Creek. The site pictures from the Caltrans report show woody debris in the stream in 1981 (Caltrans, 2016). Similar woody debris is currently present in Little Mill Creek. Over the year of site visits, debris was present in the upstream reach and at the confluence with the Smith River. During a site visit on January 9, 2020 there was new debris immediately upstream of the crossing (see Figure A-6 in APPENDIX A). Additional photos of debris can be found in APPENDIX A. Debris at Little Mill Creek seems significant to the stability of the banks upstream of the crossing. The location and migration of woody debris is not easily predictable, so design criteria guaranteeing a crossing opening wide enough to pass the expected debris, which is true for the current structure, is essential.

Current conditions

Currently under the Little Mill Creek crossing, the backwatering caused by the Smith River created conditions to deposit sediment on the right bank under the crossing structure. Currently, the sediment deposits are approximately seven feet higher than the channel thalweg and cover the lower portion of the right bank RSP (based on site visits in 2020).

Figure 6. Picture of Little Mill Creek bridge (Highway 197) taken by Mike Love on 5/9/2019. Photo taken from upstream looking downstream.

The channel geometry currently at Little Mill Creek bridge differs from the reference reach. The bankfull width at the crossing is 32.8 feet, while the bankfull width in the reference reach is approximately 30.7 feet. The active channel width at the crossing is 23.8 feet and in the reference reach is 24.6 feet. The wetted channel width at the crossing is 12.8 feet, while the wetted width in the reference reach is 11.6 feet. The longitudinal profile of the stream along the thalweg is shown in APPENDIX E.

North Fork Ryan Creek

North Fork Ryan Creek is a tributary to Ryan Creek which flows to Outlet Creek, which then discharges to the Upper Main Eel River. The drainage area upstream of the North Fork Ryan Creek stream crossing is 0.67 square miles and a mean annual precipitation of 51 inches is used to be consistent with flows simulated in the hydraulic analysis for the Ryan Creek Culvert Replacement Project Final Report; however, there is

no source available for the values used in the report (AECOM, 2014)(Figure 7). The current mean annual precipitation from USGS StreamStats is 56.1 inches (USGS, 2020). The target species for fish passage and habitat are: Northern CA Steelhead (threatened), Northern CA Coast Coho (threatened), and CA Coastal Chinook (threatened) (CalFish & Caltrans, 2020). Pacific lamprey (*Lampetra tridentate*) are also identified as inhabitants of Ryan Creek (AECOM, 2014). The new stream crossing is classified as 'not a barrier' to fish passage (CalFish & Caltrans, 2020).

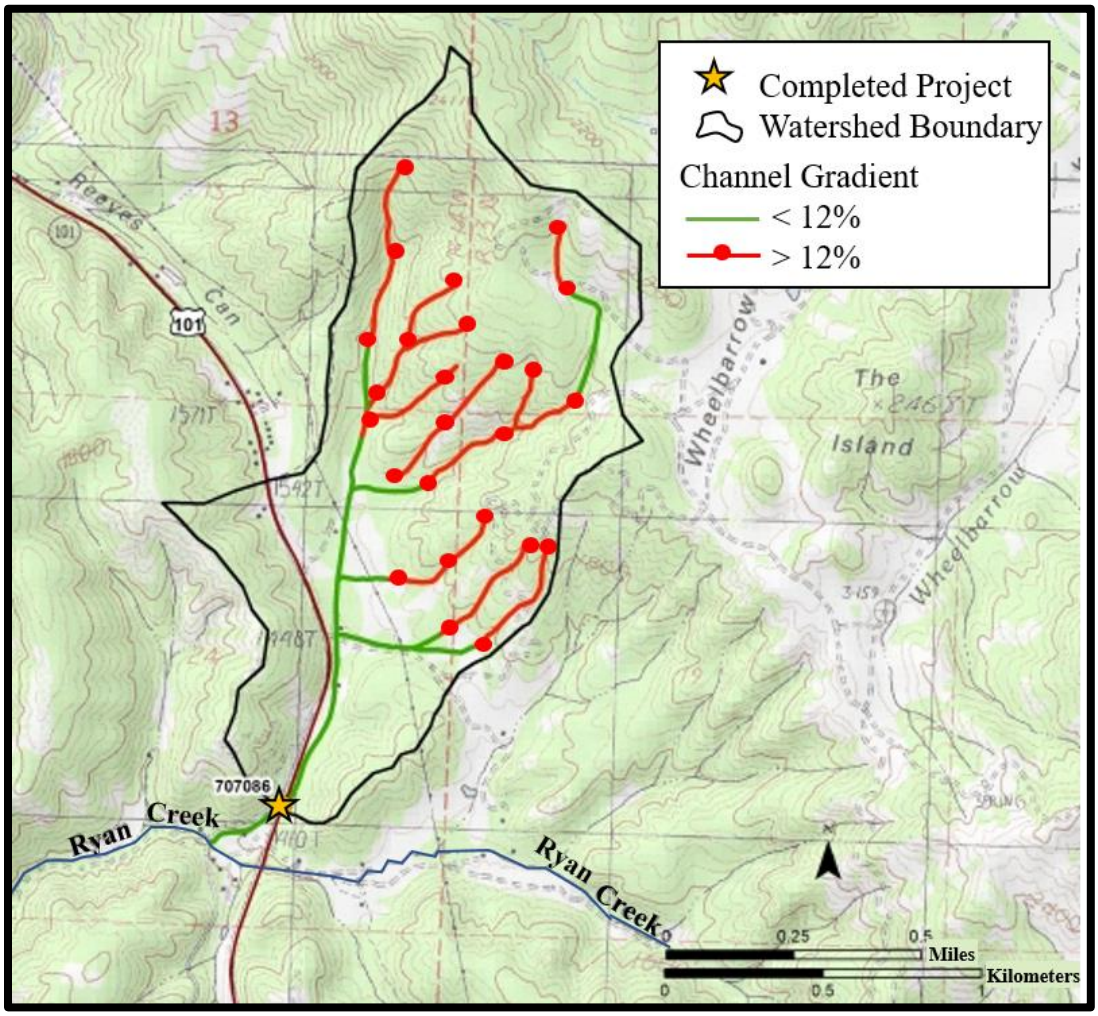

Figure 7. North Fork Ryan Creek site map showing project location relative to watershed boundary with stream gradients identified (adapted from CalFish and Caltrans 2020). The North Fork Ryan Creek project is located at a latitude of 39.479 and a longitude of -123.361 degrees. Images of North Fork Ryan Creek crossing are found in APPENDIX A.

Replacement of the North Fork Ryan Creek crossing to restore fish passage was used to satisfy mitigation requirements for the Willits Bypass Project, which constructed a new freeway alignment of US 101 to the east of and around Willits, CA (AECOM, 2014). The previous culvert, a 5-foot diameter corrugated metal pipe (CMP), had a perched outlet which prevented fish passage for all species and life stages of the fish of interest (Lang, 2005). The CMP was replaced with a 12-ft span by 10-ft rise reinforced concrete box (RCB) countersunk 24 inches (AECOM, 2014)(Figure 8). The top of the structure is approximately 13 feet above the constructed streambed (AECOM, 2014).

Figure 8. Photo on left of culvert outlet pre-treatment taken by Humboldt State University of 12/15/2002 (perspective: downstream looking upstream). Photo on right of culvert inlet post-treatment taken by Caltrans on 01/09/2018 (perspective: upstream looking downstream)(adopted from CDFW BIOSViewer as of 2020).

The height from streambed to culvert invert elevation was designed to be eight feet. There were two upstream rock weirs installed and nine downstream rock weirs (see

as-built design drawings in APPENDIX E). The report states that the existing reference reach streambed was 84 inches wide, which the design width of the crossing was based on (AECOM, 2014). It is unclear whether the stated streambed width is a bankfull width, as there is no description of how this value was determined.

Current conditions

Currently at North Fork Ryan Creek crossing, the structure is no longer technically full-spanning because the banks have eroded upstream of the crossing inlet and the crossing now constricts the flow area at the 2-year flow and above. The channel geometry currently at North Fork Ryan Creek crossing has changed from the installed design. The bankfull width currently upstream of the crossing inlet is 18.4 feet, compared to the crossing width of 12 feet (Figure 9). The wetted channel width upstream of the crossing is approximately 15.5 feet.

Figure 9. Photo of North Fork Ryan Creek crossing inlet taken by Margaret Lang on 02/27/2019. Photo taken upstream looking downstream.

There is no evidence of woody debris transport at the North Fork Ryan Creek crossing. Upstream of the reference reach in North Fork Ryan Creek there is large woody debris, but the debris is less likely to be transported because of the small channel width and small flow magnitudes.

Data Collection

Data was collected over the course of 2019 and 2020 for the two project sites: Little Mill Creek and North Fork Ryan Creek. The topographic surveys were done using a Topcon GTS 226 Total Station. The Little Mill survey data was collected on 08/08/2019, 11/11/2019, and 11/14/2019 with the following crew members present on various days: Tyler Caseltine, Chris Fabbri, Marcie Jimenez, Margaret Lang, Antonio

Llanos, David Riveras, and Alyssa Virgil. The North Fork Ryan survey data was collected 01/14/2020 and 3/16/2020 with crew members: Tyler Caseltine, Margaret Lang, and Alyssa Virgil. Data was collected in both the stream crossing reach, including the stream channels directly upstream and downstream of the crossing and within the crossing, and in upstream reference reaches. Survey data collected includes longitudinal thalweg profile, wetted channel boundary, active channel boundary, slope breaks, boundaries defining different surface roughness such as RSP, boundaries of the stream crossing structures, and boundaries of terraces. Cross sections were surveyed upstream and downstream of the crossings, as well as, in the upstream reference reach.

Pebble counts were done in the reference reaches and stream crossing reaches using the Wolman pebble count method (Wolman, 1954). A pebble count was done at Little Mill Creek, but not at North Fork Ryan Creek. The grain size distribution determined from the pebble count is presented in Table 3.

Table 3. Grain size distribution for Little Mill Creek under the crossing based on Wolman pebble counts (Wolman, 1954).

% Finer	**D_i**	**Particle Diameter (mm)**	**Particle Diameter (in)**
98%	D_{98}	237.2	9.34
95%	D_{95}	181	7.13
90%	D_{90}	128	5.04
84%	D_{84}	105.5	4.15
50%	D_{50}	42.8	1.69
35%	D_{35}	20.1	0.79
30%	D_{30}	16	0.63
16%	D_{16}	6	0.24
10%	D_{10}	2.8	0.11
5%	D_5	<2	--

For Little Mill Creek, the longitudinal profile extended from the crossing structure 620 feet upstream and 135 feet downstream to the confluence with the Smith River (Figure 10). There were six cross-sections surveyed, four near the crossing and two in the upstream reference reach. The cross-sections near the crossing structure bounded the RSP, with XS1 at the downstream boundary of the RSP, XS2 at the downstream crossing wall, XS3 at the upstream crossing wall, and XS4 at the upstream boundary of the RSP. The top of the sediment deposits located on the right bank under Little Mill Creek bridge and sediment deposits on the left bank upstream were also surveyed. Additional features were surveyed that are not included in Figure 10, including wetted channel, active channel, bankfull width extents, floodplain extents, and breaks in slope.

For North Fork Ryan Creek, the longitudinal profile extended 253 feet upstream and 182 feet downstream of the crossing structure (Figure 11). There were 19 cross-sections surveyed, four in the upstream reference reach, two upstream of the crossing, one at the inlet headwall, three in the crossing, one at the outlet headwall, and seven downstream of the crossing. More cross-sections were surveyed at North Fork Ryan Creek, compared to six at Little Mill Creek, because there were more rock weirs and the crossing structure was directly affecting the flow area. Cross-sections were surveyed at each discernible rock weir structure, both upstream and downstream of the crossing. Key boulders that were expected to obstruct flow based on field observations were also surveyed. Additional features were surveyed that are not included in Figure 11.

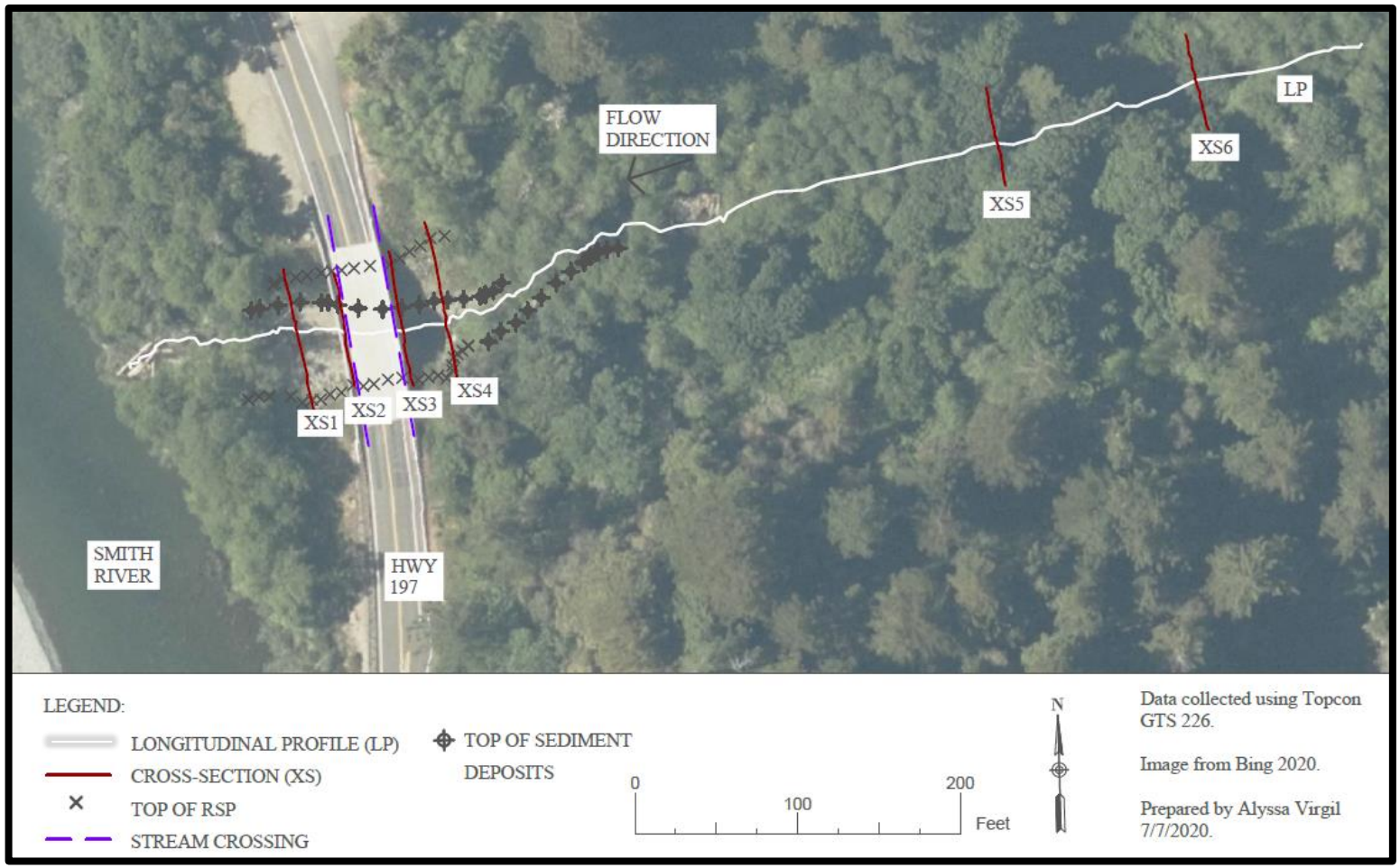

Figure 10. Site map of Little Mill Creek with surveyed cross-sections, longitudinal profile, top of RSP, deposits, and flow direction shown.

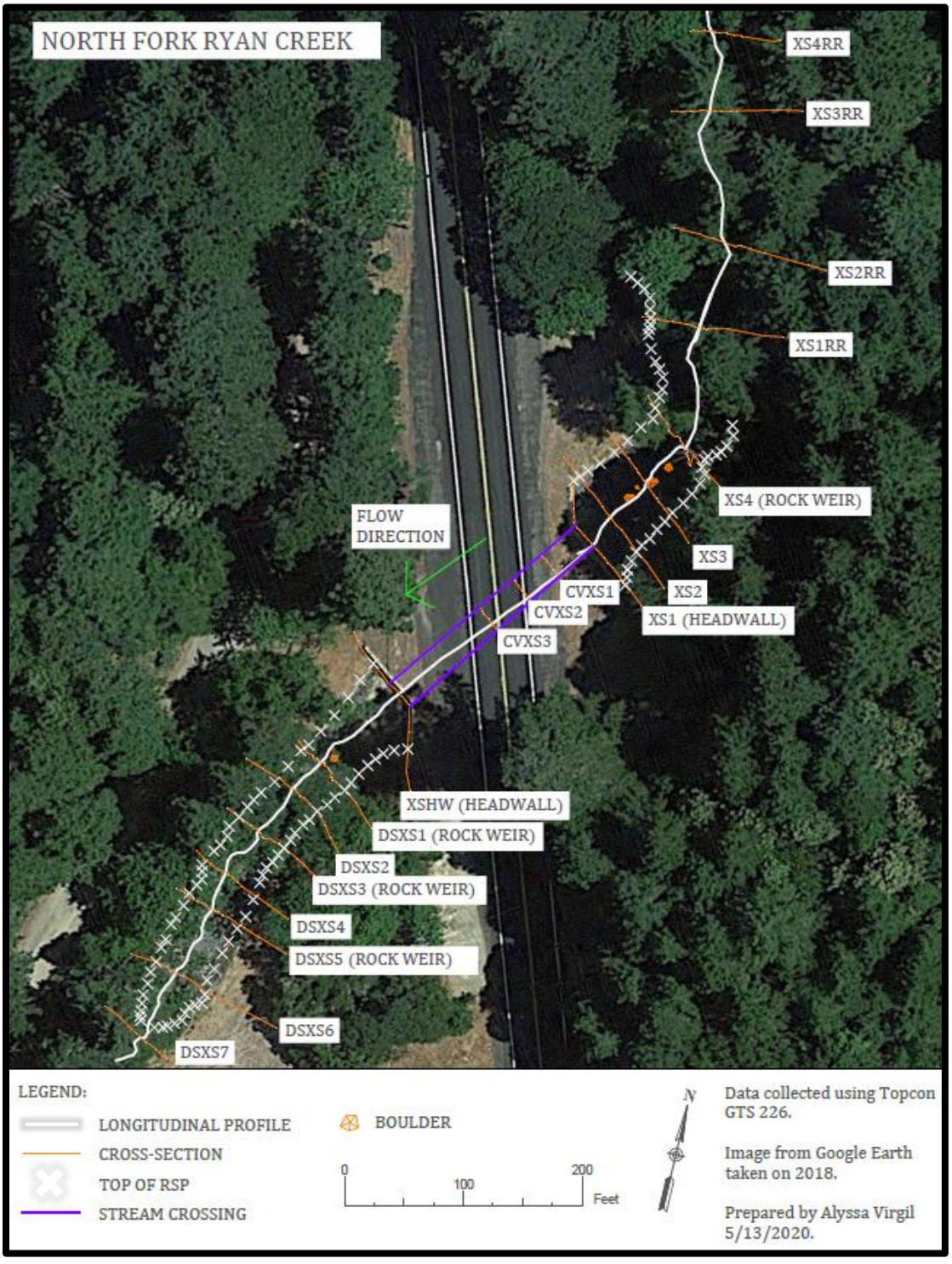

Figure 11. Site map of North Fork Ryan Creek with surveyed cross-sections, longitudinal profile, top of RSP, key boulders, and flow direction shown.

Collecting survey data for 2-D hydraulic models

The topographic data collected was driven by the model requirements to include slope breaks and adequate density of data points. For Little Mill Creek wetted channel, active channel, bankfull channel, top of RSP, toe of RSP, top of right bank sediment deposits, top of terrace, and other slope breaks were surveyed. For North Fork Ryan Creek, the same channel boundaries and slope breaks were surveyed, but this site had no significant sediment deposits. Surveying slope breaklines along the stream banks allowed for the stream geometry to be defined without the need for a high density of cross-section surveys. Elevations can be linearly interpolated between slope breaklines since there was not a significant change in the slope between the surveyed points. Wetted, active, and bankfull channel lines made increasing the resolution of the stream channel mesh easier because these define breaklines and provide boundaries for triangulation of the scatter points within the model mesh. Physical obstructions to flow, including boulders and rock weirs, were also surveyed in detail. The key boulders in the streams were surveyed for the base elevations around the bottom of the boulders and a survey point at the highest elevation of the boulder. Rock weirs were surveyed along the crest and the base of the weir.

The longitudinal thalweg profile was surveyed to establish the main flow pathway (see longitudinal profiles in APPENDIX E). In the North Fork Ryan model, the longitudinal profile was also used to initially calculate the subcritical normal depth outlet boundary condition (until water surface elevations were output by the model). In the Little Mill model, the outlet boundary condition was supercritical due to the slope of the

channel at the confluence with the Smith River. The floodplains were extended for Little Mill Creek, using knowledge of the site terrace boundaries, to make a realistic mesh surface.

The design flows of interest for both sites were expected to inundate the floodplain; thus, the upper elevations surveyed included the threshold elevation that needs to be overtopped to enter the floodplain. The top of bank generally served as this upper boundary between the channel and the floodplain. The terrace extent along the reference reach at Little Mill Creek is about 3.25 times wider than the channel and is bounded by steep valley slopes, so the survey included some points at the boundaries of the floodplain and terrace extents. The floodplain in the reference reach at North Fork Ryan Creek is about 1.5 times as wide as the channel and bounded by milder sloping valley hillsides, so more detailed cross-sections spanning the entire floodplain were collected.

There is greater average survey point density in the channel and lower bank section because a majority of the water is routed through this section (Table 4 and Table 5). In addition to this difference, the distribution of the survey points within these two sections is uneven, with greater point density at cross-sections.

Table 4. Little Mill Creek survey point density for the entire model domain, main channel area, and upper bank/floodplain area.

Area name	Area size	Density of survey points
Entire Little Mill Creek model domain	131,936 square feet (appx. 0.005 square miles)	0.009 points per square foot (113 square feet per survey point)
Main channel	-	0.029 points per square foot (34.3 square feet per survey point)
Upper bank and floodplain	-	0.003 points per square foot (290 square feet per survey point)

Table 5. North Fork Ryan Creek survey point density for the entire model domain, main channel area, and upper bank/floodplain area

Area name	Area size	Density of survey points
Entire North Fork Ryan Creek model domain	23,239 square feet	0.049 points per square foot (20.2 square feet per survey point)
Main channel	-	0.077 points per square foot (12.9 square feet per survey point)
Upper bank and floodplain	-	0.034 points per square foot (29.5 square feet per survey point)

Modeling Procedure

This project uses the Sedimentation and River Hydraulics 2-D (SRH-2D) model version 3 developed by Yong Lai at the U.S. Bureau of Reclamation in Surface Water Modeling System (SMS) program version 13.0.11 developed by Aquaveo, LLC (Lai, 2008). The SRH-2D model is capable of modeling hydraulics, sediment, and temperature. The SMS program allows for complete construction and use of surface water models, with a graphical user interface for building model elements and viewing model results.

The general procedure used for creating the 2-D hydraulic models in SRH-2D is summarized in Figure 12. To begin, the topographic survey data was collected during on-

site ground surveys. The survey data and breaklines defined by sets of survey points were then used to make a mesh in the SMS software, along with coverages for defining boundary conditions, material roughness areas, and monitoring points. The mesh and coverages were used to define model parameters and run the SRH-2D model. Details for most of this model development procedure is included as 0. Those aspects of model development with the greatest impact on the simulation results, the boundary conditions and the material roughness polygons, are described here.

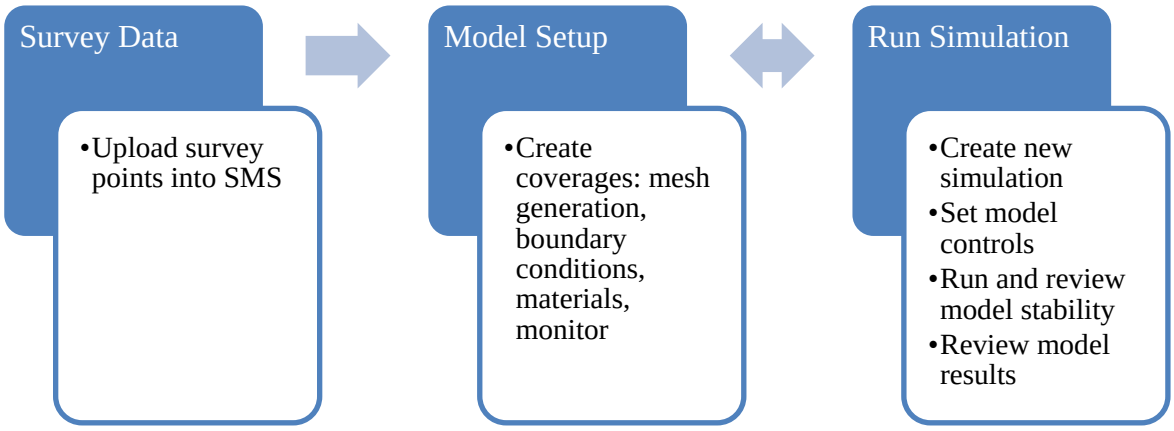

Figure 12. Modeling procedure for 2-D hydraulic modeling in SRH-2D.

SMS:SRH-2D model set-up

Using the SMS interface, a SRH-2D model is created from a group of coverages, including a mesh (further described in 0), boundary conditions, materials, and monitor coverages.

Boundary conditions

The boundary conditions are coverages that are defined using a SRH-2D package in SMS. This package uses arcs to set the inlet and outlet boundary conditions. For the

inlet boundary condition, the flow distribution for this project was set to “Q”. The Q flow distribution is a constant unit discharge that is assumed to flow normal to the inlet boundary. The flow can become unstable at the inlet, so a simple trapezoidal channel extended upstream of the surveyed data can stabilize the flow before it reaches the analysis area (Figure 13; see

APPENDIX B.3 for effect of upstream channel extension). However, for the North Fork Ryan Creek model, the upstream channel extension did not change the results once the model stabilized.

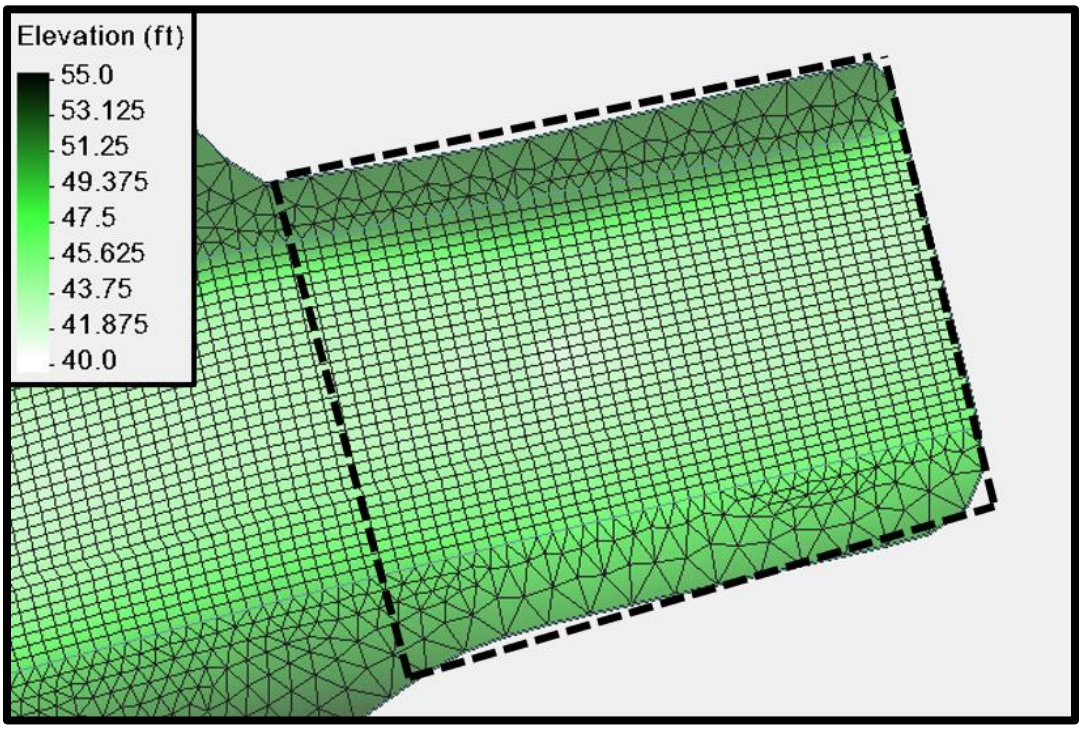

Figure 13. Example of an extended upstream channel from the Little Mill Creek model. Dashed line shows the extent of the added upstream channel.

Little Mill Creek

Little Mill Creek 2-D model simulations were run for the 2-, 10-, 25-, 50-, and 100-year return period flows. The return period flow values for the 10-, 25-, 50-, and 100-year return period from the Little Mill Creek Bridge Hydraulic Report were used to allow direct comparison with the Caltrans' previous 1-D HEC-RAS hydraulic model results (Caltrans, 2016) (Table 6). The 2-year return period flow was also simulated to evaluate hydraulic conditions at approximately the high fish passage flows. The effect of

backwater from the Smith River was simulated in the model by changing the outlet boundary condition to the water depth caused by various flow magnitudes in the Smith River (Caltrans, 2016; J. Pallares, personal communication, n.d.). For consistency with the 1-D HEC-RAS hydraulic model analysis scenarios, the same five scenarios for Little Mill Creek and Smith River flow event concurrences evaluated in Caltrans' Little Mill Creek Bridge (Culvert Replacement) Final Hydraulic Report (1-D analysis) were included in the SRH-2D hydraulic model analysis (Table 7) (Caltrans, 2016).

Table 6. Flow rates for the Little Mill Creek Basin (adapted from Caltrans 2016 Table 1). Drainage area (A) of 3.96 sq. miles and mean annual precipitation (P) of 90.49 inches.

Notation	**Recurrence Interval (years)**	**North Coast Equations (Region 1)[1]**	**Flow (cfs)**
Q2	2	$1.82A^{0.904}\ P^{0.983}$	529
Q10	10	$14.8A^{0.880}\ P^{0.696}$	1,143
Q25	25	$26.0A^{0.874}\ P^{0.628}$	1,466
Q50	50	$36.3A^{0.870}\ P^{0.589}$	1,707
Q100	100	$48.5A^{0.866}\ P^{0.556}$	1,955

[1] regional regression equations from USGS report "Methods for Determining Magnitude and Frequency for Floods in California, Based on Data through Water Year 2006"

Table 7. Simulations were conducted to match those from Caltrans' Little Mill Creek Bridge Hydraulic Report (Caltrans 2016) and two additional simulations for the 2-year and 25-year return period flows (shown in bold). Smith River backwater elevations are from the Bureau of Land Management using Bulletin 17B and FEMA, and are used in the Caltrans simulations.

Simulation Number	**Little Mill Creek flow**	**Smith River backwater elevation**
1	Q_{25}	Q_{100} WSE = 47 feet
2	Q_{100}	Q_{25} WSE = 42 feet
3	Q_{10}	None
4	Q_{50}	None
5	Q_{100}	None
6	**Q2**	**None**
7	**Q25**	**None**

For the Little Mill model simulations without backwatering, the outlet boundary condition is located in a supercritical flow zone, with Froude numbers greater than 1, so the ‘Exit-SC’ boundary is used because a normal depth calculation is not valid (Figure 14).

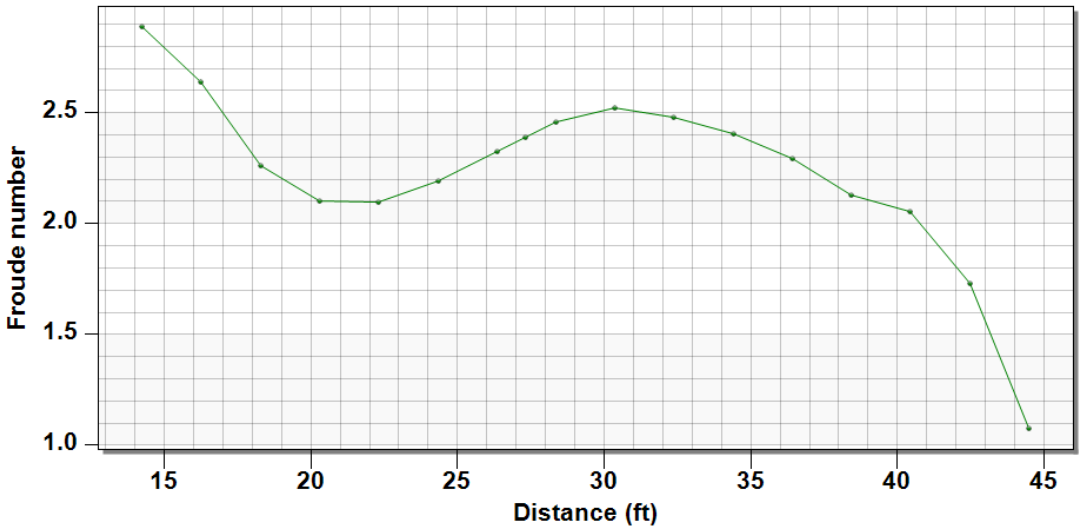

Figure 14. Froude numbers across the outlet boundary condition arc from left-to-right bank for Little Mill Creek model at the 2-year return period flow.

North Fork Ryan Creek

North Fork Ryan Creek was modeled for the 2-, 10-, 25-, 50-, and 100-year return period flows (Table 8). For the North Fork Ryan model, the outlet boundary condition is located in a subcritical zone, having Froude numbers less than 1 (Figure 15) at all simulated conditions. Thus, a normal depth outlet boundary condition was used. The normal depth is calculated using values and options shown in Table 9.

Table 8. Flow rates used for the North Fork Ryan Creek analysis completed by AECOM (2014). The AECOM analysis used the NRCS TR-55 method for flows with a drainage area (A) of 0.67 square miles and mean annual precipitation (P) of 51 inches.

Recurrence Interval (years)	**Notation**	**Flow (cfs)**
2	Q2	33
10	Q10	115
25	Q25	170
50	Q50	217
100	Q100	263

Table 9. Outlet boundary condition inputs for North Fork Ryan Creek.

Input	**North Fork Ryan Creek**
Outlet Type	Exit-H (subcritical)
Geometry	Surface with upstream channel extension
Composite Manning's	0.045
Slope	0.045, water surface slope
Flow	Value input for Inlet boundary condition

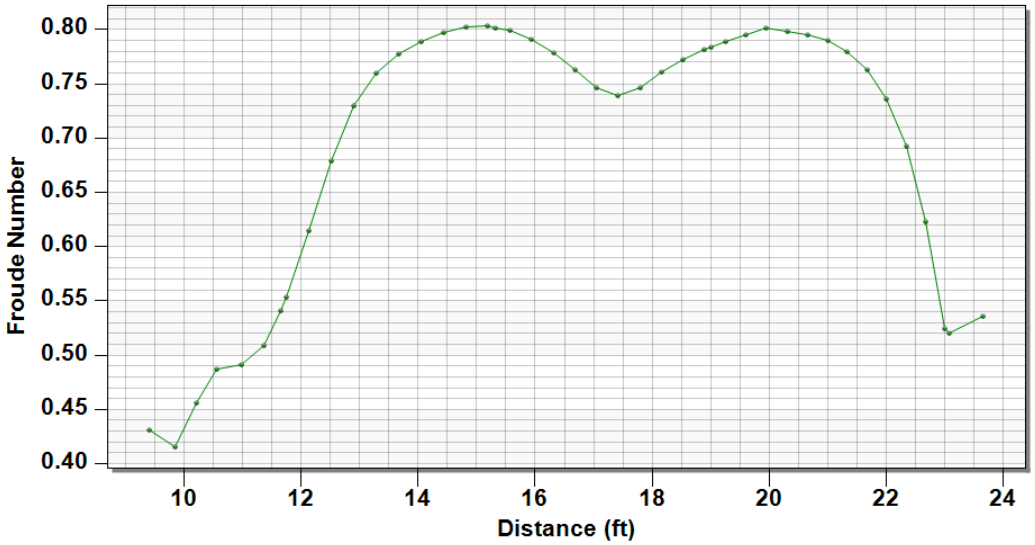

Figure 15. Froude numbers across the outlet boundary condition arc from left-to-right bank for North Fork Ryan Creek model at the 2-year return period flow.

Materials roughness

Similar to the boundary conditions, the material roughnesses are defined as coverages using tools included in SRH-2D. However, the material roughness coverages are defined by polygons. The materials coverage assigns a Manning's roughness n-value to specified areas of the model. An efficient method for creating the materials coverage polygons is to duplicate the mesh generator coverage, change its type to 'materials' (located in the right-click drop-down menu), and then define the different roughness sub-polygons. Alternatively, the materials layer can be created separately, using the field data and mesh generator coverage as a guide.

The assigned model materials coverages are based on the ground cover and streambed substrate observed during the field visits to both sites. For Little Mill Creek, materials include RSP, gravel streambed, tree vegetation, and grass vegetation (Figure

16). The RSP lies on the banks of the channel almost up to the top of the abutments, the vegetation is less dense above the RSP next to the abutments, and the floodplain is covered in dense mixed vegetation. The in-channel woody debris are not included in the model's materials coverage because the woody debris are mobile and were found to not affect stream hydraulics at or near the crossing structure.

For North Fork Ryan Creek, materials include RSP, gravel streambed, silt streambed, tree vegetation, and grass vegetation (Figure 17). The RSP lines the banks from the crossing upstream to the rock weir and downstream to the end of the model domain. The grass vegetation occurs on the floodplain where RSP has been installed and on the upstream reference reach left bank floodplain. Where RSP has not been installed, the banks are lined by trees and vegetation moving upstream into the reference reach. The majority of the streambed is a gravel substrate, but silt is deposited in the reach leading up to the rock weir. Woody debris is not included in the materials coverage because the existing woody debris is upstream of the reference reach and is unlikely to reach the crossing during design return period flows.

The materials coverages for this project had constant roughness values (Table 10). With the exception that the Little Mill Creek model did not use the 'Streambed – silt' materials coverage. The Manning's roughness values ranged from 0.03 to 0.06 in this project's models. The roughness values were kept constant over all water depths, so that it could be compared to previous 1-D HEC-RAS models, which also had constant roughness values. The values used in the 1-D model were not available to check, so instead a sensitivity analysis was done on Manning's roughness values (see the 'Results'

section). When creating an independent model, if the stream has larger streambed substrate, it may be beneficial to add a rating curve for the relative roughness values, so that the roughness values change with water depth.

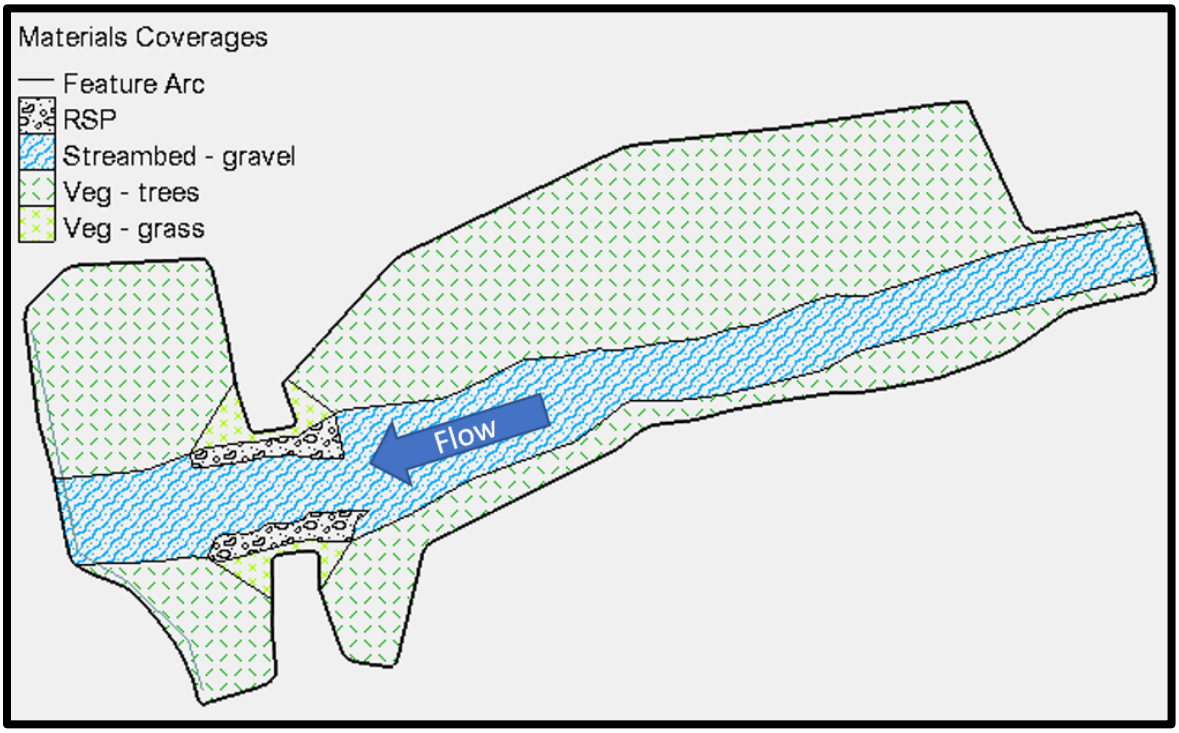

Figure 16. Materials coverage map to specify Manning's roughness values for Little Mill Creek model.

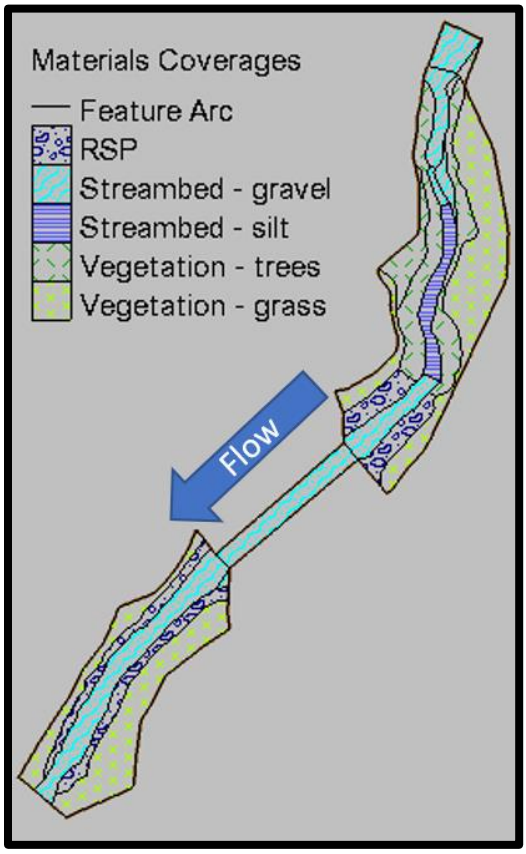

Figure 17. Materials coverages map to specify Manning's roughness values for North Fork Ryan Creek model.

Table 10. Materials coverages with associated Manning's roughness (n) values.

Material	**Manning's roughness, n**
RSP	0.050
Streambed – gravel	0.045
Streambed – silt	0.035
Vegetation – trees	0.060
Vegetation – grass	0.030

Monitor coverage

The monitor coverage consists of lines/arcs and points defining locations within the model domain to monitor fluxes (flow) and point values (e.g. WSE), respectively. The monitor lines and points are drawn manually in areas of interest within the model

domain. Monitor lines were created at the inlet and outlet boundaries of the model to verify the flow is consistent at the inlet and outlet. Monitor point locations were included in both site models at the crossing structure to check the WSE. The monitor lines and points are displayed in the simulation run window and updated during run time.

Running simulations

A simulation is created for specific flow conditions, and a unique set of the mesh, boundary conditions, materials coverage, and monitor coverage. The model control then needs to be set by indicating the time step and the output time interval. In general, a smaller timestep becomes necessary as the number of mesh elements increases.

In the Little Mill Creek model, there are 38,014 mesh elements with the vertices distributed 1.8 feet apart in the main channel and approximately 5 feet apart on the floodplain. The model time step used for this number of elements is 0.1 seconds over a simulated time period of 0.5 hours. The model stabilizes before the end of the simulated 0.5-hour time period, so it could be reduced to lower the total run time, which varied between 15 and 30 minutes for the final models (see Figure 64 for model computation run times in relation to number of mesh elements). The run time would be reduced by approximately the fraction of time that the simulation time period is reduced by. In the North Fork Ryan model, when the vertices were distributed to 0.75 feet at the channel and 2.0 feet at the edge of the floodplain, there were approximately 54,277 mesh elements. A simulation time step of 0.1 seconds became necessary to stabilize the model

and achieve residuals of zero. The model stabilizes at about 0.08 hours, so this simulation time period could also be reduced from 0.5 hours (Figure 18).

The model stability can be determined from the inlet and outlet flows, the mass residual value, and the stability of both flows and residuals. The inlet and outlet flows should be equal, preserving continuity; the mass residual value should be approximately zero; and timeseries plots of flow and mass residuals should show stable convergence (Figure 18 and Figure 19). If the mass residual is not reaching zero, the mass residual can often be lowered by reducing the model control simulation time step.

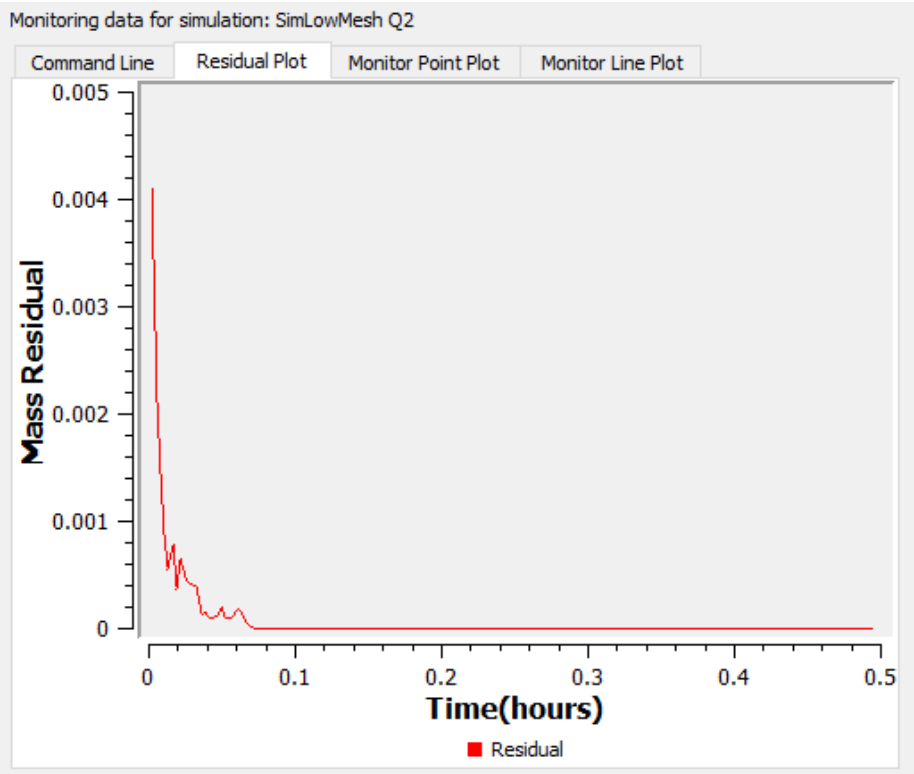

Figure 18. Model residual plot stable at zero at about 0.08 hours into the simulation. North Fork Ryan Q2 used as an example.

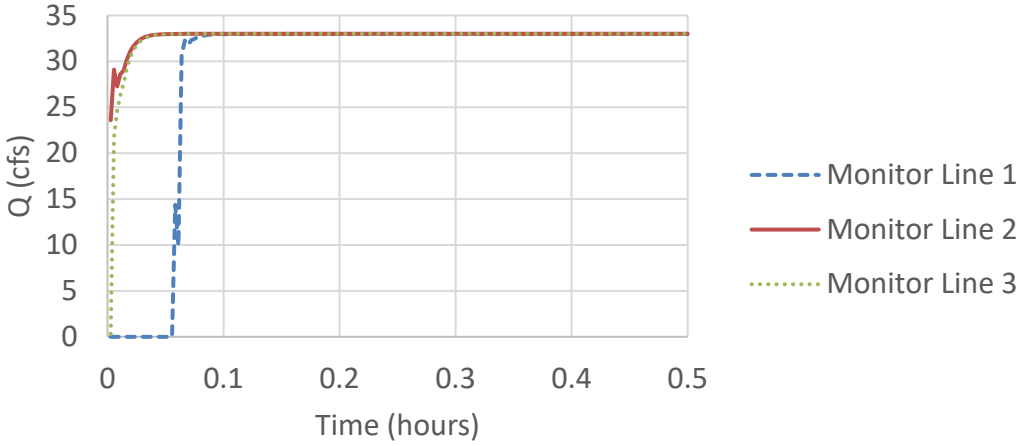

Figure 19. Monitor line plot with Arc1 near the inlet and Arc3 near the outlet boundary conditions, with stable flows at the same value. North Fork Ryan at Q2 used as an example.

Exporting results

General information from each model, like model average, maximum, and minimum of results, was taken from the model information (in the right-click menu). Observation arcs were used to export water depth, water surface elevation, bed elevation, and velocity data at specific cross-sections. Averages of velocity over cross-sections were calculated by dividing the discharge by the flow area through the cross-section. Average depths at the cross-sections were acquired by redistributing the vertices to be equidistant on the observation arcs used to export the data points and taking the average of the data.

The water depth, velocity, and shear stress result contour maps were taken at the same timestep. For the water depth figures, the results had to be filtered to remove water depths less than zero. In the Manning's roughness sensitivity analysis, when taking differences between base run and sensitivity run results, the velocity and filtered water

depth results were sampled at the end timestep and individually differenced between the correlated base and sensitivity run results.

Additional Analyses

Scour analysis

Abutment scour is calculated for the Little Mill Creek Bridge abutments using the methods described in Section 8.6.3 NCHRP 24-20 Abutment Scour Approach of the document '*Evaluating Scour at Bridges, Fifth Edition*' (Arneson et al., 2012). The abutment scour computed from the NCHRP approach is total scour at the abutment; it is not added to contraction scour because it already includes contraction scour. The abutment scour computed from the NCHRP approach accounts for contraction scour and is the total scour at the abutment. The contraction scour depth, as part of the NCHRP approach, is calculated using flow depths and unit discharges in Equation 1 (Equation 8.5, Arneson et al., 2012). With 2-D model results available, the unit discharge is obtained by multiplying the velocity and water depth at the abutments or embankment covering the abutment at the water's edge. When 1-D model results are available additional steps are required to determine suitable unit discharges, including determining the setback ratio (ratio of the setback length, or distance from edge of main channel to toe of abutment, to channel flow depth) of each abutment and determining which velocity and flow area to use.

$$y_c = y_1 \left(\frac{q_{2c}}{q_1}\right)^{6/7} \quad (1)$$

y_c = Flow depth including live-bed contraction scour (ft)

y_1 = Upstream flow depth (ft)

q_{2c} = Unit discharge in the constricted opening accounting for non-uniform flow distribution (ft^2/s)

q_1 = Upstream unit discharge (ft^2/s)

The flow depth accounting for live-bed contraction scour (y_c) is then multiplied by a scour amplification factor determined in Figure 8.9 (live-bed, spill-through abutment) or Figure 8.10 (live-bed, wingwall abutment) to get the maximum flow depth (y_{max}), as shown in Equation 2 (Equation 8.3, Arneson et al., 2012). The scour depth is calculated by subtracting the original flow depth by the maximum flow depth resulting from abutment scour, as shown in Equation 3 (Equation 8.4, Arneson et al., 2012).

$$y_{max} = \propto_A y_c \quad (2)$$

$$y_s = y_{max} - y_0 \quad (3)$$

$y_{\max}$ = Maximum flow depth resulting from abutment scour (ft)

$\propto_A$ = Scour amplification factor for live-bed conditions

y_c = Flow depth including live-bed contraction scour (ft)

y_s = Abutment scour depth (ft)

y_0 = Flow depth prior to scour (ft)

For North Fork Ryan Creek, scour on the streambed is estimated with two methods: using abutment scour calculations to determine scour depth and by analyzing bed stability of the channel material and channel protection installed under the channel material. The channel material was excavated at the beginning of construction and mixed into the engineered streambed material. The size gradations of the streambed material and the streambed sub-layer were estimated using the material quantities and standard rock sizes. Abutment scour is calculated using the methods described above and Equations 1 through 3 but using Figure 8.10 in '*Evaluating Scour at Bridges, Fifth Edition*' to determine the scour amplification factor (Arneson et al., 2012). Bed material sizing methods used are from Section 5.5.5 Bed Material Sizing of Caltrans' '*Fish Passage Design for Road Crossings Manual'* (Caltrans et al., 2007). Either the Modified Shields method or the Critical Unit Discharge method are used, depending on bed particle size, bed particle gradation, and bed slope. The Modified Shields method was applicable for Little Mill Creek using Equations 5 and 6. Both the Modified Shields and Critical Unit Discharge methods require grain size distribution, so an alternative critical shear stress analysis was done on North Fork Ryan Creek, since pebble counts were not done at this site.

$$\tau_c = \gamma R_c S_e \tag{5}$$

$$\tau_{c-D84} = 102.6\tau_{D50} D_{84}^{0.3} D_{50}^{0.7} \tag{6}$$

Parameters: Bed slope < 5%

$R_c/D_{84} > 5$ (D_{84} in feet)

$D_{84}/D_{50} < 25$

Bed particle range between 0.39" – 9.75"

τ_c = Driving Force: Boundary Shear Stress (psf)

γ = Unit weight of water (lb/cu.ft.)

R_c = Hydraulic Radius (ft)

S_e = Energy slope or bed slope (ft/ft)

D_{84} = 84^{th} percentile particle size (ft)

D_{50} = 50^{th} percentile particle size (ft)

τ_{c-D84} = Critical shear to entrain D_{84} particle (psf)

τ_{D50} = Shields Parameter to entrain D_{50} particle (dimensionless)

Scour potential at RSP is calculated indirectly by sizing RSP material using the methods of Section 5 California Layered RSP Design Method in Caltrans' '*California Bank and Shore RSP Design Guide*' (Racin et al., 2000). Water velocity, specific gravity of rock, and bank slope are used in Equation 7 (Equation 1, Racin et al., 2000). If only the average channel velocity is known, as would be the case with 1-D model results, the velocity is multiplied by a factor based on flow orientation. If 2-D results are available, the channel velocity at the toe of the RSP can be used directly in the following equation.

$$W = \frac{0.00002\, v^6\, SG}{(SG-1)^3 \sin^3(r-a)} \tag{7}$$

W = theoretical minimum rock weight which resists forces of flowing water and remains stable on slope of stream bank (lbs)

v = Velocity to which bank is exposed (fps)
- for parallel flow multiply average channel velocity by 0.67
- for impinging flow multiply average channel velocity by 1.33

SG = Specific gravity of rock (2.65 for granite)

r = 70 degree, constant

a = Outside slope face angle with horizontal (degrees)

Based on the minimum rock weight, the outer-layer RSP size is chosen from Table 5-1 in the '*California Bank and Shore RSP Design Guide*' (Racin et al., 2000). If the minimum rock weight calculated falls on a standard weight, the rock size should be chosen from the next weight up to be conservative. Further analysis of size gradation is done when designing RSP, but for the purpose of comparing RSP design in this project, the size of the outer layer of RSP is used. The RSP sizes calculated using the 2D model results are then compared to the sites' RSP design specifications. The RSP sizes determined in the results and discussion within this report are given in the old standard sizes in order to compare with the installed RSP sizes. The Caltrans standards for RSP sizes were changed in the *Highway Design Manual* in 2016 to a modified version of the Hydraulic Engineering Circular (HEC) 23 gradations (Caltrans, 2020; Craggs, 2016)(see new standards in Appendix D).

Rock weirs are also analyzed for stability using a critical shear stress analysis using Equation 8 (Equation 7.3, Lagasse et al., 2012; Equation E.4, USFS Stream

Simulation Working Group, 2008). The critical shear stress is compared to bed shear stress from the model results, to determine if the analyzed particle sizes are stable.

$$\tau_c = (\gamma_s - \gamma_f)\tau^* D_{50} \quad (8)$$

$$\tau_c = 102.6\ \tau^* D_{50}$$

τ_c = Critical shear stress for initial particle motion (lb/ft2)

τ^* = Shields parameter, ranges from 0.03 to 0.10 (0.054 for any size of 128 mm, from Table E.1 in Appendix E of USFS 2008)

γ_s = Specific weight of sediment (165 lb/ft3)

γ_f = Specific weight of fluid (62.4 lb/ft3)

D_{50} = Particle size diameter (ft)

RESULTS

Caltrans' 1-D Model Results

One-dimensional (1-D) hydraulic HEC-RAS models were used in the Caltrans design analyses for the current installed structures. The 1-D hydraulic models were not available for either of the projects, so the 1-D model results summarized and presented in the final project reports were used for comparison with 2-D model results from this analysis. Both the 1-D and 2-D models were not calibrated to depth and velocities observed at the project sites.

Little Mill Creek – North Bank Road

Caltrans Structures Hydraulics and Hydrology engineers completed the hydraulic analysis for Little Mill Creek bridge using HEC-RAS 1-D in 2016 (Caltrans, 2016). The bridge was designed to replace a 14-foot diameter SSPP culvert that was thought to be damaged by bedload and had created sinkholes in the overlying roadway. The hydraulic analyses were completed for the 10-, 50-, and 100-year return period flows in Little Mill Creek without considering backwater effects of the Smith River. Additional simulations were also conducted using the 25-year return period flow coinciding with a 100-year backwater event in the Smith River and the 100-year return period flow with a Smith River 25-year backwater event (Table 11). The likely combinations for coincident flows of the Smith River and Little Mill Creek were determined by Caltrans using the NCHRP Report "Estimating Joint Probabilities of Design Coincident Flows at Stream

Confluences" (Caltrans, 2016). The Smith River water elevation can backwater the channel through the Little Mill Creek bridge during coincident high return period flows in both channels. With the addition of backwater from Smith River water surface elevations, the velocities decrease and the water depths rise at Little Mill Creek Bridge. For a Little Mill Creek 100-year flow, the addition of backwater from a Smith River 25-year water surface elevation increases elevation by 5.25 feet from 36.75 feet to 42 feet (Table 11). The increase in water depth results in a decrease in velocity of 8.45 feet per second.

Table 11. Little Mill Creek bridge design hydraulic modeling results for the 10-, 50-, and 100-year return period flows and the 25-year return period flow with a Smith River 100-year backwater event and the 100-year return period flow with a Smith River 25-year backwater event. Results for under the bridge include velocity, depth, water surface elevation, and freeboard (based on a soffit elevation of 47.78 feet) (adopted from Caltrans 2016).

Little Mill Creek Frequency	**Flow rate (cfs)**	**Velocity (fps)**	**Depth (ft)**	**Smith River Frequency**	**WSE (ft)**	**Freeboard (ft)**
Q10	1,143	14.62	4.46	None	35.37	12.41
Q50	1,707	14.74	5.52	None	36.43	11.35
Q100	1,955	14.95	5.84	None	36.75	11.03
Q25	1,466	2.3	16.09	Q100	47 [1]	0.78
Q100	1,955	6.5	11.09	Q25	42 [1]	5.78

[1] WSE (water surface elevations) controlled by the Smith River backwater elevation

In Caltrans' analysis, the predicted water depths and velocities were also used to estimate scour at Little Mill Creek Bridge. Scour depths in the Caltrans' Little Mill Creek analysis used the equations in "*Evaluating Scour at Bridges*" Section 8.6.3 "NCHRP 24-20 Abutment Scour Approach" (Arneson et al., 2012). The short term (local) and long-

term (degradation and contraction) scour depths were estimated as zero in this previous analysis (Caltrans, 2016).

North Fork Ryan Creek – HWY 101

Caltrans engineers developed a 1-D HEC-RAS model of North Fork Ryan Creek, which was included in a project report completed by AECOM in 2014 (AECOM, 2014). The new culvert was designed to meet fish passage and peak flow conveyance standards. The installation of the 12-foot by 10-foot reinforced concrete box (RCB) culvert decreased the headwater depth created by the undersized culvert, a 5-foot diameter CMP, and eliminated the 4.5-foot drop at the previous outlet. Rock weirs were installed to re-establish the stream gradient. Water depths at rock weirs were modeled using broad-crested weir flow. Additionally, the structure was found to have "more than adequate freeboard during peak flow events" reducing the headwater depths at high flows (AECOM, 2014).

Caltrans' 1-D HEC-RAS model could not be attained and there are limited quantitative results in the final project report by AECOM (2014). The results include the ranges of the water depth and average water velocity from the 1-D HEC-RAS model results when simulating a 'high fish passage flow' of 16 cfs over the entire model, which are less applicable for comparison to this project. The report also presents the predicted velocity range at the rock weirs when simulating a 100-year flow in the HEC-RAS 1-D model. The predicted velocity range at the rock weirs during the 100-year flow event is 1.5 to 6.9 feet per second (AECOM, 2014). The 100-year flows were also used for the

design of bank RSP and rock weir boulder sizes. The final hydraulic report for the current design at North Fork Ryan Creek states that 10-year and 100-year flow events were modeled in the HEC-RAS 1-D model and the proposed culvert design met criteria for both these flow events (AECOM, 2014). The culvert design criteria stated in the report include: (1) accommodate the 10-year flow without causing the headwater elevation to rise above the crown of the culvert; and (2) accommodate the 100-year flow without causing headwater to rise above an elevation that would cause objectionable backwater depths or outlet velocities (AECOM, 2014).

In the Caltrans hydraulic report, there is also a HEC-RAS 1-D water surface profile of North Fork Ryan Creek for the 10-year and 100-year simulated flows, from which water surface elevations were extracted (see Appendix C.4). In the Caltrans HEC-RAS 1-D model results, the water depth during the 100-year flow at the culvert inlet is predicted to be approximately 4.2 feet, while the depth through the culvert is predicted to be approximately 3.5 feet. The RCB culvert in North Fork Ryan Creek was designed to be countersunk 24 inches, which is 20 percent of the RCB culvert height, leaving 8 feet of available head. During a preliminary site visit on September 12, 2019, the height from the top of the culvert opening to substrate was approximately 6.8 feet at the upstream inlet opening and 7.5 feet at the downstream outlet opening.

2-D Model Results

The two-dimensional hydraulic model results at the 2-, 10-, 25-, 50-, and 100-year return period flows for Little Mill Creek and North Fork Ryan Creek are presented in this

section. Results include velocity, water depth, shear stress, and accompanying interpretations relating to scour, deposition, and flow conveyance. Special attention is paid to conditions and locations in the project area with clear 2-D flow behavior that would not be identified by a 1-D model.

Little Mill Creek – North Bank Road (Highway 197)

Results of the Little Mill Creek model simulations focus on three key sections of the stream: reference reach, upstream debris, and crossing (Figure 20). The reference reach is a stretch of Little Mill Creek that was untouched by the bridge crossing construction and is upstream of the hydraulic and geomorphic influences of the existing and previous crossings. The reference reach serves as a baseline for comparing crossing conditions to the natural stream channel. The upstream debris area is located at a slope break in the stream, which combined with the large woody debris, affect the streamflow depths and velocities. The conditions at the crossing are of primary interest to determine the stability of the crossing structure during high flow events and the evaluation of the water depth and velocity conditions through the crossing design. Results are presented as water depth contour maps overlain by velocity vectors. The 2-year and 25-year return period flows are presented, along with the 25-year flow with a Smith River 100-year backwater event and the 100-year flow with a Smith River 25-year backwater event. Additional figures showing water depths, velocities, and shear stress for the simulated flows can be found in Appendix C.1.

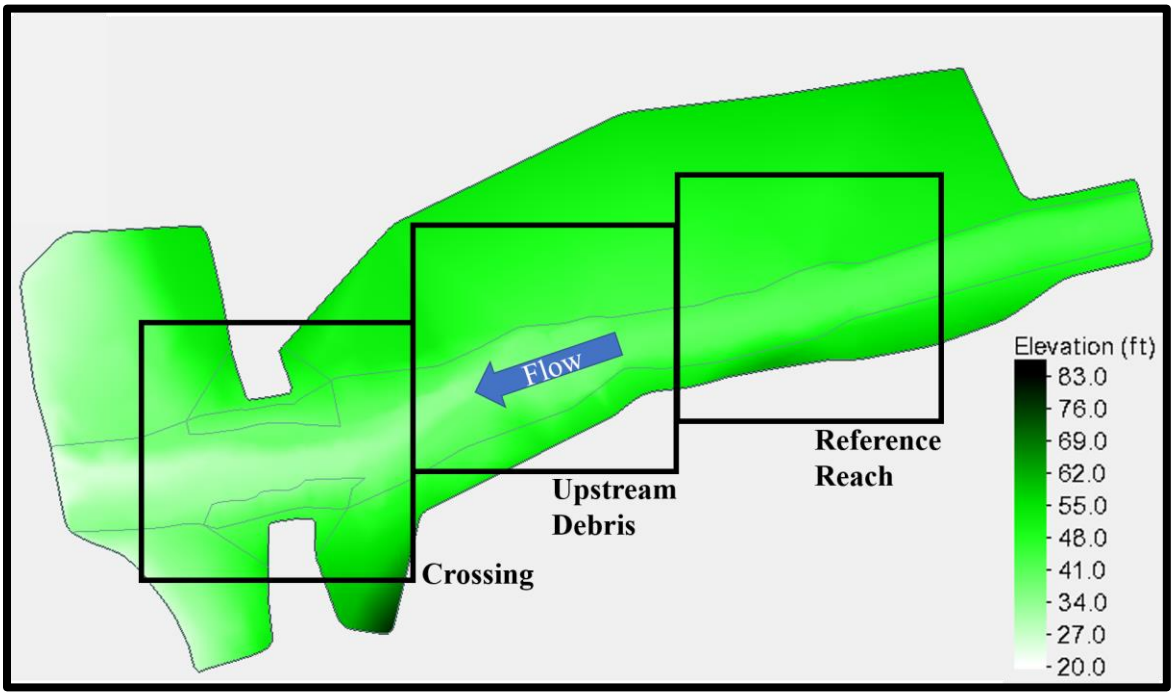

Figure 20. Plan view of Little Mill Creek model domain with elevation contours in feet. The labeled squares indicate the locations for key figures included throughout the following section.

Maximum water depth, velocity, and shear stress predicted within the model domain occur at the confluence of Little Mill Creek with the Smith River. Results at the confluence are not pertinent to the analysis of conditions at the bridge site itself, so the maximum ranges of water depth, velocity, and shear stress predicted at the confluence are not presented.

Within the Little Mill Creek model domain, the highest velocities moving from upstream to downstream are predicted at four distinct locations: the slope break upstream of the woody debris, downstream of the woody debris, upstream of the crossing, and at the confluence with the Smith River (Figure 21). The velocities are diminished when greater water depths occur due to inclusion of the Smith River backwater events (Figure

22, Figure 23). The Smith River right bank at the downstream end of the model and the Little Mill Creek right bank floodplain terrace experience the largest change in inundation when the Smith River backwater elevations are included in the simulation. Eddies form on the floodplains of Little Mill Creek and the Smith River (downstream section of Little Mill Creek model), as well as next to the right bank bridge abutment (Figure 22).

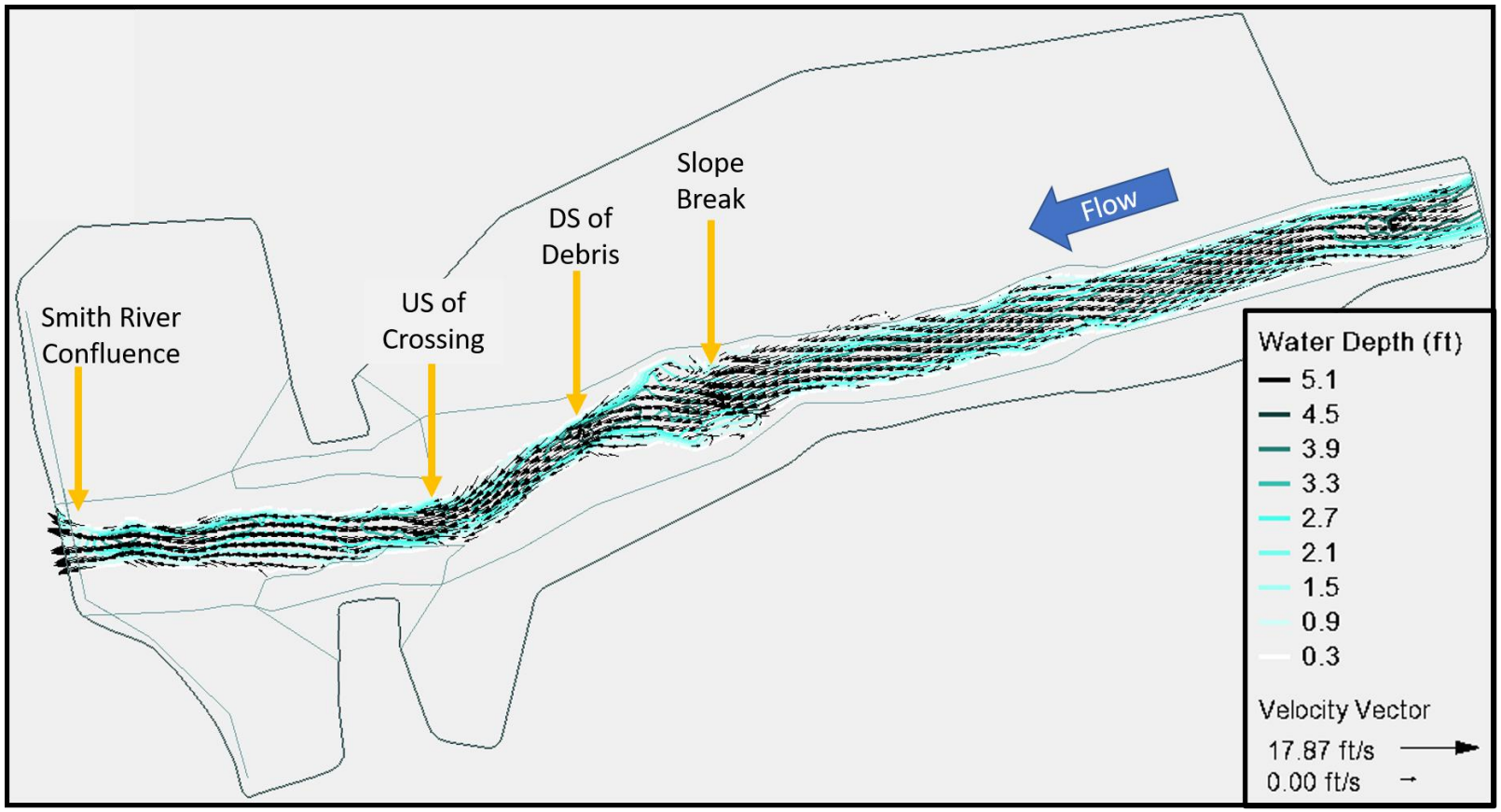

Figure 21. Plan view of Little Mill Creek full model domain with water depth contours (feet) and velocity vectors (feet per second) for the 2-year return period flow of 529 cfs.

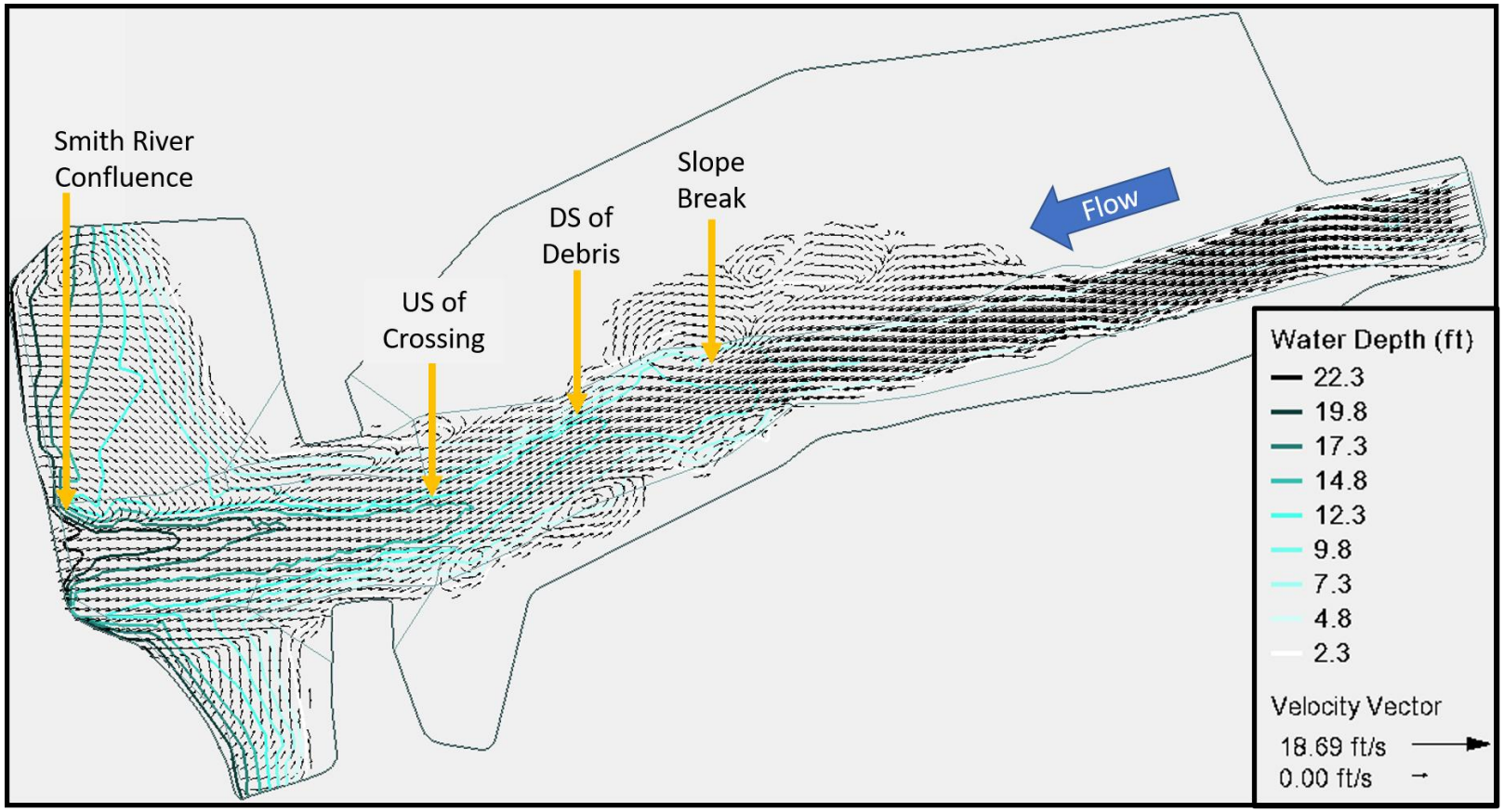

Figure 22. Plan view of Little Mill Creek full model domain with water depth contours (feet) and velocity vectors (feet per second) for the 25-year return period flow of 1,466 cfs with a Smith River 100-year backwater elevation of 47 feet.

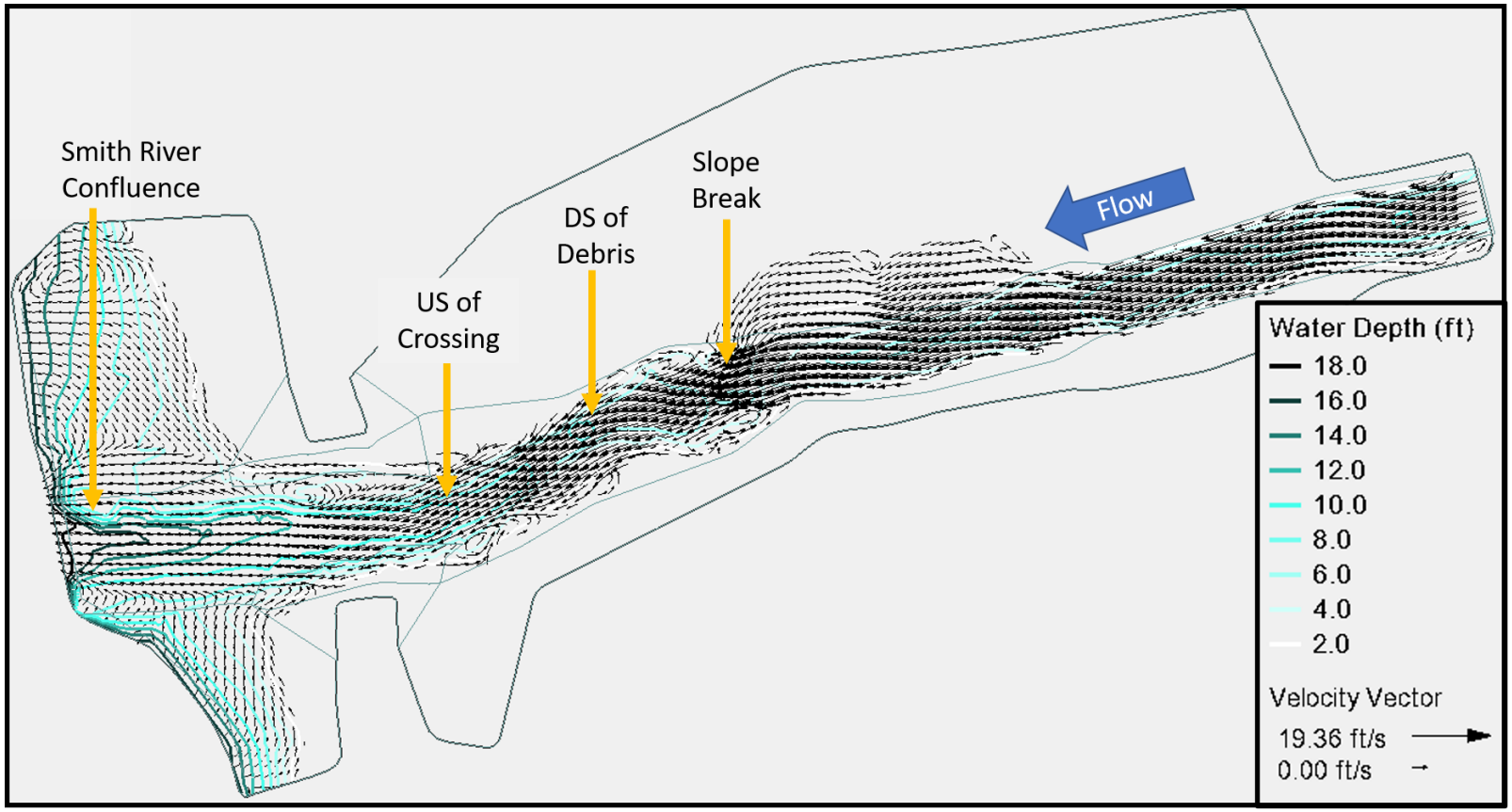

Figure 23. Plan view of Little Mill Creek full model domain with water depth contours (feet) and velocity vectors (feet per second) for the 100-year return period flow of 1,955 cfs with a Smith River 25-year backwater elevation of 42 feet.

Reference reach region results

In the reference reach, flow is confined in an incised channel by steep slopes on both the left and right banks. The left bank continues upward as a steep slope with dense vegetation. The right bank transitions to a terrace approximately 45 feet wide with dense vegetation. The reference reach cross-section indicated in Figure 24 is located on XS 5 of the survey data (survey data shown in Figure 10). The reference reach XS 5 is located approximately 380 feet upstream of Little Mill Creek bridge.

The flow simulations for the 2-year and 25-year flows, as well as the 25-year flow with a 100-year Smith River backwater and the 100-year flow with a 25-year Smith River backwater, are presented in the following results. The channel width, water depth, and velocity results for these flow events are presented in Table 12. At the 2-year return period flow of 529 cfs, the flow remains within the steep slopes on the left and right banks (Figure 24). A similar pattern is predicted during the 25-year return period flow of 1,466 cfs (Figure 25). During the 25-year flow of 1,466 cfs with a Smith River 100-year backwater elevation of 47 feet, the flow in the reference reach remains within the steep slopes on the left and right banks, but flows onto the floodplain terrace immediately downstream of XS 5 (Figure 26). During the 100-year flow of 1,955 cfs with a Smith River 25-year backwater elevation of 42 feet, the flow remains bounded by steep slopes on the left and right banks, but also overtops the banks immediately downstream of the cross-section (Figure 27).

Table 12. Wetted channel width, water depth, and velocity results at XS5 in the reference reach for the following flows: 2-year; 25-year, 25-year with Smith River 100-year backwater; 100-year with Smith River 25-year backwater.

Flow simulation	Wetted channel width (ft)	Avg. Water Depth (ft)	Max Water Depth (ft)	Avg. Velocity (fps)	Max Velocity (fps)
2-year	30.8	2.3	3.8	6.1	7.3
25-year	36.1	3.7	5.9	9.2	10.7
25-year with Smith River 100-year	36.1	3.9	6.1	8.9	10.3
100-year with Smith River 25-year	37.5	4.2	6.6	10.6	12.2

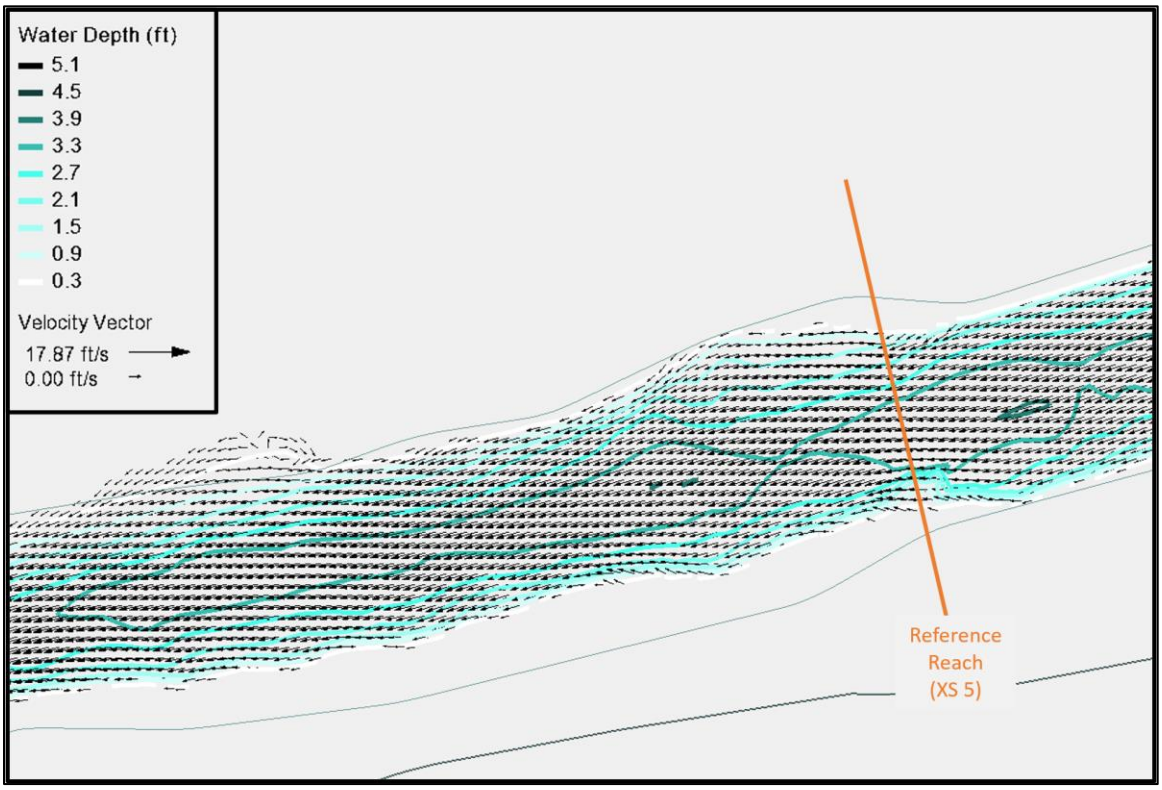

Figure 24. Plan view of reference reach location in Little Mill Creek with water depth contours (feet) and velocity vectors (feet per second) for the 2-year return period flow of 529 cfs.

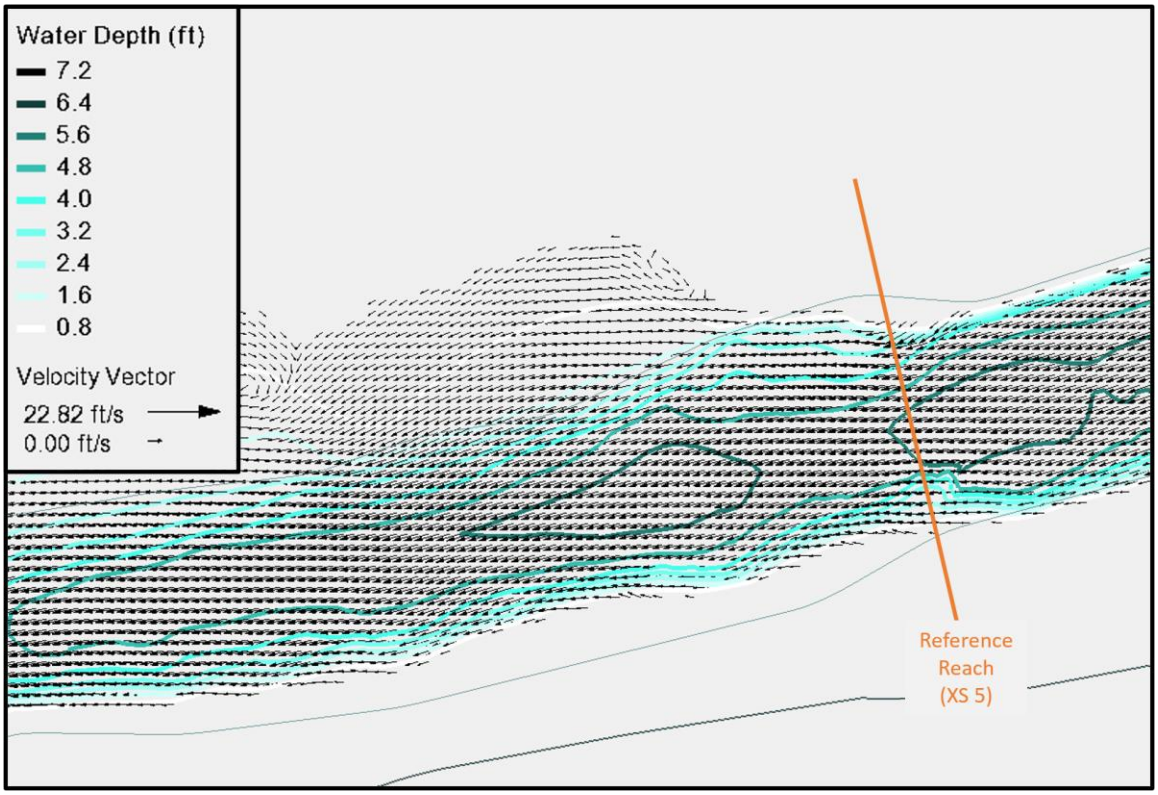

Figure 25. Plan view of reference reach location in Little Mill Creek with water depth contours (feet) and velocity vectors (feet per second) for the 25-year return period flow of 1,466 cfs.

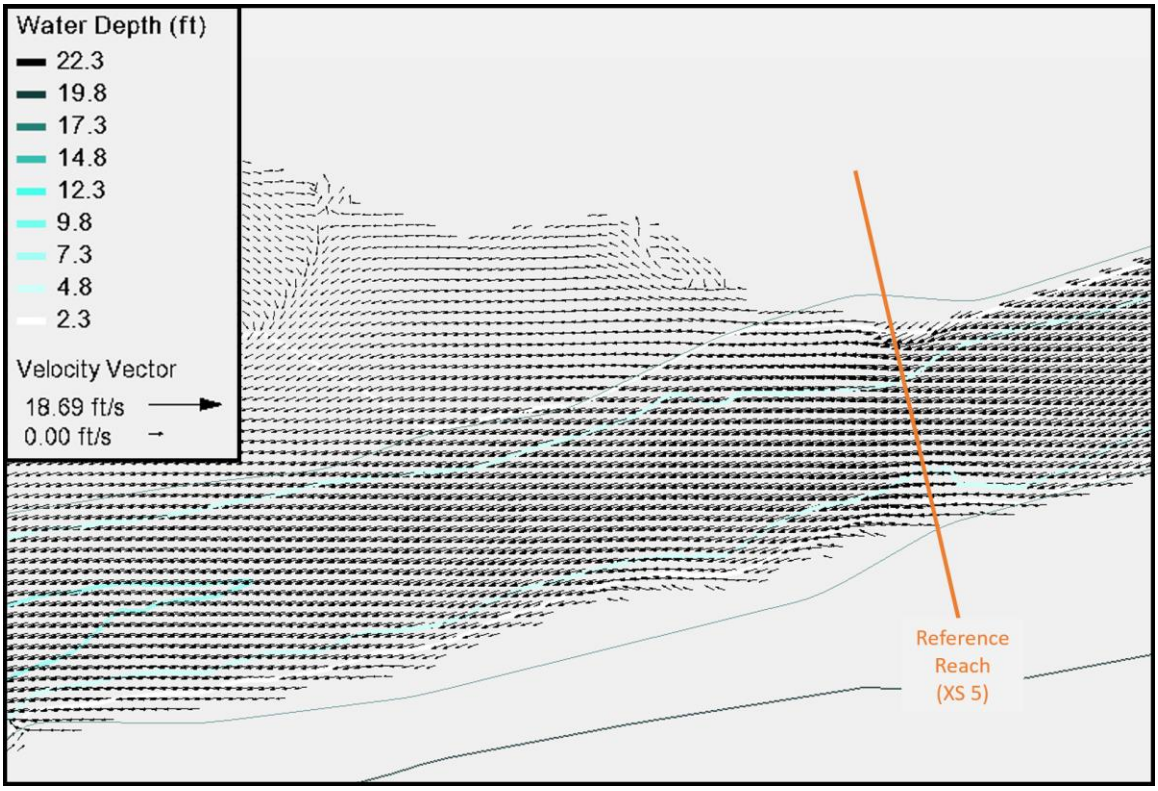

Figure 26. Plan view of reference reach location in Little Mill Creek with water depth contours (feet) and velocity vectors (feet per second) for the 25-year return period flow of 1,466 cfs and a Smith River 100-year return period backwater event with a water surface elevation of 47 feet.

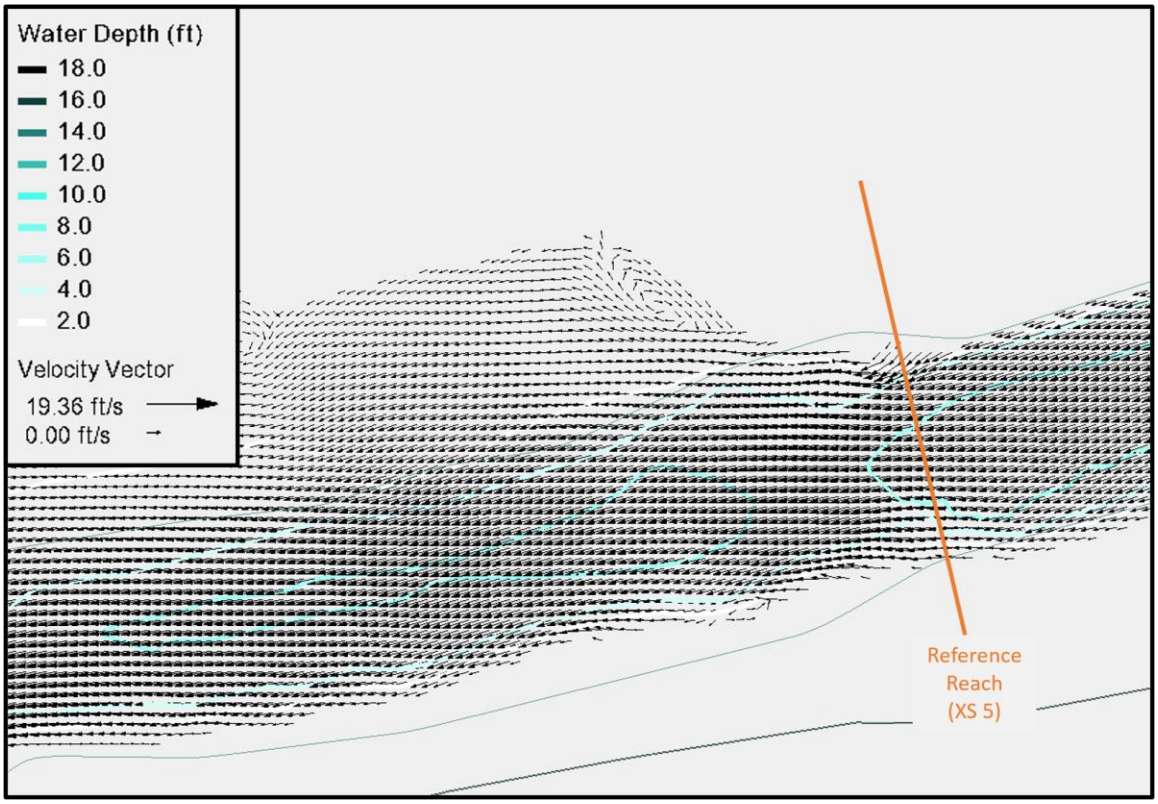

Figure 27. Plan view of reference reach location in Little Mill Creek with water depth contours (feet) and velocity vectors (feet per second) for the 100-year return period flow of 1,955 cfs and a Smith River 25-year return period backwater event with a water surface elevation of 42 feet.

The reference reach cross-section XS 5, shown in Figure 28, spans the channel from left to right bank. The channel is relatively symmetrical, with the main flow pathway in the center of the wetted channel. The maximum depth is at the same location during all flow scenarios. The influence of the Smith River is noticeable when comparing the water depths of the 25-year flow with and without a Smith River 100-year backwater event. The scenario that includes the backwater slightly increases water depth over the entire cross-section, with an increase in maximum water depth from 5.8 to 6.1 feet.

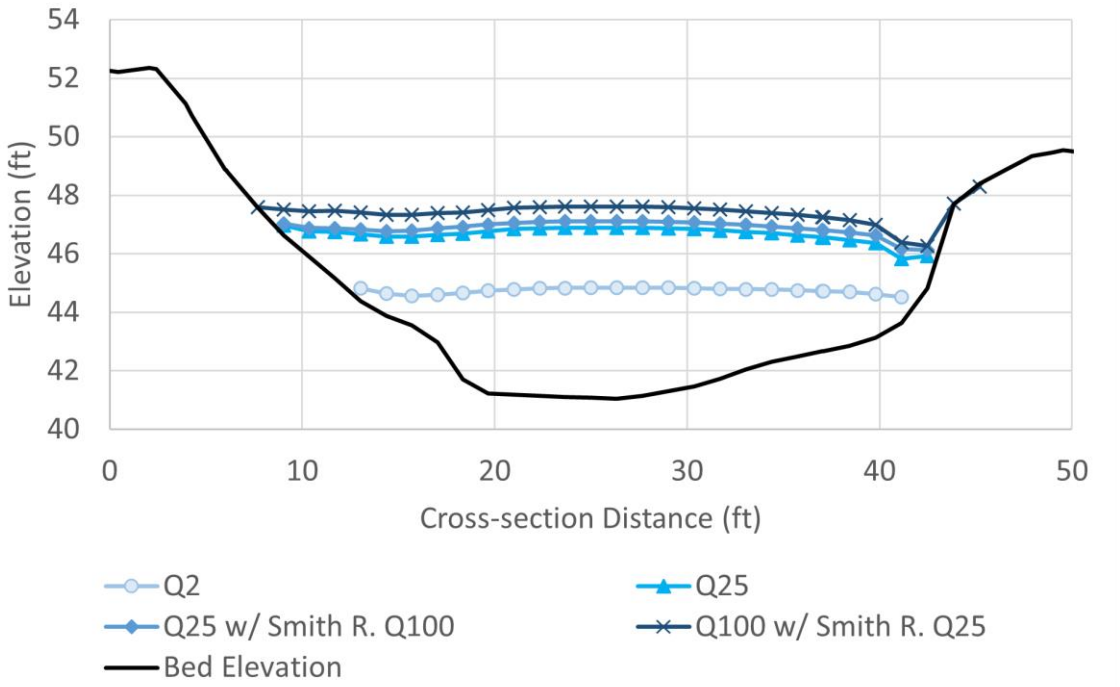

Figure 28. Little Mill Creek water surface elevations at the reference reach XS (XS5) during the 2-year flow, 25-year flow with and without a Smith River backwater 100-year event, and 100-year flow with and without a Smith River backwater 25-year event.

The velocity is distributed evenly across XS 5, with a rapid decrease in velocity moving towards each bank (Figure 29). The 100-year return period flow has the maximum velocity of the four scenarios at 15.7 feet per second. The maximum velocity during the 25-year flow decreases by 0.4 feet per second with the addition of the Smith River 100-year backwater event. The decrease in velocity is expected due to the increase in water depth shown in Figure 28 from the addition of the Smith River 100-year backwater.

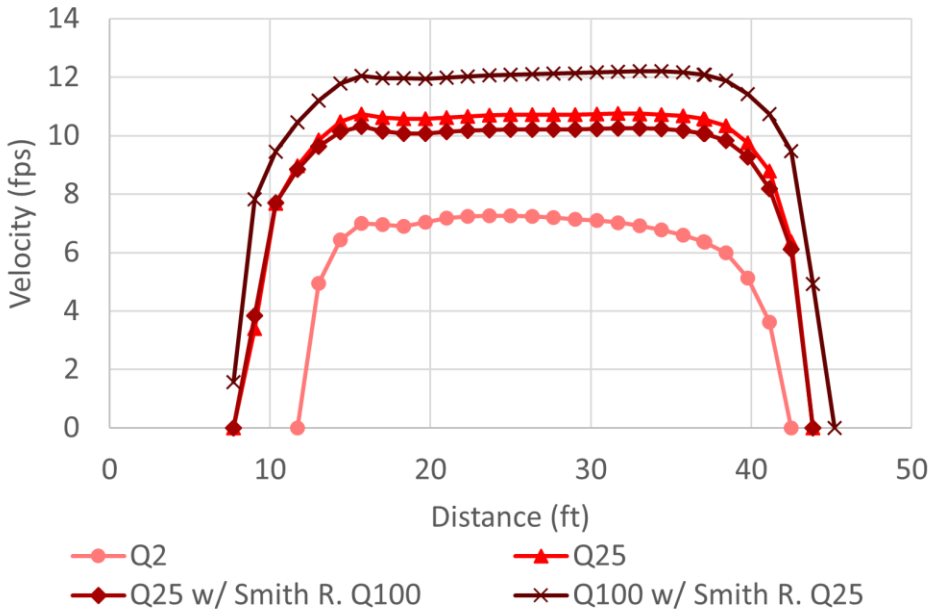

Figure 29. Little Mill Creek velocities at the reference reach XS during the 2-year flow, 25-year flow with and without a Smith River backwater 100-year event, and 100-year flow with and without a Smith River backwater 25-year event.

Upstream Debris Region Results

Flowing downstream from the reference reach, the stream reaches a slope break in a location that has accumulated large woody debris. The slope changes from 0.03 upstream to 0.05 downstream (see longitudinal profile in APPENDIX E). At the slope break, the stream channel widens and is maintained moving downstream towards the crossing. The large woody debris spans the full channel width. At flows at and below the 2-year return period flow of 529 cfs, the debris is expected to act as an obstruction to flow with water flowing under and around the debris. The 2-year flow is not modeled with the obstructions from the debris included because the effect of the debris on water depth and velocity at the crossing is assumed to be negligible. At flows larger than the

25-year return period flow of 1,466 cfs, the debris will generally be overtopped and can be simulated as increased streambed roughness. Because the debris is 170 feet upstream of the crossing, the increase in material roughness of that particular area was found to have a negligible effect on the crossing water depths and velocities (see

APPENDIX B.3 for differences in 2-D model results when an independent materials roughness value was used for the debris compared to the base case).

At the 2-year return period flow of 529 cfs, the water depths decrease and velocities increase as flow reaches the large woody debris deposited throughout the channel and the channel area expands (Figure 30). The slope break cross-section indicated in Figure 30 is 230 feet upstream of the crossing and immediately upstream of the debris. At this flow, an average water depth of 2.0 feet and average velocity of 6.6 feet per second exist on this cross-section, compared to the reference reach XS 5 with an average water depth of 2.3 feet and average velocity of 6.1 feet per second. The maximum water depth is 3.5 feet and the maximum velocity is 8.9 feet per second, which are located in the main flow pathway near the left bank (Table 13).

At the 25-year return period flow of 1,466 cfs, the flow upstream of the crossing travels through the large woody debris deposit (Figure 31). The flow is bounded by the left bank slope and extends onto the terrace on the right bank. At the channel slope break cross-section, the average water depth of 2.2 feet and the average velocity of 5.8 feet per second, compared to the conditions in the reference reach at XS 5 with an average water depth of 3.7 feet and average velocity of 9.2 feet per second.

During the 25-year flow of 1,466 cfs with a Smith River 100-year backwater elevation of 47 feet, the wetted channel extends onto the right bank floodplain and forms eddies (Figure 32). Smaller eddies also form on the left bank. The channel width at the slope break cross-section is predicted to be 90 feet compared to 66 feet during the 25-year return period flow with no backwater effect. Additionally, compared to the 25-year

flow with no backwater effect, the maximum water depth has increased by 2.1 feet while the maximum velocity has decreased by 4.4 feet per second.

During the 100-year flow of 1,955 cfs with a Smith River 25-year backwater elevation of 42 feet, the wetted channel extends into the floodplain, but few eddies are formed (Figure 33). Compared to the 25-year flow with no backwater effect, the maximum water depth has risen by 0.7 feet and the maximum velocity has increased by 0.8 feet per second.

Table 13. Summary table of wetted channel width and average and maximum depth and velocity results at Little Mill Creek upstream debris region. The flow simulations summarized are the 2-year, 25-year, 25-year with Smith River 100-year event, and 100-year with Smith River 25-year event.

Flow simulation	**Wetted channel width (ft)**	**Avg. Water Depth (ft)**	**Max Water Depth (ft)**	**Avg. Velocity (fps)**	**Max Velocity (fps)**
2-year		2.0	3.5	6.6	8.9
25-year	66	2.2	5.4	5.8	11.5
25-year with Smith River 100-year	90	3.4	7.5	2.8	7.1
100-year with Smith River 25-year	75.4	2.5	6.1	6.1	12.3 (near left bank)

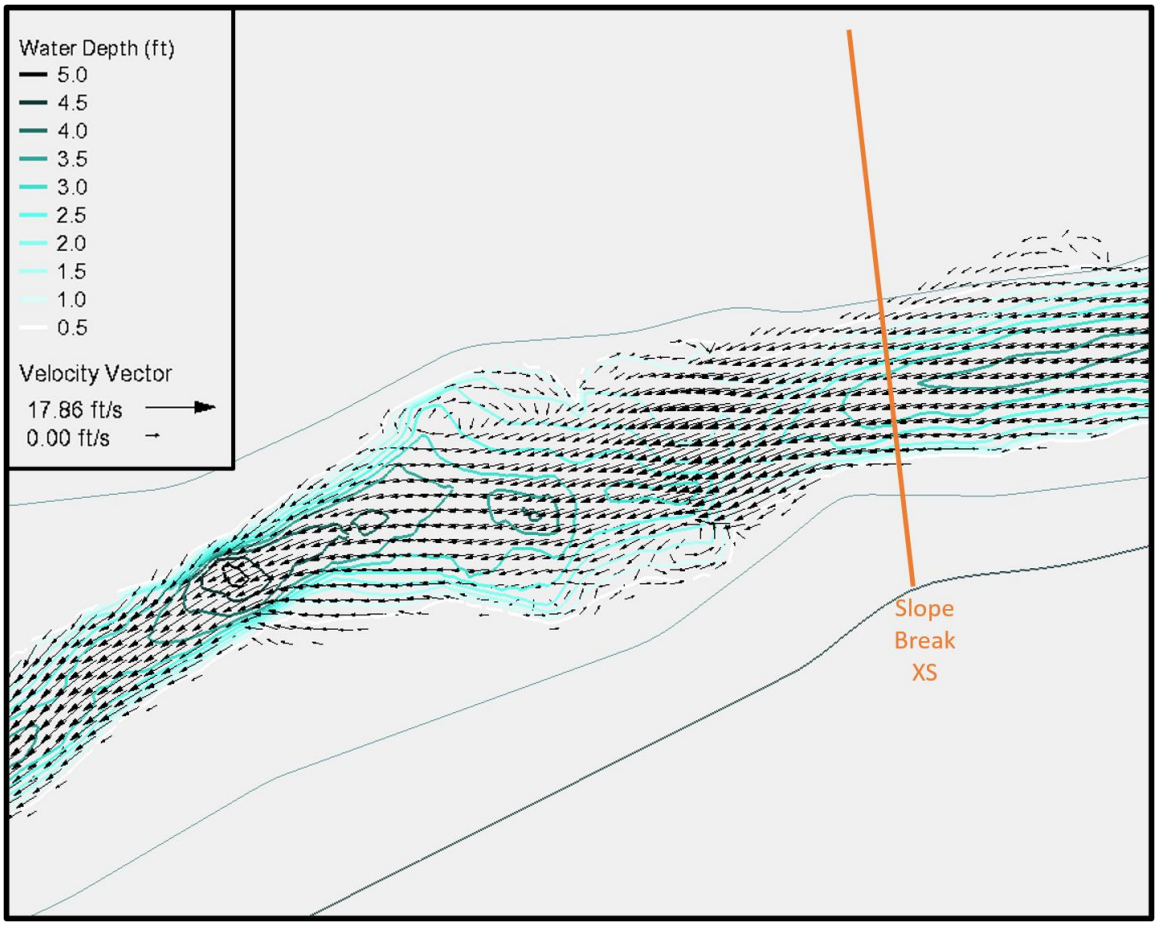

Figure 30. Plan view of upstream debris location in Little Mill Creek with water depth contours (feet) and velocity vectors (feet per second) for the 2-year return period flow of 529 cfs.

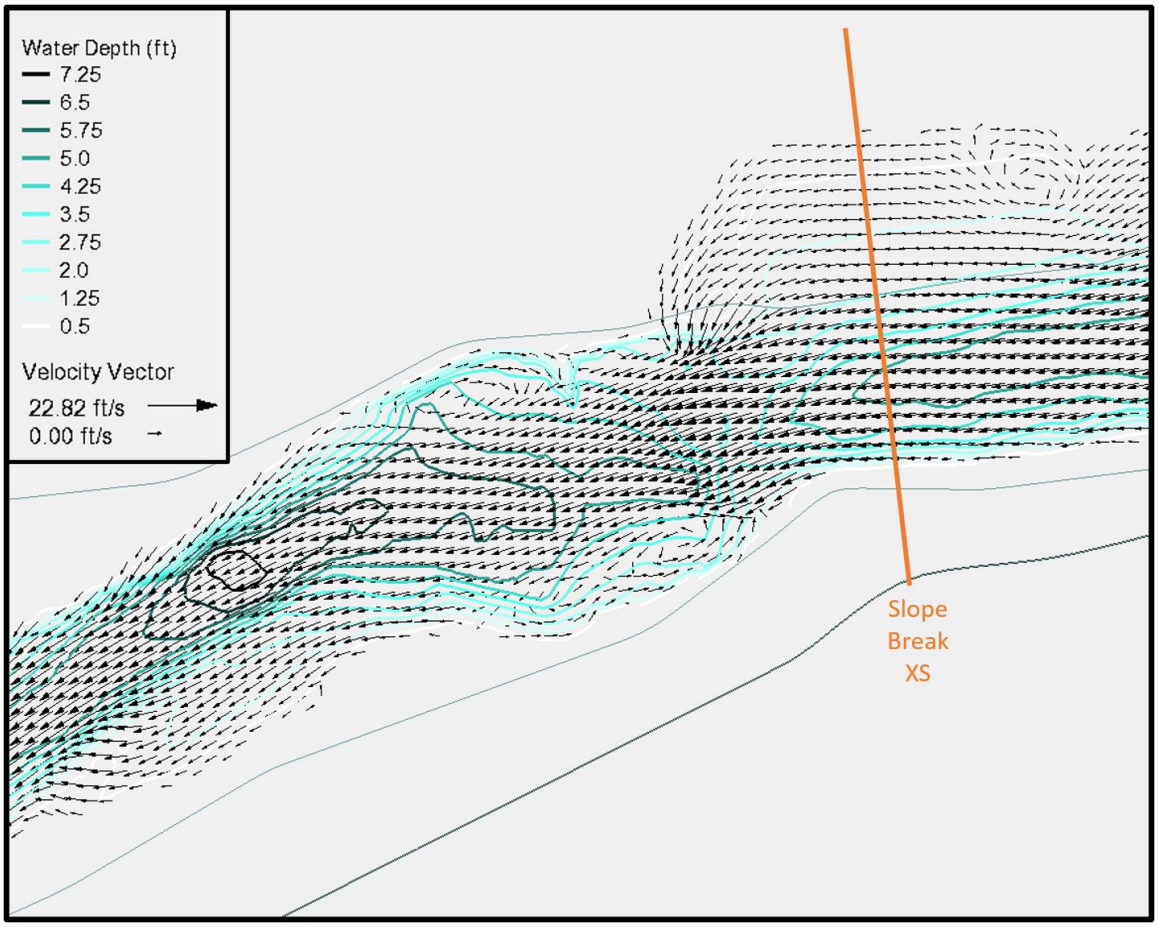

Figure 31. Plan view of upstream debris location in Little Mill Creek with water depth contours (feet) and velocity vectors (feet per second) for the 25-year return period flow of 1,466 cfs.

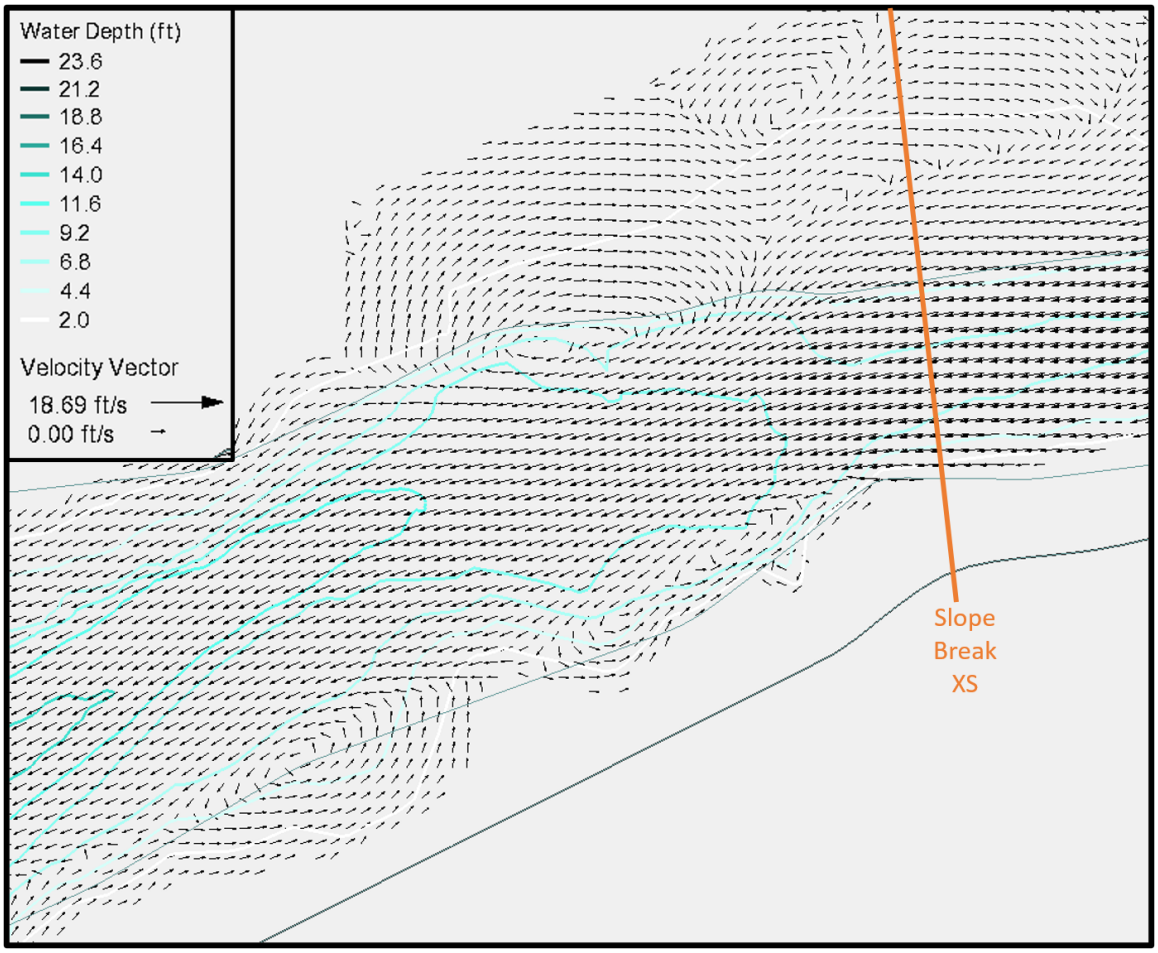

Figure 32. Plan view of upstream debris location in Little Mill Creek with water depth contours (feet) and velocity vectors (feet per second) for the 25-year return period flow of 1,466 cfs with a Smith River 100-year return period backwater event with a water elevation of 47 feet.

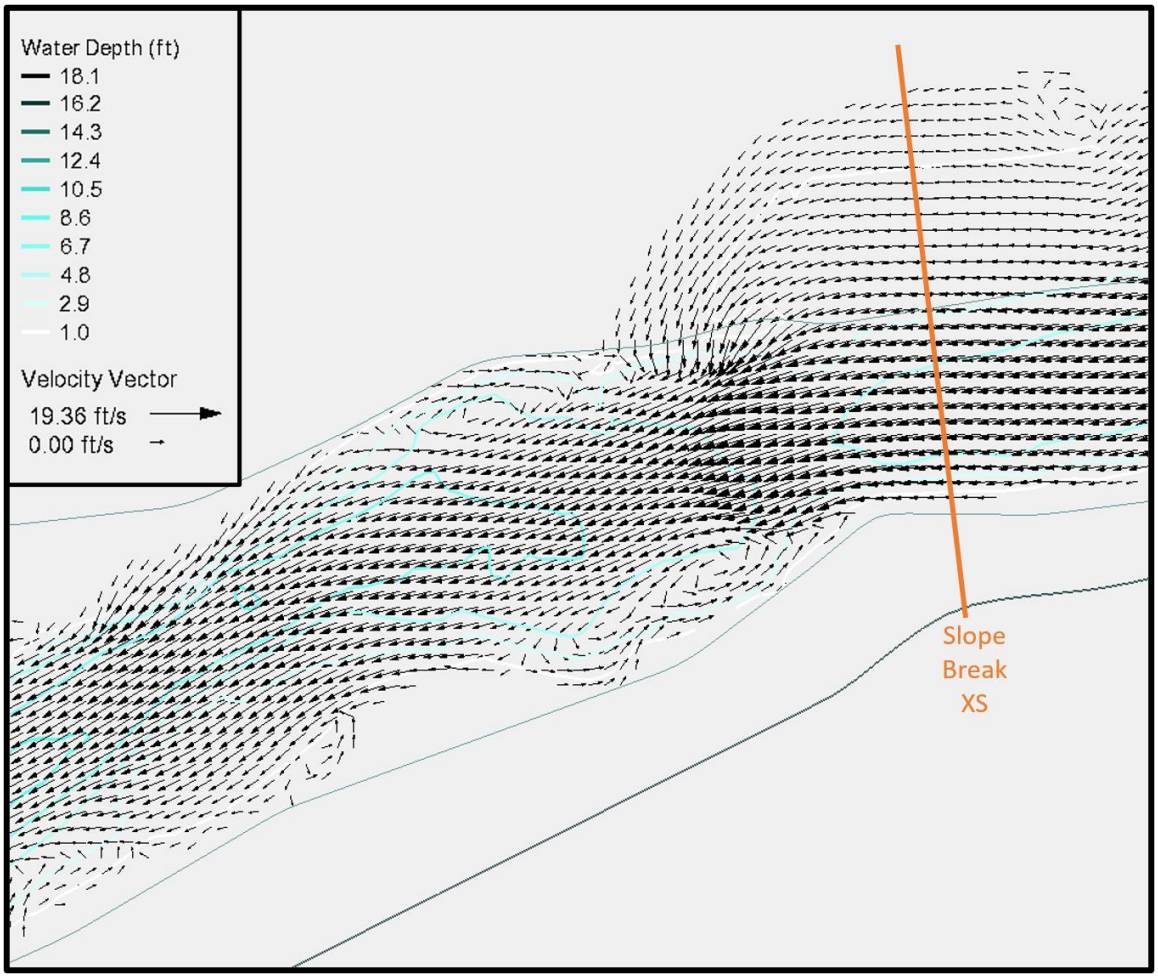

Figure 33. Plan view of upstream debris location in Little Mill Creek with water depth contours (feet) and velocity vectors (feet per second) for the 100-year return period flow of 1,955 cfs with a Smith River 25-year return period backwater event with a water elevation of 42 feet.

The slope break cross-section data shown in Figure 34 spans the channel from left to right bank. From the left bank, the water depth increases quickly for the main flow pathway, and then slowly decreases moving towards the right bank. The maximum depth is at the same location for all four flow scenarios. Little Mill Creek is influenced by the Smith River backwater at the slope break, approximately 410 feet upstream from the

confluence of Little Mill Creek with the Smith River. The 25-year flow maximum water depth increases from 5.3 feet to 7.4 feet with a Smith River 100-year backwater event.

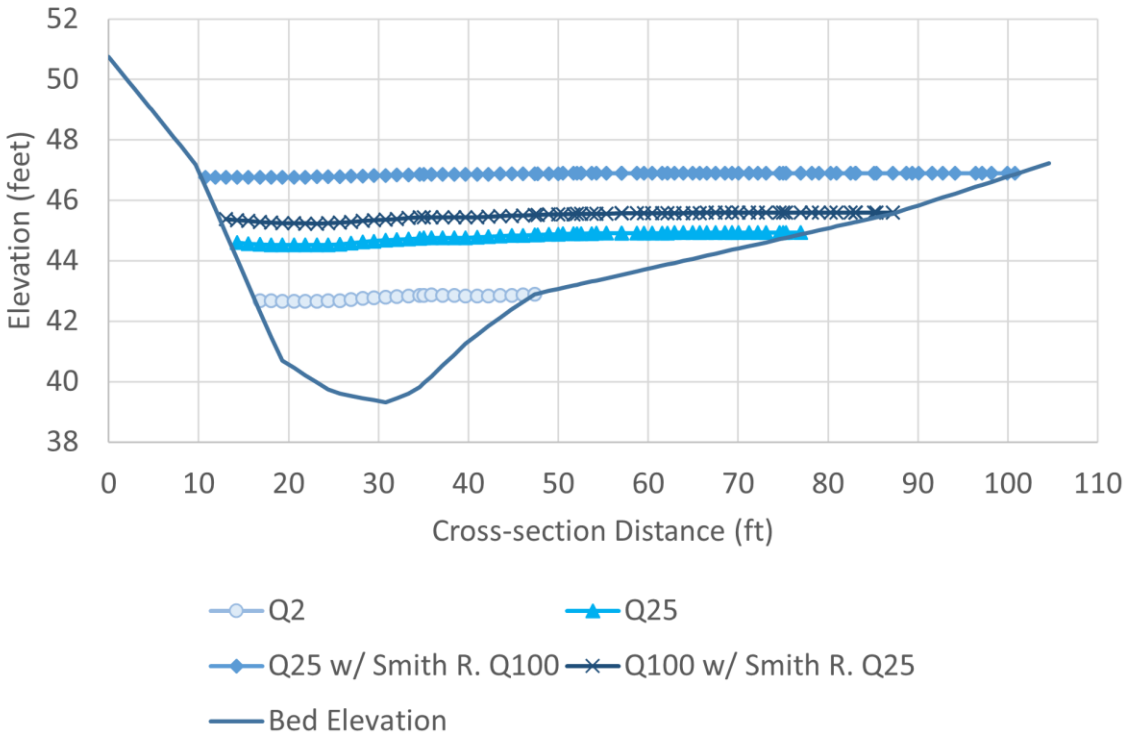

Figure 34. Little Mill Creek water surface elevations at the slope break upstream of the woody debris at the 2-year flow, 25-year flow with and without a Smith River backwater 100-year event, and 100-year flow with and without a Smith River backwater 25-year event.

The velocity distribution across the slope break cross-section has the maximum velocity on the left side of the channel (Figure 35). The 2-year and 25-year return period flows have maximum velocities of 8.8 and 11.5 feet per second, respectively. The 25-year flow with a Smith River 100-year backwater event reduces the maximum velocity at the cross-section to 5.9 feet per second and shifts the location of the maximum velocity.

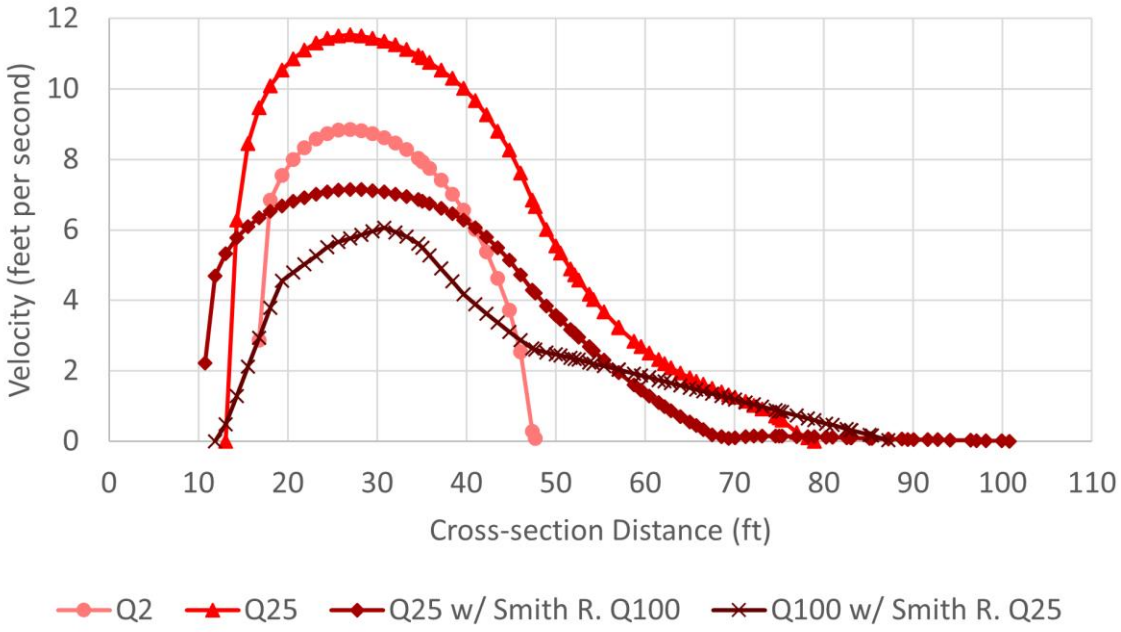

Figure 35. Little Mill Creek velocities at the slope break upstream of the woody debris at the 2-year flow, 25-year flow with and without a Smith River backwater 100-year event, and 100-year flow with and without a Smith River backwater 25-year event.

Crossing Region Results

At the 2-year return period flow of 529 cfs, the flow through the crossing travels through the main channel (Figure 36). The flow under the crossing is bounded by sediment deposits that rise about 7.1 feet above the streambed on the right bank and the installed RSP on the left bank. The average and maximum water depths and velocities moving under the crossing are summarized in Table 14. The edge velocities under the crossing 1.2 feet from the right bank deposits and left bank RSP are 3.5 feet per second and 1.5 feet per second, respectively.

During the 1,466 cfs, 25-year return period flow, the flow remains in the main channel (Figure 37). The flow is bounded by sediment deposits on the right bank and the

installed RSP on the left bank. An eddy may form upstream of the crossing on the left bank. The edge velocities under the crossing are 2.4 feet per second against the right bank deposits and 1.9 feet per second against the left bank RSP.

During the 25-year return period flow of 1,466 cfs with a 47-foot Smith River backwater elevation, the flow overtops the RSP on both banks (Figure 38). Under the crossing, the water depth rises 10.7 feet, from an average elevation of 36.3 feet at the 25-year return period flow without a Smith River backwatering event to an elevation of 47.0 feet with a 100-year backwatering event. The flow under the crossing is bounded by the abutments on the right and left banks. Eddies are predicted to form upstream of the crossing on the left and right banks parallel to one another. These eddies are larger than those formed during the 100-year return period flow without backwater scenario. An eddy also occurs next to the right bank abutment. Additional eddies on both sides of the channel occur downstream of the crossing. The water moving under the crossing has a minimum depth of 1.16 feet and a maximum depth of 16.0 feet. The average water depth of flow over the sediment deposits is 9.06 feet. The average velocity is 1.81 feet per second including flow over the sediment deposits. The edge velocities of flow moving under the crossing are 0.4 feet per second against the right bank abutment and 0.9 feet per second against the left bank abutment.

During the 100-year return period flow of 1,955 cfs with a Smith River backwater elevation from the 25-year return period event of 42 feet, the flow rises along the RSP on both banks (Figure 39). Under the crossing, the water depth rises 4.6 feet, from an elevation of 37.2 feet during the 100-year return period flow without a Smith River

backwatering event to an elevation of 41.8 feet with a 25-year backwatering event. The flow under the crossing is bounded by the RSP on the right and left banks. Eddies are expected to form upstream of the crossing on the left and right banks parallel to one another, similar to the Little Mill Creek 25-year return period flow with Smith River 100-year backwater effect scenario. Under the crossing, an eddy forms on the right bank over the sediment deposit terrace. Additional eddies on both sides of the streambank occur downstream of the crossing, where the Smith River backwater effect would be influenced by the stream discharge from Little Mill Creek. The average and maximum water depth and velocity moving under the crossing in the main channel are summarized in Table 14. The average water depth over the sediment deposits is 3.82 feet. The edge velocities moving under the crossing are 0.35 feet per second against the right bank RSP, 2.6 feet per second at the edge of the right bank deposits, and 0.9 feet per second against the left bank RSP.

Table 14. Summary table of wetted channel width and average and maximum depth and velocity results at Little Mill Creek crossing region. The flow simulations summarized are the 2-year, 25-year, 25-year with Smith River 100-year event, and 100-year with Smith River 25-year event.

Flow simulation	**Wetted channel width (ft)**	**Avg. Water Depth (ft)**	**Max Water Depth (ft)**	**Avg. Velocity (fps)**	**Max Velocity (fps)**
2-year	28.3	2.35	3.10	8.26	9.72 (near right bank)
25-year	35.9	3.7	5.2	12.0	13.7 (center of channel)
25-year with Smith River 100-year	84 (entire crossing)	14.92 (main channel)	15.75	2.40	2.42 (center of channel)
100-year with Smith River 25-year	64.5	9.92 (main channel)	10.75 (main channel)	4.75 (main channel)	6.76 (main channel)

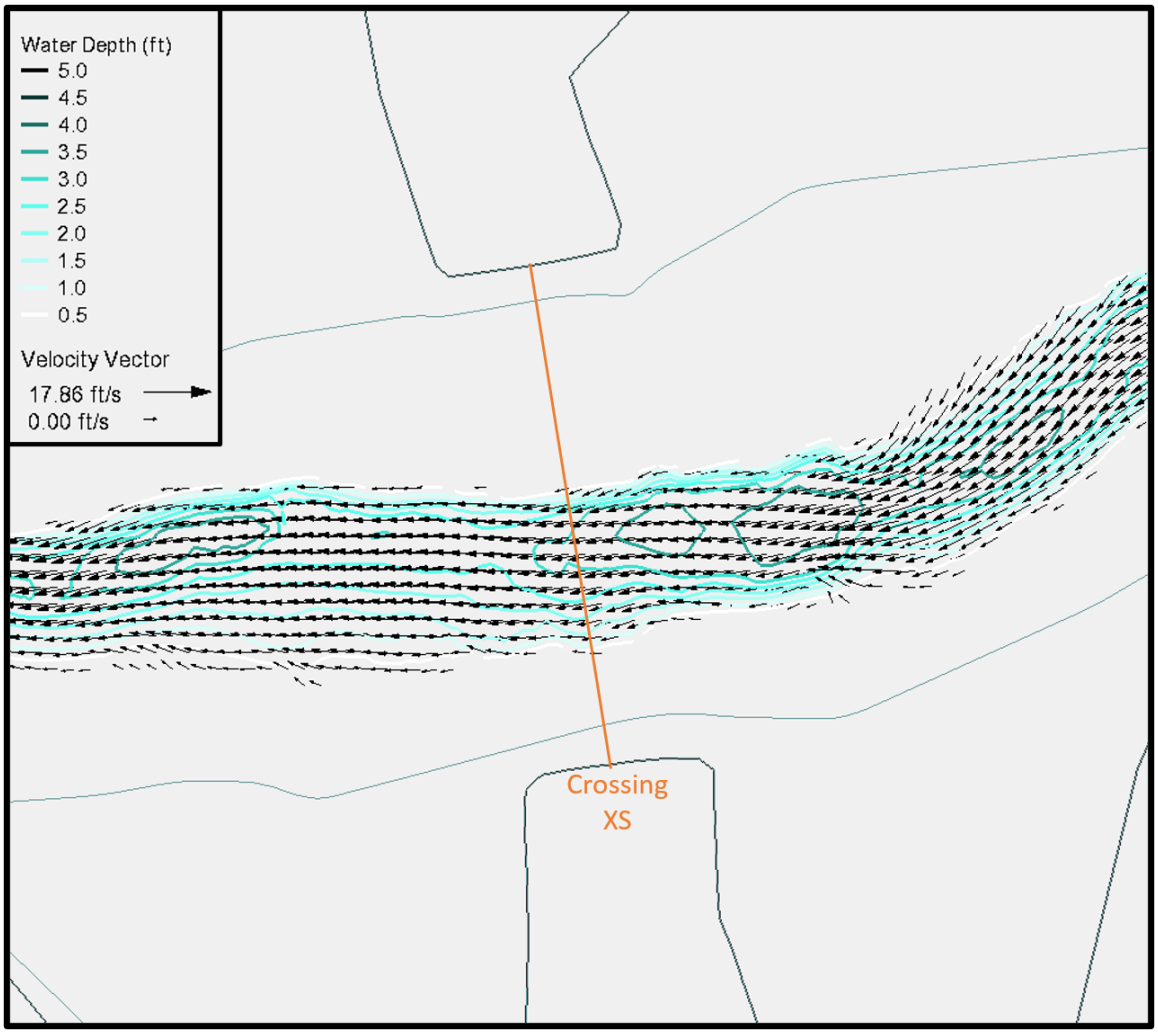

Figure 36. Plan view of crossing at Little Mill Creek with water depth contours (feet) and velocity vectors (feet per second) for the 2-year return period flow of 529 cfs.

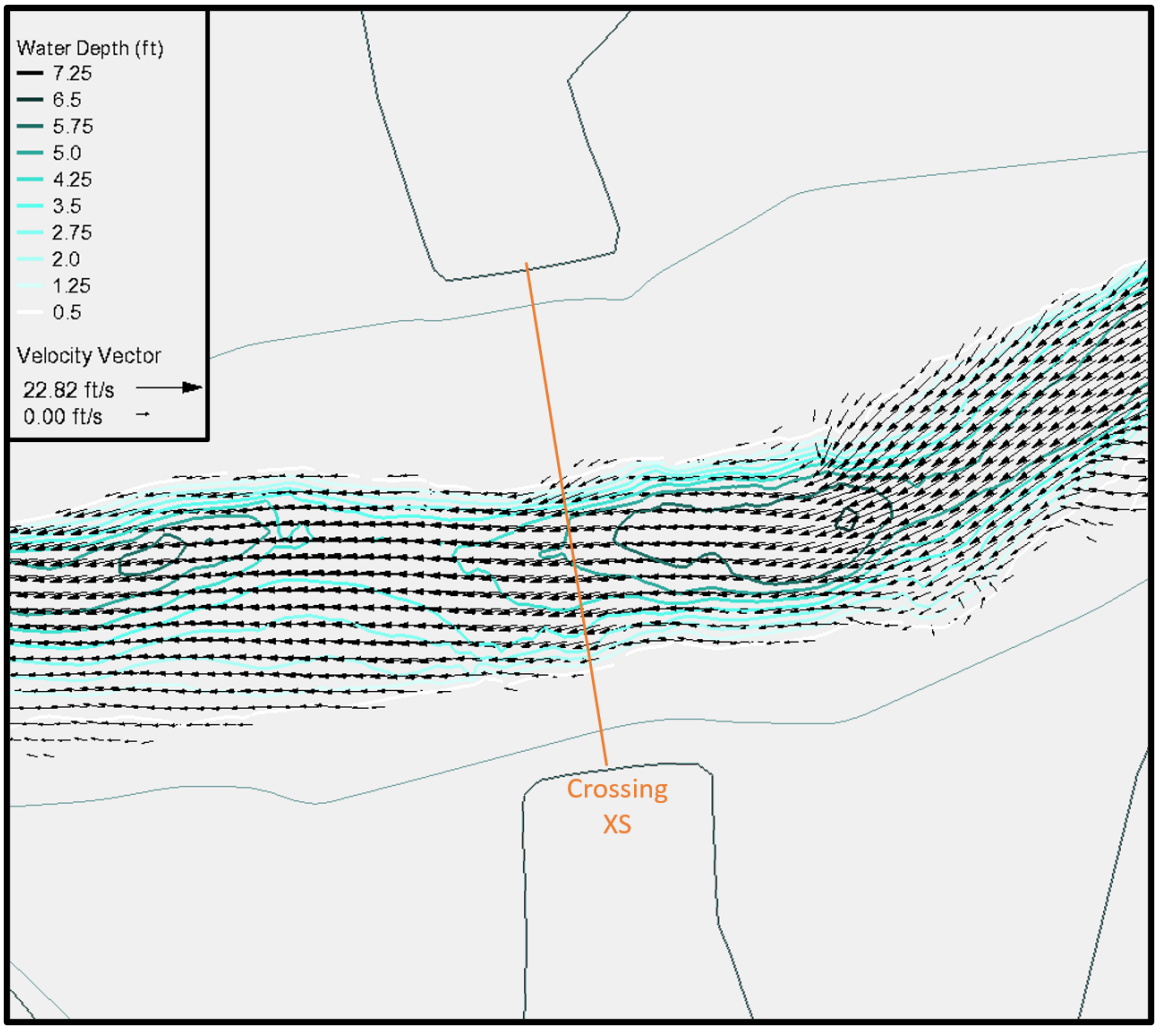

Figure 37. Plan view of crossing at Little Mill Creek with water depth contours (feet) and velocity vectors (feet per second) for the 25-year return period flow of 1,466 cfs.

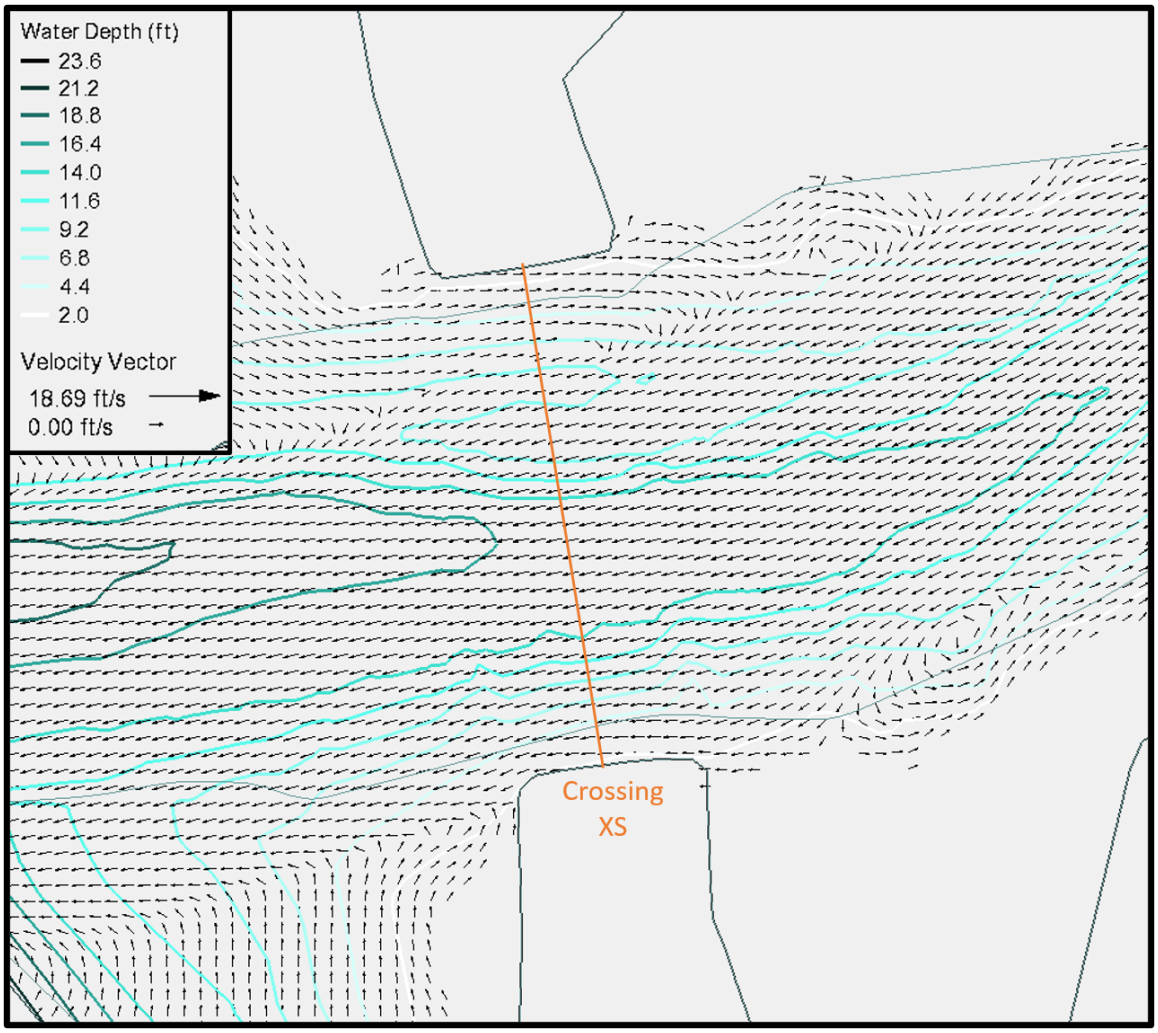

Figure 38. Plan view of crossing at Little Mill Creek with water depth contours (feet) and velocity vectors (feet per second) for the 25-year return period flow of 1,466 cfs and a Smith River backwater elevation for the 100-year return period flow event of 47 feet.

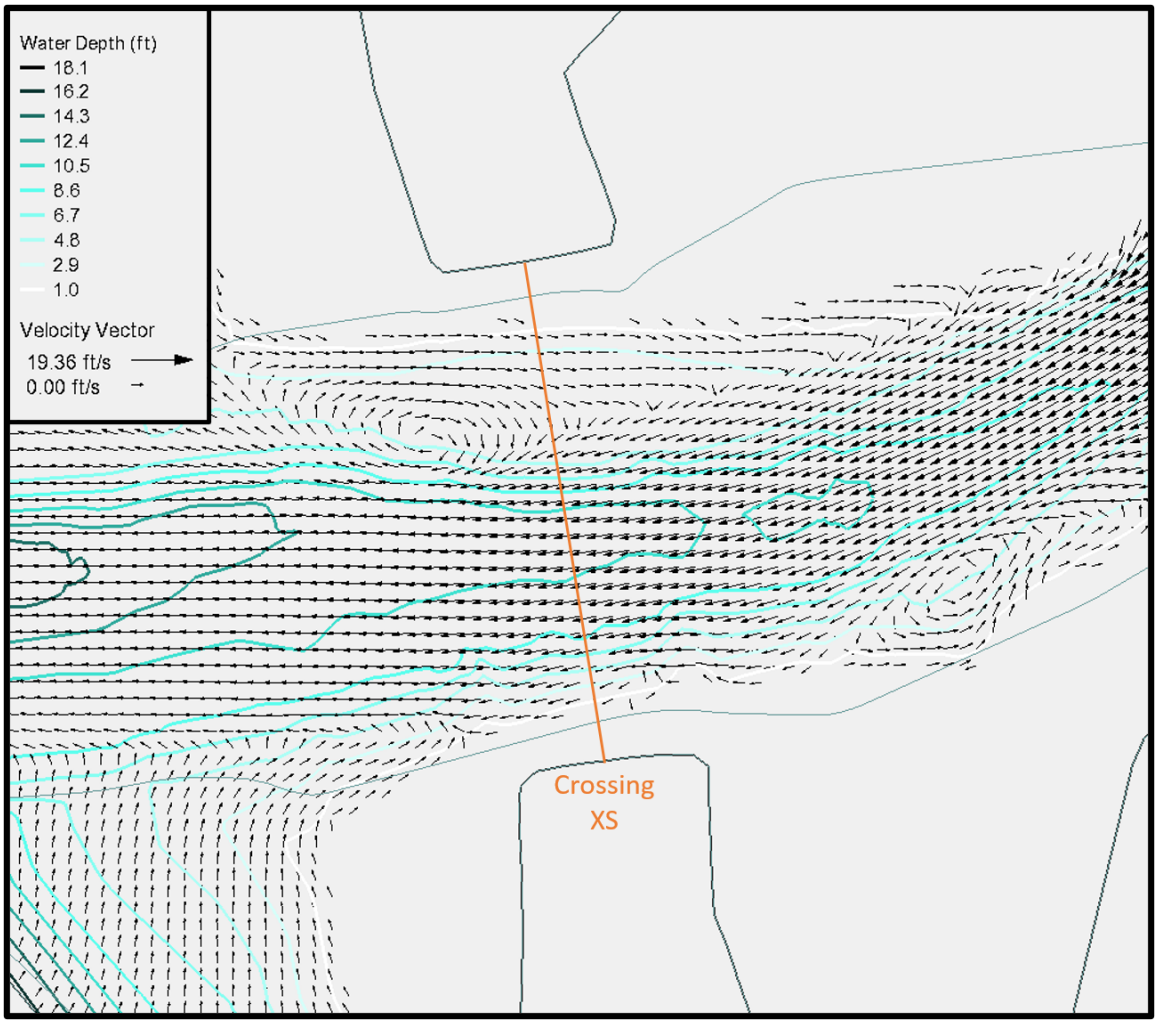

Figure 39. Plan view of crossing at Little Mill Creek with water depth contours (feet) and velocity vectors (feet per second) for the 100-year return period flow of 1,955 cfs and a Smith River backwater elevation for the 25-year return period flow event of 42 feet.

Water depths at the crossing show the geometry of the cross-section, with the main channel from station 21.3 to 51.4 feet and the sediment deposits from 51.4 to 65.8 feet (Figure 40). The backwater events from the Smith River have a significant effect on water depths and velocities. The water depths during the 25-year flow increase by a maximum of more than three times from the scenario without a backwater compared to

the scenario with a 100-year backwater event. The magnitude of the Smith River backwater event is significant, with the 25-year backwater elevation at 42 feet and the 100-year backwater elevation at 47 feet. The water depths during the 100-year flow increase by at most 1.8 times with the addition of a Smith River 25-year backwater event.

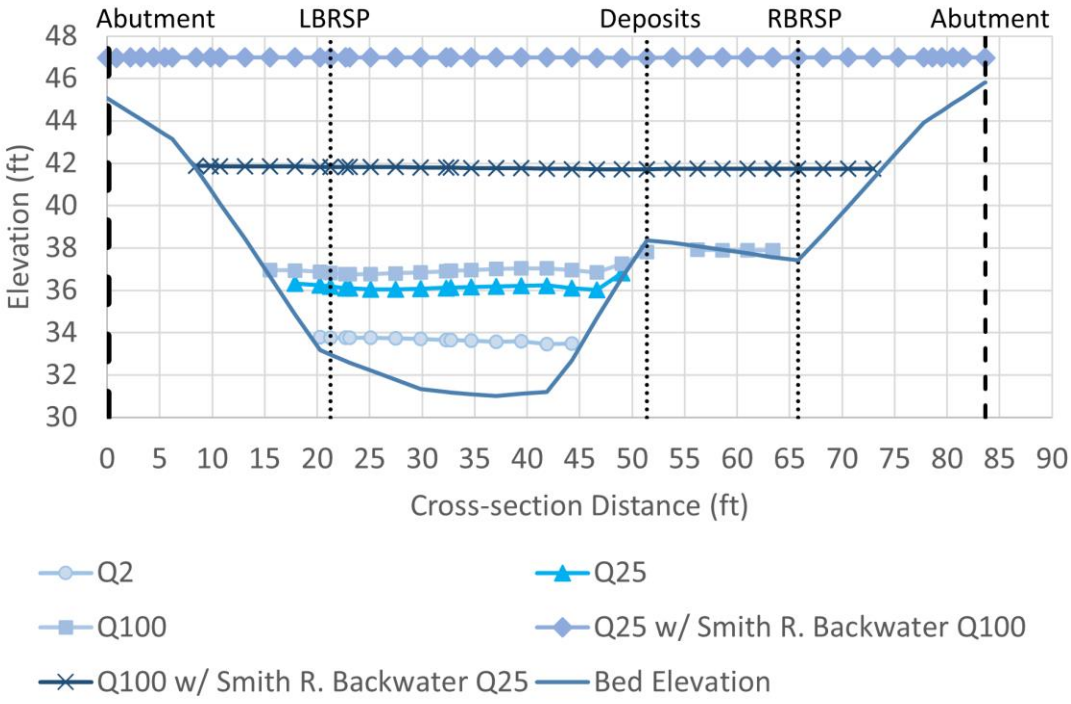

Figure 40. Little Mill Creek water surface elevations under the crossing at the 2-year flow, 25-year flow with and without a Smith River backwater 100-year event, and 100-year flow with and without a Smith River backwater 25-year event.

The velocity distribution across the crossing cross-section has the maximum velocity on the left side of the channel (Figure 41). The 2-year, 25-year, and 100-year return period flows have maximum velocities of 9.7, 13.7, and 14.8 feet per second, respectively. The 25-year flow with the addition of a Smith River 100-year backwater event reduces the maximum velocity by 11.3 feet per second at the cross-section to 2.4

feet per second. The decrease in velocity is expected due to the increase in water depth from the addition of the Smith River 100-year backwater shown in Figure 40.

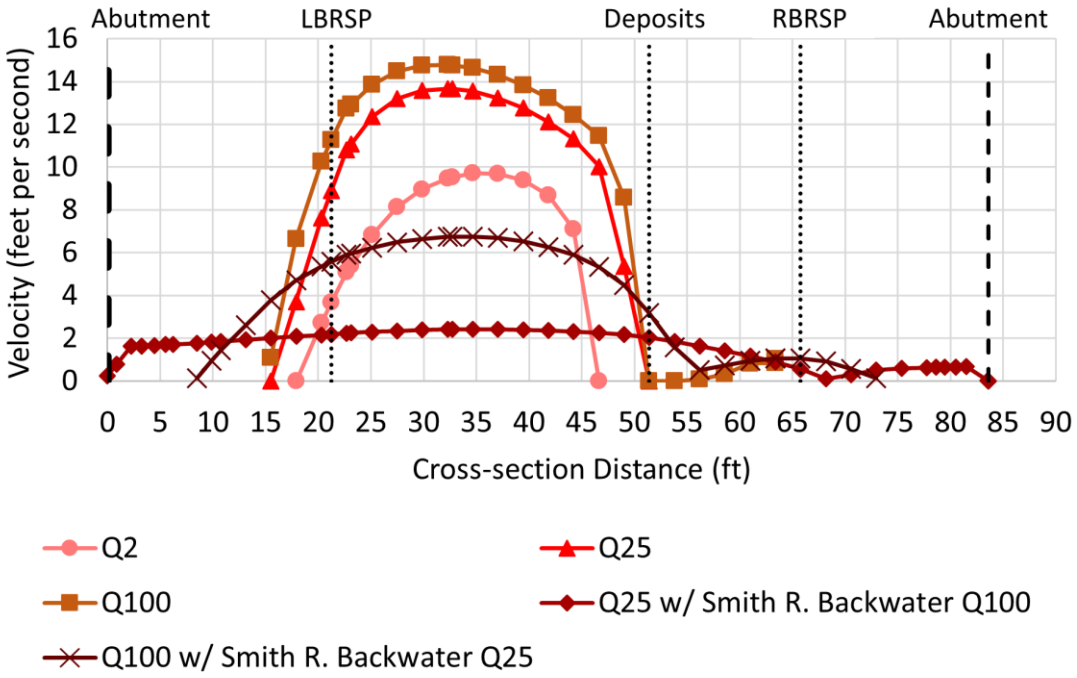

Figure 41. Little Mill Creek velocities, in feet per second, under the crossing at the 2-year flow, 25-year flow with and without a Smith River backwater 100-year event, and 100-year flow with and without a Smith River backwater 25-year event.

North Fork Ryan Creek – HWY 101

The North Fork Ryan Creek model simulations focus on three key sections of the stream: upstream rock weir, crossing inlet, and crossing outlet (Figure 42). The upstream rock weir is a key design element that alters flow reaching the entrance of the stream crossing and maintains the bed elevation of the upstream channel. The inlet and outlet of the stream crossing affect the hydraulics entering and exiting the crossing structure. Most results are presented as water depth contour maps overlain by velocity vectors.

Additional figures showing water depths, velocities, and shear stress for 2-, 10-, 25-, 50-, and 100-year return period flows can be found in

APPENDIX C.

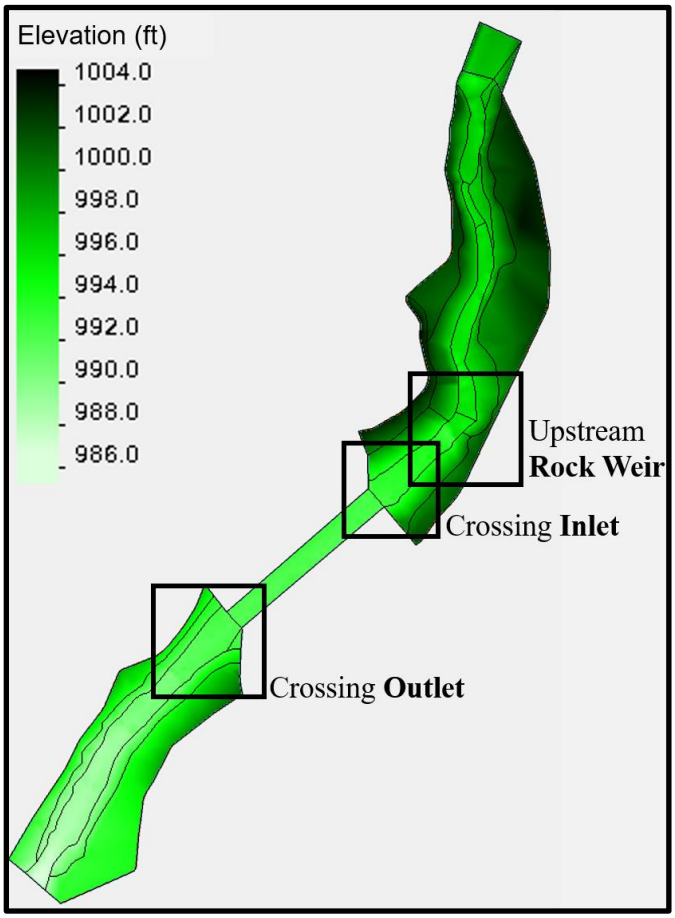

Figure 42. Plan view of North Fork Ryan Creek model extents with elevation contours. The labeled squares indicate the locations for key figures included throughout the following section.

Maximum water depth, velocity, and shear stress predicted by the model at each flow are summarized in Figure 43. Velocity and shear stress experience around a 4 unit increase in maximum values from the 2-year to the 100-year flow, while water depth experiences a 2.9-foot increase in maximum values from the 2-year (33 cfs) to the 100-year flow (263 cfs) (Figure 43).

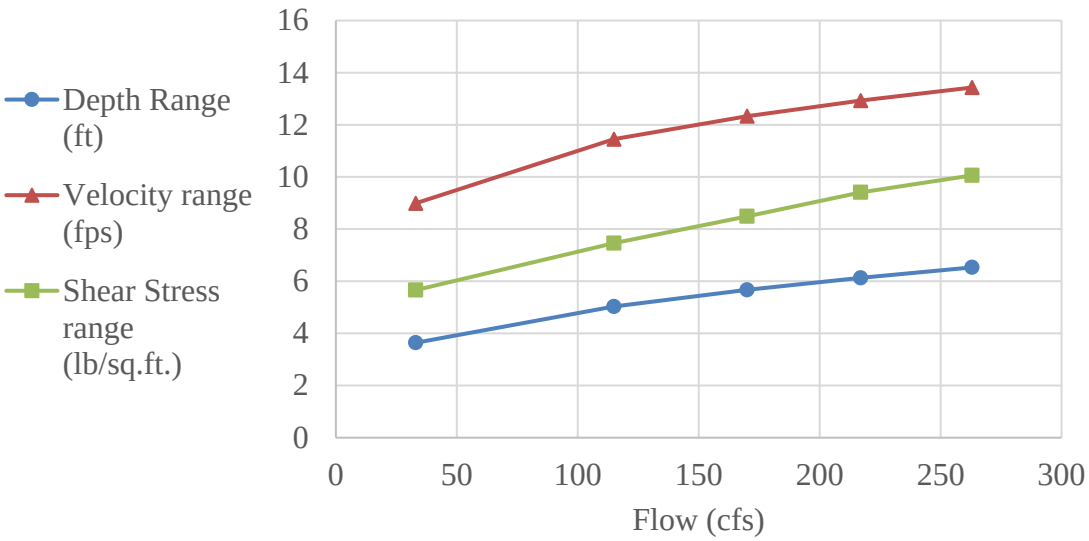

Figure 43. North Fork Ryan Creek. Maximum values for water depth, velocity, and shear stress for the 2-, 10-, 25-, 50-, and 100-year return period flows.

Rock Weir results

At the 2-year return period flow of 33 cfs, the flow is split into two major pathways (Figure 44) as it moves around a large boulder, one of the many that make up the rock weir structure. Eddies form on both banks immediately downstream of the rock weir, circulating towards the banks with upstream velocity along both banks. An additional eddy occurs in the middle of the channel between the two main flow pathways. The eddy formed on the right bank is 3.0 feet wide and the eddy formed on the left bank is 2.7 feet wide, while the wetted channel width is 13.7 feet. The flow width between the eddies is 8.0 feet, while the flow width above the rock weir is 11.7 feet. The maximum velocity of upstream flow along the right bank is 2.46 feet per second, as is the downstream-moving flow of that same eddy further into the channel. Moving towards the left bank, the maximum velocity in the larger flow pathway is 3.61 feet per second, then

decreases to 0.4 feet per second in the mid-stream eddy and increases back to 2.3 feet per second in the secondary flow pathway. The eddy formed on the left bank has maximum velocity of 1.6 feet per second for the downstream-moving flows and 1.06 feet per second upstream-moving flows closest to the bank. The edge velocities adjacent to the zero-boundary condition are 1.0 and 0.83 feet per second for the right and left banks, respectively.

Divergence in the velocity vectors shows the flow splitting around the two key boulders (BLDR3 and BLDR4) indicated in Figure 44, downstream of the rock weir. The importance of mesh sizing becomes clear here, as smaller mesh elements increase the mesh resolution and allow the large boulders in the stream channel to be accurately represented in the mesh element elevations. The flow moves around the boulders as flow obstructions in the mesh. BLDR4 is located approximately 9 feet downstream of the rock weir, which is also where the pool created by the rock weir begins to taper off. Maximum depth within this pool is 2.7 feet, and the water depths leading up to BLDR4 are still around 1.4 feet compared to depths of 1.0 feet and below further downstream around BLDR3. The height from streambed to boulder top of BLDR4 and BLDR3 are 1.93 and 0.84 feet, respectively. The effect of BLDR4 on the surrounding velocities is difficult to discern because of the proximity to the eddies formed by the rock weir, but BLDR4 does seem to deflect flow and lower velocities immediately downstream. The water to the left of BLDR4 has velocities around 2 feet per second, while most velocities in the main flow pathway are over 3 feet per second. Contrary to its lesser height compared to BLDR4, BLDR3 has a more pronounced effect on the surrounding velocity distribution because

the flow around BLDR3 is becoming more uniform and the peak of BLDR3 is further upstream creating a larger obstructive face perpendicular to flow than BLDR4. The minimum velocity immediately downstream of BLDR3 decreases to 0.49 feet per second.

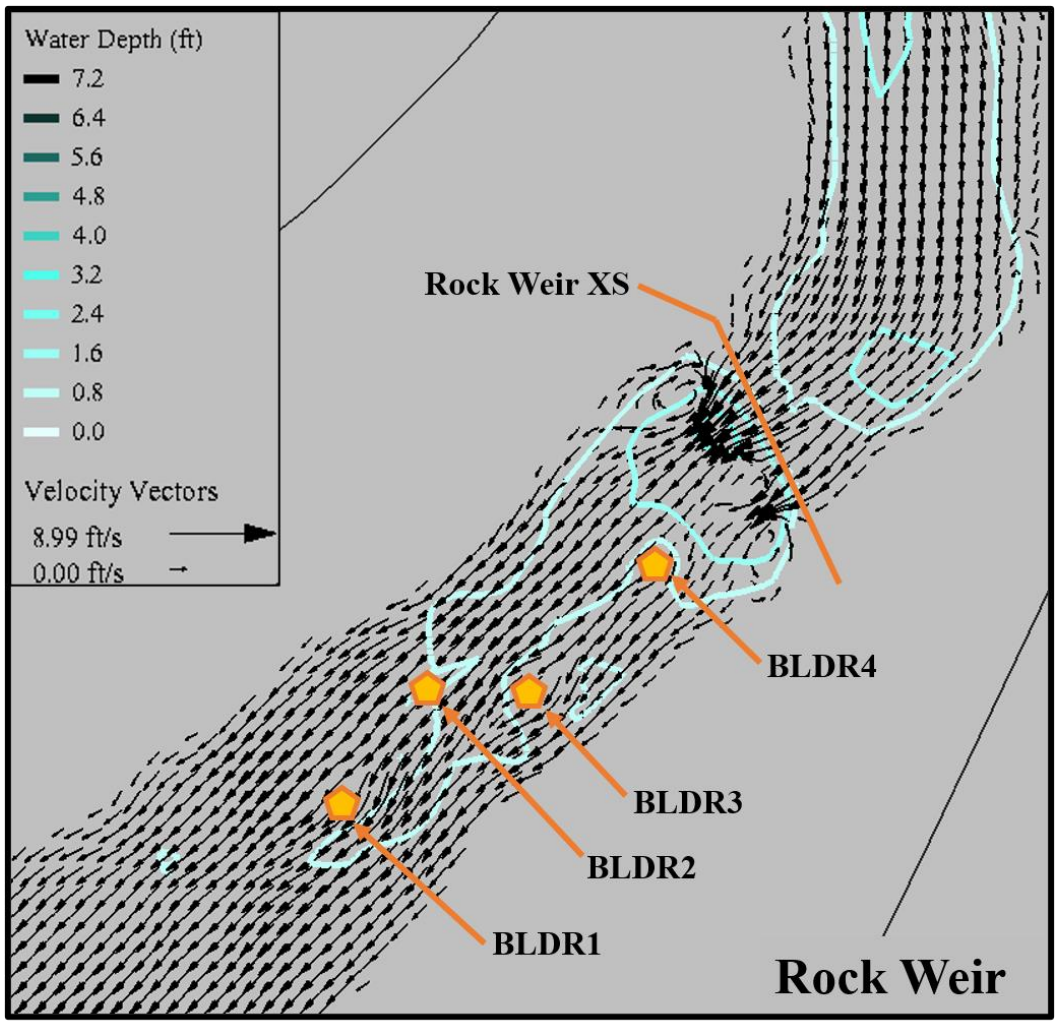

Figure 44. North Fork Ryan Creek rock weir location, 2-year return period flow water depth (feet) contour lines with velocity vectors.

At the 25-year return period flow of 170 cfs, the flow of water at the rock weir is no longer split (Figure 45). Flow overtops the entire rock weir structure and the key boulders downstream of the rock weir. The eddies observed along the bank at the 2-year

flow still form immediately downstream of the rock weir and have the same circulation pattern. The eddy formed on the right bank is 7.85 feet long and the eddy formed on the left bank is 6.11 feet long. The maximum velocity of upstream-moving flow within the eddy is 3.04 feet per second. Moving from the center of the eddy towards the center of flow within the channel, the velocity increases to 6.1 feet per second. Although flow over the rock weir is not split by a flow obstruction like in the 2-year flow, the velocity behind the previous flow obstruction is slower at 3.22 feet per second, but then returns to 4.5 feet per second on the left-hand side of the channel. The velocity starts to decrease moving into the left bank eddy, falling to 0.4 feet per second near the center of the eddy. Moving from the center of the eddy to the left bank the velocity increases in the upstream-moving flow to 2.15 feet per second at a distance of 0.7 feet from the water's edge. The edge velocities adjacent to the zero-boundary condition are 1.16 and 1.51 feet per second for the right and left banks, respectively.

The key boulders that were visible in the 2-year flow results are overtopped during the 25-year flow (Figure 45). The minimum water depths over BLDR4 and BLDR3 are 0.82 and 1.12 feet, respectively. BLDR4 immediately downstream of the rock weir does influence channel velocity resulting in slower velocities in the left side of the channel, where the maximum channel velocity is 4.5 feet per second, compared to 6.1 feet per second in the main flow pathway. BLDR3 no longer creates decreased downstream velocities and does not redirect the flow pathway since it no longer obstructs the full depth of flow. The velocities in the partially obstructed flow of water above BLDR3 increase to a maximum of 8.07 feet per second and immediately downstream of

BLDR3 the minimum velocity is 6.11 feet per second, but the velocity drops down below 6.0 feet per second to the left of BLDR3 and above the upstream left corner of BLDR3. In the right adjacent main channel, maximum velocity is 7.93 feet per second.

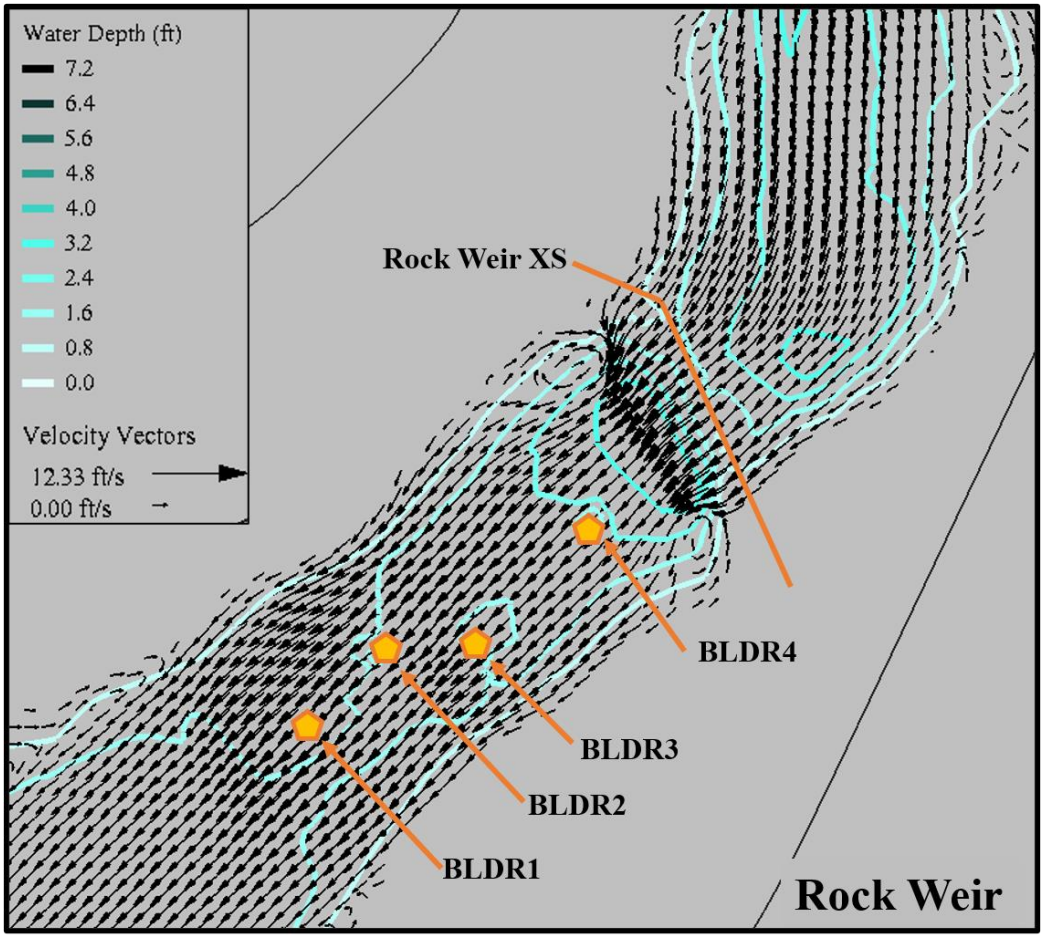

Figure 45. North Fork Ryan Creek rock weir location, 25-year return period flow water depth (feet) contour lines with velocity vectors.

At the 100-year return period flow of 263 cfs, flow also overtops the entire rock weir structure and the key boulders downstream of the rock weir (Figure 46). The eddies still form along the bank downstream of the rock weir and have the same circulation pattern. During the 100-year flow, the eddy formed on the right bank is 4.8 feet wide and

the eddy formed on the left bank is 3.2 feet wide, while the wetted channel width is 20.2 feet. The flow width between the eddies is 12.2 feet, while the flow width above the rock weir is 18.0 feet. The maximum velocity of upstream-moving flow within the eddy is 3.16 feet per second. Moving from the center of the eddy towards the center of flow within the channel, the velocity increases to 6.94 feet per second. Velocities slow nearing the left bank where the most upstream boulder following the rock weir is located. The velocity continues to decrease moving into the left bank eddy, falling to 0.42 feet per second near the center of the eddy. Moving from the center of the eddy to the left bank the velocity increases in the upstream-moving flow to 2.7 feet per second at a distance of 1.0 feet from the water's edge. The edge velocities adjacent to the zero-boundary condition are 0.96 and 1.40 feet per second for the right and left banks, respectively.

The velocity distribution patterns predicted around the key boulders for the 25-year flow are also observed in the 100-year flow results. BLDR4 continues to have lower velocities upstream around 5 feet per second compared to 7 feet per second in the main flow pathway. Immediately downstream of BLDR3, the minimum velocity is 7.21 feet per second compared to the right adjacent main channel velocity of over 8.0 feet per second. The velocity drops below 7.0 feet per second to the left of BLDR3 and partially above BLDR3, similar to the 25-year return period flow.

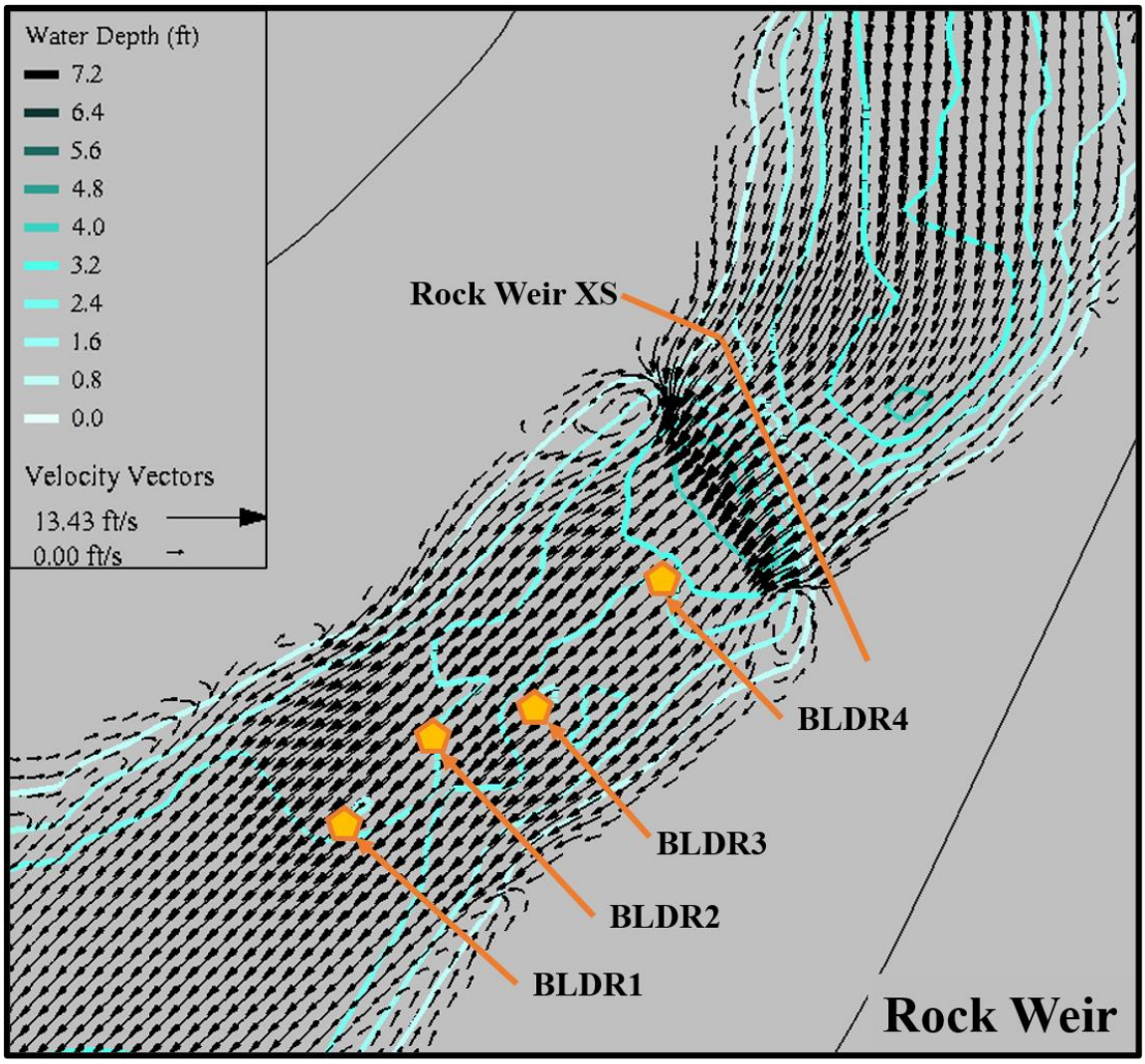

Figure 46. North Fork Ryan Creek rock weir location, 100-year return period flow water depth (feet) contour lines with velocity vectors.

The water depths at the crest of the rock weir vary because of the presence of the large rock components forming a series of notches along the weir (Figure 47). The maximum water depth increases over three-fold, from 0.54 feet during the 2-year return period flow to 1.78 feet during the 100-year return period flow. The vertical difference in water elevation between the top of the rock weir (995.5 feet) and in the pool downstream

(994.3 feet) of the rock weir at the 2-year flow is 1.2 feet. The design criteria in Caltrans' North Fork Ryan Creek project report is a maximum water surface drop of 0.5 feet for juvenile salmonids and 1.0 feet for adult salmonids (AECOM, 2014; CDFG, 2002; NMFS, 2001).

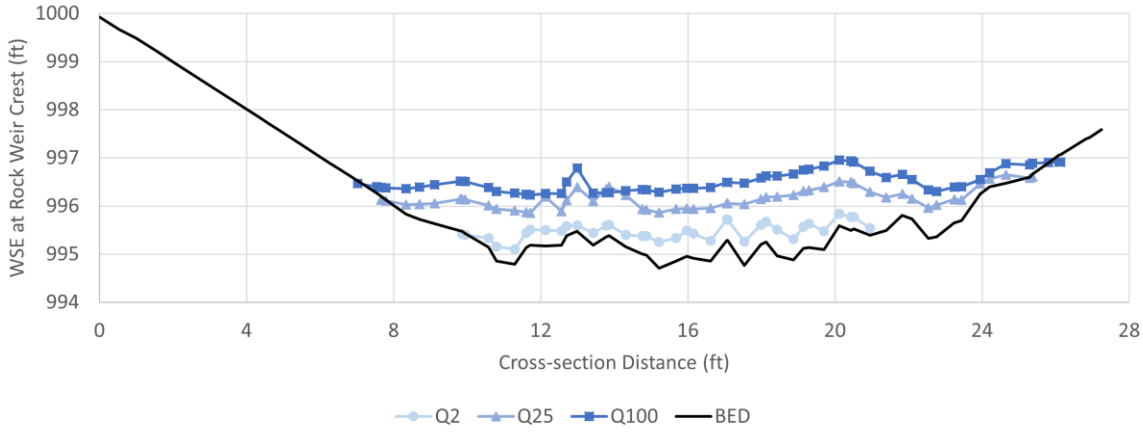

Figure 47. Water surface elevations at the Rock Weir crest (XS4) for the 2-, 25-, and 100-year return period flows. The perspective of the plot is looking downstream towards the rock weir crest, so the left side of the plot is the left bank and the right side represents the right bank.

The velocities passing over the rock weir crest increase by approximately 3 feet per second between the 2-year and the 25-year flow, while the increase from the 25-year to the 100-year flow is about 1 foot per second (Figure 48).

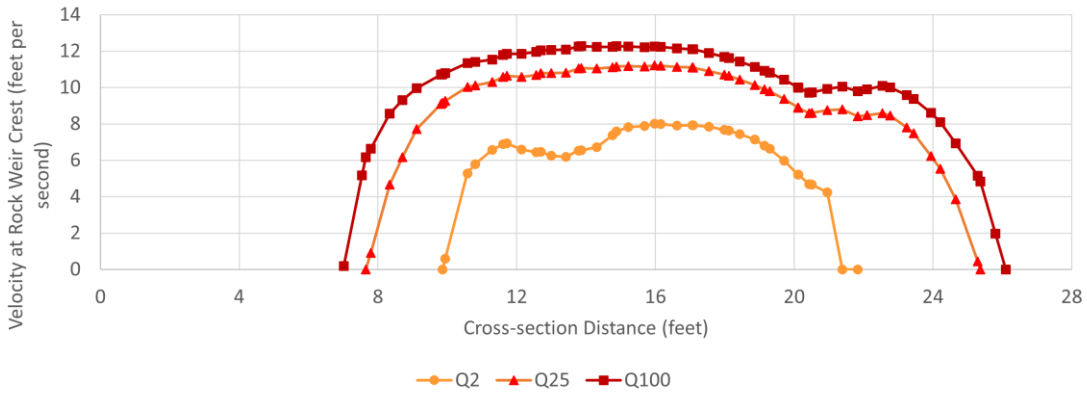

Figure 48. Velocities (in feet per second) at the Rock Weir crest (XS4) for the 2-, 25-, and 100- year return period flows. The perspective of the plot is looking downstream towards the rock weir crest, so the left side of the plot is the left bank and the right side is the right bank.

Crossing Inlet results

During a 2-year return period flow of 33 cfs, the velocities within the culvert range from 1.1 to 3.8 feet per second with faster velocities on the left bank (Figure 49). Along the inlet headwall, the velocities are much smaller with a maximum of 0.64 feet per second. The average velocity over the inlet headwall cross-section is 1.6 feet per second, while the average velocity at the inlet opening is 2.6 feet per second. A small eddy possibly forms at the intersection of the right bank with the inlet headwall (Figure 49). The maximum velocity in this eddy is 0.15 feet per second and there is no eddy present on the left bank. The simulation predicts that the flow width at the 2-year flow is at least 18.9 feet, which is larger than the culvert inlet width of 12 feet. The edge velocities adjacent to the zero-boundary condition on the bank RSP are 2.6 and 3.1 feet per second for the right and left banks, respectively.

The two lines perpendicular to flow in Figure 49 represent observation arcs at the inlet and upstream of the inlet where water depth and velocity results were extracted from the simulation (see Figure 53 and Figure 54). The water depth and velocity results were also examined in the direction of flow, spanning the left, center, and right of the crossing opening. These values extend 10 feet upstream and downstream of the crossing opening. During the 2-year flow, the water depth entering the middle of the crossing increases from 0.5 feet to 1.2 feet and the velocity decreases from 4.5 feet per second to 2.5 feet per second.

The key boulders, BLDR1 and BLDR2, identified in Figure 49, are submerged during the 2-year flow, but BLDR1 does influence the flow pathway. BLDR2 does not have a significant effect on the flow pathway. BLDR2 is less prominent in the streambed with a top elevation 0.24 feet lower than BLDR1. The velocities immediately downstream of BLDR1 reach a minimum of 2.42 feet per second, compared to velocities around 5 feet per second adjacent to BLDR1. Velocities immediately downstream of BLDR2 are not predicted to change and remain the same magnitude as adjacent velocities.

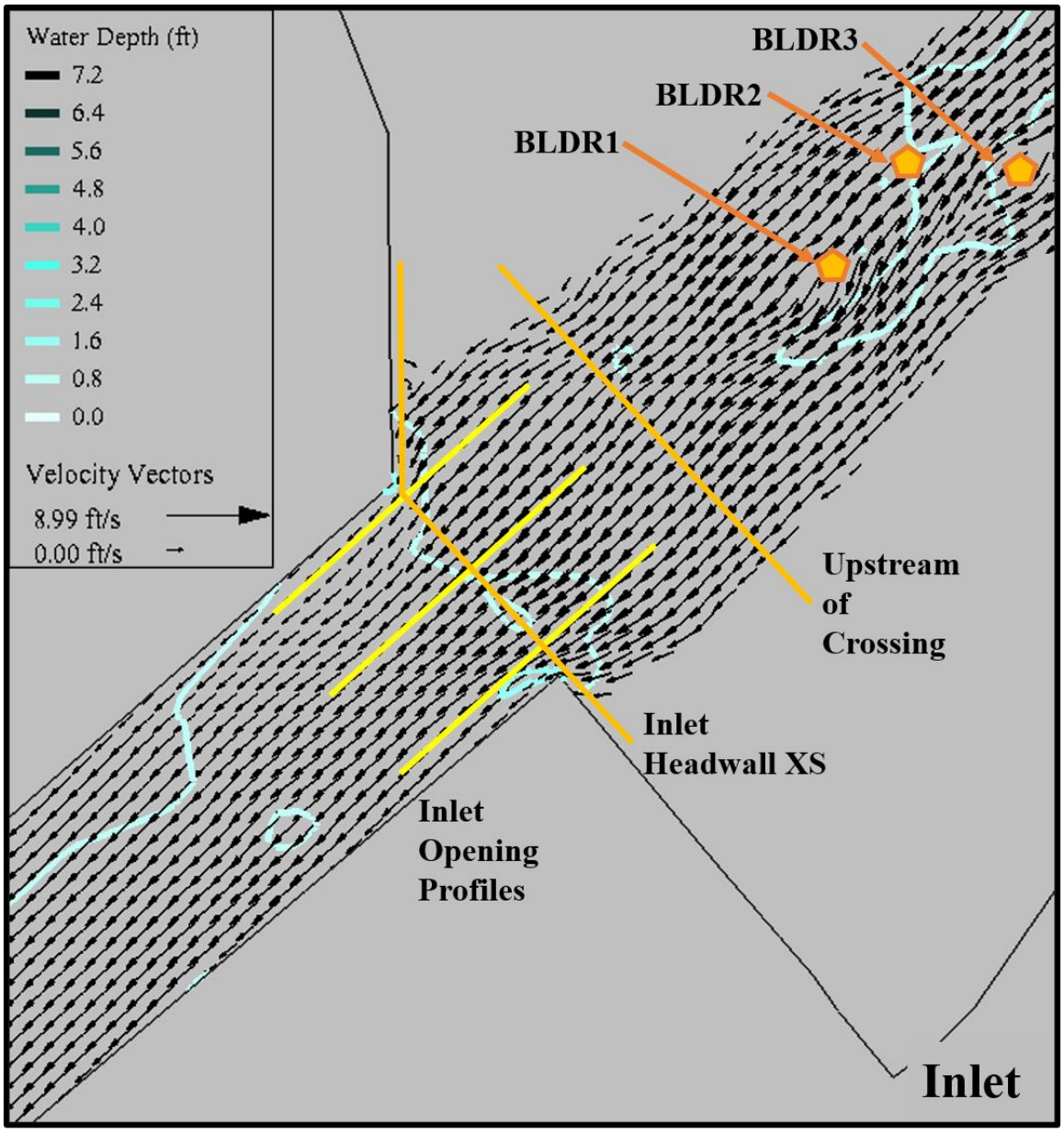

Figure 49. North Fork Ryan Creek crossing inlet location, 2-year return period flow water depth (feet) contour lines with velocity vectors.

At the 25-year return period flow of 170 cfs, larger eddies have formed at the intersection of the stream banks with the inlet headwall (Figure 50). The model simulation predicts a clockwise eddy on the right bank and velocity vectors suggest a

similar, but less pronounced, eddy structure on the left bank. Along the inlet headwall, velocities ranged from 0 to 0.8 feet per second. The average velocity over the inlet headwall cross-section is 2.5 feet per second, while the average velocity at the inlet opening is 4.9 feet per second. On the right bank, the eddy formed has a maximum velocity of 1.2 feet per second moving upstream along the bank. The velocity in the middle of the channel reaches 5.45 feet per second, then decreases to the center of the left bank eddy. The velocity then increases once more to 1.31 feet per second, with the water moving upstream along the bank at a distance of 0.4 feet from the water's edge, before reaching zero at the water's edge. The edge velocities adjacent to the zero-boundary condition along the RSP are 0.5 feet per second for both the right and left banks.

Similar to the 2-year flow, results predicted across the channel arcs spanning 10 feet upstream and downstream of the crossing opening, continue to show an increase in water depth as water enters the crossing in the 25-year flow. Entering the middle of the crossing during the 25-year flow, the water depth increases from 2.0 feet to 2.9 feet and the velocity oscillates around 5.2 feet per second by about +/- 0.1 feet per second. Unlike in the 2-year flow, the key boulders BLDR1 and BLDR2 do not significantly affect the stream hydraulics or the velocities at the 25-year flow.

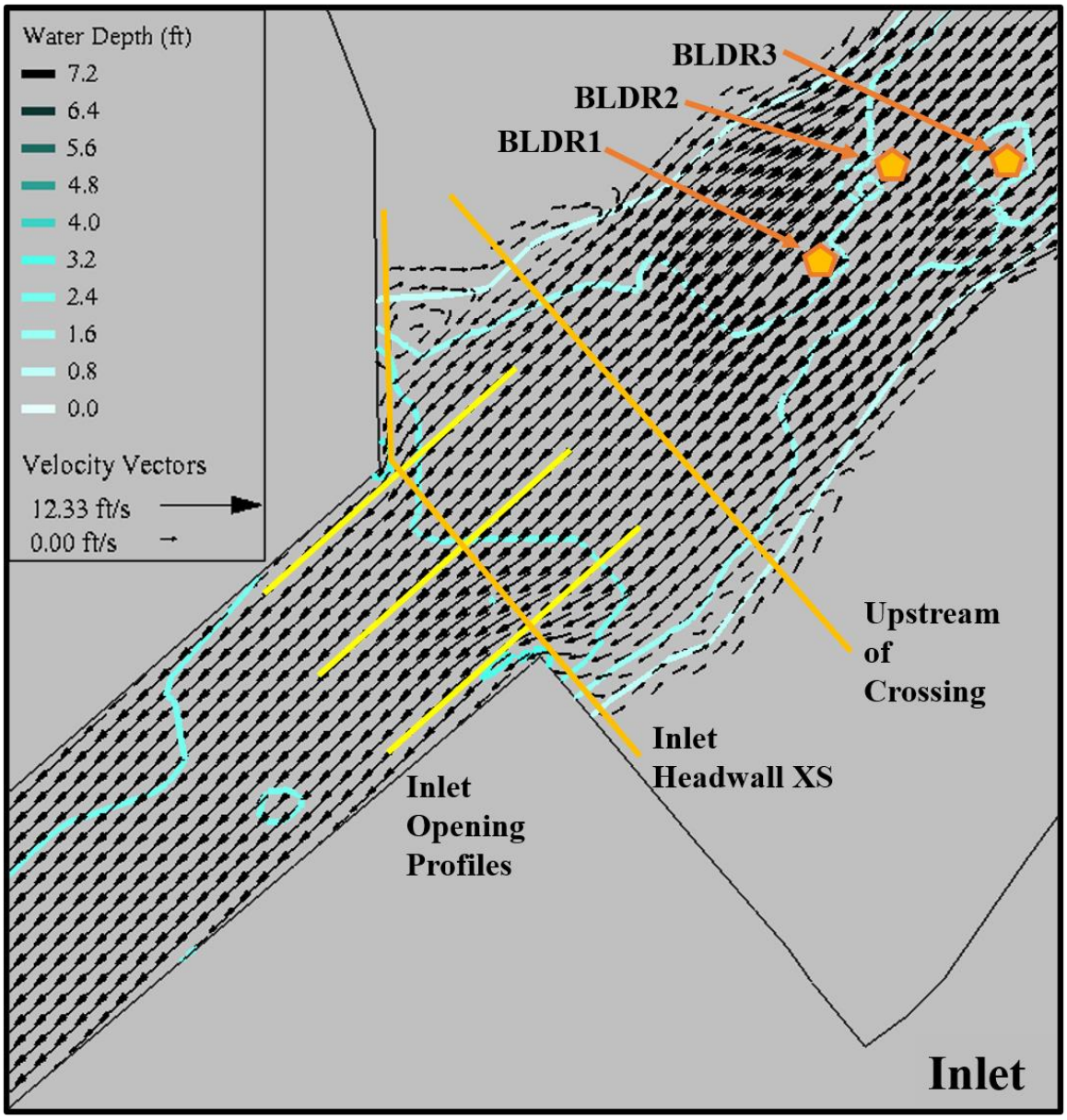

Figure 50. North Fork Ryan Creek crossing inlet location, 25-year return period flow water depth (feet) contour lines with velocity vectors.

During the 100-year return period flow of 263 cfs, the water depths and velocities increase and the eddies expand to include upstream portions near the water's edge (Figure 51). The average velocity over the inlet headwall cross-section is 2.8 feet per

second, while the average velocity at the inlet opening is 5.8 feet per second. The eddy on the left bank is now much more pronounced whereas the right bank eddy remains in approximately the same longitudinal location but becomes wider. The eddy on the right bank has a maximum velocity of 1.46 feet per second moving upstream along the bank, approximately 1.3 feet from water's edge. The water velocity then decreases to 0.06 feet per second at the center of the eddy. Moving towards the center of the channel, velocities increase to a maximum of 5.58 feet per second between the right and left bank eddies. Moving towards the left bank, velocities decrease until reaching the center of the left bank eddy, and then increase to 1.97 feet per second as flow comes back to flow upstream along the left bank. This maximum eddy velocity of 1.97 feet per second is located 1.6 feet away from the water's edge. The velocity then decreases until a zero-velocity at the edge of the water. The edge velocities adjacent to the zero-boundary condition along the RSP are 1.0 and 1.6 feet per second for the right and left banks, respectively. The low velocities are due to the eddies that occur on both banks upstream of the crossing inlet. The velocities directly above the RSP toe line are 3.3 and 3.1 feet per second for the right and left banks, respectively.

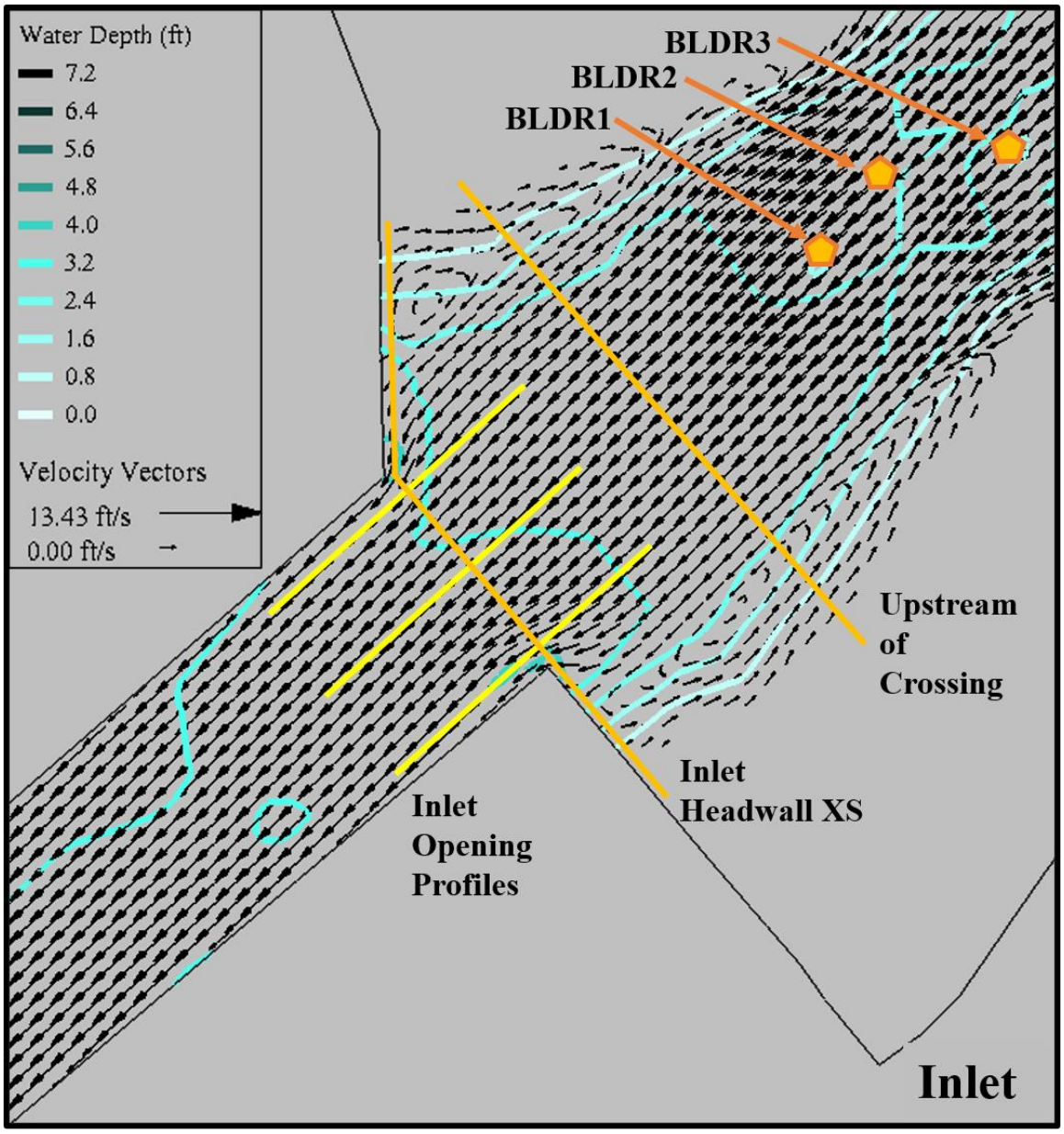

Figure 51. North Fork Ryan Creek crossing inlet location, 100-year return period flow water depth (feet) contour lines with velocity vectors.

Similar to the 2-year and 25-year flow, results along perpendicular channel arcs spanning 10 feet upstream of the crossing to 10 feet downstream into the crossing opening show an increase in water depth as water enters the crossing in the 100-year

flow. During the 100-year flow, the water depth entering the middle of the crossing increases from 2.9 feet in the channel 10 feet upstream of the crossing opening to 3.7 feet into the crossing by 5 feet (Figure 52). The velocity varies when entering the crossing, with an increase from 5.7 to 6.3 feet per second from upstream to the opening, then a decrease to 6.1 feet per second 6 feet into the crossing, and then an increase back to 6.3 feet per second at 10 feet into the crossing.

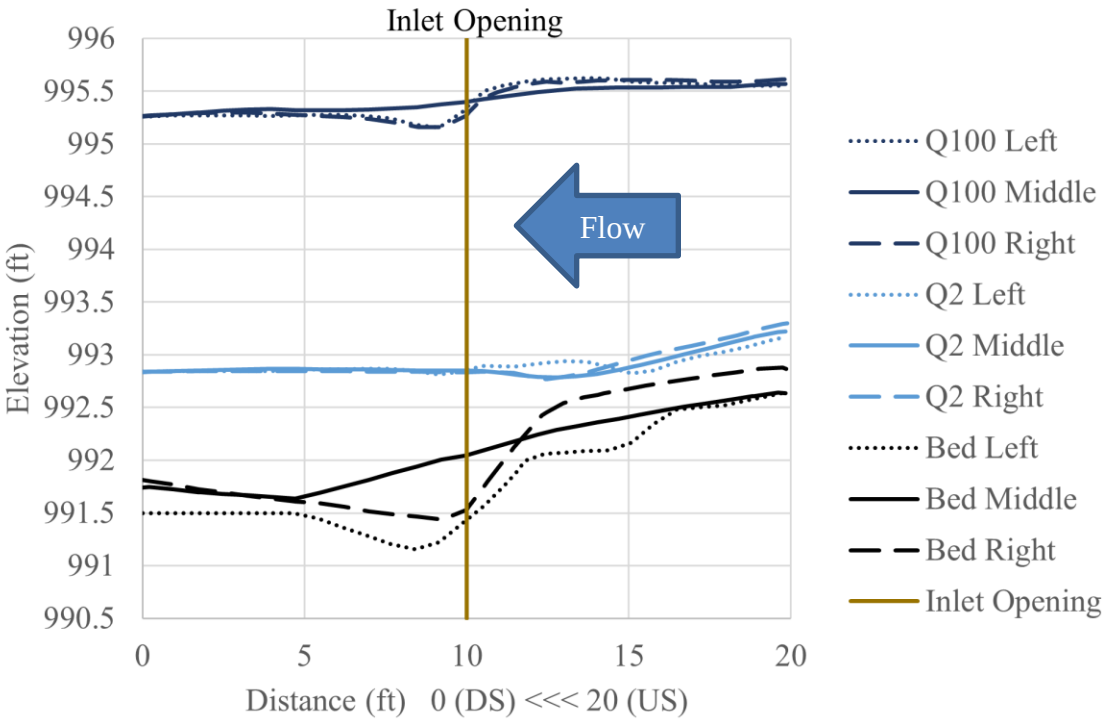

Figure 52. North Fork Ryan Creek. Water surface elevations (ft) in the direction of flow for the 2-year and 100-year return period flows. Arcs represent the left, middle, and right sides of the inlet opening. The bottom group of three lines represent the bed elevations, the middle group of lines represent the 2-year flow water surface elevations, and the top group of lines represent the 100-year flow water surface elevations. The inlet opening is at 10 feet, moving downstream from 20 to 0 feet.

The crossing inlet data spans the channel from the left to right headwall in Figure 53. On both the left and right sides there is an increase in depth moving away from the banks and into the main channel, until the water depth decreases at the opening of the crossing inlet. The deepest water depths of 1.7, 3.4, and 4.3 feet are located at the left side of the crossing opening for the 2-, 25-, and 100-year flows, respectively. The water depths entering the opening decrease by a maximum of 1.0, 1.1, and 1.2 feet compared to the peak water depths at the 2-, 25-, and 100-year flows (Figure 53). Entering the crossing, the water depth is slightly greater on the left, by a minimum of 0.1 feet consistently through the three flows, likely due to the underlying bed topography. Average water depth across the inlet opening increases from 1.0 feet during the 2-year flow to 2.7 feet during the 25-year flow to 3.5 feet during the 100-year flow.

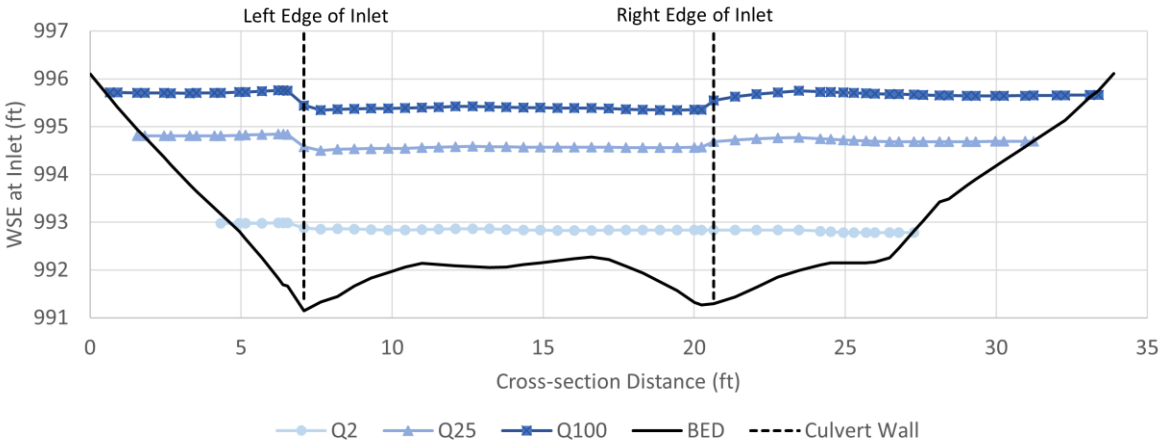

Figure 53. Water surface elevations and bed elevation (in feet) at the crossing inlet cross-section (XS1) for the 2-, 25-, and 100-year return period flows.

The velocities next to the inlet headwall (approximately 0.2 feet away from the structure boundary) change exponentially at the inlet opening in the 2-, 25-, and 100-year

flows (Figure 54). On the right boundary, the velocity increase is slightly more gradual because the right headwall is angled and water is guided in the direction of channel flow, compared to the perpendicular obstruction of the left headwall. The increasing and decreasing velocities of the eddies upstream of the inlet are not visible in these plots because of their proximity to the headwall structure. Within the crossing opening, the average water velocity increases from 2.6 feet per second during the 2-year flow to 4.6 feet per second during the 25-year flow to 5.5 feet per second during the 100-year flow.

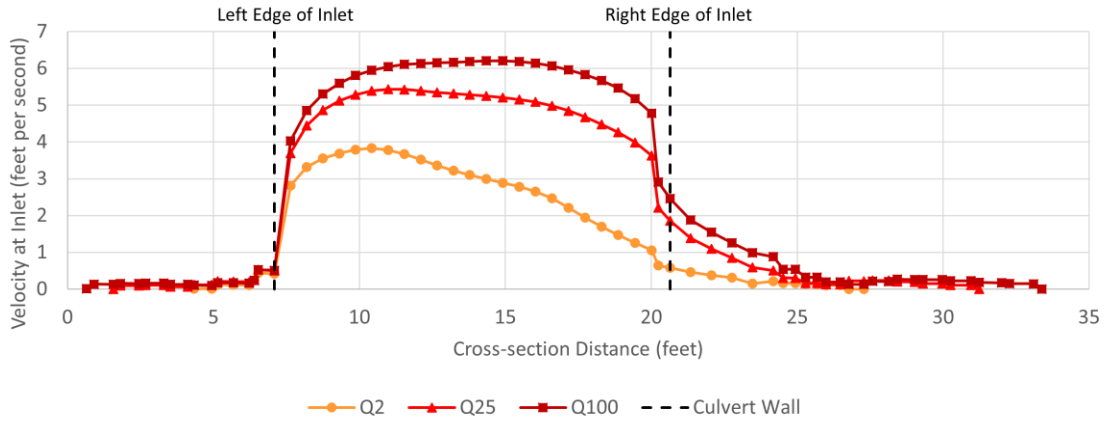

Figure 54. Velocities (in feet per second) at the crossing inlet headwall (XS1, appx. 0.2 feet away from the structure boundary) for the 2-, 25-, and 100-year return period flows.

Crossing Outlet results

At the crossing outlet during the 2-year return period flow of 33 cfs, there are eddies occurring on both sides of the stream as the water exits the crossing (Figure 55). The right bank eddy moves in a clockwise direction, while the left bank eddy moves in a counter-clockwise direction. In the eddy along the right bank, the maximum velocity moving upstream along the bank is 0.75 feet per second. In the channel center, the greatest velocity between the right and left bank eddies is 3.0 feet per second. The

velocity decreases moving from the main flow to the center of the left bank eddy then increases to a maximum of 0.6 feet per second in the upstream direction before decreasing at the water's edge.

The water depth and velocity results were also extracted in the direction of flow, spanning the left, center, and right of the crossing opening. The extracted values extend 10 feet upstream and downstream of the crossing opening. During the 2-year flow the water depth entering the middle of the crossing decreases from 1.0 feet to 0.85 feet and the velocity varies as the water exits the crossing and flows over the key rocks located around the opening. Velocities range from 2.3 to 3.0 feet per second, over the 20-foot segment of stream exiting the crossing outlet opening.

Downstream of the crossing outlet, there are three 'key rocks' and one boulder, BLDR0 (Figure 55). The key rocks are less prominent in the channel compared to the boulders identified upstream and downstream of the crossing and are fully submerged at the 2-year flow. Key rock 1 has the largest effect on stream velocities, increasing velocities from 2.6 to 3.5 feet per second as water is forced over them, and velocities decrease to 2.4 feet per second downstream of the rock. Key rock 3 also affects stream velocities, increasing from 2.7 to 3.1 feet per second as water passes over the rock, and decreasing to 2.7 feet per second downstream of the rock. The boulder BLDR0 is not completely submerged at this flow, creating divergences in the velocity vectors in the middle of the channel (Figure 55). The velocity directly behind the peak of BLDR0 is zero, and the velocities downstream of BLDR0 drop to a minimum of 0.2 feet per second. Velocities quickly return to around 3 feet per second as the flow goes over the first rock

weir downstream of the crossing outlet. The velocities upstream of BLDR0 are also around 3 feet per second, and the velocities on the left and right sides of BLDR0 reach 4 feet per second.

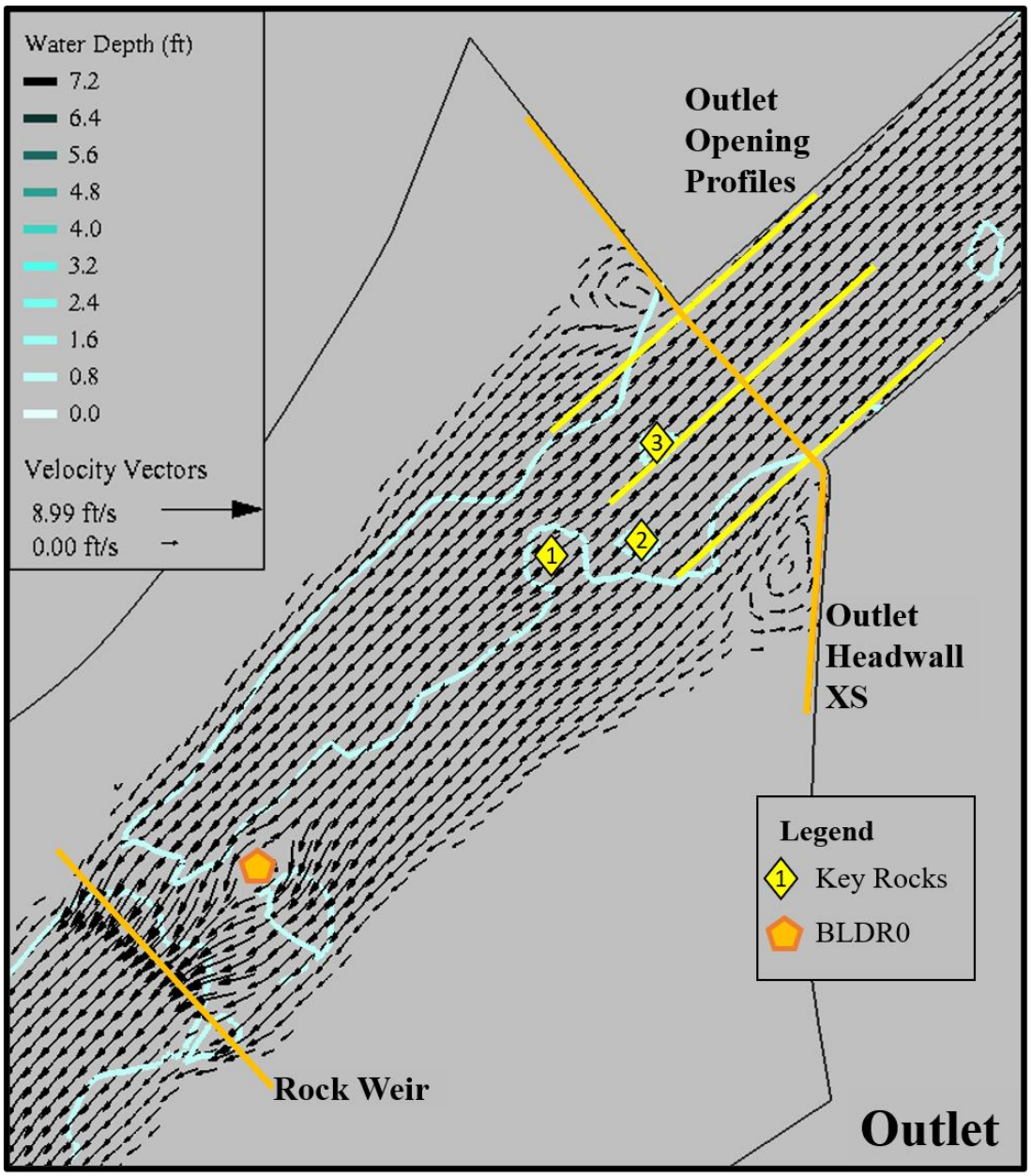

Figure 55. North Fork Ryan Creek crossing outlet location, 2-year return period flow water depth (feet) contour lines with velocity vectors.

During the 25-year return period flow of 170 cfs, the eddies increase in size both laterally and longitudinally, but the locations of the eddies remain the same as in the 2-year flow (Figure 56). The increase in size of the right bank eddy is more pronounced and is likely an effect of the slight angle of the crossing. The velocities along the outlet headwall range from 0.25 to 1.4 feet per second. The maximum velocity moving upstream along the right bank towards the headwall is 2.55 feet per second. That water then turns at the headwall, moving downstream with the main channel flow. Moving from the edge of the right eddy to the middle of the channel, the velocity increases at the right edge of outlet opening, from 0.5 to 7.0 feet per second, and remains around 7.0 feet per second in the middle of the channel (Figure 59). Continuing towards the left bank, the velocity decreases to 2.3 feet per second at the left edge of the outlet, where the left bank eddy begins. The velocities drop moving left towards the center of the eddy, and then increase to a maximum of 2.3 feet per second flowing in the upstream direction towards the headwall at 1.1 feet from the left bank water's edge. The edge velocities adjacent to the zero-boundary condition on the banks are 0.8 and 1.3 feet per second for the right and left banks, respectively.

Similar to the 2-year flow, results spanning 10 feet upstream and downstream of the crossing opening show a decrease in water depth as water exits the crossing in the 25-year flow. During the 25-year flow the water depth entering the middle of the crossing decreases from 2.3 feet to 1.7 feet at 10 feet upstream into the crossing to 6 feet downstream of the outlet opening, respectively. At 6 feet downstream of the crossing outlet opening, the water is above key rock 3, so water depth increases to 1.9 feet as the

topography drops down between key rock 1 and 3. The velocity increases moving out of the crossing, with an increase from 6.2 to 7.0 feet per second from 10 feet upstream in the crossing to the opening. Another increase in velocity from 7.0 to 7.2 feet per second occurs from 4 feet to 6 feet downstream (above key rock 3) of the opening. The velocity then begins decreasing to 6.3 feet per second at 10 feet downstream of the crossing, where water depths increase between key rock 3 and key rock 1. Velocity then decreases to 5.2 feet per second immediately downstream of key rock 1.

In the 25-year flow, BLDR0 is submerged by at least 0.62 feet of water and continues to obstruct flow. Velocities following BLDR0, decrease to 6.1 feet per second compared to velocities of 7.0 feet per second adjacent to BLDR0 on the left and right. Water flowing over BLDR0 reaches a maximum of 7.7 feet per second, starting from 6.0 feet per second immediately upstream of the boulder.

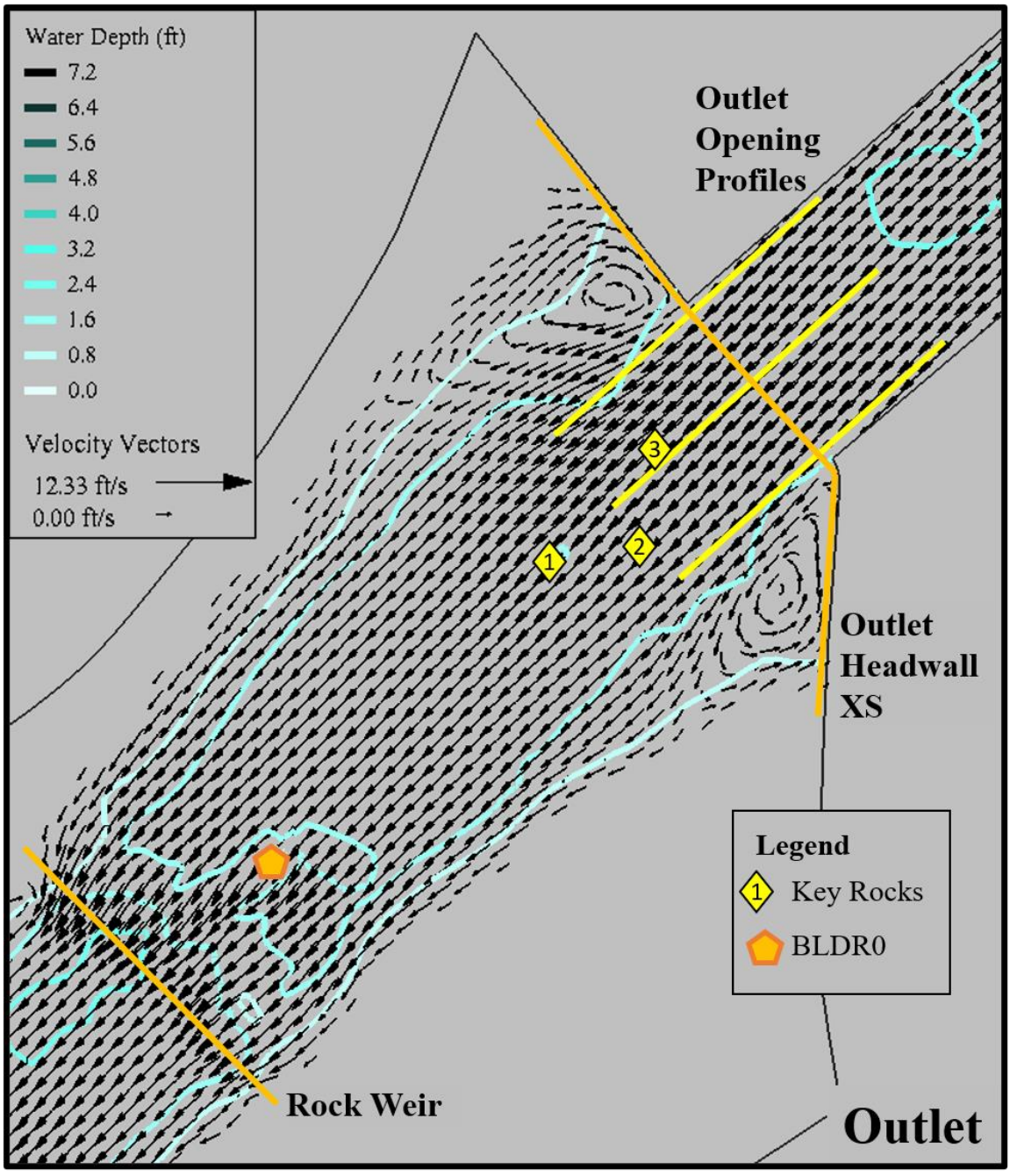

Figure 56. North Fork Ryan Creek crossing outlet location, 25-year return period flow water depth (feet) contour lines with velocity vectors.

During the 100-year return period flow of 263 cfs, the eddies remain at the same locations and only increase in size laterally (Figure 57). The maximum velocity moving upstream along the right bank towards the headwall is 3.41 feet per second. Moving from the edge of the right eddy to the middle of the channel, the velocity drastically increases at the beginning of the outlet, from 0.7 to 8.6 feet per second. The velocity increases moving towards the middle of the channel to a maximum velocity of 9.6 feet per second. Continuing towards the left bank, the velocity decreases drastically once again from 8.3 to 0.3 feet per second at the boundary of the outlet, where the left bank eddy begins. The velocities decrease moving towards the center of the eddy, and then begin to increase to 3.03 feet per second flowing in the upstream direction towards the headwall, until decreasing to zero velocity at the edge of water on the left bank. The edge velocities adjacent to the zero-boundary condition along the banks are 1.6 and 1.4 feet per second for the right and left banks, respectively.

Similar to the 2-year and 25-year flow, results spanning 10 feet upstream and downstream of the crossing opening show a decrease in water depth as water exits the crossing in the 100-year flow. During the 100-year flow the water depth exiting the middle of the crossing decreases from 3.0 feet to 2.5 feet. The velocity increases when exiting the crossing, with an increase from 7.4 to 9.5 feet per second from 10 feet upstream in the crossing to 6 feet downstream of the opening, above key rock 3. Velocity then begins to decrease to 8.6 feet per second at 10 feet downstream of the opening.

In the 100-year flow, key rocks 1 and 3 continue to affect velocities exiting the crossing opening. BLDR0 is submerged under a minimum of 0.9 feet of water, and still

influences water velocities. The maximum velocities shift to the downstream end of the obstructions. Velocities increase from 9.0 to 9.5 feet per second, moving from upstream of key rock 3 to above the downstream end of the rock, and then decrease to 7.4 feet per second between key rock 1 and 3. The velocity above the downstream end of key rock 1 increases to 7.7 feet per second before decreasing to 6.4 feet per second for the next 15-foot section of channel downstream. At BLDR0 velocities increase from 7.4 feet per second upstream of the boulder to 8.9 feet per second at the downstream end of the boulder. Velocities decrease to 7.7 feet per second following BLDR0, but quickly increase to above 10 feet per second because of the rock weir downstream.

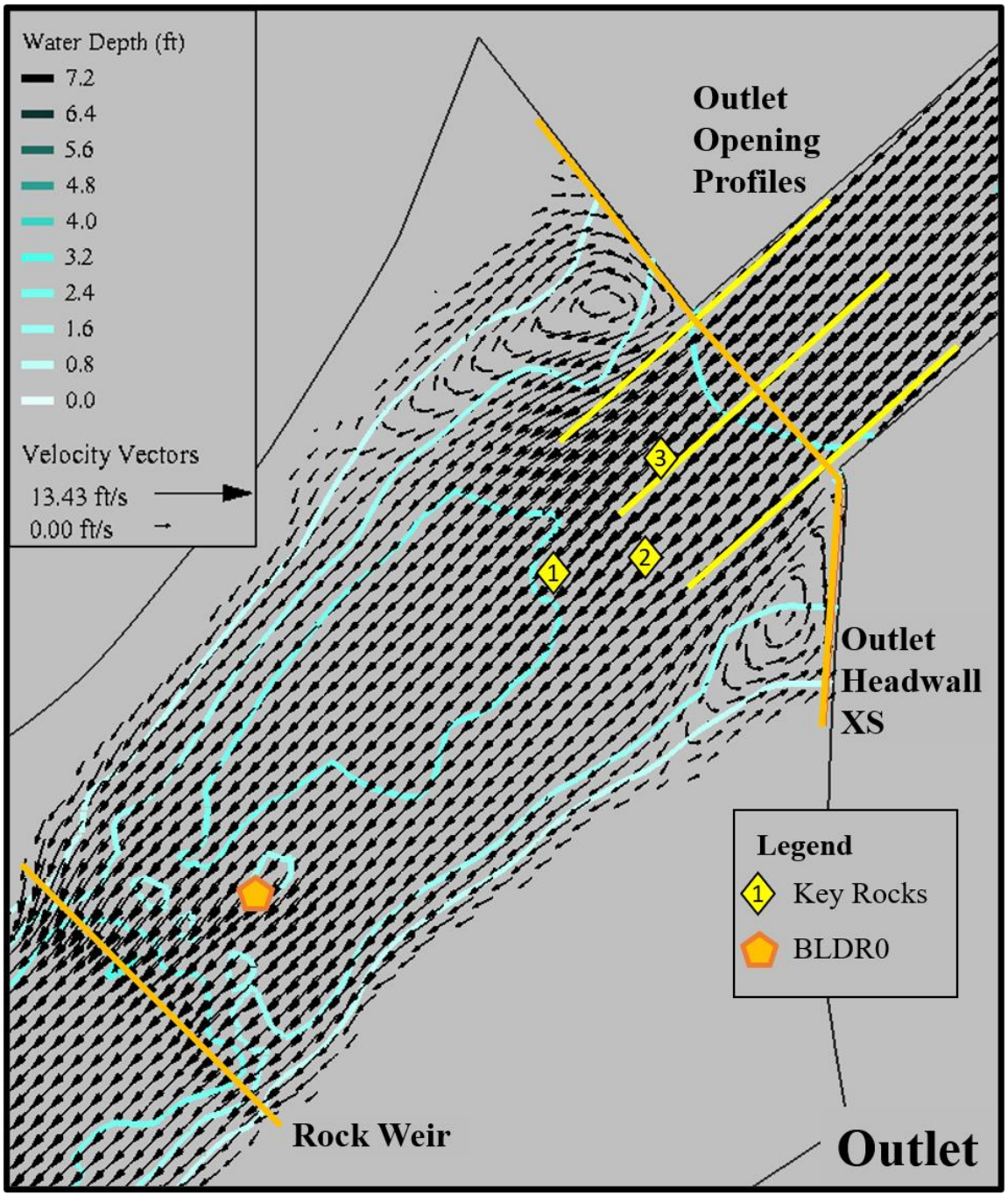

Figure 57. North Fork Ryan Creek crossing outlet location, 100-year return period flow water depth (feet) contour lines with velocity vectors.

The crossing inlet results span the channel from left to right bank in Figure 58. On the left and right sides, the depth increases moving away from the banks and into the main channel, until the water depth increases rapidly at the opening of the crossing inlet. The water depth exiting the outlet is slightly greater on the right, by about 0.2 feet. The deepest water depths are located at the center right side of the crossing opening for the 2-, 25-, and 100-year flow, respectively. Average water depth across the inlet opening increases from 1.0 feet during the 2-year flow to 2.0 feet during the 25-year flow to 2.4 feet during the 100-year flow.

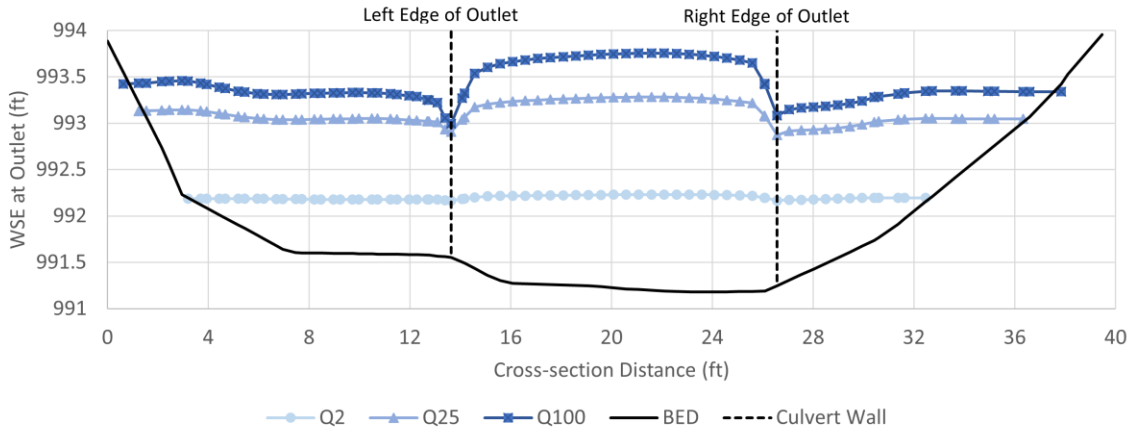

Figure 58. Water surface elevations, in feet, at the crossing outlet headwall (appx. 0.2 feet from the structure boundary) for the 2-, 25-, and 100-year return period flows. Flow direction is moving into the page.

Similar to the crossing inlet, the velocities next to the crossing outlet headwall (approximately 0.2 feet away from the structure boundary) change exponentially at the outlet opening. The velocities increase from 0.5, 1.3, and 1.9 feet per second adjacent to the opening to 2.7, 6.5, and 8.3 feet per second at the edge of the opening in the 2-, 25-, and 100-year flows (Figure 59). Moving through the crossing, the average velocities

changed from 2.6, 4.6, and 5.5 feet per second at the inlet to 2.6, 6.5, and 8.2 feet per second at the outlet for the 2-, 25-, and 100-year flows (Figure 54 and Figure 59).

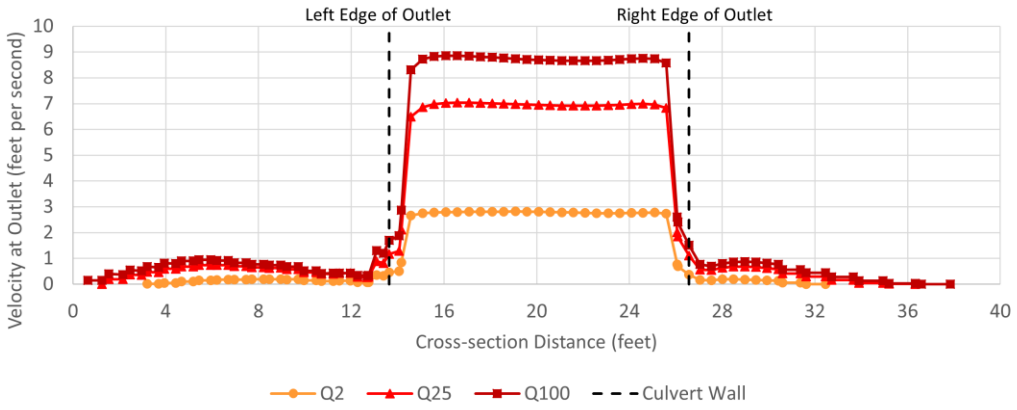

Figure 59. Velocities at the crossing outlet headwall cross-section (appx. 0.2 feet from the structure boundary) for the 2-, 25-, and 100-year return period flows.

Scour potential

The potential for scour to occur was estimated for both study sites at the simulated flow events using critical velocities for the site-specific substrate (RSP and streambed) and comparing these to velocities predicted by the 2-D model simulations. RSP and streambed sizing methods were also used to determine if differences in water depths and velocities affected the recommended substrate sizes based on both the 2-D and 1-D modeling results. Additionally, the abutment scour estimates for the Little Mill Creek bridge were compared for the 2-D and 1-D modeling results.

Little Mill Creek

At Little Mill Creek bridge scour potential was estimated for the left bank RSP, rock weirs, streambed, and the abutments during high flows. During the 100-year return period flow, the average channel velocity predicted using SRH-2D is 12.0 feet per

second, which is first adjusted for the orientation angle of the channel leading towards the left bank RSP. In this case, the adjustment factor for the average velocity is 1.33 because of the impinging flow from the stream orientation in relation to the bank. The adjusted velocity of 15.96 feet per second results in a required stone weight of 1,093 pounds. A ½-ton is 1,000 pounds, so the recommended RSP is sized up a class to 1-ton. When using edge velocities under the bridge during the 100-year flow, of 8.0 feet per second on the right bank and 6.9 feet per second on the left bank, the resulting recommended RSP size is ‘Light’ for the top of both banks (‘Light’ RSP size is equivalent to a minimum stone weight of 200 pounds, see

APPENDIX D.1). This would suggest that the installed rock at the top of the bank could be a lower class than at the toe of the bank slope. While using the velocity above the left bank RSP toe line at the 100-year flow of 14.0 feet per second, the resulting required stone weight is 498 pounds. A ¼-ton is 500 pounds, so the recommended RSP is sized at ¼ -ton. However, it would be practical to size up to the ½ -ton RSP size because the calculation of minimum stone weight is sensitive to velocity values and the model result velocities are estimates. Using the new Caltrans RSP size standards, the recommended RSP size is 3/8-ton, which correlates to a diameter 3 inches less than the old standard recommended size.

The rock weirs were designed with a crest of 2-ton rock, layered on top of 1-ton footing rock, and placed on coarse aggregate or competent streambed material. The shear stress at the first rock weir is approximately 5.8 pounds per square foot during the 100-year flow, while the critical shear stress for a 2-ton rock is 15.7 pounds square foot and for a 1-ton rock is 13.2 pounds per square foot.

The streambed is expected to be mobile during the 2-year flow and above. The critical shear stress for entrainment of the D_{84} particle is 0.98 pounds per square foot. During the 2-year flow, maximum shear stress in the reference reach is 3.3 pounds per square foot, while shear stress within the crossing reaches 6.4 pounds per square foot (near the first rock weir at XS4) and 5.4 pounds per square foot against the right bank sediment deposits.

Scour at the bridge abutments was calculated using live-bed contraction scour equations because a critical velocity analysis determined the bed was mobile between the

2-year to the 100-year flows. Additionally, the abutments are covered by ¼-ton RSP slopes and the exposed portions of the abutments are out of the floodplain. A critical velocity analysis of the RSP found it to be stable because critical velocity was greater than the average channel velocities (and even the maximum velocities). The estimated abutment scour depth is 1.7 feet during the 25-year flow and 3.9 feet during the 100-year flow. These results differ from the Caltrans' scour analysis that determined there was an abutment scour depth of zero feet. The difference could be due to using local unit discharges (from velocity and water depth) in flow adjacent to the abutment compared to using an average velocity and water depth, but the 1-D calculations are not available to confirm this explanation. The difference could also be due to a smaller cross-sectional shape resulting from the deposition under the crossing.

North Fork Ryan Creek

At North Fork Ryan Creek culvert, scour potential was estimated at the upstream rock weir, the RSP upstream of the crossing inlet, and the streambed throughout the crossing. The rock weirs were designed as ½ -ton rock with Backing Class No. 1 as footing and interstitial filling (AECOM, 2014). The shear stress at the upstream rock weir is a maximum of 9.7 pounds per square foot during the 100-year flow. Using the 9.7 pounds per square foot as a critical shear stress, the minimum diameter of rock weir material is 1.75 feet, which corresponds to a $^{3}/_{8}$-ton rock size. With a footing of Backing Class No. 1, the critical shear is 3.9 pounds per square foot, which is less than the 5.6 pounds per square foot bed shear stress downstream of the weir during the 2-year flow and 9.9 pounds per square foot during the 100-year flow. The ½-ton rock will remain

stable, but the footing is Backing Class No. 1 which has the potential to become mobile during the 100-year event and undermine the ½-ton rock. With the size of material used in the footing expected to be mobile during the 100-year flow, the bed is also expected to be mobile. If the bed scours downstream of the rock weir and the footing is not buried sufficiently, failure of the rock weir might occur.

During the 100-year return period flow, the average velocity in the channel reach, upstream of the crossing and downstream of the rock weir, is 4.14 feet per second. The velocity is adjusted by a factor of 0.67 because the flow is parallel to the RSP banks and the resulting recommended RSP size is the smallest of the standard RSP sizing, Backing Class No. 3. While using the velocities above the RSP toe lines at the 100-year flow of 7.8 feet per second on the right bank and 8.0 feet per second on the left bank, the resulting recommended RSP size is Backing Class No. 2. Using the new Caltrans standard RSP sizes, the weight is below the D_{50} weight range for any of the standard RSP Class groupings.

The scour at the culvert walls was calculated using live-bed abutment scour equations. A critical velocity analysis determined the bed subgrade layer was not mobile between the 2-year to the 100-year flows; however, the abutments are within the active channel, so the live-bed equations are applicable. The estimated abutment scour depth is 0.5 feet during the 25-year flow and 1.0 feet during the 100-year flow.

The streambed in the crossing experiences average bed shear stress of 0.4 pounds per square foot during 2-year flows (maximum of 0.7 pounds per square foot) and 1.5 pounds per square foot during the 100-year flows (maximum of 3.4 pounds per square

foot). During the 2-year flow, shear stress is mostly uniform through the crossing and through the outlet downstream, while the inlet and upstream have higher shear stress (up to 2.4 pounds per square foot). During the 100-year flows, the shear stress increases moving downstream in the crossing, with an average of 1.5 pounds per square foot in the upstream half of the crossing and reaching an average of 2.0 pounds per square foot 20 feet from the downstream outlet and a maximum of 3.4 pounds per square foot exiting the outlet opening. There is the potential for scour downstream of the outlet, with a maximum bed shear stress of 4.2 pounds per square foot predicted approximately 7 feet downstream of the outlet opening. The design did include RSP backfill placed under the clean sand and gravel layer at the outlet because of previous severe scour (AECOM, 2014). During the 100-year flow, a streambed with a D_{50} of 3.4-inch rock (classified 'fine cobble') would be expected to be mobilized in the crossing. Near the outlet of the crossing, a streambed of 7.4-inch rock (classified 'coarse cobble') would be expected to mobilize at the outlet of the crossing.

Sensitivity Analysis

A sensitivity analysis on model inputs and simulation properties was conducted to identify parameter values and their impact on simulation predictions. The parameters and simulation properties evaluated included Manning's roughness values, mesh size, and model simulation timestep. The range of conditions assessed is summarized in Table 15. This section describes the results from these sensitivity analyses.

Table 15. Summary of sensitivity analysis parameters, the change in the value, and the use of the changed parameter within the model.

Parameter	Parameter Change	Use of Changed Parameter
Manning's roughness value	+/- 0.005	Entire model material coverage
Manning's roughness value	+/- 0.005	Streambed material coverage
Manning's roughness value	+/- 0.005	RSP material coverage
Mesh size	30,000 to 120,000 elements	Mesh Generator Coverage
Model simulation timestep	1.0 seconds 0.5 seconds 0.1 seconds	Model setup

Manning's roughness

The sensitivity analysis for the Manning's roughness values included twelve simulations per site to analyze three variations to materials roughness values: (1) the entire model domain surface, (2) only the RSP regions, and (3) only the active channel streambed. The Manning's roughness values were increased or decreased by 0.005 for each sensitivity analysis simulation. For each of the material variations, the 2-year and 100-year return period flows were evaluated to examine the extremes for the model simulations. The simulations run with a model-wide increase or decrease of the Manning's roughness value were to show the overall effect of roughness on the stream hydraulic conditions. The simulations run with an increase or decrease of the streambed or the RSP were to show the effect of changing roughness values at boundaries of the material coverages.

Little Mill Creek

The Little Mill Creek model has four materials coverages, consisting of RSP, streambed, vegetation – trees, and vegetation – grass (Figure 16). The base case Manning's roughness values associated with each of the four materials are summarized in Table 16. The sensitivity analysis examines a 0.005 decrease and a 0.005 increase in Manning's roughness values. The water depth and velocity results figures are shown as differences, sensitivity analysis simulation minus base case simulation results (see results figures in

APPENDIX C.3).

Table 16. Materials coverages and associated Manning's roughness values for Little Mill Creek.

Material	Manning's roughness, n
RSP	0.050
Streambed	0.045
Vegetation - trees	0.060
Vegetation - grass	0.030

In all Manning's roughness sensitivity analysis runs, the greatest changes in water depth and velocity occur near a grade control feature 25 feet upstream of the crossing and in a pool downstream of the upstream debris reach, approximately 200 feet upstream of the crossing. In general, when material roughness values were decreased, water depths decreased and velocity increased, and vice versa.

For the 2-year return period flow of 529 cfs, water depths decrease on average by 0.13 feet (Table 17). With an increase of 0.005 in the materials coverage roughnesses, water depth on average increases by 0.13 feet. Velocities increase by an average of 0.31 feet per second with a decrease of 0.005 in the Manning's roughness for the entire model domain's materials coverages (Table 17). With an increase of 0.005 in the entire model's materials coverage roughnesses, velocity decreases by a maximum of 2.52 feet per second and an average of 0.26 feet per second.

Table 17. Little Mill Creek, Q2. The change in water depth and velocity results from base case due to increases and decreases of 0.005 in Manning's roughness value over the

model domain. The water depth and velocity differences are presented for locations of interest along with the average of maximum differences.

Manning's Roughness Change	**-0.005**	**-0.005**	**+0.005**	**+0.005**
Location	**Water Depth Diff. (ft)**	**Velocity Diff. (fps)**	**Water Depth Diff. (ft)**	**Velocity Diff. (fps)**
Grade Control 25' US of Crossing	-0.81	+3.48	+0.55	-0.85
Pool DS of US Debris Reach	-0.11	+2.39	+0.51	-2.52
Average over model domain	-0.13	+0.31	+0.13	-0.26

For the 100-year return period flow of 1,955 cfs, a decrease of 0.005 in the Manning's roughness causes water depths to decrease by an average of 0.22 feet (Table 18). The maximum changes from the base case occur at both the location downstream of the grade control feature near the upstream bridge face and at a pool downstream of the large woody debris deposited in the stream channel. The only increases in water depth are located on the floodplain and on the deposits. The increases could be due to water reaching elements that were not previously 'wet' in the base case scenario because of a lower resistance to flow. With an increase of 0.005 in the entire model's materials coverage roughnesses, the increase in water depth from the base case is an average of 0.20 feet.

Table 18. Little Mill Creek, Q100. The change in water depth and velocity results from base case due to increases and decreases of 0.005 in Manning's roughness value over the

model domain. The water depth and velocity differences are presented for locations of interest and the average and maximum differences.

Manning's n Change	**-0.005**	**-0.005**	**+0.005**	**+0.005**
Location	**Water Depth Diff. (ft)**	**Velocity Diff. (fps)**	**Water Depth Diff. (ft)**	**Velocity Diff. (fps)**
Grade Control 25' US of Crossing	-1.2	+3.0	+0.77	-2.0
Pool DS of US Debris Reach	-1.2	+3.1	+1.3	-2.0
Average over model domain	-0.22	+0.38	+0.20	-0.31

Velocities increase when Manning's roughness values are decreased during the 100-year flow. At the downstream end of a large woody debris deposit velocity increases by 3.1 feet per second (Table 18). The majority of velocity decreases occur on the water's edge and on the floodplain terrace. On average over the entire model domain, velocities increase by 0.38 feet per second. With an increase of 0.005 in the entire model's materials coverage roughnesses, the velocity decreases on average by 0.31 feet per second (Table 18). The maximum change occurs downstream of the grade control feature upstream of the crossing and downstream of in-stream large woody debris. The dark stretches along the left bank under the crossing and both banks downstream of the crossing are increases in velocity by up to 8.5 feet per second, which occur because the wetted boundary has expanded to areas that were not 'wet' in the base case simulation.

The water depth difference ranges span over positive and negative values largely because of the conditions after the exit boundary condition, which is not relevant to the

model (Figure 60). The exit boundary condition is the edge of the controlled flow within the model, so any flow downstream of the exit boundary condition is not bounded by any set conditions and therefore produces unreliable results in those areas.

The changes in roughness over the entire model and the active channel bed roughness result in similar water depth results because the streambed is a majority of the model domain area. However, the 2-year flow depths with a decrease in the streambed roughness values have a significantly larger upper range because the water depth increases after the exit boundary condition. The velocity difference ranges vary from positive to negative values because of the presence of the eddies forming in the inundated floodplains; shifts in the eddy locations between the sensitivity analysis simulations both increase and decrease predicted local velocity values (Figure 61). The changes in roughness on the entire model and the bed roughness result in similar velocity results because the streambed is a majority of the model domain area. A change in only RSP roughness results in less change in both water depth and velocity relative to changing the entire model domain roughness values or the streambed roughness values. The RSP makes up less area than the streambed within the model domain.

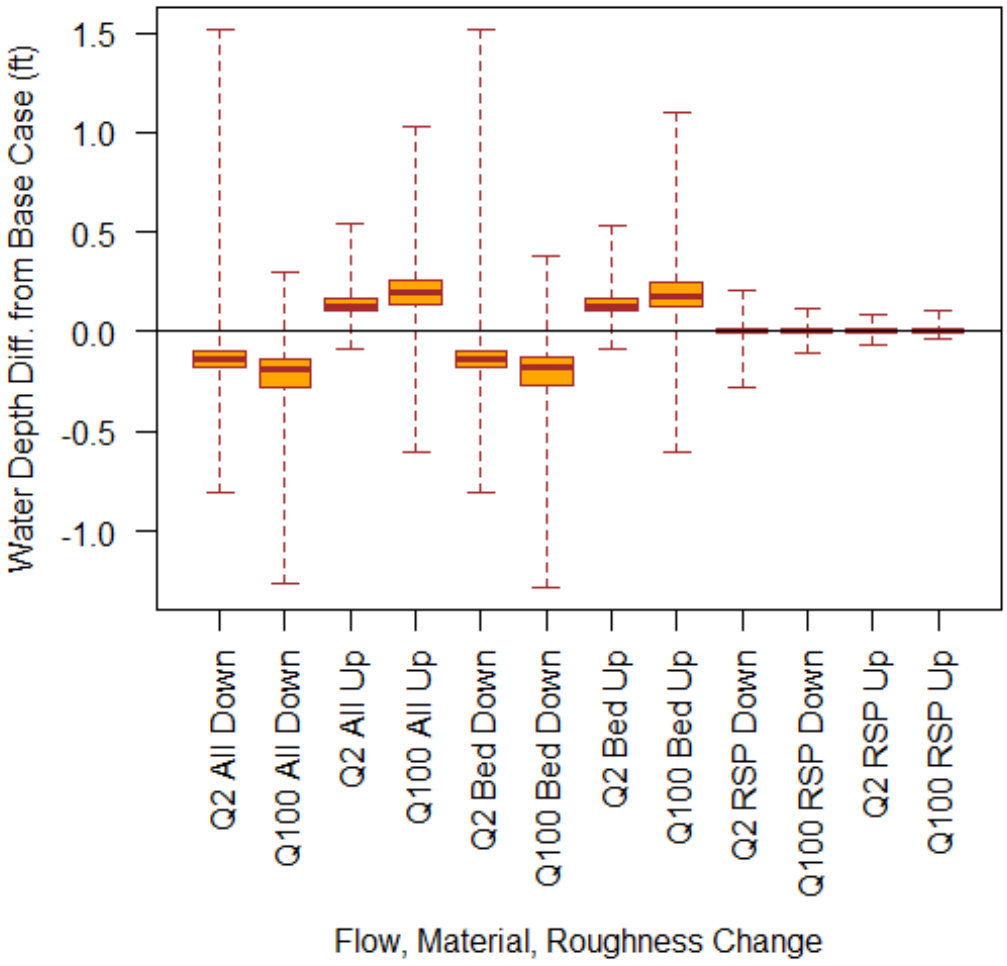

Figure 60. Range of water depth differences from base case (in feet) for the 2-year flow and the 100-year flows, with increases (up) and decreases (down) of 0.005 in Manning's roughness coefficient for the entire model, the streambed, and the RSP, independently.

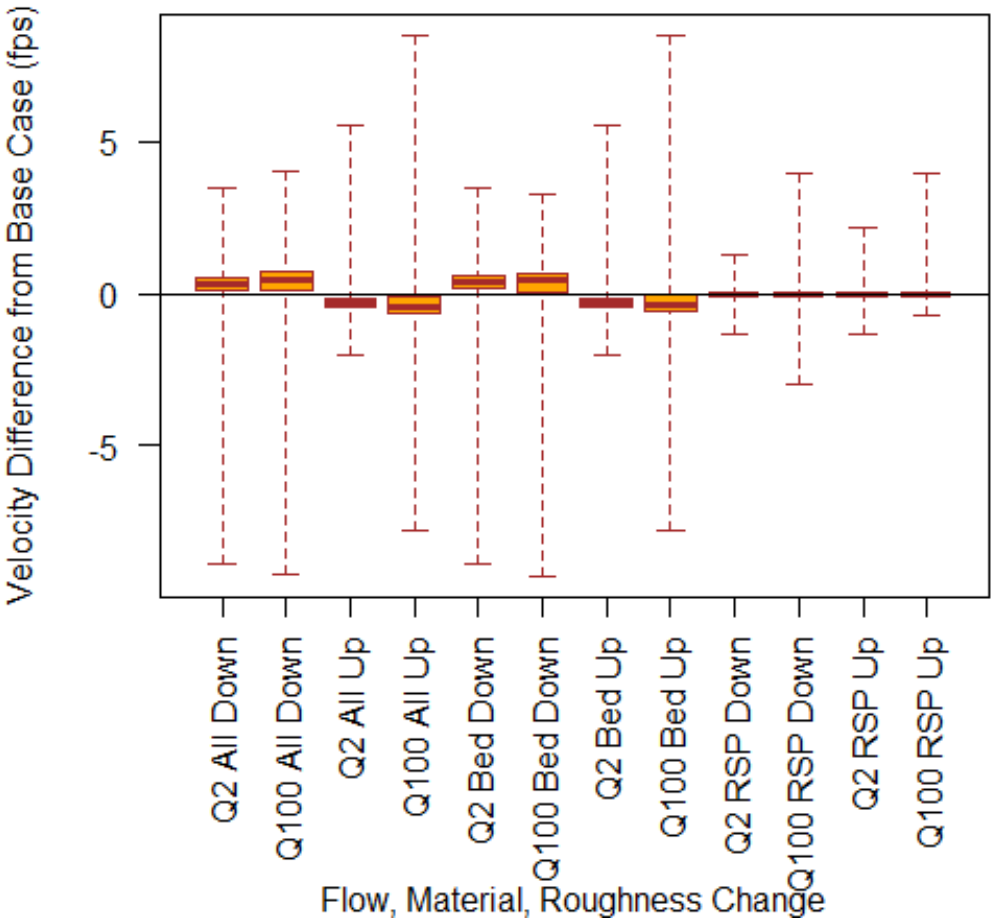

Figure 61. Range of velocity differences from base case (in feet per second) for the 2-year and 100-year flows, with increases (up) and decreases (down) of 0.005 in Manning's roughness coefficient for the entire model, the streambed, and the RSP, independently.

North Fork Ryan Creek

The North Fork Ryan Creek model included five materials coverages, consisting of RSP, streambed – gravel, streambed – silt, vegetation – trees, and vegetation – grass (Figure 17). The base case Manning's roughness values associated with each of the five materials are summarized in Table 19. The sensitivity analysis results for the changed Manning's roughness values are presented in

APPENDIX C.3. The water depth and velocity results are shown as differences, sensitivity analysis simulation minus base case simulation results.

Table 19. Materials coverages and associated Manning's roughness values for North Fork Ryan Creek.

Material	Manning's roughness, n
RSP	0.050
Streambed – gravel	0.045
Streambed – silt	0.035
Vegetation – trees	0.060
Vegetation – grass	0.030

Water depths decrease with a decrease of 0.005 in the Manning's roughness for the entire model domain's materials coverages (Table 20). For the 2-year return period flow of 33 cfs, water depths decrease by a maximum of 0.13 feet and on average by 0.04 feet when Manning's roughness is decreased by 0.005. With an increase of 0.005 in the materials coverage roughnesses, water depth increases by a maximum of 0.11 feet and on average increases by 0.04 feet.

Velocity experiences the opposite effect as water depth with changes in Manning's roughness values. Velocities increase an average of 0.13 feet per second with a decrease of 0.005 in the Manning's roughness for the entire model domain's materials coverages (Table 20). With an increase of 0.005 in the entire model's materials coverage roughnesses, velocity decreases by an average of 0.11 feet per second.

The increases in water depth are either occurring where the wetted channel width becomes constricted or after relatively rapid drops in elevation. Increases in water depth

correspond to a decrease in velocity, which is generally what is seen in the figures of velocity distribution (see

APPENDIX C.3).

Table 20. North Fork Ryan Creek, Q2. The change in water depth and velocity results from base case due to increases and decreases of 0.005 in Manning's roughness value over the model domain. The water depth and velocity differences are presented for locations of interest, as well as the average and maximum differences.

Manning's n Change	**-0.005**	**-0.005**	**+0.005**	**+0.005**
Location	**Water Depth Diff. (ft)**	**Velocity Diff. (fps)**	**Water Depth Diff. (ft)**	**Velocity Diff. (fps)**
Bottom of US Rock Weir	-0.06	+1.95 (max)	+0.06	-0.39
DS of BLDR1	-0.08	+0.70	+0.07	-0.54
Crossing Inlet Opening	-0.13 (max)	+0.88	+0.11 (max)	-0.68
Base of DS rock weirs	-0.12	+0.87	+0.10	-0.80 (max)
Average over model domain	-0.04	+0.13	+0.04	-0.11

For the 100-year return period flow, the changes in water depth and velocity remain at some of the same locations as the 2-year simulations, with the greatest magnitude of difference occurring immediately downstream of rock weirs; however, not directly at the crossing inlet opening. Additional locations of significant difference occur immediately downstream of BLDR1 further upstream of the crossing inlet and key rocks 1-3 downstream of the crossing outlet.

Water depths decrease with a decrease of 0.005 in the Manning's roughness for the entire model domain's materials coverages (Table 21). For the 2-year return period

flow of 33 cfs, water depths decrease on average by 0.11 feet when Manning's roughness is decreased by 0.005. With an increase of 0.005 in the materials coverage roughnesses, water depth increases on average increases by 0.10 feet.

Velocity experiences the opposite effect as water depth with changes in Manning's roughness values. Velocities increase an average of 0.24 feet per second with a decrease of 0.005 in the Manning's roughness for the entire model domain's materials coverages (Table 21). With an increase of 0.005 in the entire model's materials coverage roughnesses, velocity decreases by an average of 0.20 feet per second.

Table 21. North Fork Ryan Creek, Q100. The change in water depth and velocity results from base case due to increases and decreases of 0.005 in Manning's roughness value over the model domain. The water depth and velocity differences are presented for locations of interest, as well as the average differences.

Manning's n Change	**-0.005**	**-0.005**	**+0.005**	**+0.005**
Location	**Water Depth Diff. (ft)**	**Velocity Diff. (fps)**	**Water Depth Diff. (ft)**	**Velocity Diff. (fps)**
Bottom of US Rock Weir	-0.22	+0.84	+0.21	-0.77
DS of BLDR1	-0.61 (max)	+2.14	+0.40	-1.31
Crossing Outlet	-0.29	+1.90	+0.22	-1.50
Base of DS rock weirs	-0.44	+2.58	+0.41 (max)	-2.75
Average over model domain	-0.11	+0.24	+0.10	-0.20

In all sensitivity analysis runs, it was found that areas immediately downstream of rock weirs and outside of the crossing inlet and outlet experience the greatest change in

water depth and velocity. In general, when material roughness values were decreased, water depth decreases and velocity increases, and vice versa. The water depth difference ranges span over positive and negative values, but the 100-year flows show the general pattern of a decrease in depth with a decrease in the Manning's roughness value (Figure 62). The velocity difference ranges vary from positive to negative values because of the presence of the eddies; shifts in the eddy locations between the sensitivity analysis simulations both increase and decrease predicted local velocity values (Figure 63).

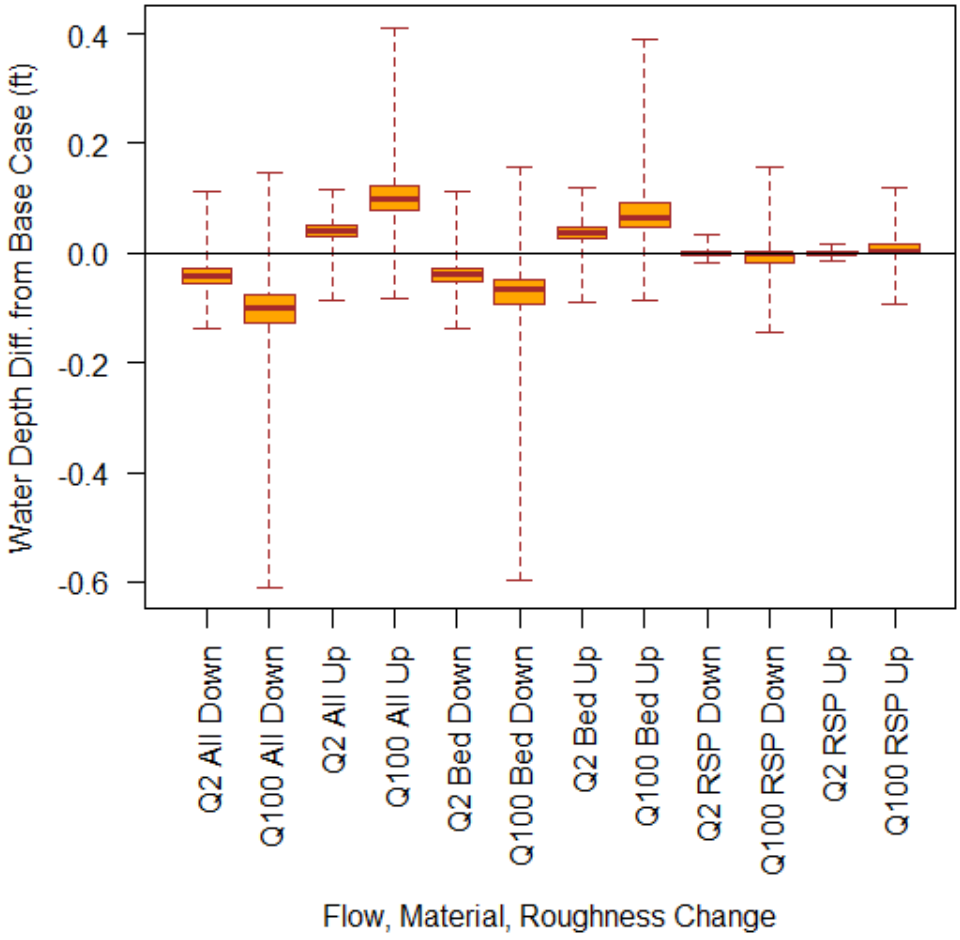

Figure 62. Range of water depth differences from base case (in feet) for 2-year and 100-year flows, with increases (up) and decreases (down) of 0.005 in Manning's roughness coefficient for the entire model, the streambed, and the RSP, independently.

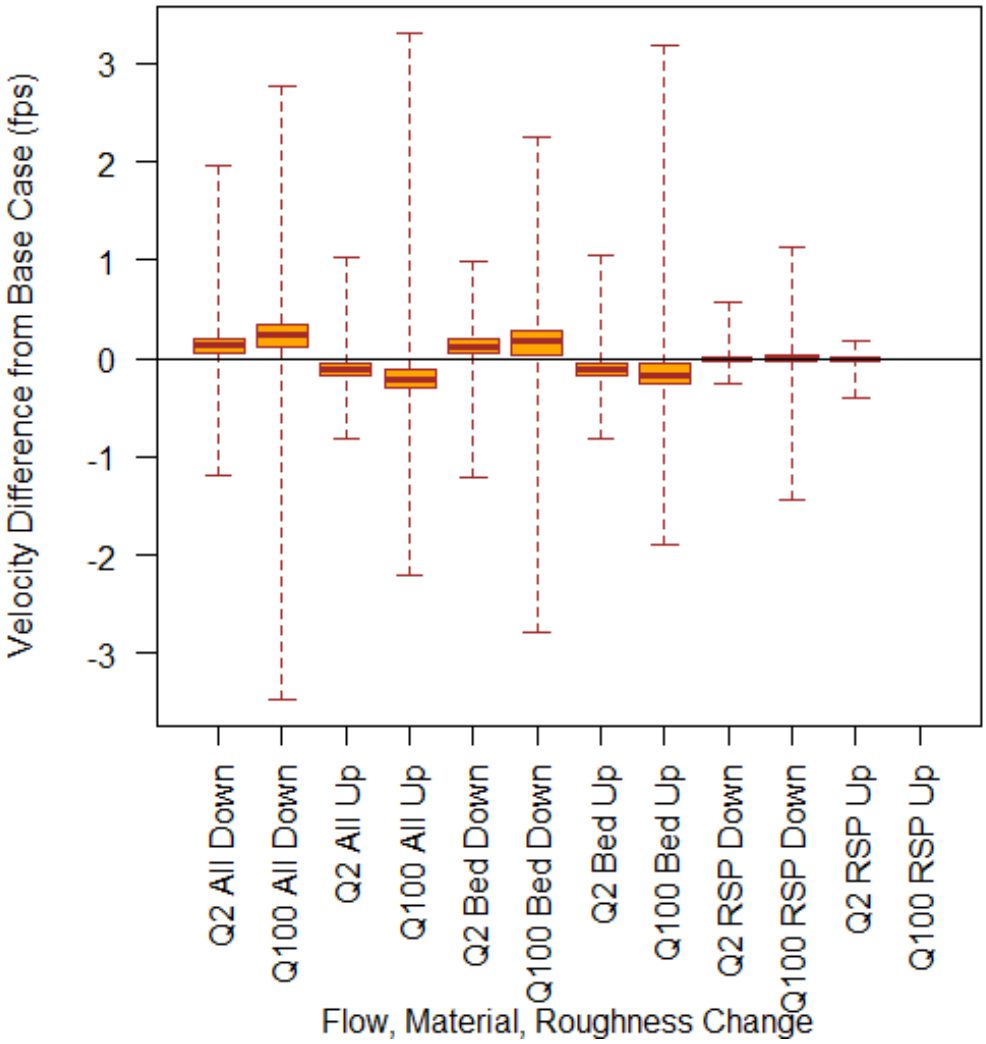

Figure 63. Range of velocity differences from base case (in feet per second) for 2-year and 100-year flows, with increases (up) and decreases (down) of 0.005 in Manning's roughness coefficient for the entire model, the streambed, and the RSP, independently.

Mesh resolution and simulation run time

Meshes with varying numbers of elements were run in similar simulations, to determine the required model computation time. Model computation time increases

linearly as the number of mesh elements increases (Figure 64). The model computation times are from model runs with a timestep of 0.1 seconds and a simulation time period of one hour.

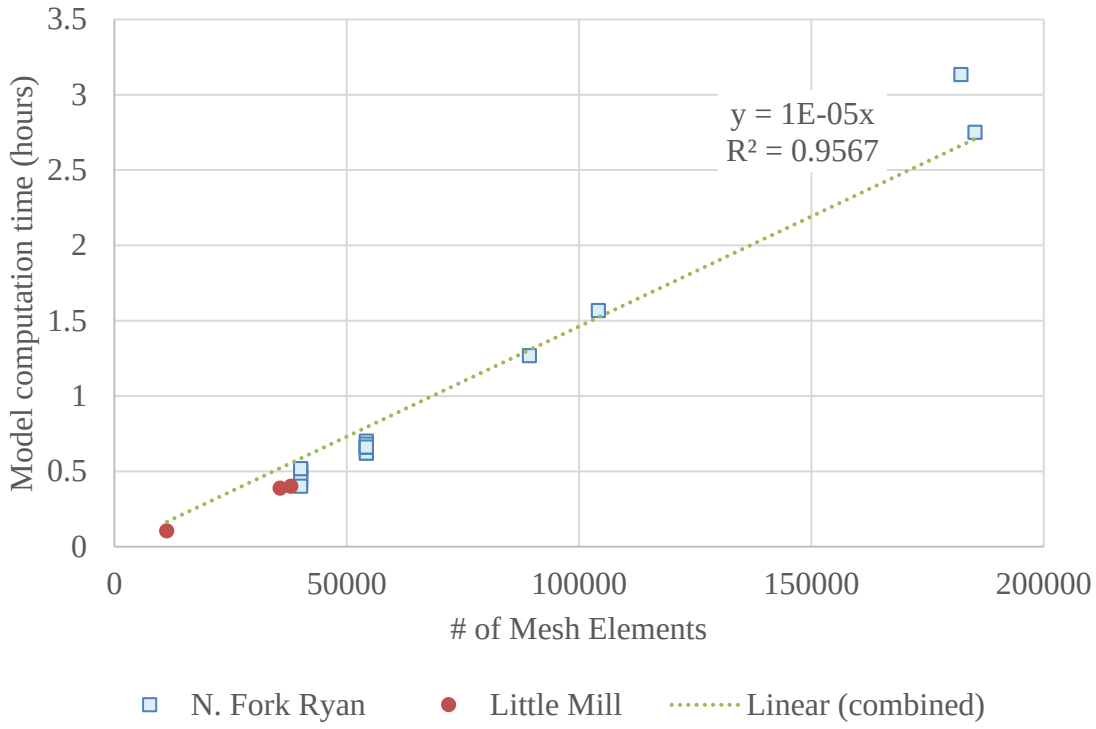

Figure 64. Plot of number of mesh elements (x) with model computation time in hours (y). The Little Mill Creek and North Fork Ryan Creek meshes with simulations runs done had a range of 11,303 to 185,242 elements.

DISCUSSION

This section compares 1-D and 2-D model predictions and design recommendations. Average water depths and velocities are compared directly. The potential for scour on the banks, streambed, and at rock weirs is evaluated and compared with the 1-D model-informed design specifications. Additionally, eddies at the crossing structures are identified and their impact is discussed because these features are not simulated with 1-D models.

A synthesis of 2-D modeling effort is also included, with recommendations for modeling different site scales. Observations of the incremental gains resulting from the number of mesh elements compared to the simulation computer processing time are also discussed.

Average water depths and velocities

The thalweg water depths are compared between the 1-D and 2-D model results to assure comparison of equivalent prediction locations. To compare 1-D and 2-D model velocity results, the average water depths and velocities from 2-D simulations are calculated across cross-sections because 1-D model velocity results are averages over a channel cross-section. The maximum edge velocities from 2-D model results are also discussed because the maximum edge velocities at banks or abutments are more indicative of the shear forces and potential for scour. The 2-D model results presented are

extracted at the Crossing XS for Little Mill Creek and at the Crossing Inlet XS for North Fork Ryan Creek.

Little Mill Creek

At the Crossing XS, the difference between thalweg depths for all analyzed return periods from Caltrans' HEC-RAS 1-D model and from the SRH-2D simulations are shown in Figure 65. The analyzed return periods in the 1-D model are the 10-year, 50-year, 100-year return period flows with no backwater; and the 25-year flow with a 100-year Smith River backwater and 100-year flow with a 25-year Smith River backwater. The analyzed return periods for the 2-D simulations are the 2-, 10-, 25-, 50-, and 100-year flows with no backwater, along with the 25-year flow with 100-year Smith River backwater and 100-year flow with 25-year Smith River backwater. The thalweg water depths predicted by the 1-D HEC-RAS model results are within 0.15 feet of the thalweg depths predicted by the SRH-2D model results, except for the 100-year flow event with a 25-year Smith River backwater which has a 0.34-foot difference. The water depth results from the 1-D and 2-D models are similar, but the larger difference in water depth during the combined 100-year Little Mill Creek and 25-year Smith River event is potentially due to the topography at the confluence with the Smith River. There is likely different topography used for the 2-D and 1-D models because it is a dynamic location that would have changed within the few years between analyses. We do not have the 1-D model or its survey data, so this cannot be verified.

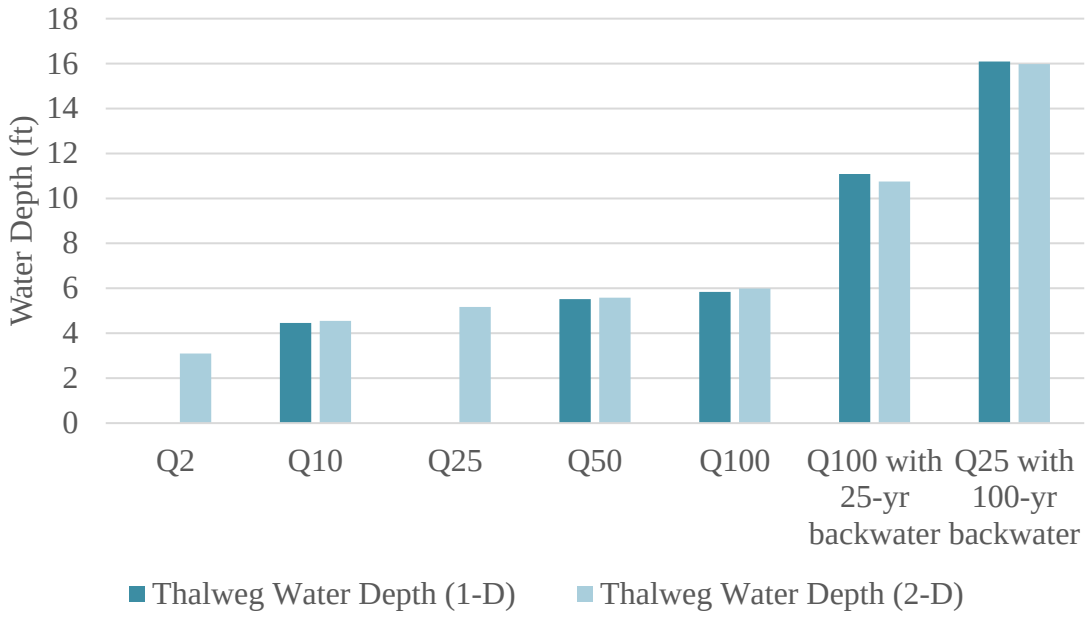

Figure 65. Comparison of thalweg water depth (feet) at the crossing between 1-D and 2-D model results of Little Mill Creek for all simulated flow events.

The difference between average velocities from the 1-D and 2-D models, along with the maximum velocities from the 2-D model at the Crossing XS are compared in Figure 66. The 100-year return period flow without backwatering resulted in the greatest magnitude velocity, with an average channel velocity under the bridge of 12.0 feet per second and maximum velocity of 14.8 feet per second. The average velocities from the 2-D model are significantly lower but are not used for any bed and bank stability analyses because actual bank velocities at specific locations are used. There is not observed data to compare the modeling results to, so it is unclear which is more accurate; however, the higher velocities are more conservative in terms of determining bed, bank, and structural stability. A balance must be found between conservative design and over-design (which would likely be more costly).

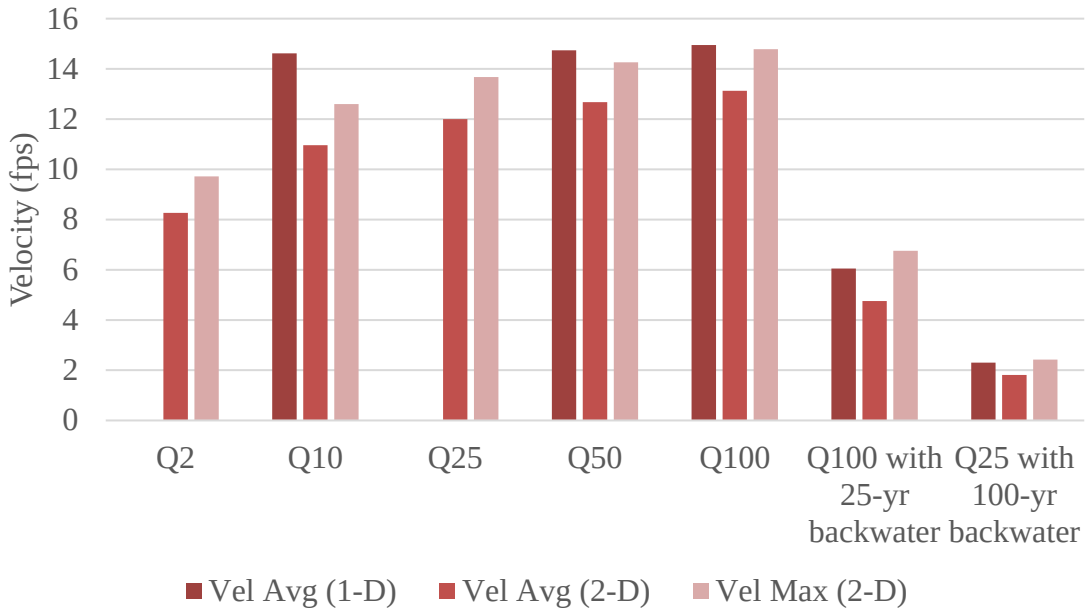

Figure 66. Comparison of velocity (feet per second) averages between 1-D and 2-D and the maximum depth from 2-D modeling of Little Mill Creek for all simulated flow events at the Crossing XS.

Effect of backwater elevation

In the Little Mill Creek 2-D model, the Little Mill Creek 100-year flow coupled with the backwater from the Smith River 25-year event affects Little Mill Creek up to approximately 390 feet upstream from the confluence. With a Little Mill Creek 25-year flow coupled with a Smith River 100-year backwater elevation, the effects are seen even further upstream of the confluence at approximately 710 feet on Little Mill Creek, reaching the surveyed extent.

For the 2-D simulation of a Little Mill Creek 100-year flow and a Smith River 25-year backwater event, the water elevation at the crossing is predicted to be 41.78 feet. The 1-D analysis assumed that the water surface elevation at Little Mill Creek Bridge

would be the same as the Smith River water surface elevation of 42 feet. Because of this the 1-D simulation of this event would likely have estimated an effect extending further upstream than what was predicted in the 2-D simulation, but the 1-D model results were not available to check this.

North Fork Ryan Creek

For the previous analysis of North Fork Ryan Creek done by AECOM for Caltrans, there are limited quantitative results to compare with; however, water surface elevations extracted from a HEC-RAS water surface profile of North Fork Ryan Creek are presented in the Ryan Creek Culvert Replacement Project Final Report (AECOM, 2014). In the Caltrans HEC-RAS model, the water depth at the culvert inlet during the 100-year flow is predicted to be 4.2 feet (Figure C-45 in

APPENDIX C.4). In the 2-D model the prediction is similar to the 1-D model prediction, the maximum water depth expected at the culvert inlet is 4.3 feet (Figure 53). The water surface elevation in both models predicts the 100-year flow will not reach the crown of the culvert and passes through the crossing without entering into pressure flow. The water surface profile from the 1-D HEC-RAS model shows a drop in water surface elevation of approximately 0.9 feet moving into the culvert during the 100-year flow (

APPENDIX C.4). The 2-D SRH-2D model predicts a drop in water surface elevations moving into the culvert of approximately 0.4 feet during the 100-year flow.

The inlet velocity estimated using the 1-D model flow and resulting flow area, is 5.1 feet per second, while the 2-D model results predict the inlet velocity to be 5.8 feet per second. In the 2-D model results, the velocity is greater and the water depth is lower at the inlet than in the 1-D results. The Caltrans report also predicts the velocity range during the 100-year return period flow is 1.5 to 6.9 feet per second at all of the rock weirs. In the 2-D model, the predicted velocity during the 100-year flow is significantly higher, up to 12.3 feet per second at the upstream rock weir. The flow width constricts from 18.0 feet upstream of the rock weir to 12.2 feet downstream of the rock weir between the eddies. The eddies are a dead-zone for downstream flow, so the water passes between the eddies and the velocity would be expected to increase. The 2-D model results account for the presence of these eddies, while the 1-D model results likely use the entire wetted channel width for calculating velocity. The effect of this disparity between the 1-D and 2-D results is further explored in terms of the rock weir sizing in the Scour Potential sub-section.

Scour potential

Little Mill Creek

Currently at Little Mill Creek, all but the most upstream installed rock weirs have been partially washed away and are missing their in-channel rocks. An analysis done on rock weir stability predicted the installed rock weirs (with a 2-ton rock crest over 1-ton

rock and a coarse aggregate footing) to be stable during the 100-year flow. The predicted shear stress was lower than the critical shear stress for the 2-ton and 1-ton rock sizes, but the three downstream weirs were displaced. The weirs could have become unstable if the stream lowered and the footing made of smaller aggregate was exposed or if debris became caught on the weirs and acted as an additional force.

Based on field observations, water flows towards the left bank RSP under the bridge. This is likely occurring because the multiple designed breaks in slope from rock weirs have been washed away and there is a large amount of sediment deposited on the right bank. This flow direction can also be seen in the 2-D model velocity vectors (Figures 34 to 36). The left bank is experiencing scour at the toe of the RSP slope and the RSP is being undercut. The loss of rock weirs, which functioned as grade control, appears to have caused the channel to downcut along the left bank. The scour at the left bank RSP toe is expected to continue because flow continues to be directed preferentially towards the left bank RSP, the material under the RSP layer is exposed, and the left bank experiences velocities up to 14.0 feet per second during the 100-year flow with no Smith River influence based on 2-D model results (Figure 41). Using the 2-D model local velocity results, the recommended surface RSP size for the left bank is ½-ton. The recommended size from the Caltrans analysis is ¼-ton rock, but this layer of rock is now missing from the toe of the installed RSP. The movement may have occurred from scouring of smaller material around and below the larger RSP material.

Caltrans' guideline for RSP sizing does need to be updated to include guidelines for 2-D model result velocities. The current guidelines only explain applying the flow

orientation adjustment factor to average channel velocities (1-D results), while the local velocities resulting from the 2-D model would likely also need an adjustment factor. The flow orientation is just as important as the speed of the water in terms of rock stability, so the benefits of 2-D model local velocity results may be negated by the lack of an adjustment factor specific to 2-D model results.

RSP was also sized based on edge velocities during the 100-year flow, and resulted in 'Light' class RSP being recommended. This suggests that the installed RSP at the top of the banks could be lower. A 2-D model could potentially allow for estimating velocities, and thereby rock sizes, from the toe to the top of the RSP. This could allow for a decreasing rock size and thickness going up the slope (and therefore cost savings).

On the right bank, stream sediment deposits form a terrace under the bridge. The sediment deposition was caused by backwatering of Little Mill Creek from the confluence with the Smith River (approximately 100 feet downstream), and the steep slope of the deposited terrace was likely carved by flow in the main channel after the backwatering recedes. The formation of this sediment deposit caused the cross-sectional area under the bridge to decrease from design conditions and therefore may affect local velocities on the opposite bank. The 2-D model used in this analysis accounted for the sediment deposit in the topography; however, there is potential for 2-D models to predict locations of sediment deposition where eddies form, which is discussed in more detail in the next section.

The abutment scour depth is estimated at 1.7 feet during the 25-year flow and 3.9 feet during the 100-year flow using the 2-D model results. These results differ from the

Caltrans' scour analysis using 1-D model results that determined there was an abutment scour depth of zero feet; however, there was scour observed at the site in 2020. The difference could be attributed to the inclusion of the sediment deposition under Little Mill Creek Bridge in the 2-D model, while the 1-D model was created with the original design topography. The sediment deposit would reduce the cross-sectional flow area under the bridge and likely affected the model predictions of water depth and velocity. The difference could also be due to the lower water depths and velocities resulting from the 1-D hydraulic modeling, but the 1-D analysis calculations are not available so this cannot be verified.

North Fork Ryan Creek

North Fork Ryan has the potential for scour at the upstream rock weir, the RSP upstream of the crossing inlet, and the streambed in the culvert.

The rock weirs are designed with ½-ton rock and Backing Class No. 1 for interstitial fill and the footing. The ½-ton rock was embedded at least 1.5 feet. The rock weir closest to the crossing inlet, about 14 feet upstream, has been washed out. The AECOM report states the rock weirs experience a velocity range of 1.5 to 6.9 feet per second during the 100-year flow, while 2-D modeling predicts a velocity of 12.3 feet per second at the middle of the crest on the most upstream rock weir during the same flow (AECOM, 2014). The footing of the upstream rock weir has a critical shear stress of 3.9 pounds per square foot (the shear stress at which the particle would begin to move), which is less than the bed shear stress downstream of the weir of 5.6 pounds per square

foot during the 2-year flow and 9.9 pounds per square foot during the 100-year flow. Bed scour downstream of the upstream rock weir is cause for concern because, if the bed scours, the critical shear stress required to move the rock weir footing is less than that of the bed shear stress. The current bed elevation drop (from weir crest to the streambed just downstream of the weir) at this weir is 2.8 feet, 0.8 feet more than the typical 2.0 feet stated in the as-builts, suggesting that there has been downstream bed erosion, but not yet enough for weir failure (AECOM, 2014)(see APPENDIX E for as-built design drawings). If the rock weir were to collapse it would create head cut potential upstream.

Upstream of the crossing, the 2-D model predicts that the bank RSP experiences velocities up to 7.8 feet per second on the right bank and 8.0 feet per second on the left bank at the 100-year design flow. From the 2-D modeling results, the recommended RSP size is Backing Class No. 2 for both banks. The installed RSP size is ¼-ton and Light, which are multiple RSP class sizes larger than Backing Class No. 2 and should remain stable during greater return period flow events.

The estimated abutment scour depth (which accounts for contraction scour) using 2-D model results is 0.5 feet during the 25-year flow and 1.0 feet during the 100-year flow. There was no analysis for scour with the 1-D model results, but the design of the streambed in the culvert has a thickness of 24 inches (AECOM, 2014). The designed streambed is expected to continue to cover the bottom of the RCB culvert after scour occurs, but, without replenishment from upstream sediment transport, the substrate in the RCB would decrease to approximately 1.0-foot thick following the 100-year flow.

Eddies at crossing structure

Little Mill Creek

The 2-D model results show that eddies occur on the right bank under Little Mill Creek Bridge and on the floodplain with the addition of backwatering (Figures 19 and 20). At lower flow events without influence from the Smith River there are no significant eddies predicted to form at the crossing structure. During the 25-year flow, there is a small eddy that forms at the beginning of the left bank RSP, where there is a bend in the main channel flow pathway. The backwatering from a 100-year Smith River event during the Little Mill Creek 25-year flow causes an eddy to occur directly along the right bank adjacent to the abutment structure. The velocity of the eddy flow moving upstream adjacent to the abutment is 0.4 feet per second. The eddies that occur on Little Mill Creek have low magnitude velocities and occur at high flows, allowing the eddies to contribute to sediment aggradation. A 100-year Little Mill Creek flow with a 25-year Smith River backwater event causes an eddy to form where the sediment deposits are located on the right bank. The ability of the 2-D model to simulate the eddies that could cause sediment deposition is a benefit to using a 2-D model compared to a 1-D model at this location. The sediment deposition would reduce the cross-sectional flow area, as was seen in the 2-D model created for Little Mill Creek in this analysis, which has the potential to change the hydraulics. The prediction of areas of sediment deposition could inform those designing stream crossings of locations where the hydraulics could change over time as sediment is deposited. This prediction of sediment deposition may have been possible at

Little Mill Creek, where eddies form on the right bank under the bridge during the 25-year flow event with 100-year Smith River backwater conditions, near the location of the current sediment deposit.

Eddies also reduce the effective flow area under Little Mill Creek Bridge. In a 1-D HEC-RAS model the user places ineffective flow markers where eddies are anticipated, but the 2-D modeling removes this user assumption of eddy location and size and instead models where the eddies are predicted to occur and their extent.

North Fork Ryan Creek

A summary of the eddies at the most-upstream rock weir during the 2-year and 100-year flows is presented in Table 22. The wetted channel width downstream of the rock weir is less than the wetted channel width; however, the eddies that form immediately downstream reduce the active flow width. During the 2-year flow the eddies reduce the flow width by 5.7 feet and during the 100-year flow the flow width is reduced by 8.0 feet. Similar to results from Little Mill Creek, the eddy location and extents resulting from 2-D models are not susceptible to user error that could occur in 1-D models. The effective flow area will impact the velocities and water depths predicted by both the 1-D and 2-D models.

When looking at the culvert opening, HEC-RAS 1-D models have the user set ineffective flow markers for sections upstream of a culvert or bridge to account for the flow contraction and loss of effective flow area. The 2-D model results predict that the active flow width (left and right eddy widths subtracted from the wetted channel width)

upstream of the culvert inlet are slightly wider than the width of the culvert (Table 23). Eddies are formed on either side of the culvert inlet opening, but they do not completely make up for the contraction of the channel width to the culvert width.

Table 22. Summary table of predicted widths of wetted channel, eddies, and active flow area for the 2-year and 100-year flow events on North Fork Ryan Creek at the upstream rock weir.

Return Period; Flow (cfs)	Wetted channel width (ft)	Right bank eddy width (ft)	Left bank eddy width (ft)	Active Flow width between eddies (ft)	Wetted channel width upstream of rock weir (ft)
2-yr; 33 cfs	13.7	3.0	2.7	8.0	11.7
100-yr; 263 cfs	20.2	4.8	3.2	12.2	18.0

Table 23. Summary table of predicted widths of wetted channel, eddies, and active flow area for the 2-year, 25-year, and 100-year flow events on North Fork Ryan Creek at the culvert inlet. Culvert width is the designed culvert width of 12 feet. The eddy, channel, and active flow widths are taken 10 feet upstream of the inlet opening.

Return Period (years); Flow (cfs)	Culvert width (ft)	Right bank eddy width (ft)	Left bank eddy width (ft)	Wetted channel width (ft)	Active Flow width (ft)
2-yr; 33 cfs	12	0	0	18.3	n/a
25-yr; 170	12	3.5	2.4	25.1	19.2
100-yr; 263 cfs	12	5.1	5.3	30.9	20.5

Synthesis – Modeling Overall

Modeling different scale of sites

The scale of the two stream crossing sites is different; however, the computer processing run time scales linearly with the number of mesh elements. Little Mill Creek is a larger stream than North Fork Ryan, with a drainage area of 3.96 square miles and a 100-year design flow of 1,955 cfs compared to North Fork Ryan Creek's drainage area of 0.67 square miles and 100-year design flow of 263 cfs. The active channel width upstream of the crossing at Little Mill Creek is approximately 25 feet and at North Fork Ryan Creek is approximately 12.2 feet.

The spacing of the mesh elements was the main procedural difference between creating the two models. The mesh elements began at larger spacing and were decreased to achieve spacing that captured changes in water depths and velocities. The mesh element width (perpendicular to the streamflow) in the main flow channel was 1.8 feet for Little Mill and 0.75 foot for North Fork Ryan. The ratio of mesh element width to active channel width is similar in both models, with 0.07 for Little Mill and 0.06 for North Fork Ryan. On the floodplain, the spacing increased to 5.0 feet for Little Mill and 2.0 feet for North Fork Ryan, and a triangular mesh was used to reduce the number of elements. These element spacings were determined based on the floodplain width and were less influential in the model flow because the banks were well defined and included in the main channel flow elements.

For Little Mill Creek the main focus of modeling was the velocity and water depths at the RSP-covered banks surrounding the bridge abutments. The water elevations were checked for high flow passage, but the main concern was the stability of the slopes protecting the abutments. For North Fork Ryan Creek, the main focus was the velocities and water depths surrounding the culvert, including the RSP, headwalls, and streambed.

Simulation computer processing time

A mesh of 50,000 elements would take approximately a half-hour to complete the simulation run, with a simulated time period of 1.0 hour and a model time step of 0.1 seconds (Figure 64). A simulated time period of 1.0 hour was more than enough time for models with up to 185,000 mesh elements to stabilize, so a smaller time period of 0.25-hour would probably be sufficient. The model time step had a greater effect on the stability of the models than the simulated time period. A change in the time step from 1.0 to 0.1 seconds resulted in stable results.

CONCLUSIONS AND RECOMMENDATIONS

Model results from SRH-2D provided additional information regarding the behavior of the stream at the crossing structures. Eddies were visible in the 2-D model results for both Little Mill Creek and North Fork Ryan Creek. In the Little Mill Creek model the locations of the eddies corresponded to the physical location of the sediment deposits under the crossing structure. Additionally, looking at the velocity vectors, the flow direction in the Little Mill Creek just upstream of the crossing is directed at the left bank, where the left bank RSP has destabilized and partially been scoured. There is potential for 2-D models to provide pertinent information for the design of stream crossing structures and streambeds in relation to eddies and peak velocities. The locations of eddies and peak velocities provided by 2-D models could aid in predicting areas of scour that may lead to structure failures and of deposition that may change flow area geometry and result in changed stream hydraulics.

The average 2-D model water depth results for Little Mill Creek are comparable to the 1-D results, while the average 2-D model velocity results are lower than the 1-D results. However, when using the local 2-D model velocities for RSP sizing and for abutment scour calculations, the recommended RSP size on the left bank is one standard size larger and the abutment scour depth is 3.9 feet greater during the 100-year return period flow than determined when using the 1-D model results. The ability to use the local velocities and water depths allows for detailed predictions of the forces experienced by the banks and abutments. For structures that are likely to cause turbulence in

streamflow, like culvert headwalls and rock weirs, the ability of 2-D models to simulate eddies provides better representation of the eddy locations and extents. The eddy location and extents resulting from 2-D models are not susceptible to user error that could occur when the user estimates and inputs eddy location and extent in 1-D models. The effective flow area (flow area not affected by the eddies) will impact the velocities and water depths predicted by both the 1-D and 2-D models, which may affect the design of the crossing and important crossing elements (RSP, in-stream structures, scour estimates, etc.).

In terms of modeling different scales of stream crossing sites, the computer processing run time scales linearly with the number of mesh elements. The number of mesh elements may increase with an increase in model domain area, but the increase in computer processing run time is approximately 1.4 hours per 100,000 mesh elements on a Windows desktop with an Intel Core i7 processor. Model run time should not be a problem for stream crossing sites that do not include expansive floodplains. To reduce the computer processing run time, the density of detail on large floodplains could be reduced by increasing the size of the mesh elements in locations where predictions of local velocities and water depths are not necessary for design calculations.

Recommendations for those using SRH-2D or other 2-D modeling software for full-span stream crossings should consider the following. Surveying breaks in slope was helpful in creating breaklines for the model mesh topography and reducing the need for multiple cross sections. Retrieve velocity and flow data if possible for model calibration. Inlet BC distribution did not significantly affect model results for the two studied sites.

The addition of an extended upstream channel to the survey data was not necessary to analyze the cross-sections in the two studied sites, but would be useful if the entire extent of surveyed points was of interest for analysis. Manning's roughness values and the boundaries between areas of different roughness values significantly affects model results. Areas of 2-D flow near the crossings, especially eddies or areas where flow is angled at the banks, should have detailed topographic measurements to develop representative mesh elements.

In future work, it would be useful to compare additional coupled 1-D and 2-D model results for a larger variety of stream crossing conditions and site characteristics. Ideally, the 1-D and 2-D models could be created simultaneously or with the same datasets, to reduce errors in comparison of results. Additionally, 2-D modeling of streams with larger floodplain would also be beneficial for quantifying the model computation run time required by significantly larger model domains. The SRH-2D model's capabilities should also be explored in more detail, especially its potential to determine areas of sediment deposition based on 2-D flow characteristics.

REFERENCES

AECOM. (2014). *Ryan Creek Culvert Replacement Project*. Prepared for Caltrans.

Aquaveo. (2018, December). *SMS:SMS User Manual 12.2*. XSM Wiki. xmswiki.com

Aquaveo. (2020, April). *SMS:SRH-2D*. XSM Wiki. xmswiki.com

Arneson, L. A., Zevenbergen, L. W., Lagasse, P. F., & Clopper, P. E. (2012). *Evaluating Scour at Bridges, Fifth Edition* (HEC-18 FHWA-HIF-12-003; Hydraulic Engineering Circular No. 18 (HEC-18)). FHWA.

Barnard, R. J., Johnson, J., Brooks, P., Bates, K. M., Heiner, B., Klavas, J. P., Ponder, D. C., Smith, P. D., & Powers, P. D. (2013). *Water Crossings Design Guidelines*. Washington Department of Fish and Wildlife, Olympia, Washington.

Barnard, R. J., Yokers, S., Nagygor, A., & Quinn, T. (2014). An evaluation of the stream simulation culvert design method in Washington state. *River Research and Applications*, *31*, 1376–1387.

Bates, K. K., & Kirn, R. (2009). *Guidelines for the Design of Stream/Road Crossings for Passage of Aquatic Organisms in Vermont*. Vermont Fish and Wildlife.

Bergendahl, B. S., & Arneson, L. A. (2014). *FHWA Hydraulic Toolbox Version 4.2 Desktop Reference Guide*.

Brunner, G. W., & CEIWR-HEC. (2016a). *HEC-RAS River Analysis System User's Manual version 5.0* (CPD-68; p. 962). Hydrologic Engineering Center (HEC), Institute for Water Resources, US Army Corps of Engineers.

Brunner, G. W., & CEIWR-HEC. (2016b). *HEC-RAS River Analysis System—2D Modeling User's Manual version 5.0* (CPD-68A; p. 171). Hydrologic Engineering Center (HEC), Institute for Water Resources, US Army Corps of Engineers.

Cafferata, P., Lindsay, D., Spittler, T., Wopat, M., Bundros, G., Flanagan, S., Coe, D., & Short, W. (2017). *Designing Watercourse Crossings for Passage of 100-year Flood Flows, Wood, and Sediment (Updated 2017)* (No. 1; California Forestry, p. 126). California Natural Resources Agency, Dept. of Forestry and Fire Protection, CalFire.

CalFish, & Caltrans. (2020). *Completed Fish Passage Remediation Locations*. Caltrans Fish Passage Priorities, Active Projects and Remediations. https://www.arcgis.com/apps/MapSeries/index.html?appid=13f6ef06050240c8a4d984544ddf45db

Caltrans. (2016). *Little Mill Creek Bridge Final Hydraulic Report*.

Caltrans, (CA Dept. of Transportation). (2020). Chapter 870—Bank Protection—Erosion Control. In *Highway Design Manual* (p. 870(32-42)).

Caltrans, CDFW (CA Dept. of Fish and Wildlife), & NMFS (National Marine Fisheries Services). (2007). *Fish Passage Design for Road Crossings: An Engineering Document Providing Fish Passage Design Guidance for Caltrans Projects*. Caltrans.

Castro, J. M., & Beavers, A. (2016). Providing Aquatic Organism Passage in Vertically Unstable Streams. *Water*, *8*(133), 20. https://doi.org/doi:10.3390/w8040133

Cayan, D. R., Maurer, E. P., Dettinger, M. D., Tyree, M., & Hayhoe, K. (2008). Climate Change Scenarios for the California Region. *Climatic Change*, *87*, 21–42. https://doi.org/10.1007/s10584-007-9377-6

CDFG, (CA Dept. of Fish and Game). (2002). *Culvert Criteria for Fish Passage*.

CDFW, (CA Dept. of Fish and Wildlife). (2009a). *California Salmonid Stream Habitat Restoration Manual: Part IX - Fish Passage Evaluation at Stream Crossings*.

CDFW, (CA Dept. of Fish and Wildlife). (2009b). *California Salmonid Stream Habitat Restoration Manual: Part XII - Fish Passage Design and Implementation*.

Cenderelli, D. A., Clarkin, K., Gubernick, R. A., & Weinhold, M. (2011). Stream Simulation for Aquatic Organism Passage at Road-stream Crossings. *Journal of the Transportation Research Board*, *2203*, 36–45.

Christiansen, C., Filer, A., Landi, M., O-Shaughnessy, E., Palmer, M., & Schwartz, T. (2014). *Cost-Benefit Analysis of Stream-Simulation Culverts*. Wisconsin Department of Natural Resources.

Craggs, T. (2016). *Implementation of Rock Slope Protection (RSP) Design*. Caltrans (CA Dept. of Transportation).

Deal, E. C., Parr, A. D., & Young, C. B. (2017). *A Comparison Study of One- and Two-Dimensional Hydraulic Models for River Environments* (Kansas Department of Transportation KS-17-02; p. 252). The University of Kansas.

Dettinger, M. (2011). Climate Change, Atmospheric Rivers, and Floods in California - A Multimodel Analysis of Storm Frequency and Magnitude Changes1: Climate Change, Atmospheric Rivers, and Floods in California - A Multimodel Analysis

of Storm Frequency and Magnitude Changes. *JAWRA Journal of the American Water Resources Association*, *47*(3), 514–523. https://doi.org/10.1111/j.1752-1688.2011.00546.x

Duffy, P., Arritt, R. W., Coquard, J., Gutowski, W. J., Han, J., Iorio, J., Kim, J., Leung, L. R., Roads, J., & Zeledon, E. (2006). Simulations of Present and Future Climates in the Western United States with Four Nested Regional Climate Models. *Journal of Climate*, *19*(6), 873–895. https://doi.org/10.1175/JCLI3669.1

Ettema, R., Nakato, T., & Muste, M. (2010). *Estimation of Scourt Depth at Bridge Abutments* (Transportation Research Board NCHRP 24-20). The University of Iowa.

Flanagan, S. A. (2005). Woody Debris Transport at Road-Stream Crossings. *Rocky Mountain Research Station - Rocky Mountain Research Station*, *3rd Quarter 2005*, 1–5.

Furniss, M. J., Ledwith, T. S., Love, M. A., McFadin, B. C., & Flanagan, S. A. (1998). *Response of Road-Stream Crossings to Large Flood Events in Washington, Oregon, and Northern California* (9877 1807P-SDTDC). Technology & Development Program, Forest Service, USDA. https://www.fs.fed.us/t-d/pubs/html/wr_p/98771807/98771807.htm

Gershunov, A., Shulgina, T., Clemesha, R. E. S., Guirguis, K., Pierce, D. W., Dettinger, M. D., Lavers, D. A., Cayan, D. R., Polade, S. D., Kalansky, J., & Ralph, F. M. (2019). Precipitation regime change in Western North America: The role of

Atmospheric Rivers. *Scientific Reports*, *9*(9944), 1–11. https://doi.org/10.1038/s41598-019-46169-w

Gillespie, N., Unthank, A., Campbell, L., Anderson, P., Gubernick, R., Weinhold, M., Cenderelli, D., Austin, B., McKinley, D., Wells, S., Rowan, J., Orvis, C., Hudy, M., Bowden, A., Singler, A., Fretz, E., Levine, J., & Kirn, R. (2014). Flood Effects on Road–Stream Crossing Infrastructure: Economic and Ecological Benefits of Stream Simulation Designs. *Fisheries*, *39*(2), 62–76. https://doi.org/10.1080/03632415.2013.874527

Harrelson, C. C., Rawlins, C. L., & Potyondy, J. P. (1994). *Stream Channel Reference Sites: An Illustrated Guide to Field Technique* (Gen. Tech Report RM-245). United States Department of Agriculture - Forest Service.

Hayhoe, K., Cayan, D., Field, C. B., Frumhoff, P. C., Maurer, E. P., Miller, N. L., Moser, S. C., Schneider, S. H., Cahill, K. N., Cleland, E. E., Dale, L., Drapek, R., Hanemann, R. M., Kalkstein, L. S., Lenihan, J., Lunch, C. K., Neilson, R. P., Sheridan, S. C., & Verville, J. H. (2004). Emissions pathways, climate change, and impacts on California. *Proceedings of the National Academy of Sciences of the United States of America*, *101*(34), 12422. https://doi.org/10.1073/pnas.0404500101

Hotchkiss, R. H., & Frei, C. M. (2007). *Design for Fish Passage at Roadway-Stream Crossings: Synthesis Report* (p. 280) [Publication]. U.S. Department of Transportation, Federal Highway Administration, Office of Infrastructure Research and Development, Turner-Fairbank Highway Research Center.

Kilgore, R. T., Bergendahl, B. S., & Hotchkiss, R. H. (2010). *Culvert Design for Aquatic Organism Passage, HEC-26* (FHWA-HIF-11-008; p. 234). Centeral Federal Lands Highway Division, FHWA.

Kim, J. (2005). A Projection of the Effects of the Climate Change Induced by Increased CO 2 on Extreme Hydrologic Events in the Western U.S. *Climatic Change*, *68*(1), 153–168. https://doi.org/10.1007/s10584-005-4787-9

Lagasse, P. F., Spitz, W. J., Zevenbergen, L. W., & Zachmann, D. W. (2004). *Handbook for Predicting Stream Meander Migration* (NCHRP Report No. 533). Transportation Research Board (TRB).

Lagasse, P. F., Zevenbergen, L. W., Spitz, W. J., & Arneson, L. A. (2012). *Stream Stability at Highway Structures, Fourth Edition* (FHWA-HIF-12-004; Hydraulic Engineering Circular No. 20 (HEC-20)). FHWA.

Lai, Y. G. (2008). *SRH-2D version 2: Theory and User's Manual*. Sedimentation and River Hydraulics Group, Technical Service Center, Bureau of Reclamation.

Lang, M. M. (2005). *Caltrans District 1 Pilot Fish Passage Asssessment Volume 1* (FHWA/CA/EN-2005/02).

Maurer, E. P. (2007). Uncertainty in hydrologic impacts of climate change in the Sierra Nevada, California, under two emissions scenarios. *Climatic Change*, *82*(3), 309–325. https://doi.org/10.1007/s10584-006-9180-9

McLaughlin, R. T., Smyth, E. R. B., Castro-Santos, T., Jones, M. L., Koops, M. A., Pratt, T. C., & Vélez-Espino, L.-A. (2012). Unintended consequences and trade-offs of

fish passage. *Fish and Fisheries*, *14*(4), 580–604. https://doi.org/10.1111/faf.12003

Mote, P. W., & Salathé, E. P. (2010). Future climate in the Pacific Northwest. *Climatic Change*, *102*(1), 29–50. https://doi.org/10.1007/s10584-010-9848-z

Neelin, J. D., Langenbrunner, B., Meyerson, J. E., Hall, A., & Berg, N. (2013). California Winter Precipitation Change under Global Warming in the Coupled Model Intercomparison Project Phase 5 Ensemble. *American Meteorological Society, Journal of Climate*, *26*, 6238–6256. https://doi.org/10.1175/JCLI-D-12-00514.1

NMFS, (National Marine Fisheries Services). (2001). *Guidelines for Salmonid Passage at Stream Crossings*. NOAA.

NOAA, (National Oceanic and Atmospheric Administration). (2020). *About Atmospheric Rivers: AR Portal*. NOAA Physical Sciences Laboratory. https://www.psl.noaa.gov/arportal/about/

Pallares, J. (n.d.). *Caltrans, Structures Hydrology/Hydraulics Branch* [Personal communication].

Pierce, D. W., Das, T., Cayan, D. R., Maurer, E. P., Miller, N. L., Bao, Y., Kanamitsu, M., Yoshimura, K., Snyder, M. A., Sloan, L. C., Franco, G., & Tyree, M. (2013). Probabilistic estimates of future changes in California temperature and precipitation using statistical and dynamical downscaling. *Climate Dynamics*, *40*(3), 839–856. https://doi.org/10.1007/s00382-012-1337-9

Poulet, N. (2007). Impacts of weirs on fish communities in a piedmont stream. *River Research and Applications*, *23*(9), 1038–1047. https://doi.org/10.1002/rra.1040

Racin, J. A., Hoover, T. P., & Crossett Avila, C. M. (2000). *California Bank and Shore Rock Slope Protection Design* (Caltrans Study No. F90TL03 FHWA-CA-TL-95-10; p. 154). Caltrans Office of New Technology and Research and FHWA.

Ralph, F. M., Coleman, T., Neiman, P. J., Zamora, R. J., & Dettinger, M. D. (2013). Observed Impacts of Duration and Seasonality of Atmospheric-River Landfalls on Soil Moisture and Runoff in Coastal Northern California. *Journal of Hydrometeorology*, *14*(2), 443–459. https://doi.org/10.1175/JHM-D-12-076.1

Rapp, C. F., & Abbe, T. B. (2003). *A Framework for Delineating Channel Migration Zones* (No. 03-06–027). Washington State DOT and Dept. of Ecology.

Schall, J. D., Thompson, P. L., Zerges, S. M., Kilgore, R. T., & Morris, J. L. (2012). *Hydraulic Design of Highway Culverts, Third Edition* (FHWA-HIF012-026; Hydraulic Design Series No. 5 (HDS-5)). FHWA (Federal Highway Administration).

Silva, A. T., Lucas, M. C., Castro-Santos, T., Katopodis, C., Baumgartner, L. J., Thiem, J. D., Aarestrup, K., Pompeu, P. S., O'Brien, G. C., Braun, D. C., Burnett, N. J., Zhu, D. Z., Fjeldstad, H.-P., Forseth, T., Rajaratnam, N., Williams, J. G., & Cooke, S. J. (2017). The future of fish passage science, engineering, and practice. *Fish and Fisheries*, *2018*(19), 340–362. https://doi.org/10.1111/faf.12258

Timm, A., Higgins, D., Stanovick, J., Kolka, R., & Eggert, S. (2017). Quantifying Fish Habitat Associated with Stream Simulation Design Culverts in Northern Wisconsin. *River Research and Applications*, *33*, 567–577.

TRB, (Transportation Research Board). (2017). *TRB Webinar Program*. TRB Online Publications. http://onlinepubs.trb.org/onlinepubs/webinars/170413.pdf

University of New Hampshire. (2009). *New Hampshire Stream Crossing Guidelines*.

USFS. (2012). *FishXing—Software and Learning Systems for Fish Passage through Culverts*. FishXing. www.fs.fed.us/biology/nsaec/fishxing/

USFS Stream Simulation Working Group. (2008). *Stream Simulation: An Ecological Approach to Providing Passage for Aquatic Organisms at Road-Stream Crossings* (Gen. Tech Report 0877 1801-SDTDC). National Technology and Development Program, U.S. Department of Agriculture.

USFWS, (U.S. Fish and Wildlife Service). (2019). *Fish Passage Engineering Design Criteria*. USFWS, Northeast Region R5.

USGS, (United States Geological Survey). (2020, June). *StreamStats* [GIS database and analytical tools]. https://streamstats.usgs.gov/ss/

Wilhere, G., Atha, J., Quinn, T., Helbrecht, L., & Tohver, I. (2016). *Incorporating Climate Change into the Design of Water Crossing Structures*. Washington Department of Fish and Wildlife, Habitat Program - Science Division, Olympia, Washington. https://wdfw.wa.gov/sites/default/files/publications/01867/wdfw01867.pdf

Wolman, M. G. (1954). A method of sampling coarse river-bed material. *Transactions American Geophysical Union*, *35*(6), 951–956.

Yochum, S. E. (2018). *Stream Channel Flow Resistance Coefficient Computation Tool* (1.1) [Excel Spreadsheet]. USFS National Stream and Aquatic Ecology Center.

Zevenbergen, L. W., Arneson, L. A., Hunt, J. H., & Miller, A. C. (2012). *Hydraulic Design of Safe Bridges* (FHWA-HIF-12-018; Hydraulic Design Series No. 7 (HDS-7)). FHWA (Federal Highway Administration).

APPENDIX A – SITE PHOTOS

A.1 Little Mill

Figure A- 1. View of Little Mill Creek Bridge looking downstream from the left streambank (taken by Mike Love 5/9/2019).

Figure A- 2. Looking downstream from under Little Mill Creek bridge towards the confluence with the Smith River (taken by Mike Love 5/9/2019).

Figure A- 3. RSP bank on left bank of Little Mill Creek under Little Mill Creek Bridge (view looking upstream) (taken by Mike Love 5/9/2019).

Figure A- 4. Sediment deposit over RSP bank on right bank of Little Mill Creek under Little Mill Creek Bridge (view looking upstream) (taken by Mike Love 5/9/2019).

Debris

Figure A- 5. View of debris upstream of Little Mill Creek Bridge looking upstream from the left streambank (taken by Mike Love 5/9/2019).

Figure A- 6. Debris directly upstream of Little Mill Creek Bridge on the left bank. Flow moving from right to left in image (taken by Alyssa Virgil on 01/09/2020).

A.2 North Fork Ryan

Figure A- 7. Looking upstream on North Fork Ryan Creek towards reference reach (taken by Margaret Lang 09/12/2019).

Figure A- 8. Looking upstream at rock weir located upstream of North Fork Ryan Creek crossing (taken by Mike Love 09/12/2019).

Figure A- 9. Looking downstream towards North Fork Ryan Creek crossing inlet (taken by Mike Love 09/12/2019).

Figure A- 10. Looking upstream towards outlet opening on North Fork Ryan Creek (taken by Mike Love 09/12/2019).

Figure A- 11. Looking downstream from on top of crossing outlet on North Fork Ryan Creek (taken by Margaret Lang 02/27/2019).

APPENDIX B – MODEL DEVELOPMENT

Survey data for this project was uploaded from a '.csv' file containing columns: point number, northing, easting, elevation, and point code/description (PNEZD format) (Figure B- 1**Error! Reference source not found.**). The point description codes were uploaded as the 'Pt Name', so that breaklines could be drawn following points labeled for active channel, bankfull width, and other significant slope breaks or features.

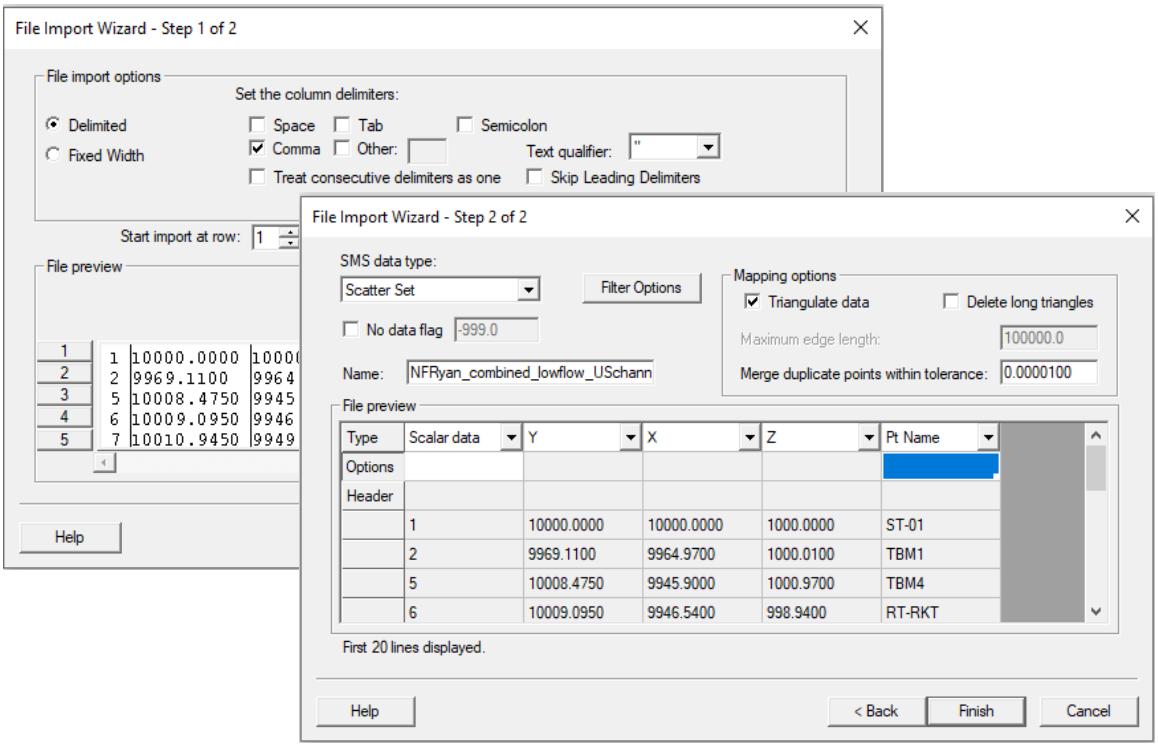

Figure B- 1. Topographic survey data import window for input into the SMS software.

The model coverages were then created to define boundary conditions using different subsets of the survey data and other input data like roughness and flow. Four different

coverages were used: the Generic ‘mesh generator’ type and the SRH-2D model ‘boundary condition’, ‘materials’, and ‘monitor’ types. The mesh generator coverage delineated the wetted channel, active channel, bankfull boundary, and slope breaks on the left and right banks. The boundary condition coverage was an inlet uniform flow condition and outlet water depth condition. The generated mesh geometry is used to calculate the inlet and outlet conditions, essentially extracting a cross-section at the location of the boundary. Input flows were estimated on-site and from return period flows estimated using the USGS regional regression equations. The materials coverage indicated areas of differing Manning’s roughness values, estimated using characteristics of the stream channel and banks (Chow, 1959). The monitor coverage consisted of arcs and points to extract and save estimated water depth and flow over the simulation time period.

B.1 Scatter Points

The survey data is loaded into SMS as scatter points and is triangulated by default. Breaklines can be added to the scatter data to maintain continuity between elements like the longitudinal profile and slope breaks (lines in Figure B- 2, Figure B- 3, and Figure B- 4). Once breaklines are placed, the ‘force breaklines’ option in the ‘Breaklines’ dropdown menu will re-triangulate. The breaklines are connected to the scatter set, so any changes to the scatter set should be made before adding breaklines.

Figure B- 2. Little Mill Creek survey points (red X) with slope breaks and model mesh breaklines (various color lines). Background satellite imagery from Google Earth taken in 2018.

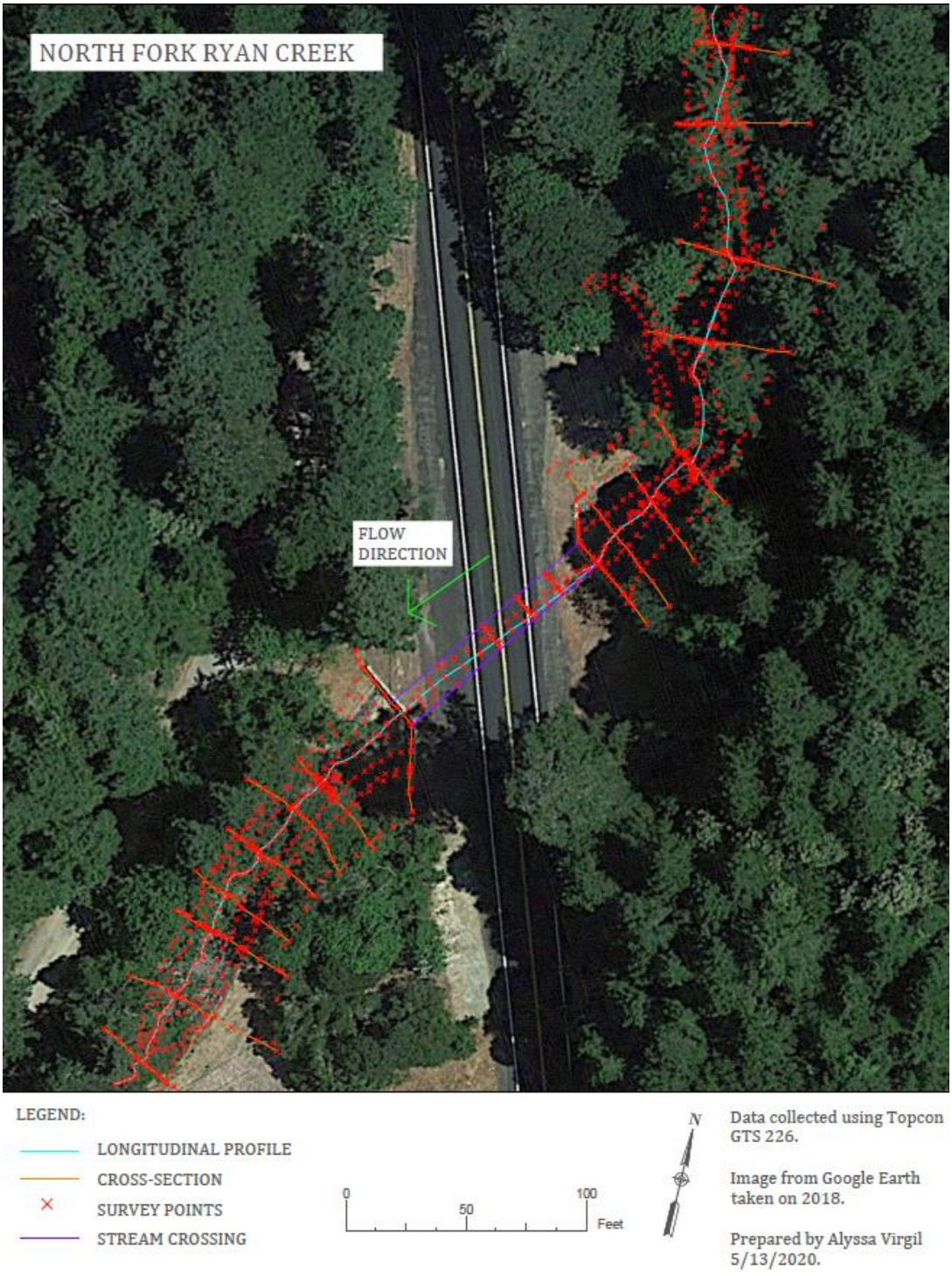

Figure B- 3. North Fork Ryan Creek survey points (red X) with slope breaks, boundaries, and model mesh breaklines (various color lines) and flow direction. Background satellite imagery from Google Earth taken in 2018.

Figure B- 4. Isolated image (no background imagery) of scatter set of topographic survey points (red dots) with breaklines (blue lines) for North Fork Ryan Creek.

Terrain

With the survey data collected at uneven spacing following slope breaks and boundary edges, there are some regions of data where the scatter points line up in a way, so that the triangulation forming the terrain is not accurate. For example in the North Fork Ryan Creek model mismatches in the thalweg longitudinal profile and water's edge survey points perpendicular to streamflow created an opportunity for water's edge points to connect with each other, seen as the darker higher elevation sections spanning the channel (Figure B- 5). These errors are fixed using breaklines to connect thalweg longitudinal profile survey points, so that interpolation of elevations in the channel will occur between the longitudinal profile points, rather than between water's edge points.

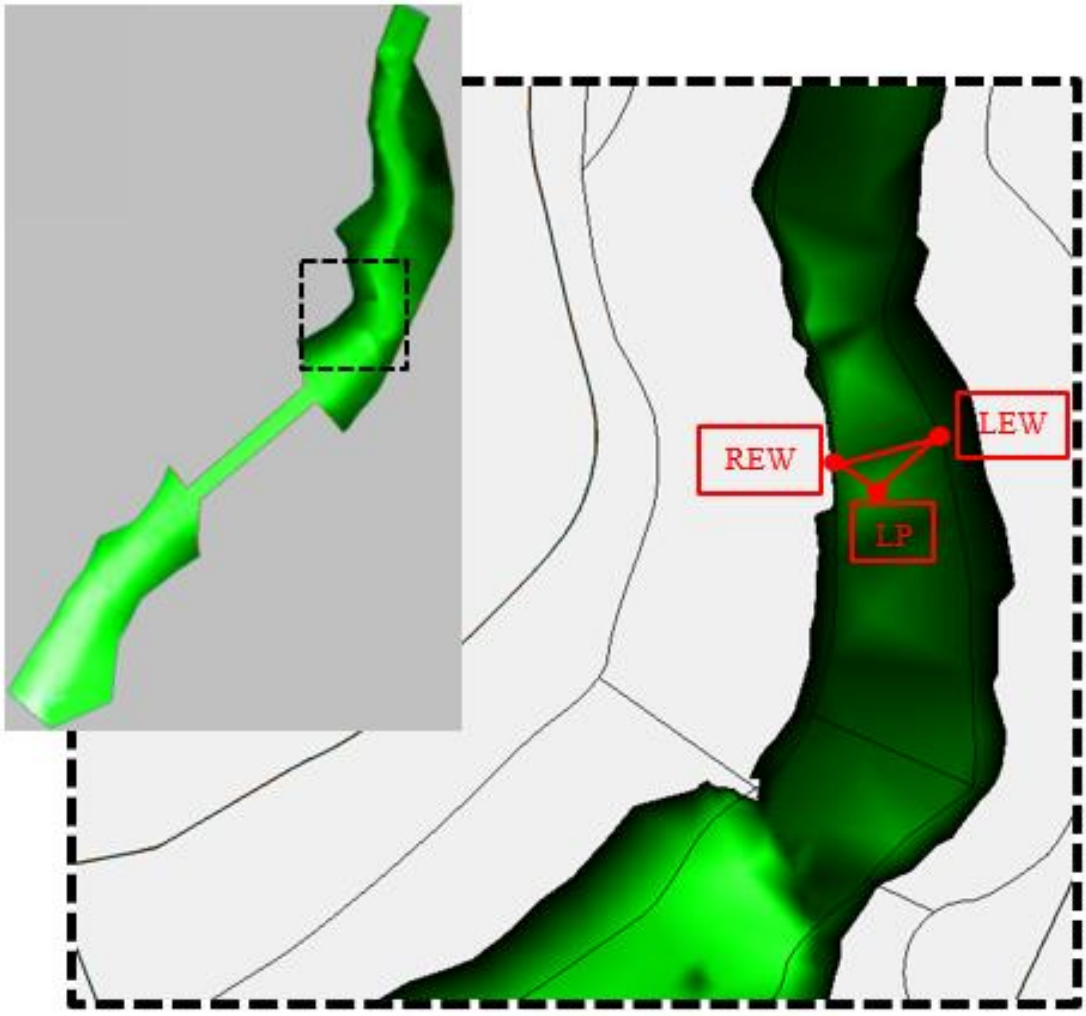

Figure B- 5. Terrain inaccuracies when not using breaklines in triangulation of survey data points. The right edge of water (REW) and left edge of water (LEW) are connecting over the channel, which creates a ridge of higher elevation than the thalweg elevation (LP).

B.2 Mesh Generator Coverage

The mesh generator coverage is part of SMS, rather than a SRH-2D package. Mesh generation is a time-intensive process, but the interaction of mesh size, mesh set up, and simulation time step were key to the success of model runs. The mesh is set up to

maintain a consistent water flow path. In the flow path, a patch (rectangular) mesh allows water mass to be calculated flowing from one mesh element to the next with consistency, instead of splitting or combining flows (Figure B- 6). The increasing or decreasing of mesh elements between two parallel arcs, ends up shifting flow values horizontally (perpendicular to flow) between mesh elements, which can lead to higher residuals in the model results. Redistributing vertices to be the same number of segments in an inlet and outlet arc is important to the stability of the model. The banks and floodplain are generally assigned a paved (triangular) mesh because there is often greater change in elevation between adjacent elements.

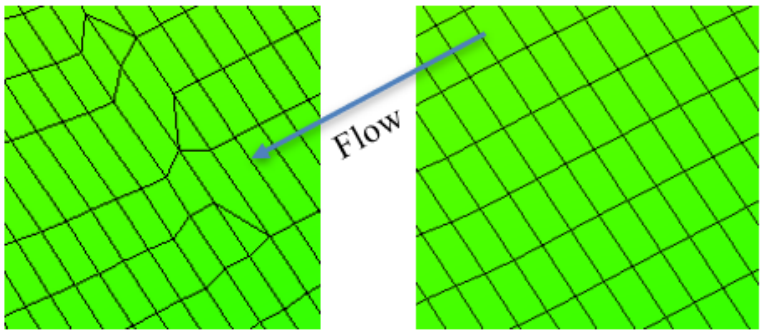

Figure B- 6. Examples of mesh with splitting and combining flow pathways (left) and uniform flow pathways (right).

Once the mesh generator coverage is sufficient, the mesh generator is converted into a mesh using the Feature Objects toolbar drop-down or a right-click on the mesh generator coverage to select “Map -> 2D Mesh”. The mesh is then generated under mesh data, and the mesh can be evaluated visually and by checking the ARR Mesh Quality (Display > Plot Wizard).

Using North Fork Ryan as an example, over the course of modeling, the mesh generator coverage was updated and improved to increase the accuracy of the model. At the beginning a coarse mesh was made, following the surveyed slope break boundaries. The vertices distribution was around 5.0 feet and everything was ‘paved’, which is made up of rectangular mesh elements. The model was run at various flows of interest, and the mesh was then refined based on the resulting wetted elements. The vertex distribution was reduced to around 1.0 feet and the channel was given a ‘patch’ mesh, which is made up of triangular elements. Another round of simulations led to the channel mesh resolution increasing to use 0.75-foot spacing, while the floodplain boundary vertices were distributed to every 2.0 feet (to limit the number of elements, and the resulting increase in the simulation time).

The final mesh used for modeling and returning results had different mesh resolution for the two models. For Little Mill Creek, a mesh size of 1.8 feet for the channel and banks worked with mesh size increasing to 4.8 feet at the edge of the floodplain. For North Fork Ryan Creek, a mesh size around 0.75 ft, created by redistributing the vertices of the mesh generation arcs, was found to work well for the channel and banks, with mesh size increasing to 2.0 feet moving into the floodplain. The difference in sufficient mesh size between the two sites is likely because of the magnitude of flows, where the 2-year return period flow at Little Mill Creek is 529 cfs and at North Fork Ryan Creek is 33 cfs.

B.3 Model Sensitivity to Inputs

Upstream Channel Extension

The upstream channel extension did not affect the results for Little Mill Creek at the areas of interest, including a majority of the reference reach, the slope break at the upstream debris, and the crossing. The same is true for North Fork Ryan Creek at the areas of interest, including the reference reach, the upstream rock weir, the crossing inlet headwall, and the crossing outlet headwall. The presence of the upstream channel did allow for lenience in the use of different inlet distributions because the results would stabilize at the same values (within a +/- 0.01 range of difference) past the extended upstream channel area (see the following section on 'Inlet Distribution').

Inlet Distribution

The type of inlet distribution, using a unit discharge ('Q' distribution) versus a conveyance calculation ('conveyance' distribution) had a negligible effect on the water depth and minimal effect on the velocity results of the model. The differences of the conveyance distribution results from the Q distribution results are presented in the following figures. Both distributions were attached to the same arc during independent simulations and all other model inputs and parameters were kept the same.

During the 2-year return period flow, the difference between the conveyance and Q inlet distribution results for water depths are within 0.01 feet from each other within the analysis area, not including the extended upstream channel area, which is not analyzed (**Error! Reference source not found.Error! Reference source not found.**).

The velocity results are different up to 0.01 feet per second into the reference reach from the edge of the extended upstream channel (**Error! Reference source not found.**).

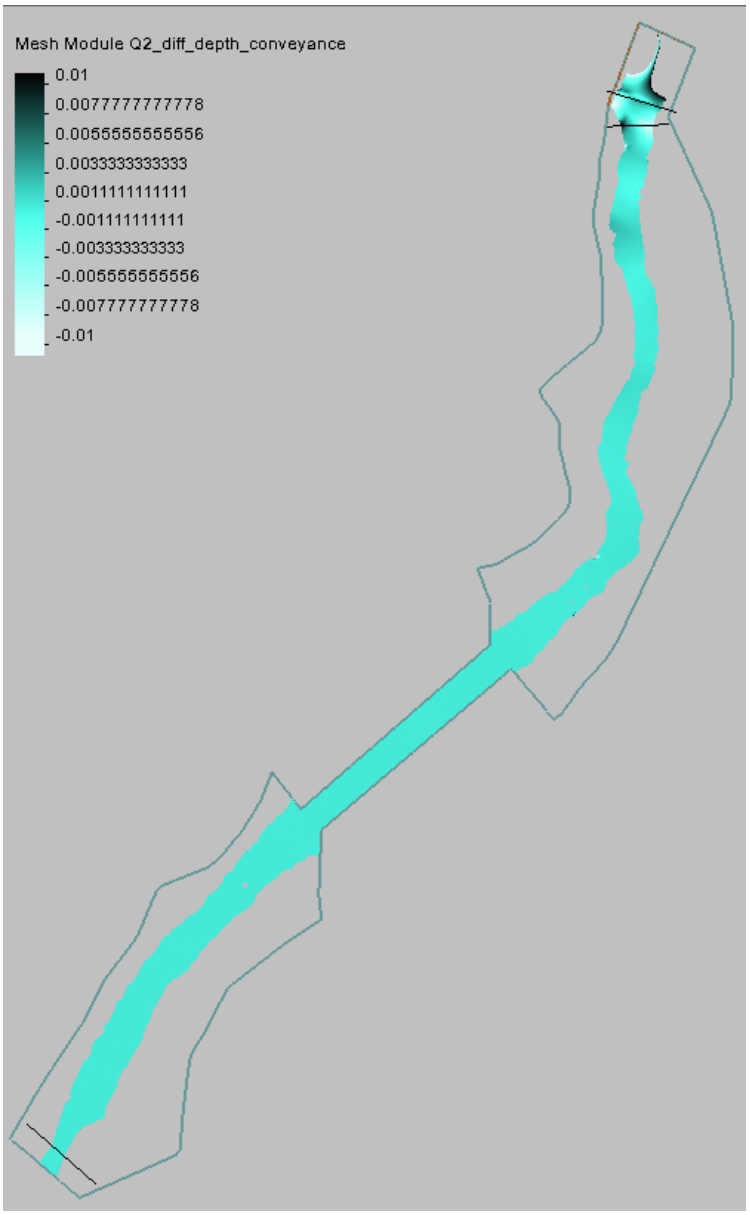

Figure B- 7. Difference in water depth results of conveyance inlet distribution from unit discharge (Q) inlet distribution, during Q2 simulation, with range from -0.01 to 0.01.

Figure B- 8. Difference in velocity results of conveyance inlet distribution from unit discharge (Q) inlet distribution, during Q2 simulation, with range from -0.01 to 0.01.

Figure B- 9. Difference in water depth results of conveyance inlet distribution from unit discharge (Q) inlet distribution, during Q100 simulation, with range from -0.01 to 0.01.

Figure B- 10. Difference in velocity results of conveyance inlet distribution from unit discharge (Q) inlet distribution, during Q100 simulation, with range from -0.01 to 0.01.

Debris Area Material Roughness (Little Mill only)

Figure B- 11. Difference in Q25 water depth results between simulation without and with a specified debris area in the materials coverage.

Figure B- 12. Difference in Q25 velocity results between simulation without and with a specified debris area in the materials coverage.

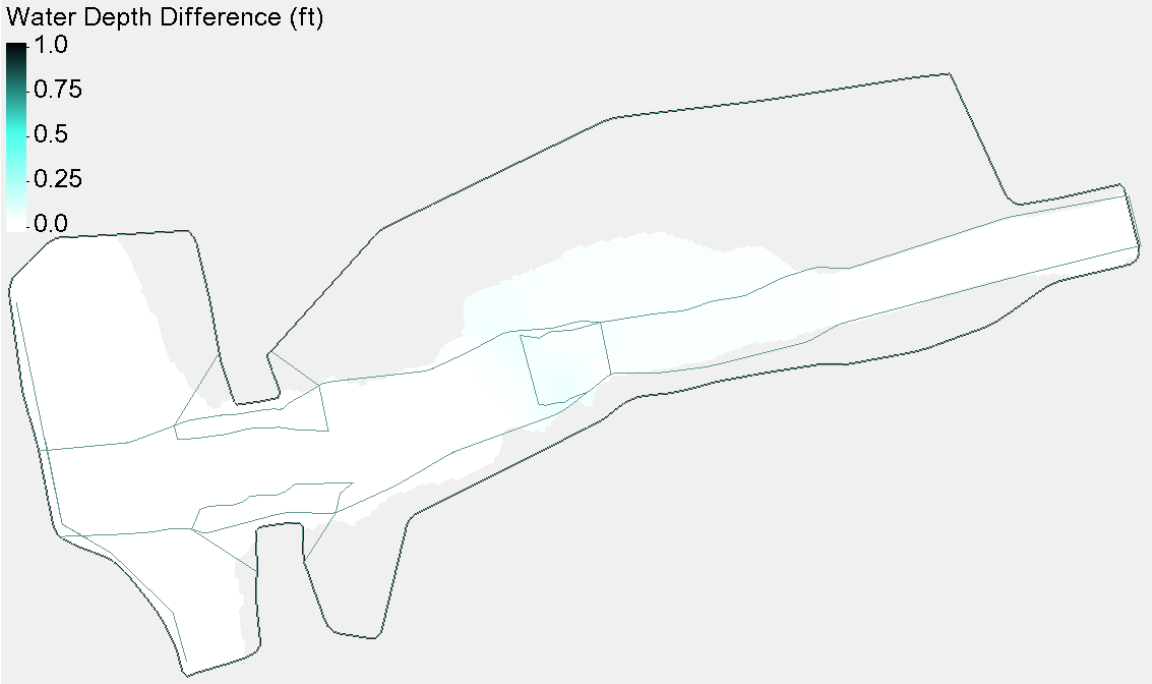

Figure B- 13. Difference in Q25 with Smith River Q100 backwater water depth results between simulation without and with a specified debris area in the materials coverage.

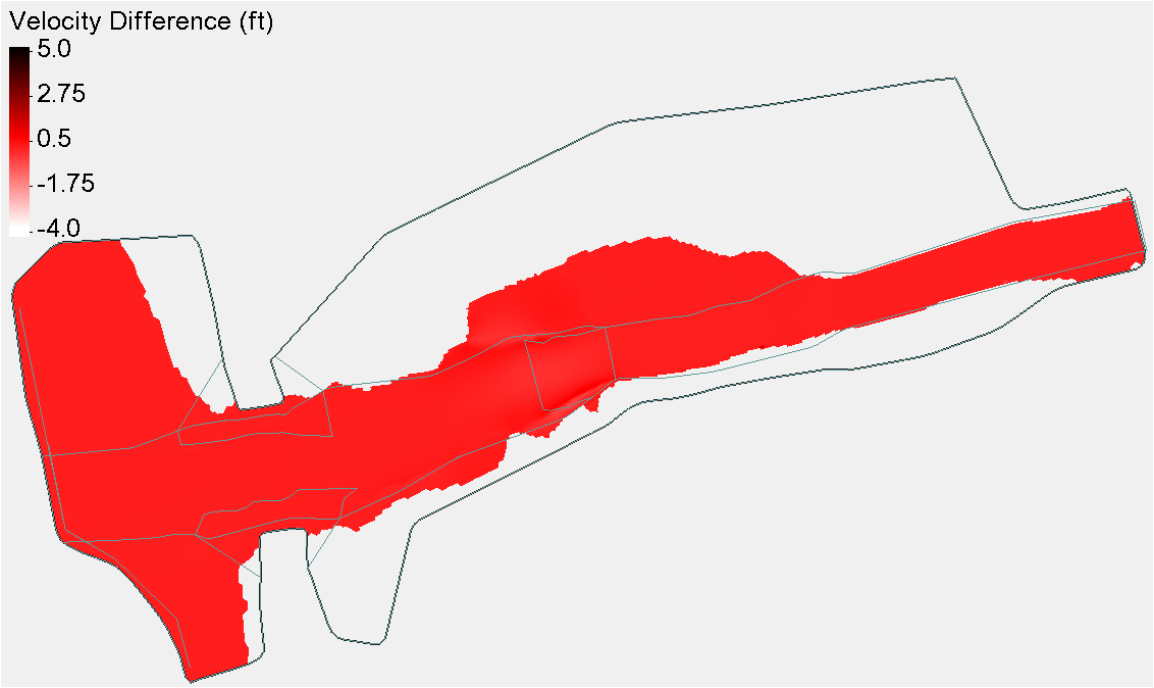

Figure B- 14. Difference in Q25 with Smith River Q100 backwater velocity results between simulation without and with a specified debris area in the materials coverage.

B.4 Model Stability

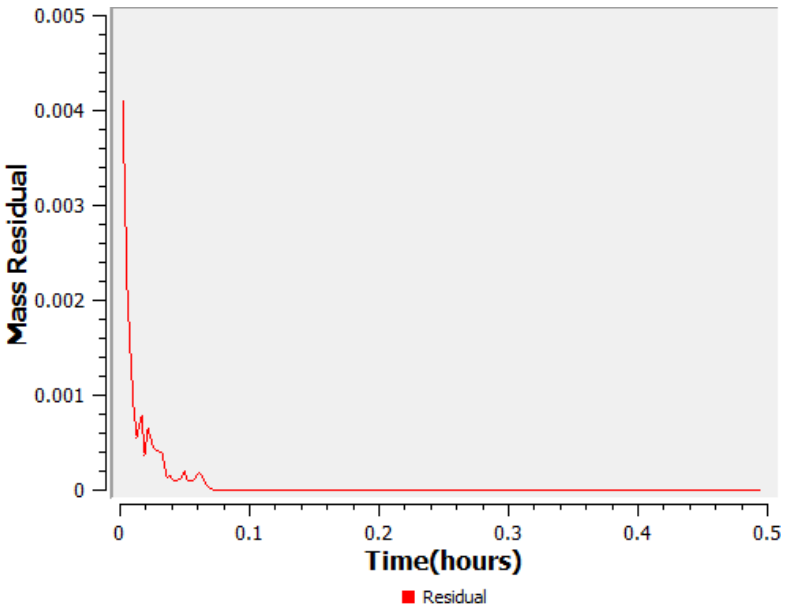

Figure B- 15. Mass residual plot for North Fork Ryan Creek simulation for the 2-year return period flow. The mass residual decreases exponentially over a 0.5-hour time period, reaching approximately zero mass residual at 0.08 hours.

APPENDIX C – EXTENDED RESULTS

C.1 Water Depth, Velocity, and Shear Stress Figures

Little Mill Creek

Water Depth/Velocity

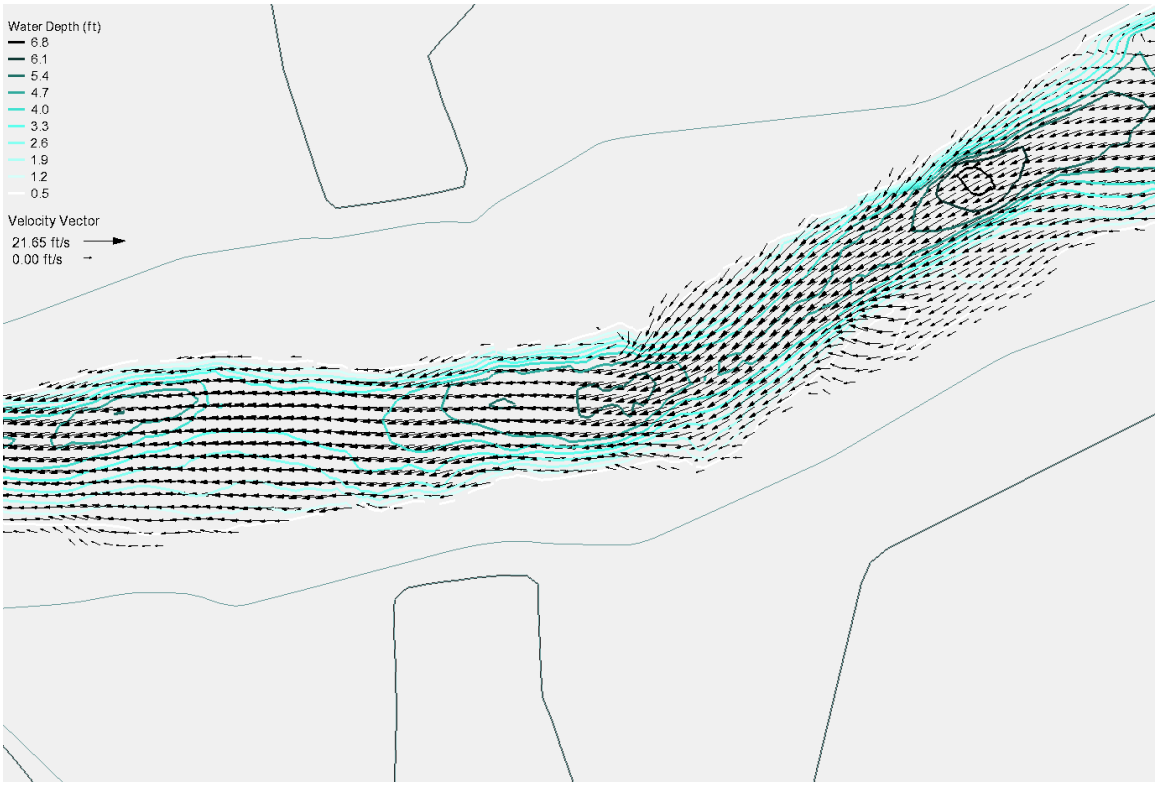

Figure C- 1. Plan view of crossing at Little Mill Creek with water depth contours (feet) and velocity vectors (feet per second) for the 10-year return period flow.

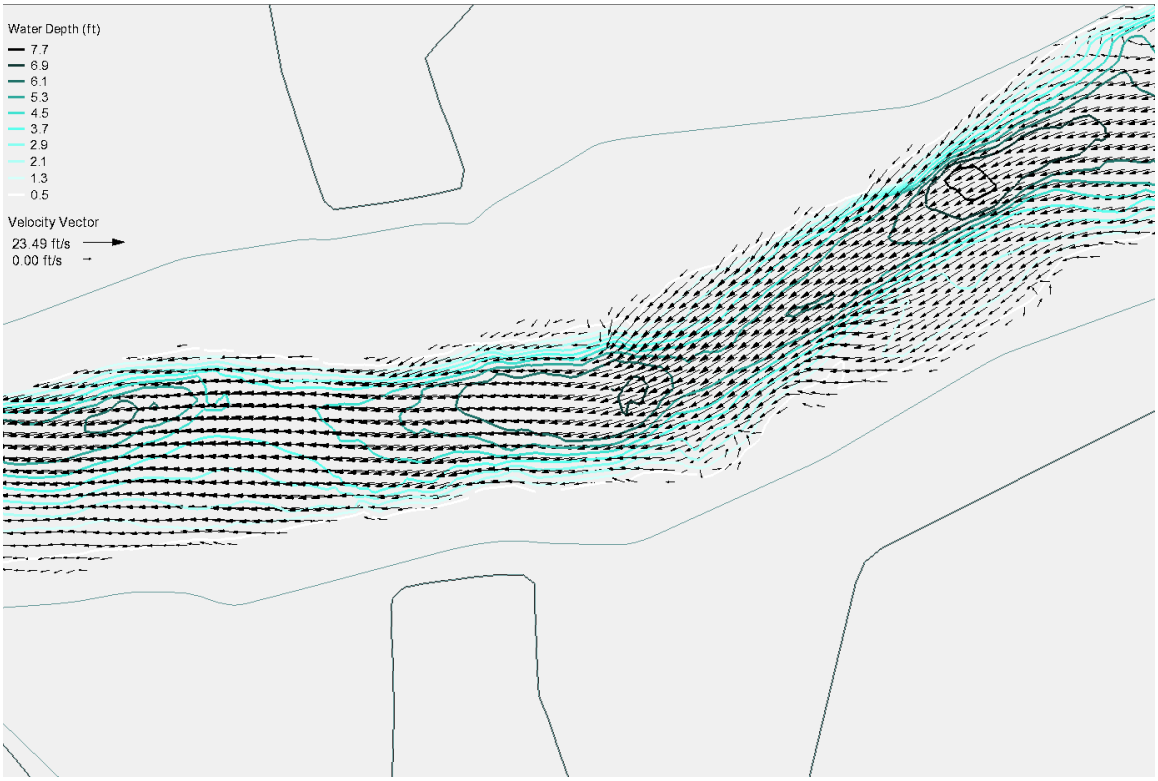

Figure C- 2. Plan view of crossing at Little Mill Creek with water depth contours (feet) and velocity vectors (feet per second) for the 50-year return period flow.

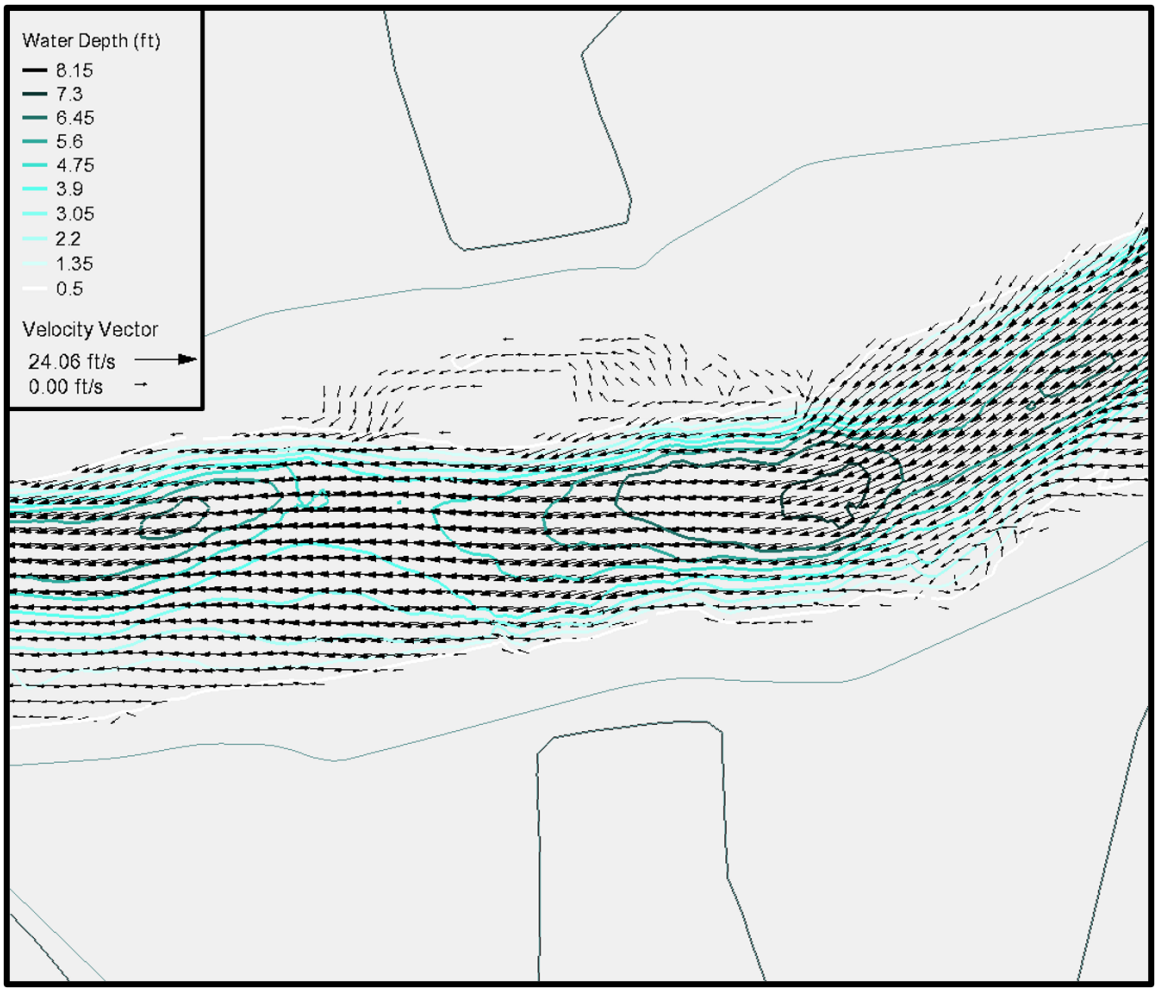

Figure C- 3. Plan view of crossing at Little Mill Creek with water depth contours (feet) and velocity vectors (feet per second) for the 100-year return period flow of 1,955 cfs. The flow splits as water is diverted onto the terrace create by the sediment deposits. An eddy is expected to form upstream of the crossing on the left and right banks parallel to one another. The average water depth moving in the main channel under the crossing is 4.19 feet, with a maximum depth of 5.99 feet. The average velocity in the main channel is 12.0 feet per second, with a maximum of 14.78 feet per second located in the center of the main channel.

Shear Stress

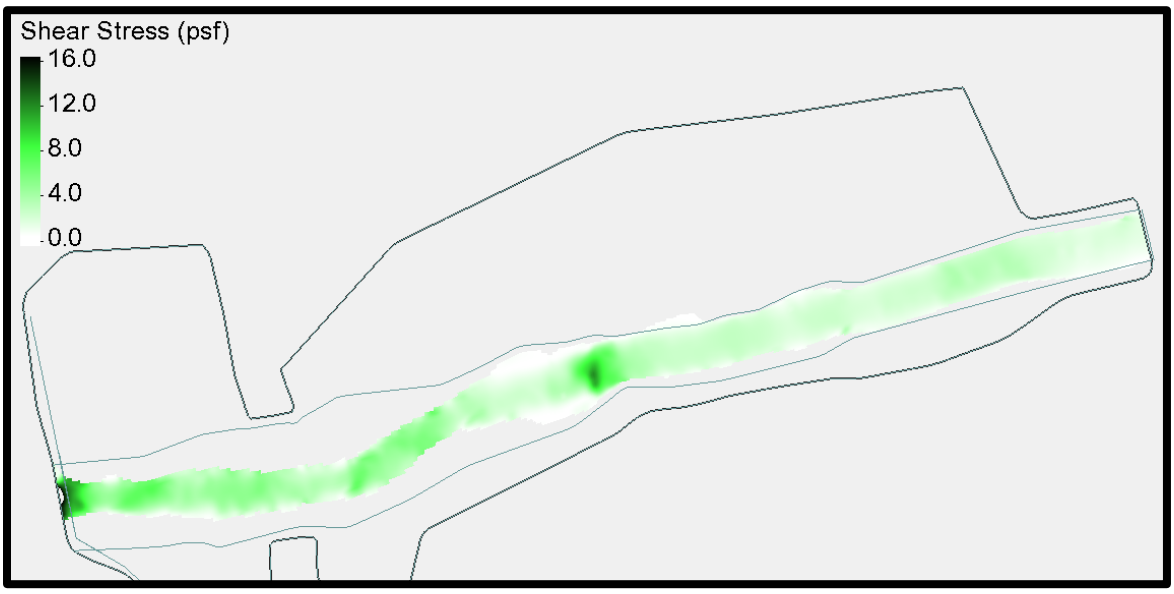

Figure C- 4. Shear stress results from Little Mill Creek model simulated for the 2-year return period flow.

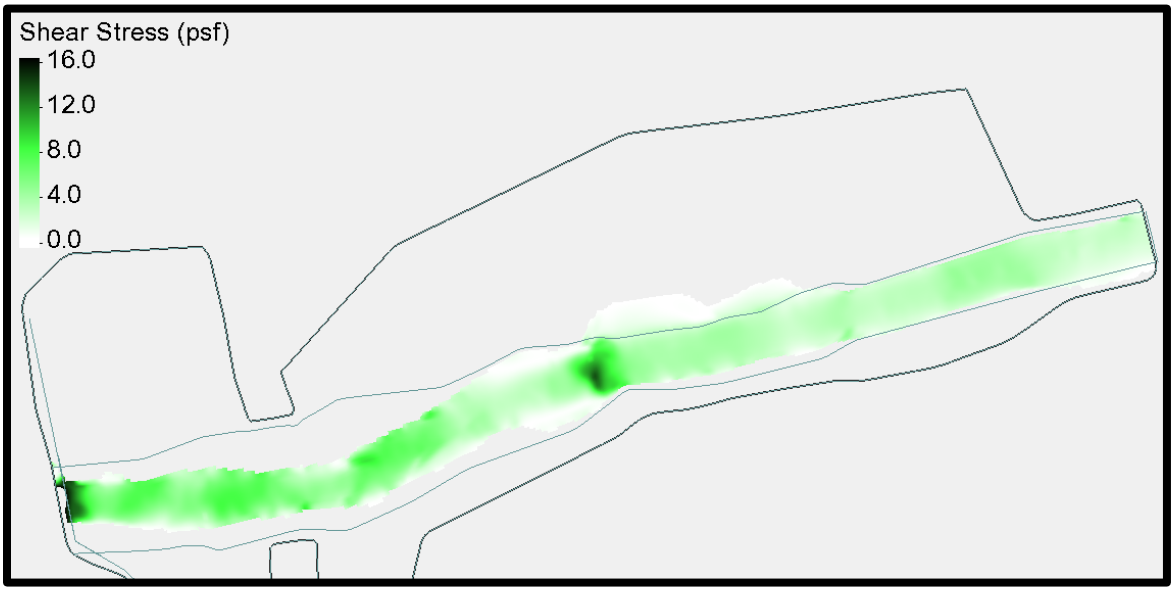

Figure C- 5. Shear stress results from Little Mill Creek model simulated for the 10-year return period flow.

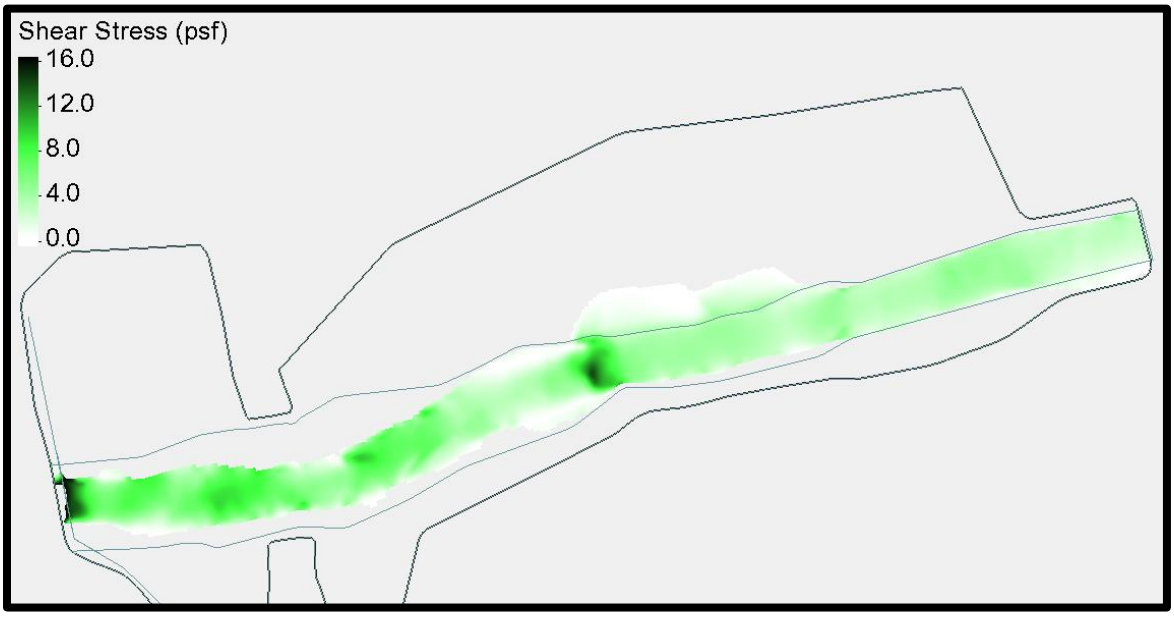

Figure C- 6. Shear stress results from Little Mill Creek model simulated for the 25-year return period flow.

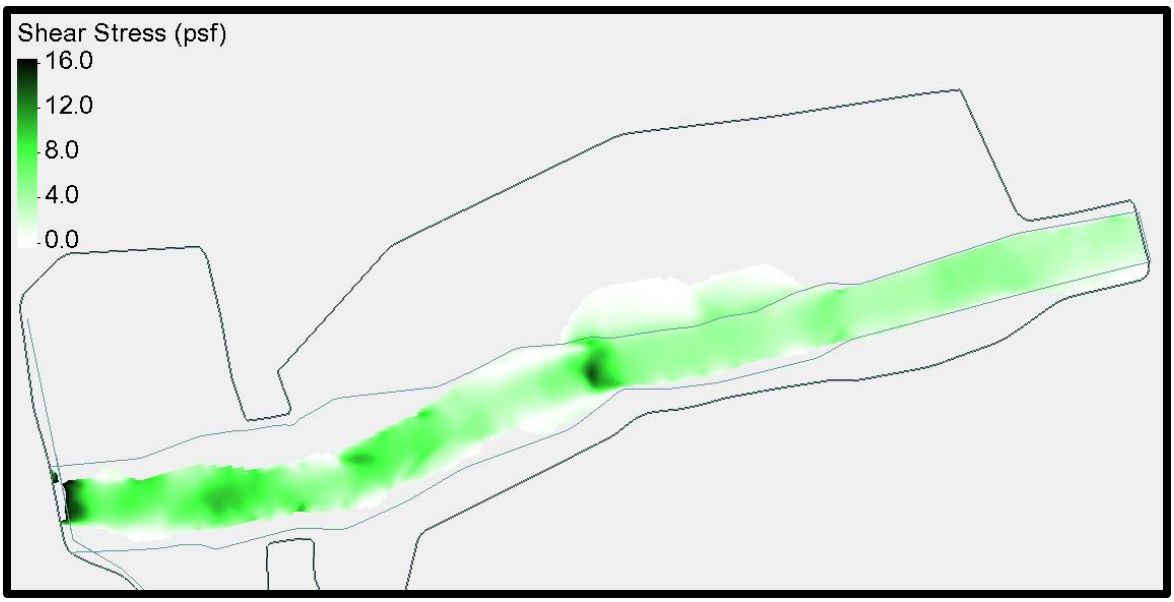

Figure C- 7. Shear stress results from Little Mill Creek model simulated for the 50-year return period flow.

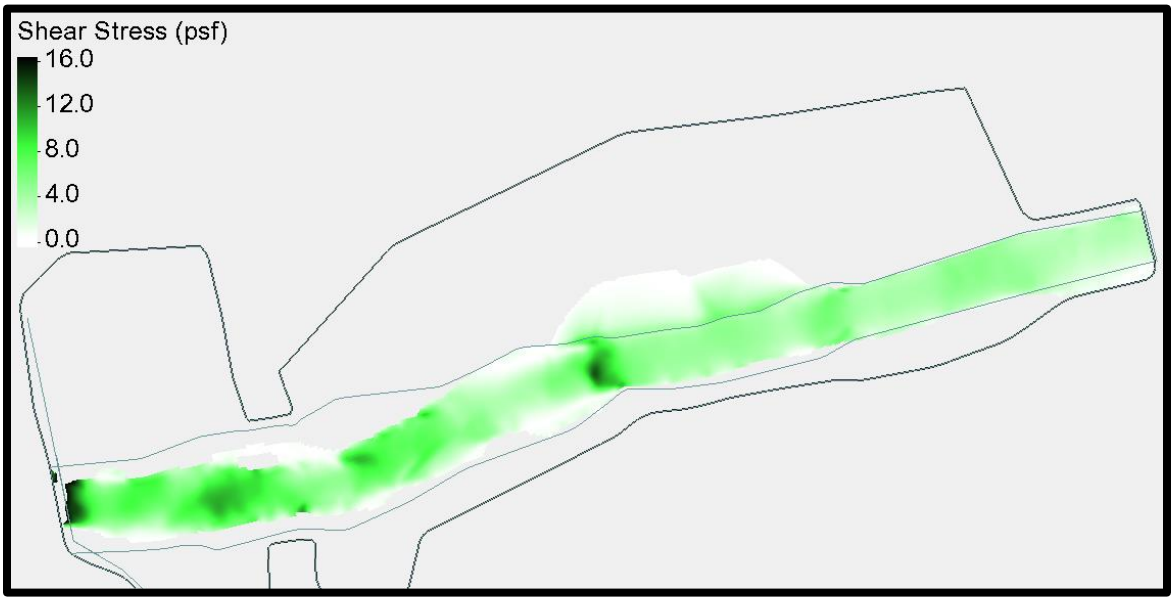

Figure C- 8. Shear stress results from Little Mill Creek model simulated for the 100-year return period flow.

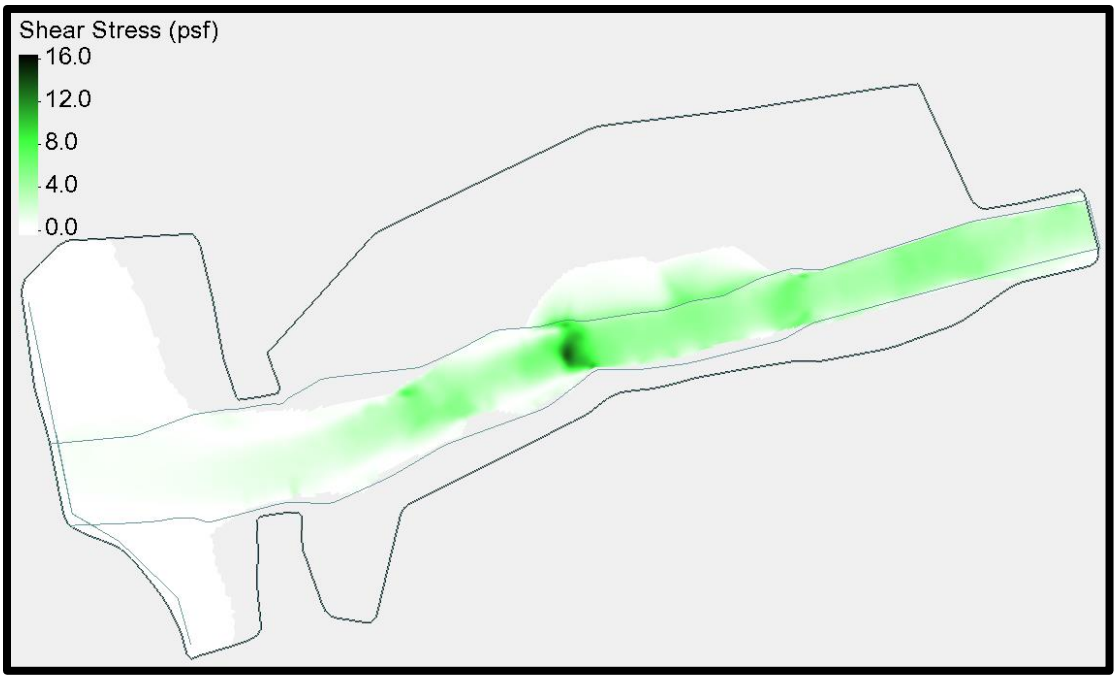

Figure C- 9. Shear stress results from Little Mill Creek model simulated for the 100-year return period flow with Smith River 25-year backwater water surface elevation.

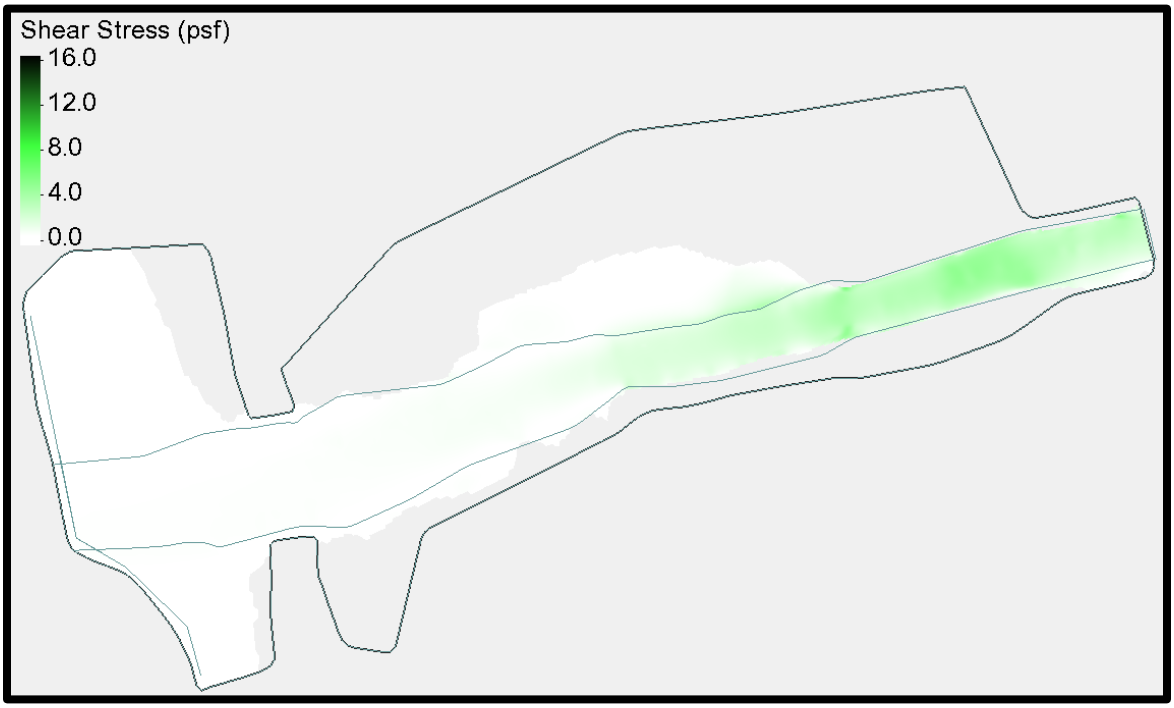

Figure C- 10. Shear stress results from Little Mill Creek model simulated for the 25-year return period flow with Smith River 100-year backwater water surface elevation.

North Fork Ryan Creek

Water Depth/Velocity

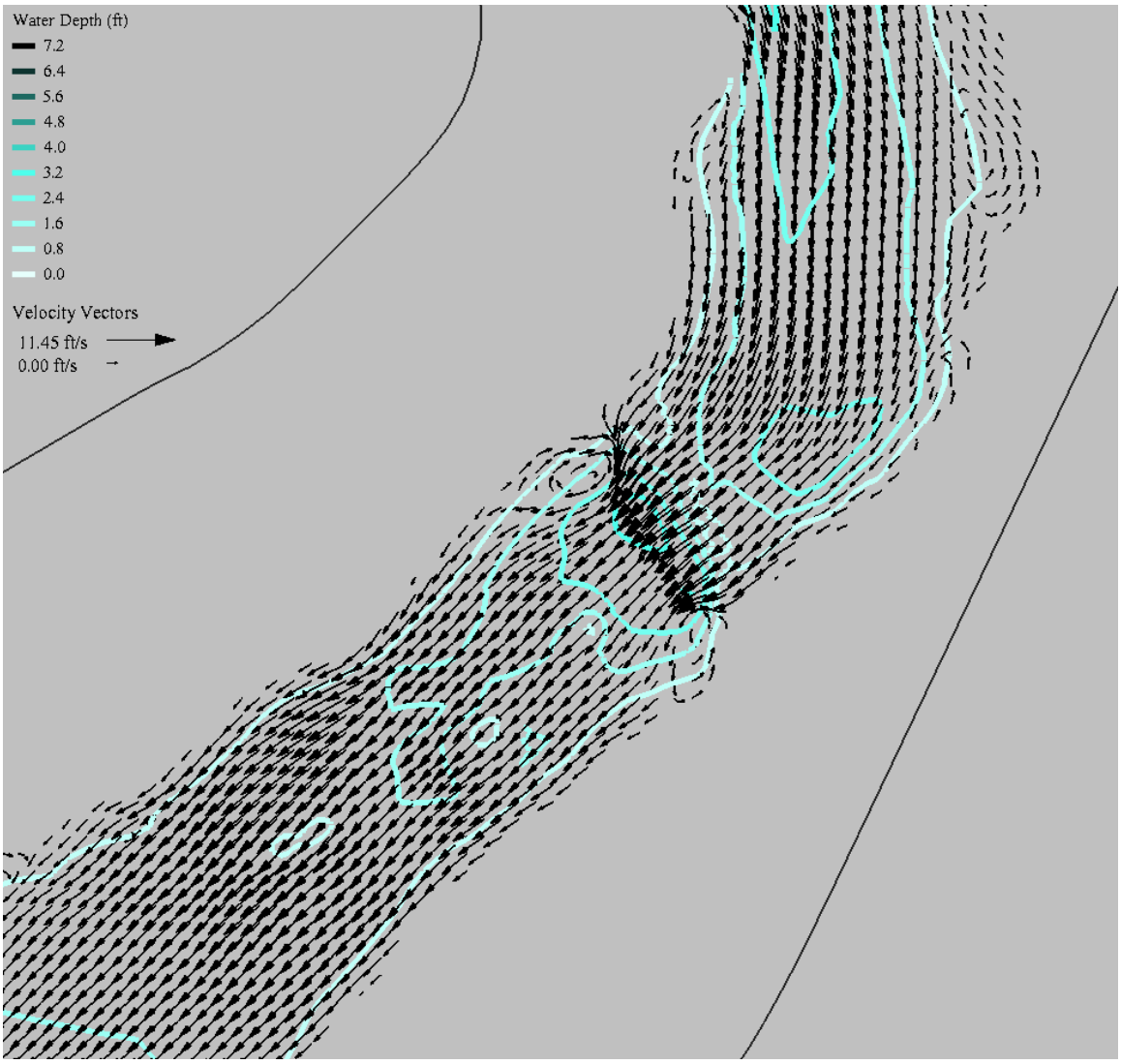

Figure C- 11. Plan view of water depth contours (feet) and velocity vectors (feet per second) at the Rock Weir XS on North Fork Ryan Creek for the 10-year return period flow.

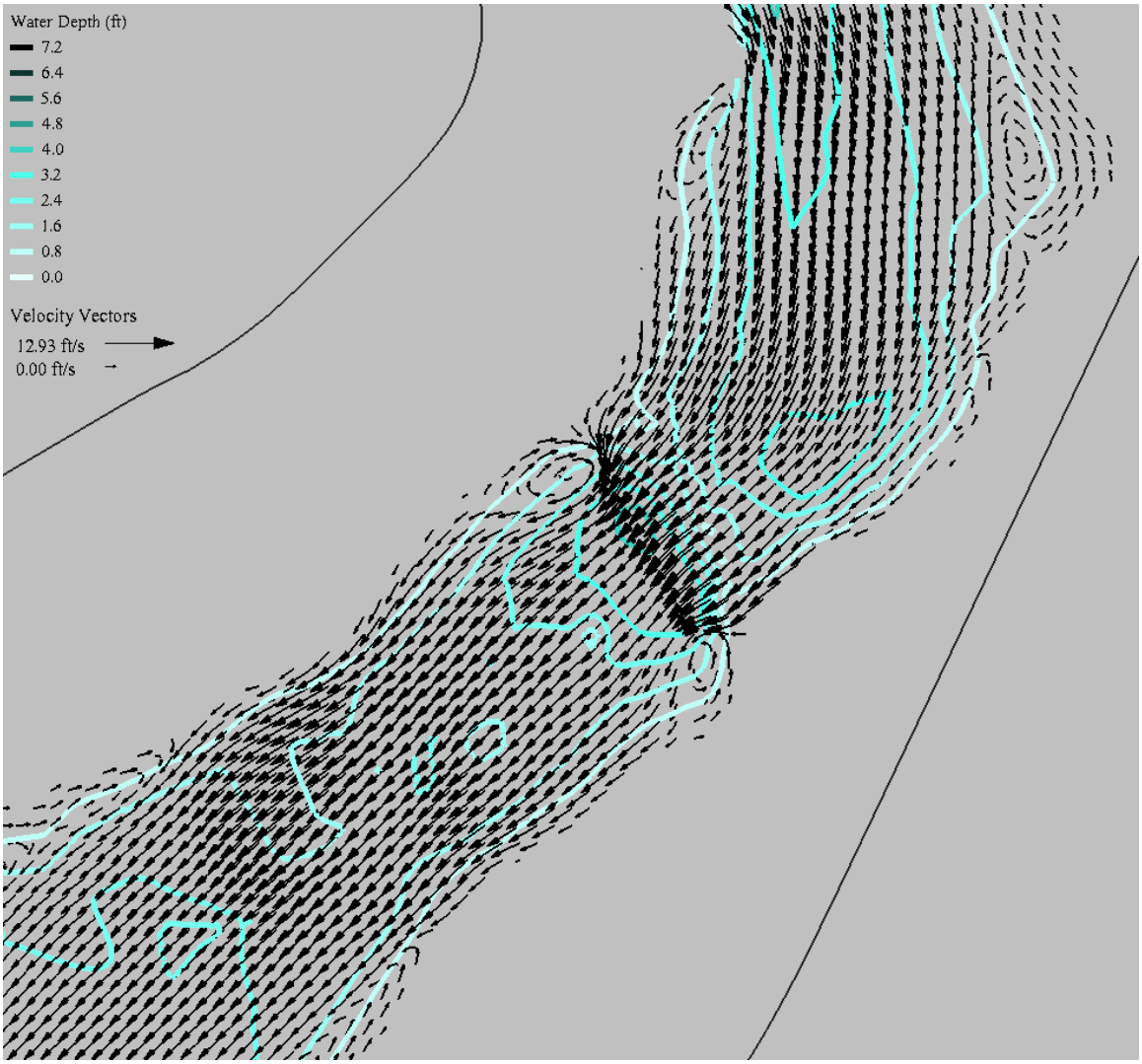

Figure C- 12. Plan view of water depth contours (feet) and velocity vectors (feet per second) at the Rock Weir XS on North Fork Ryan Creek for the 50-year return period flow.

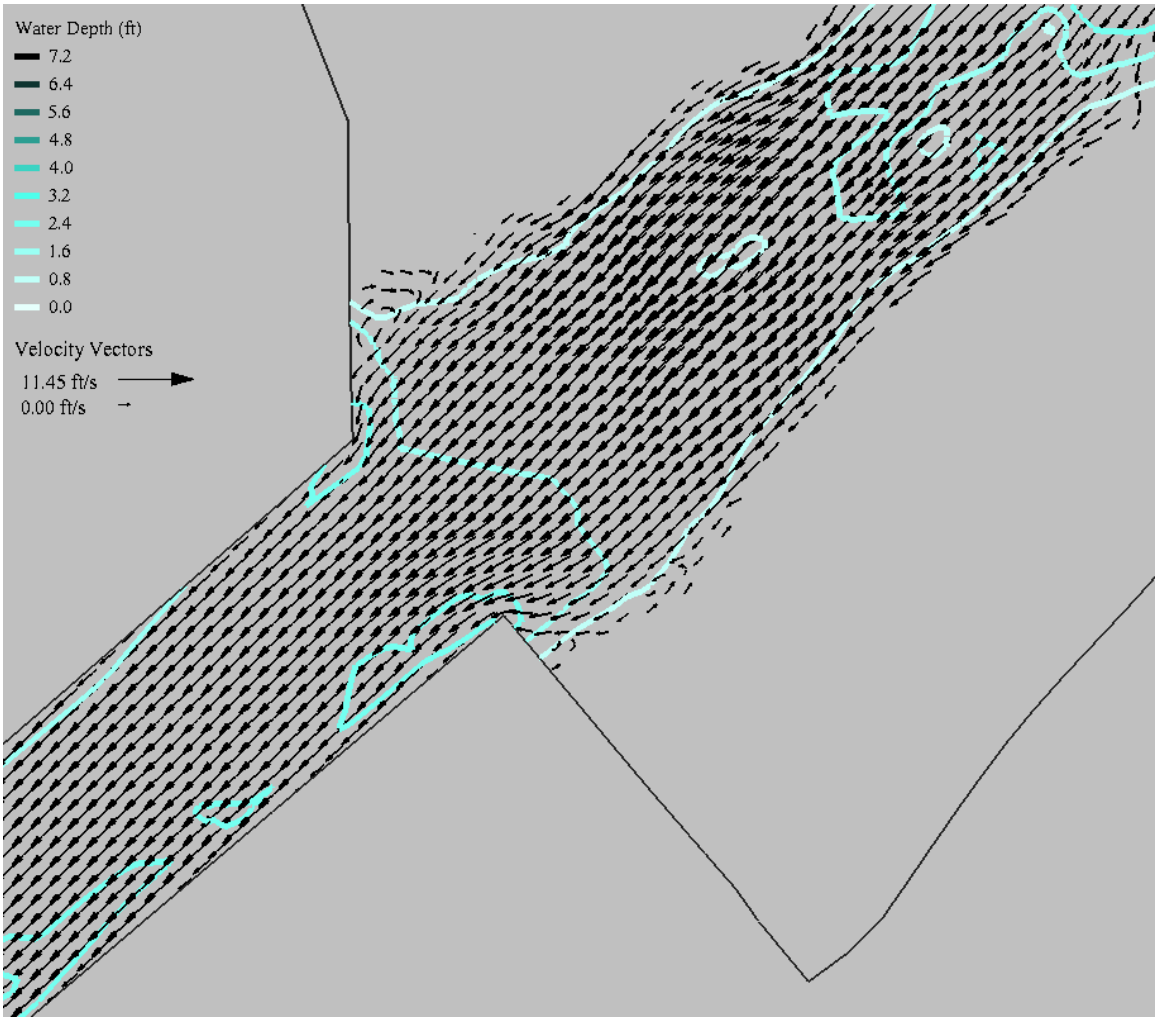

Figure C- 13. Plan view of water depth contours (feet) and velocity vectors (feet per second) at the Crossing Inlet XS on North Fork Ryan Creek for the 10-year return period flow.

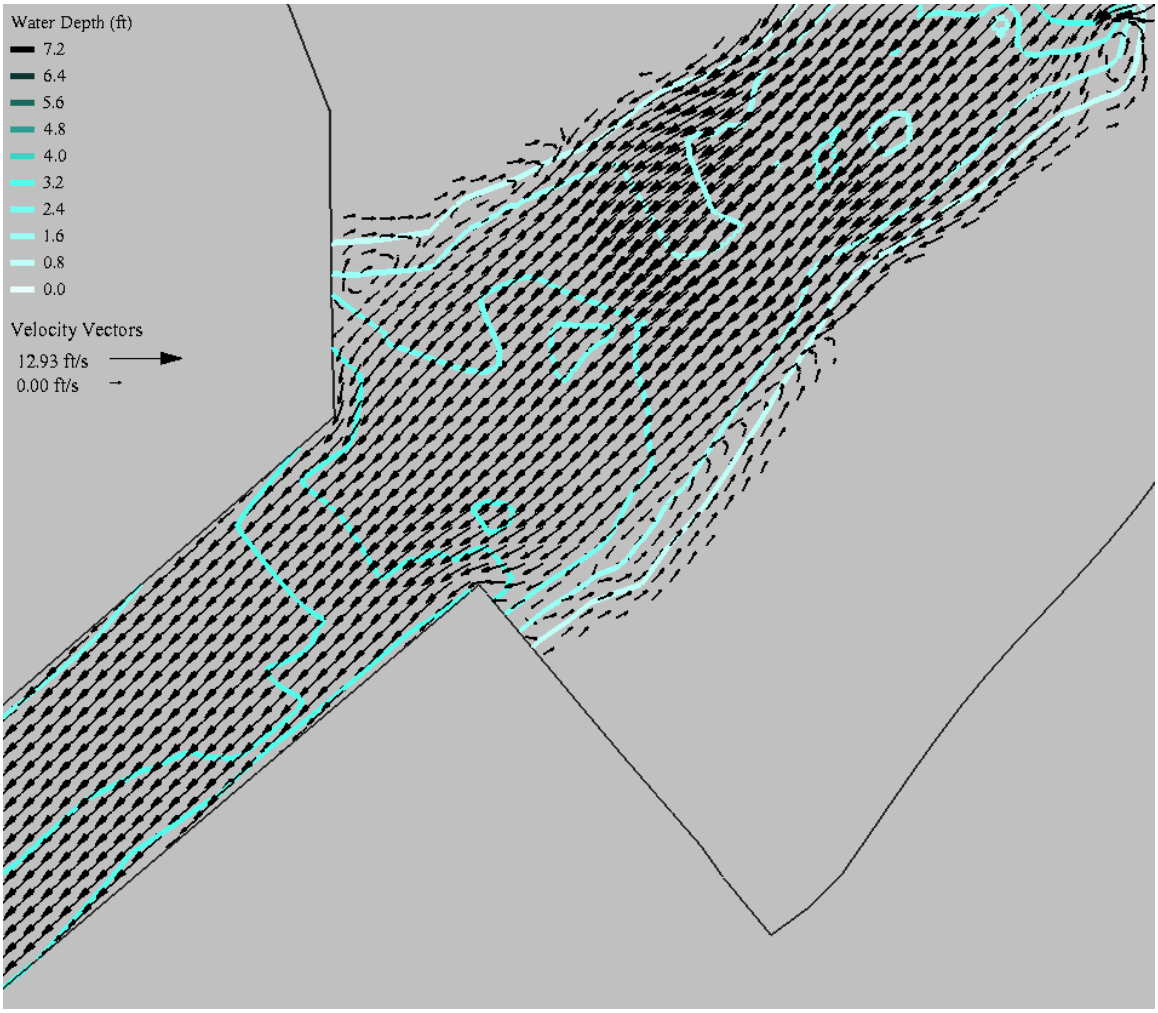

Figure C- 14. Plan view of water depth contours (feet) and velocity vectors (feet per second) at the Crossing Inlet XS on North Fork Ryan Creek for the 50-year return period flow.

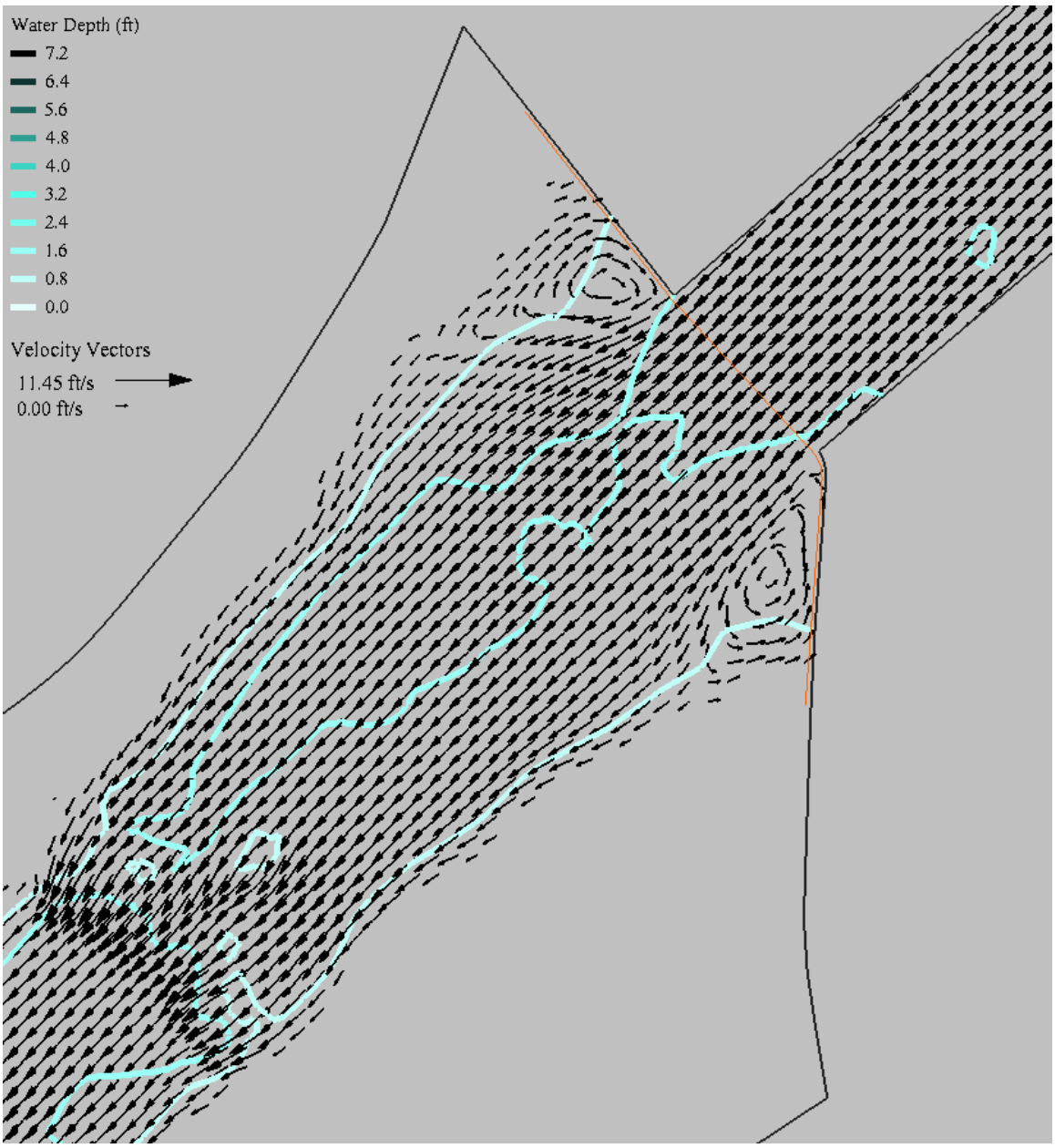

Figure C- 15. Plan view of water depth contours (feet) and velocity vectors (feet per second) at the Crossing Outlet XS on North Fork Ryan Creek for the 10-year return period flow.

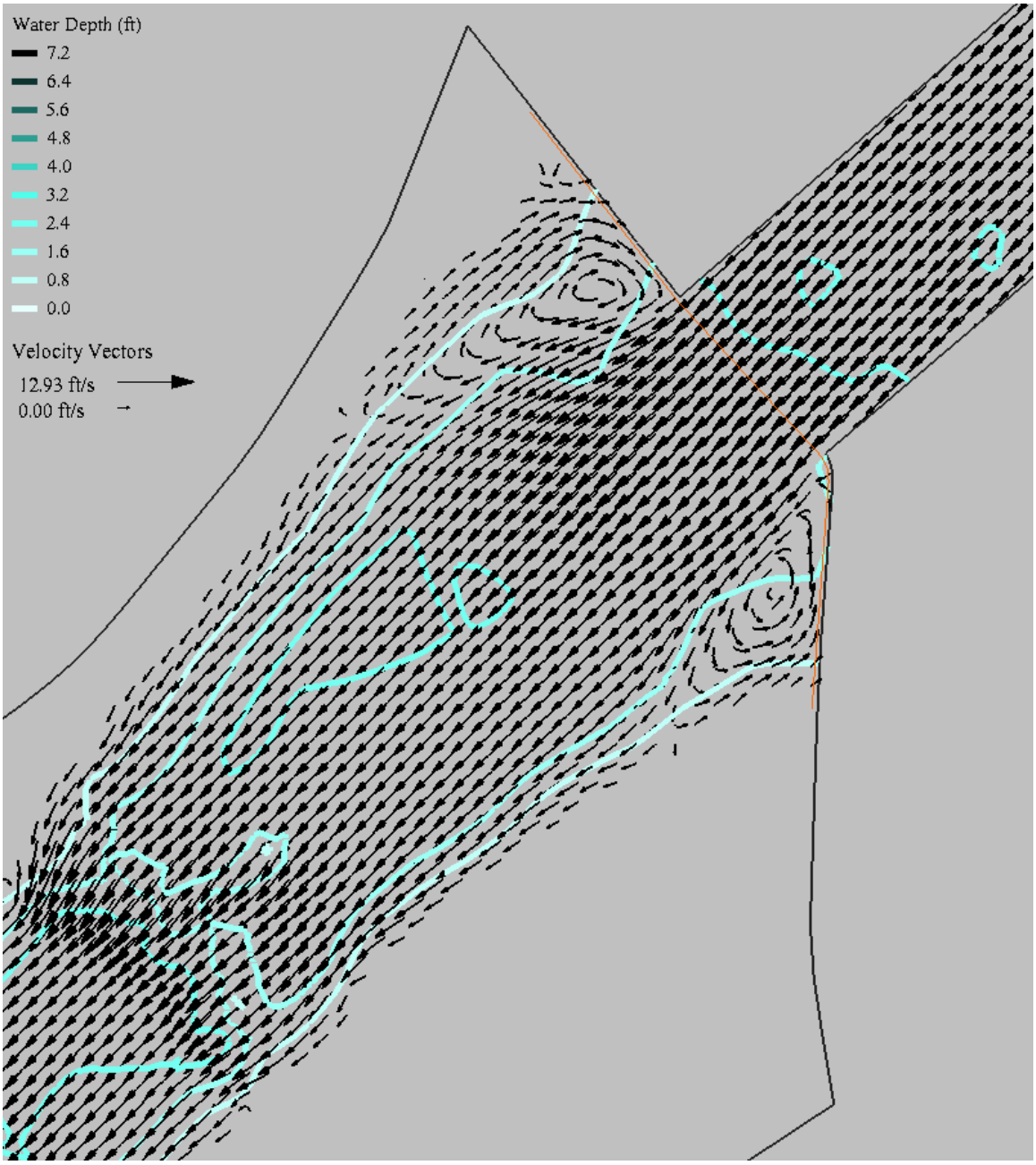

Figure C- 16. Plan view of water depth contours (feet) and velocity vectors (feet per second) at the Crossing Outlet XS on North Fork Ryan Creek for the 50-year return period flow.

Shear Stress

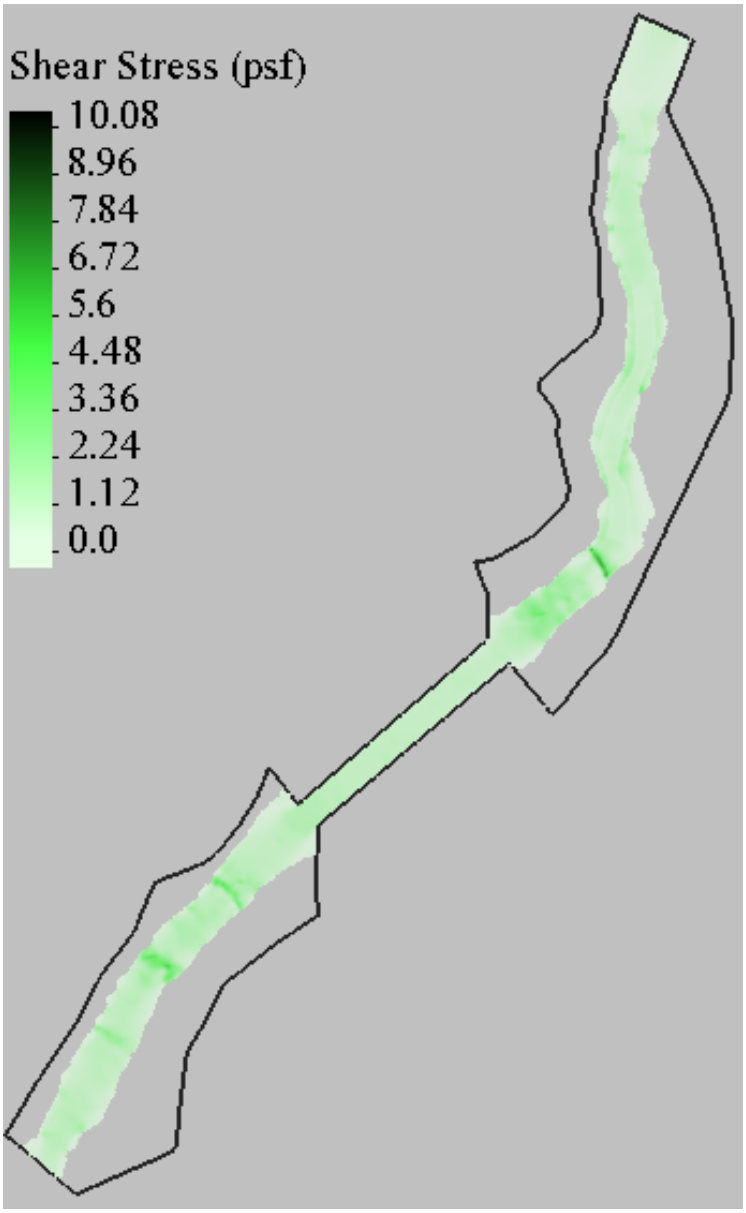

Figure C- 17. Shear stress results from North Fork Ryan Creek model simulated for the 10-year return period flow.

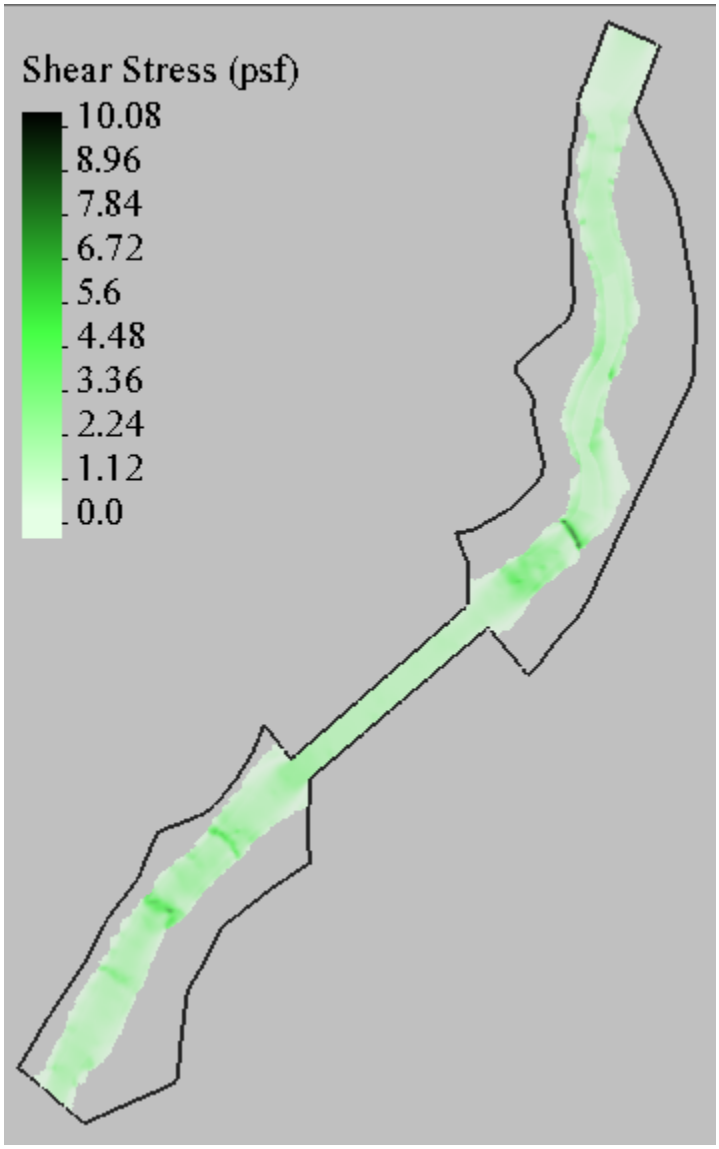

Figure C- 18. Shear stress results from North Fork Ryan Creek model simulated for the 25-year return period flow.

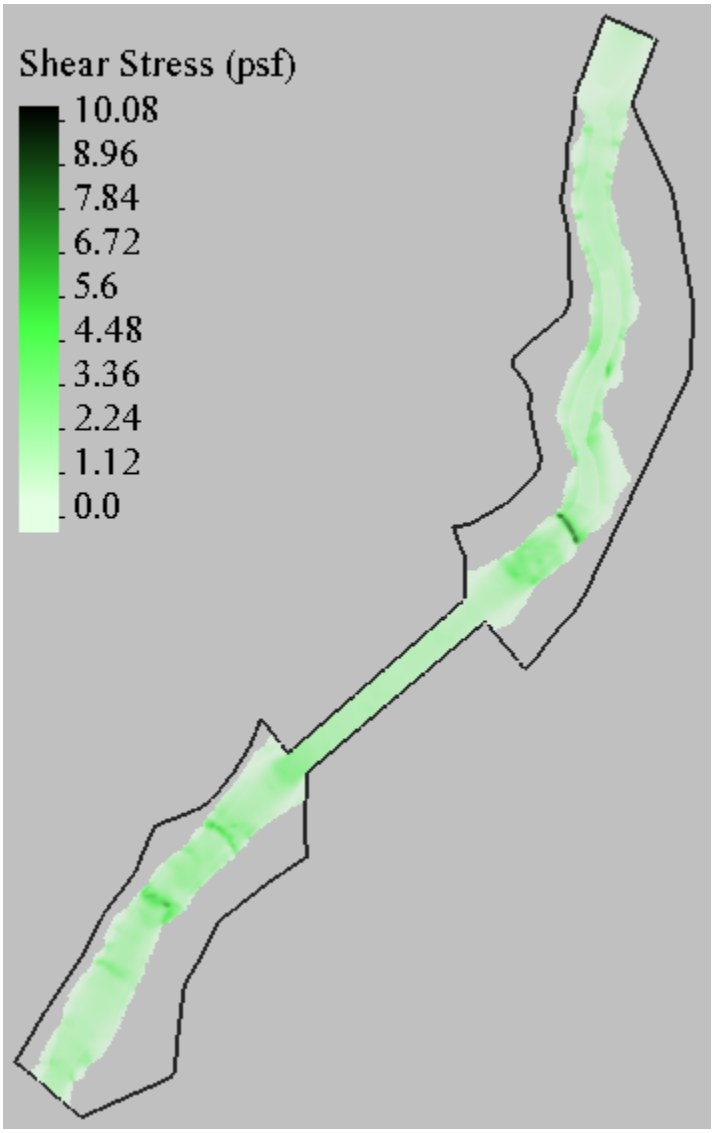

Figure C- 19. Shear stress results from North Fork Ryan Creek model simulated for the 50-year return period flow.

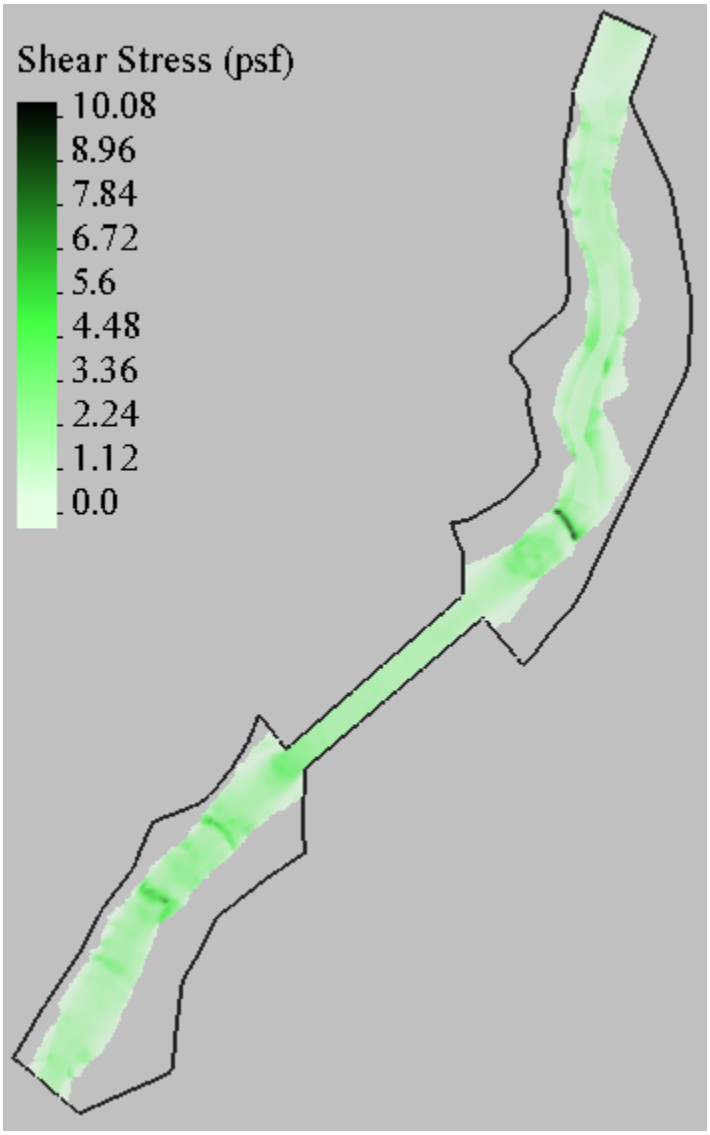

Figure C- 20. Shear stress results from North Fork Ryan Creek model simulated for the 100-year return period flow.

C.2 Water Depth and Velocity Cross-section Plots

Little Mill Creek

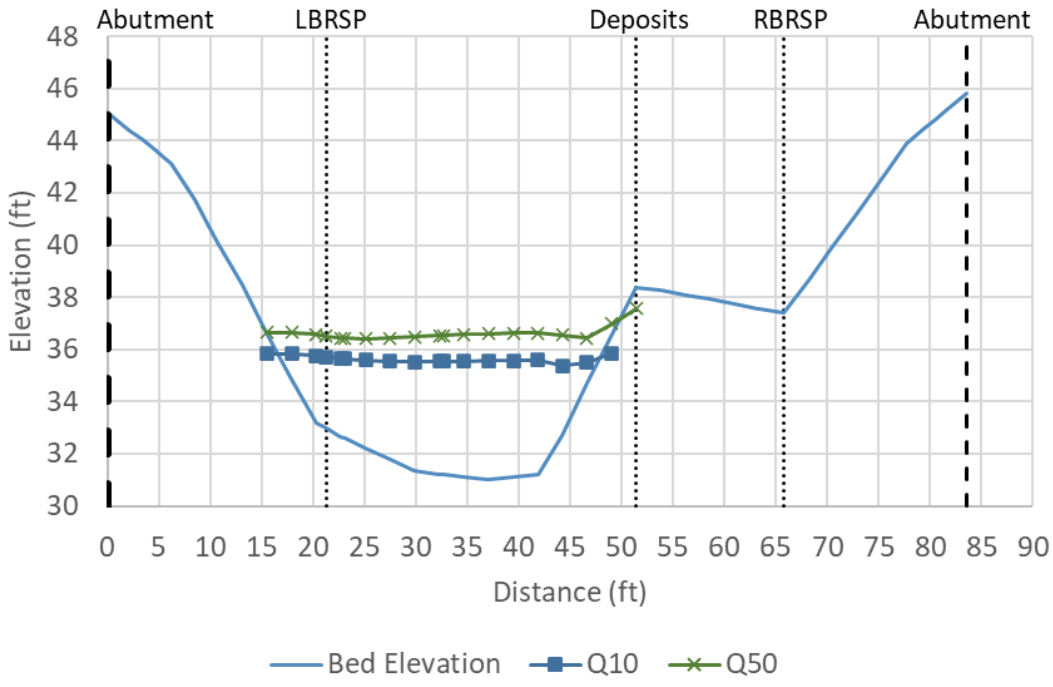

Figure C- 21. Water surface elevation (WSE) and bed elevation plot for the 10- and 50-year return period flows at the Crossing XS on Little Mill Creek.

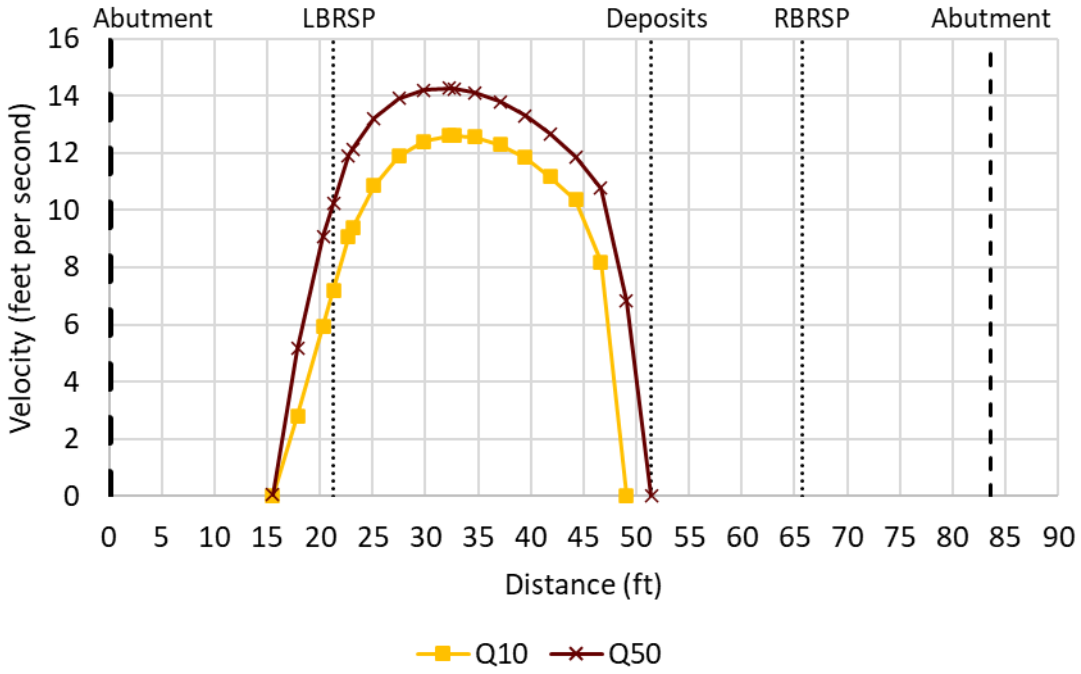

Figure C- 22. Velocity plot for the 10- and 50-year return period flows at the Crossing XS on Little Mill Creek.

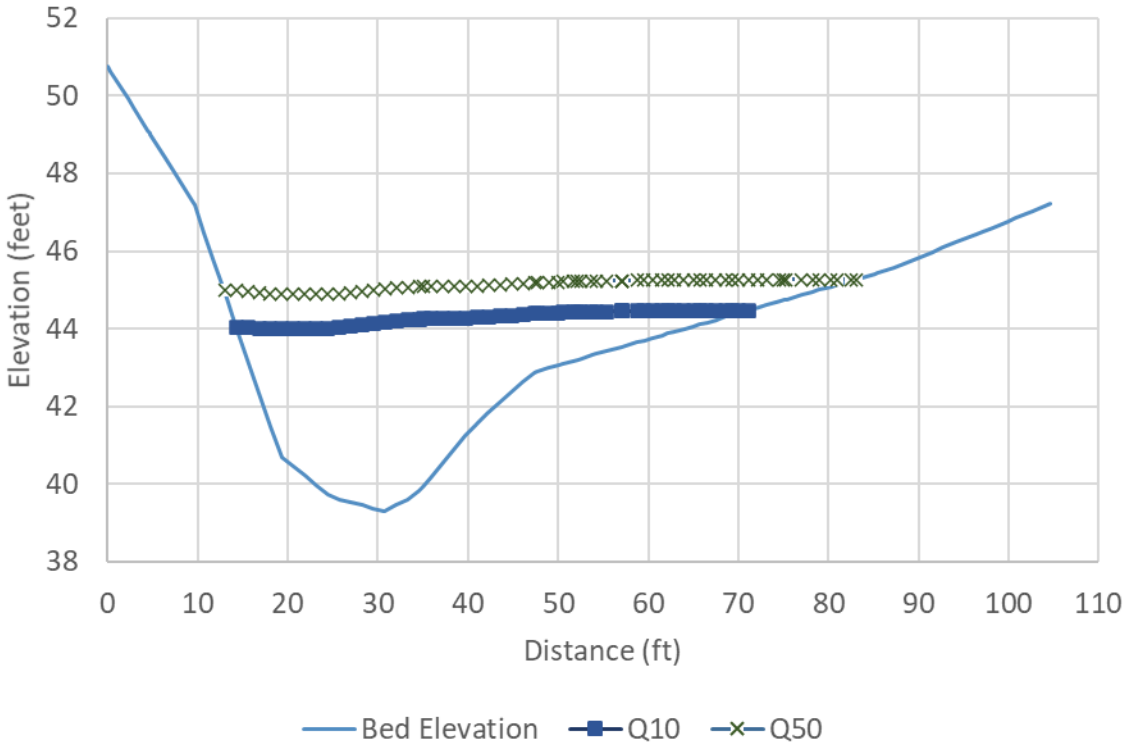

Figure C- 23. Water surface elevation (WSE) and bed elevation plot for the 10- and 50-year return period flows at the Debris XS on Little Mill Creek.

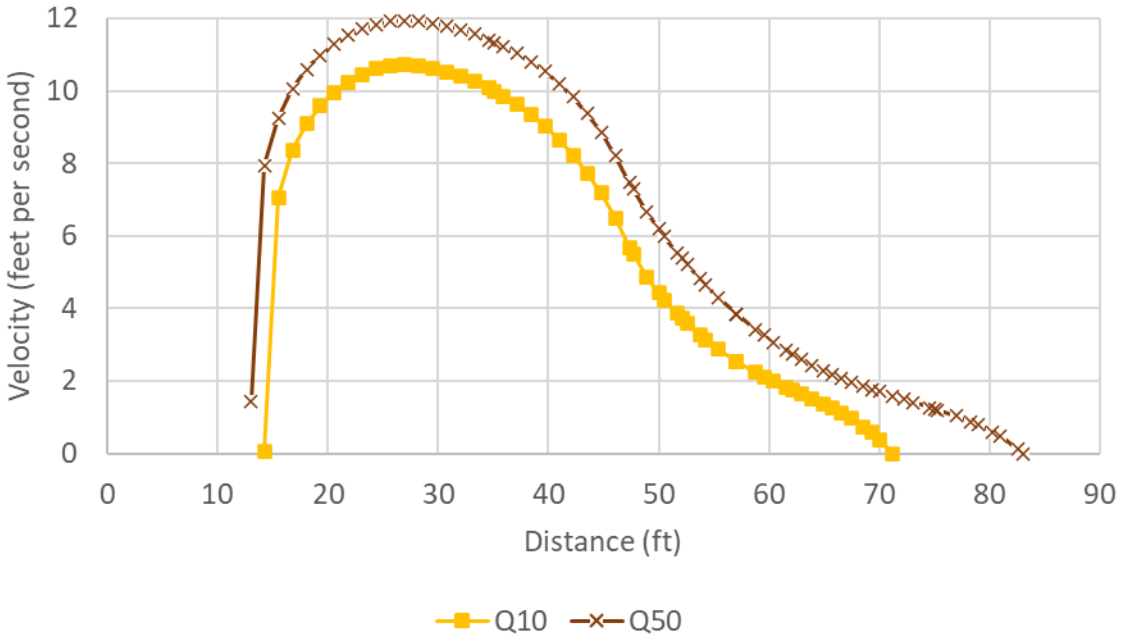

Figure C- 24. Velocity plot for the 10- and 50-year return period flows at the Debris XS on Little Mill Creek.

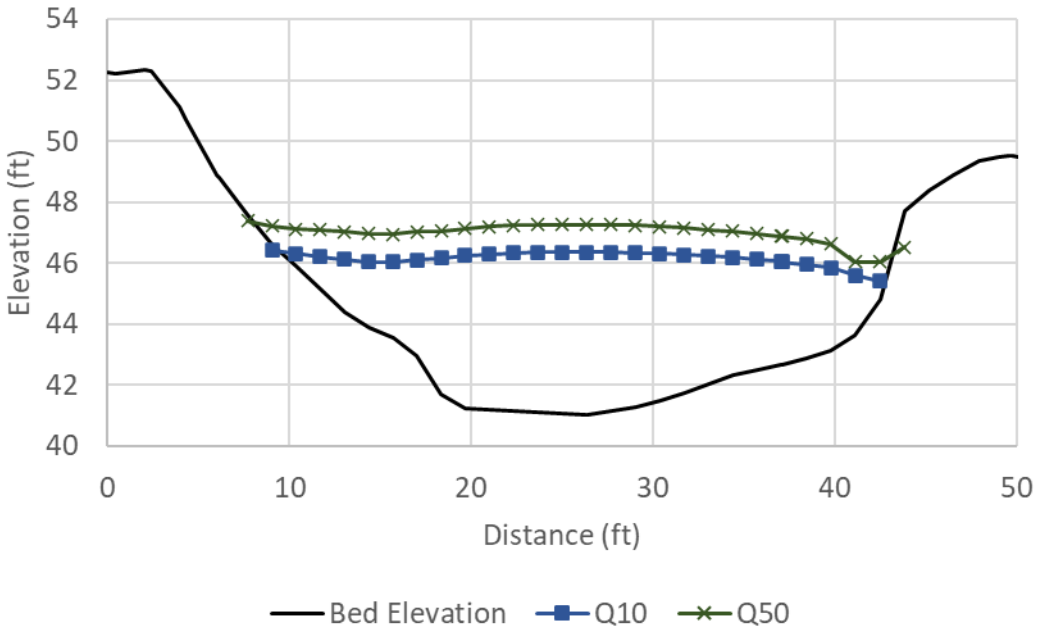

Figure C- 25. Water surface elevation (WSE) and bed elevation plot for the 10- and 50-year return period flows at the Reference Reach XS on Little Mill Creek.

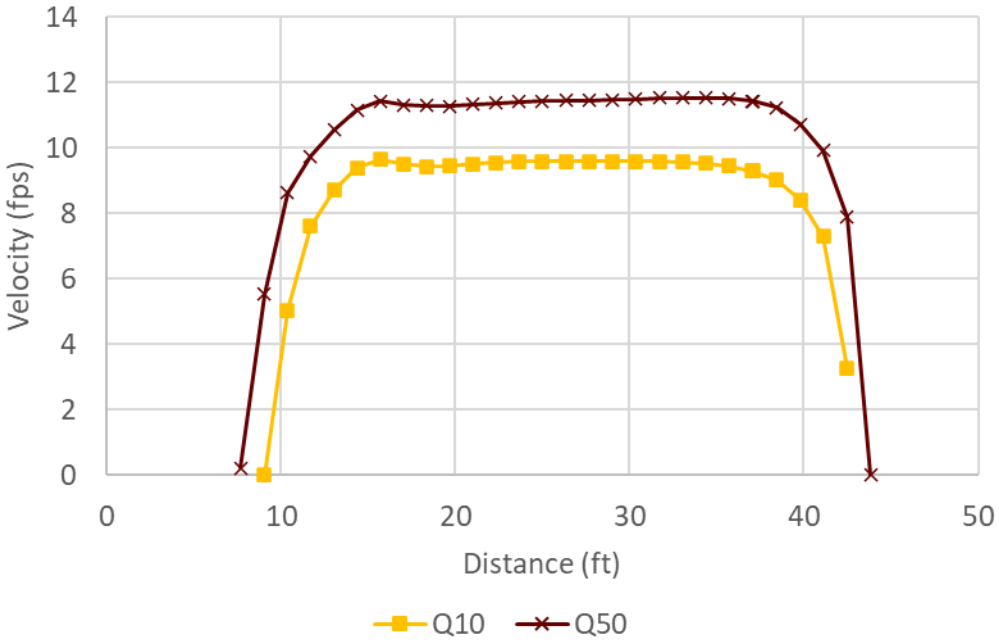

Figure C- 26. Velocity plot for the 10- and 50-year return period flows at the Reference Reach XS on Little Mill Creek.

North Fork Ryan Creek

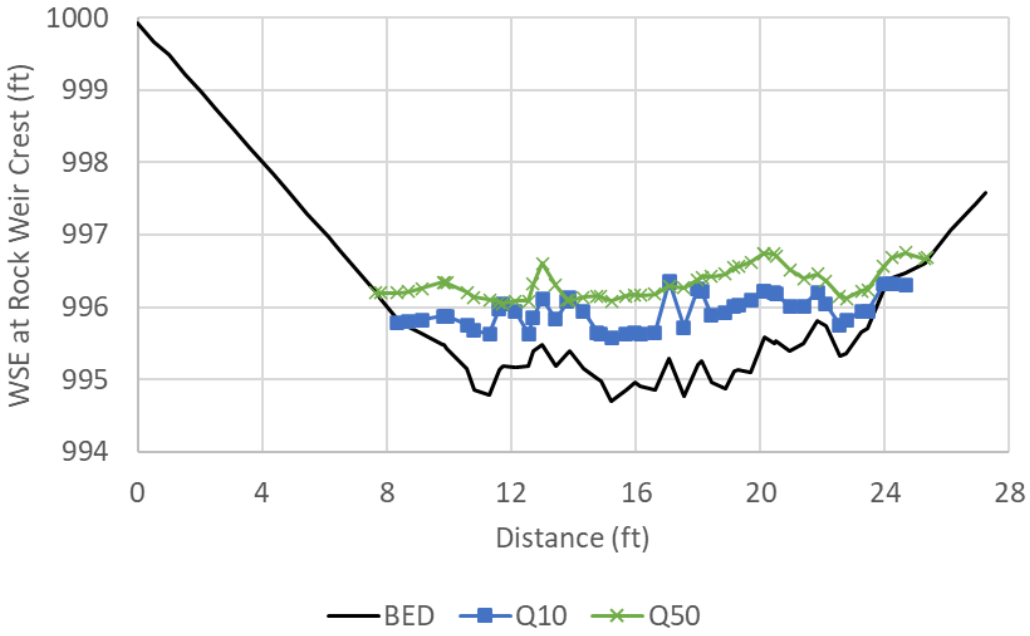

Figure C- 27. Water surface elevation plot at the Rock Weir Crest XS on North Fork Ryan Creek during the 10- and 50-year return period flows.

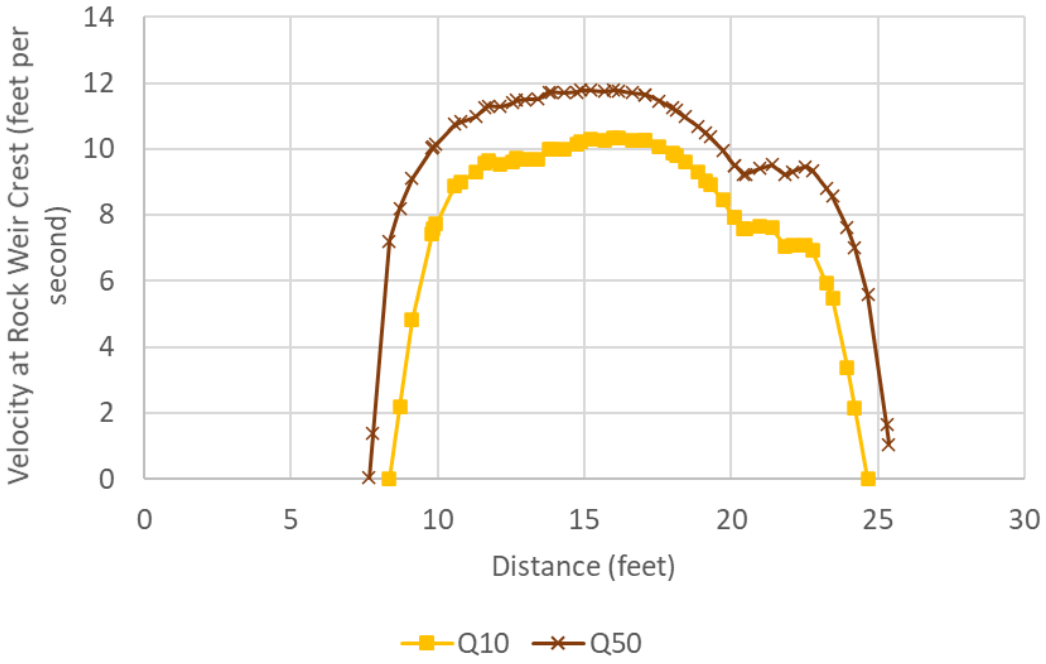

Figure C- 28. Velocities at the Rock Weir Crest XS on North Fork Ryan Creek during the 10- and 50-year return period flows.

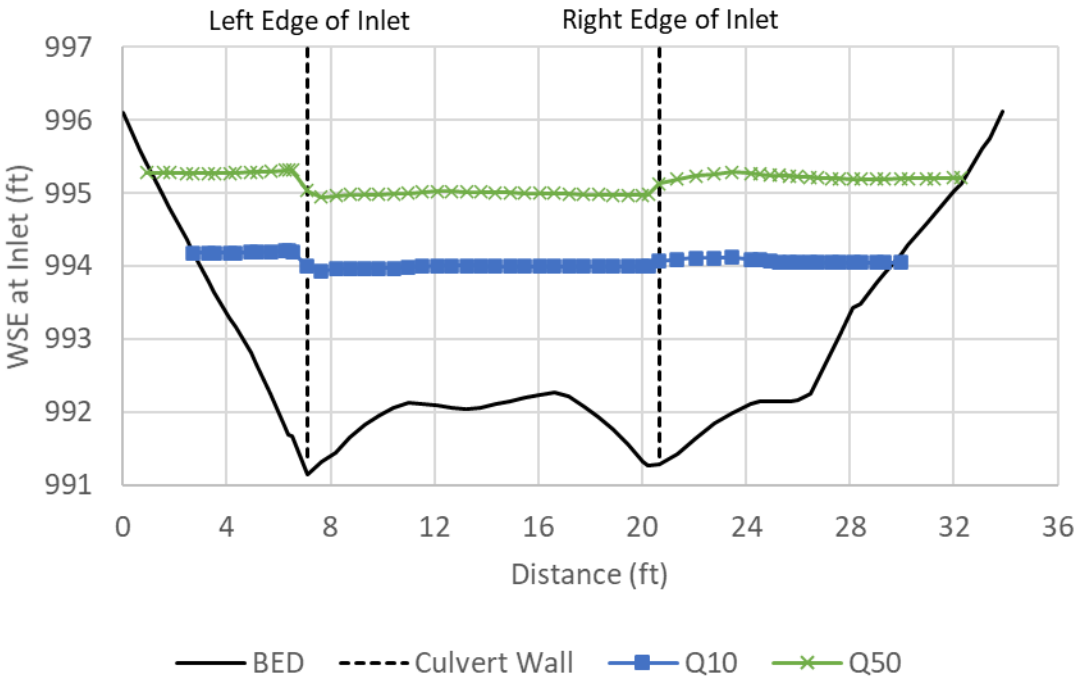

Figure C- 29. Water surface elevation plot at the Crossing Inlet XS on North Fork Ryan Creek during the 10- and 50-year return period flows.

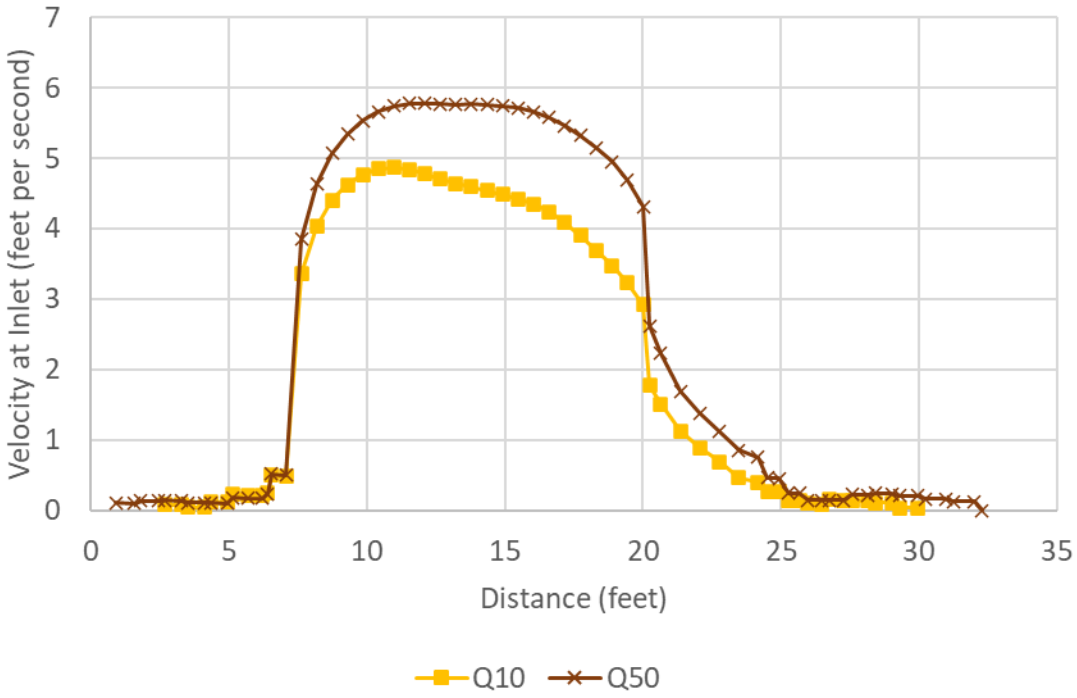

Figure C- 30. Velocity plot at the Crossing Inlet XS on North Fork Ryan Creek during the 10- and 50-year return period flows.

Figure C- 31. Water surface elevation plot at the Crossing Outlet XS on North Fork Ryan Creek during the 10- and 50-year return period flows.

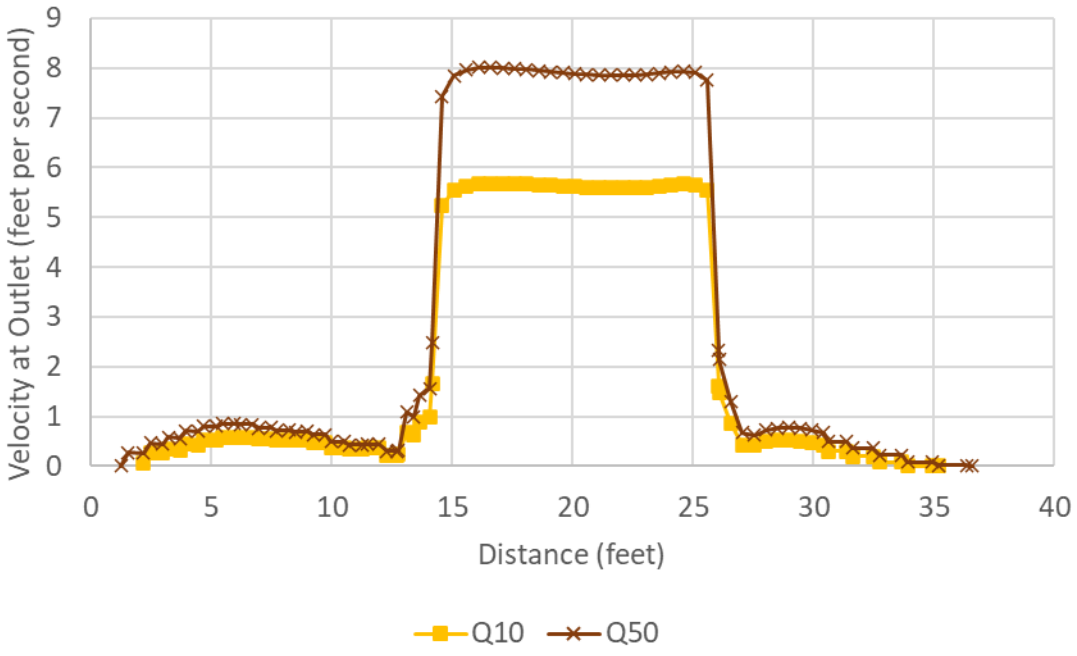

Figure C- 32. Velocity plot at the Crossing Outlet XS on North Fork Ryan Creek during the 10- and 50-year return period flows.

C.3 Sensitivity Analysis

Materials Roughness

Little Mill

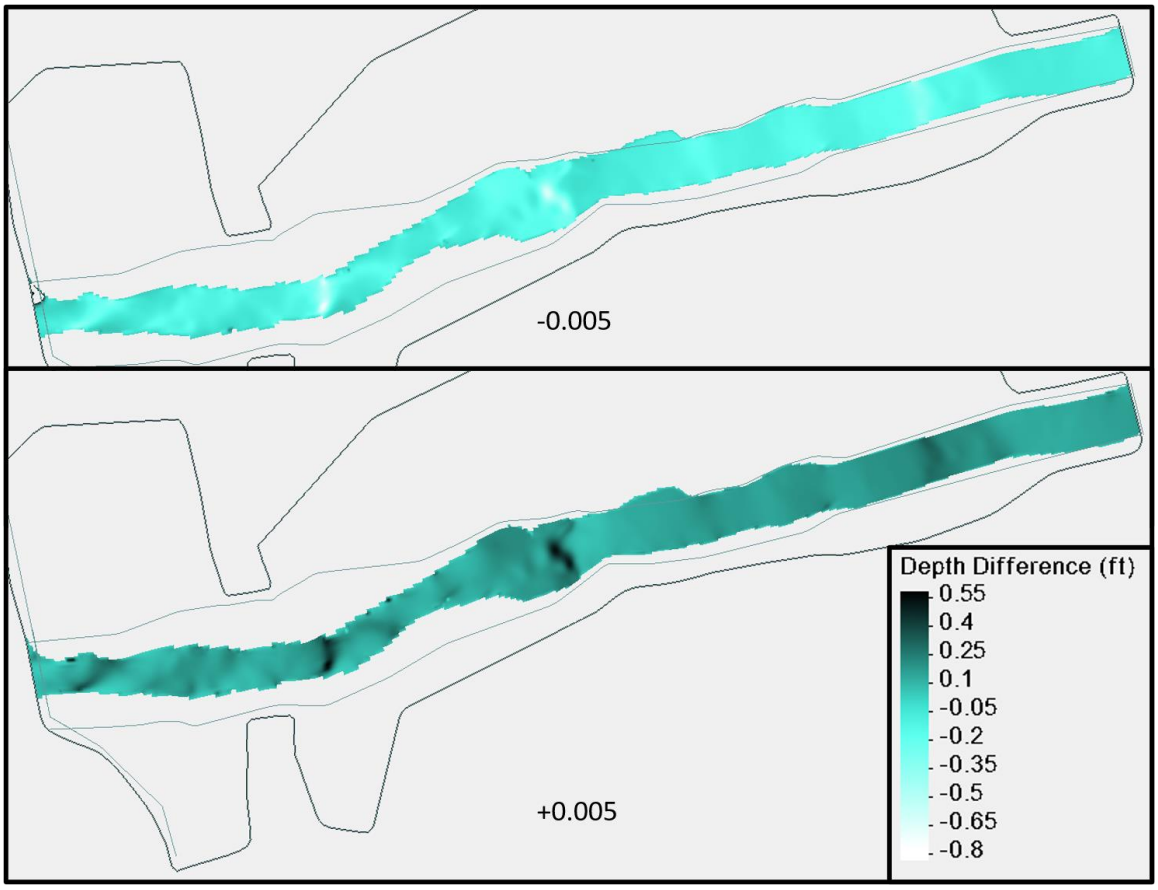

Figure C- 33. Little Mill Creek, Q2. Difference in water depth results between the base case and a sensitivity simulation with a decrease (top) and increase (bottom) of 0.005 in the entire model's materials roughness values (sensitivity case – base case).

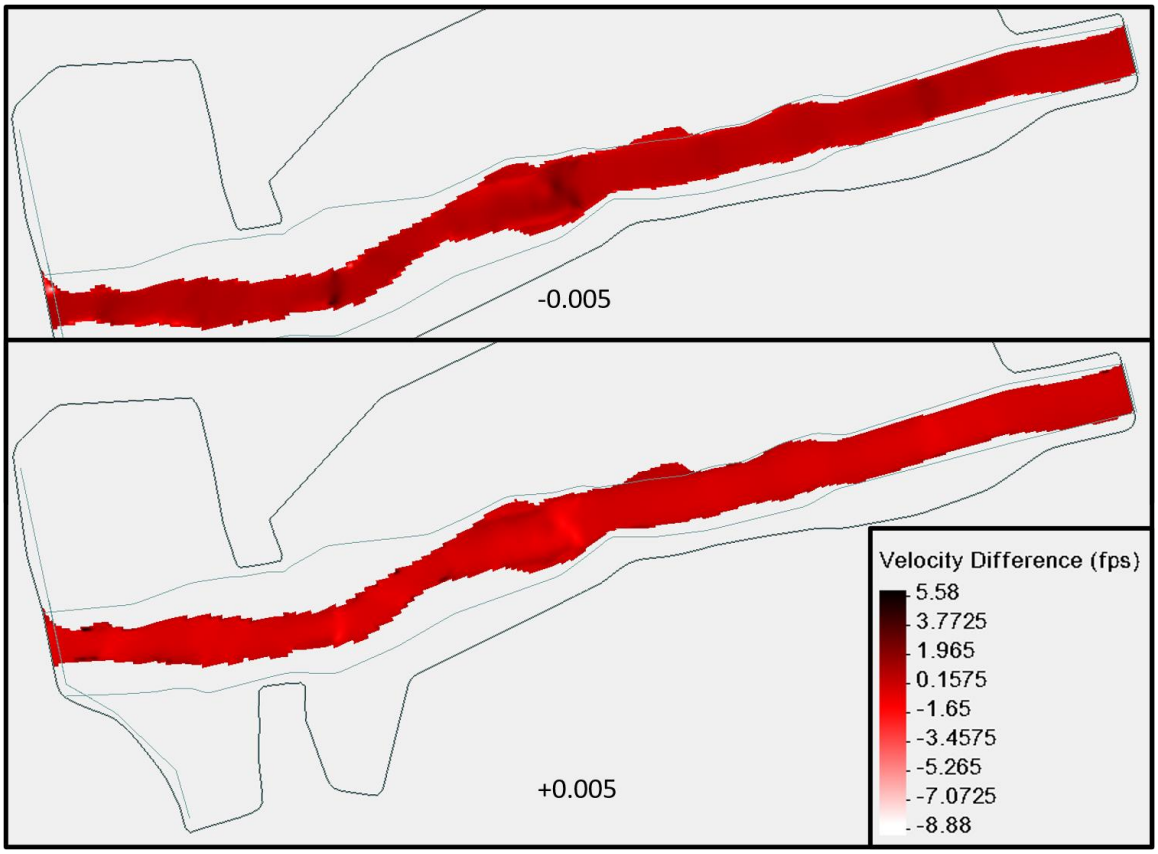

Figure C- 34. Little Mill Creek, Q2. Difference in velocity results between the base case and a sensitivity simulation with a decrease (top) and increase (bottom) of 0.005 in the entire model's materials roughness values (sensitivity case – base case).

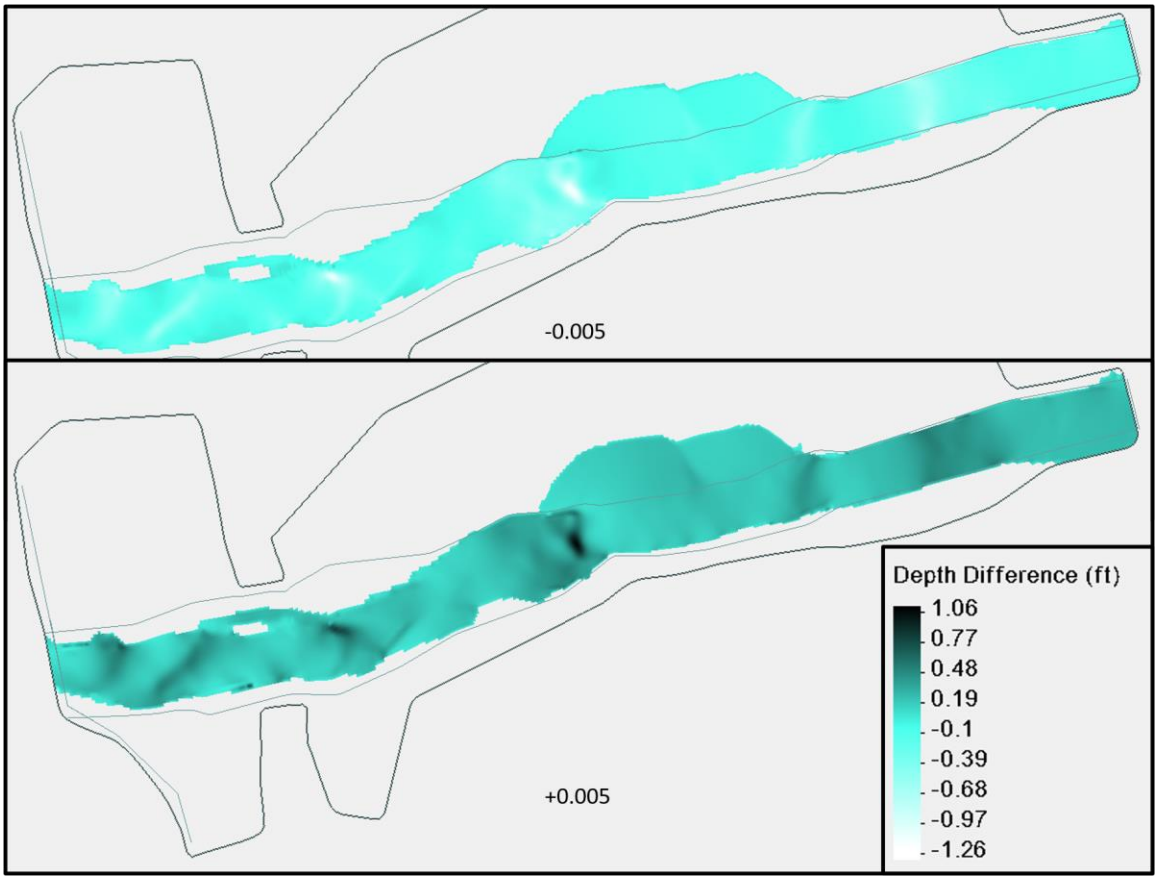

Figure C- 35. Little Mill Creek, Q100. Difference in water depth results between the base case and a sensitivity simulation with a decrease (top) and increase (bottom) of 0.005 in the entire model's materials roughness values (sensitivity case – base case).

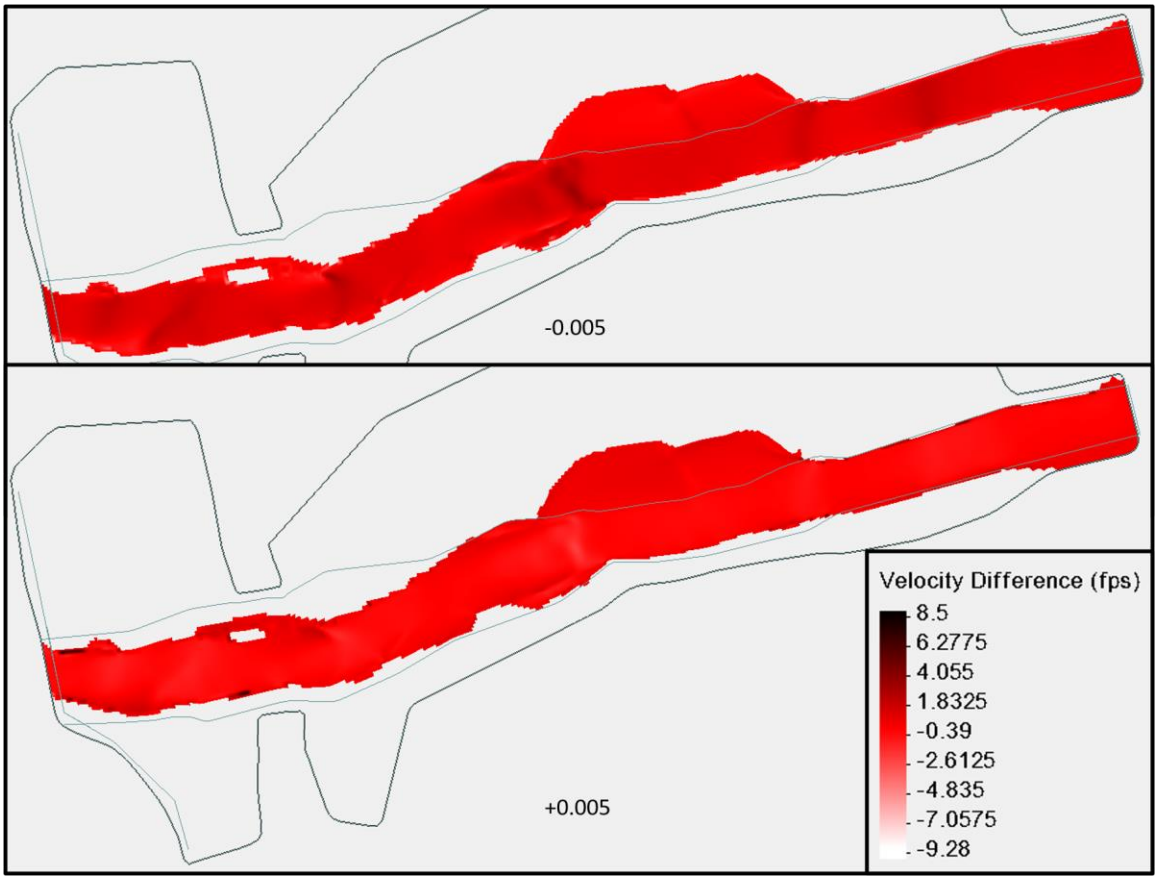

Figure C- 36. Little Mill Creek, Q100. Difference in velocity results between the base case and a sensitivity simulation with a decrease (top) and increase (bottom) of 0.005 in the entire model's materials roughness values (sensitivity case – base case).

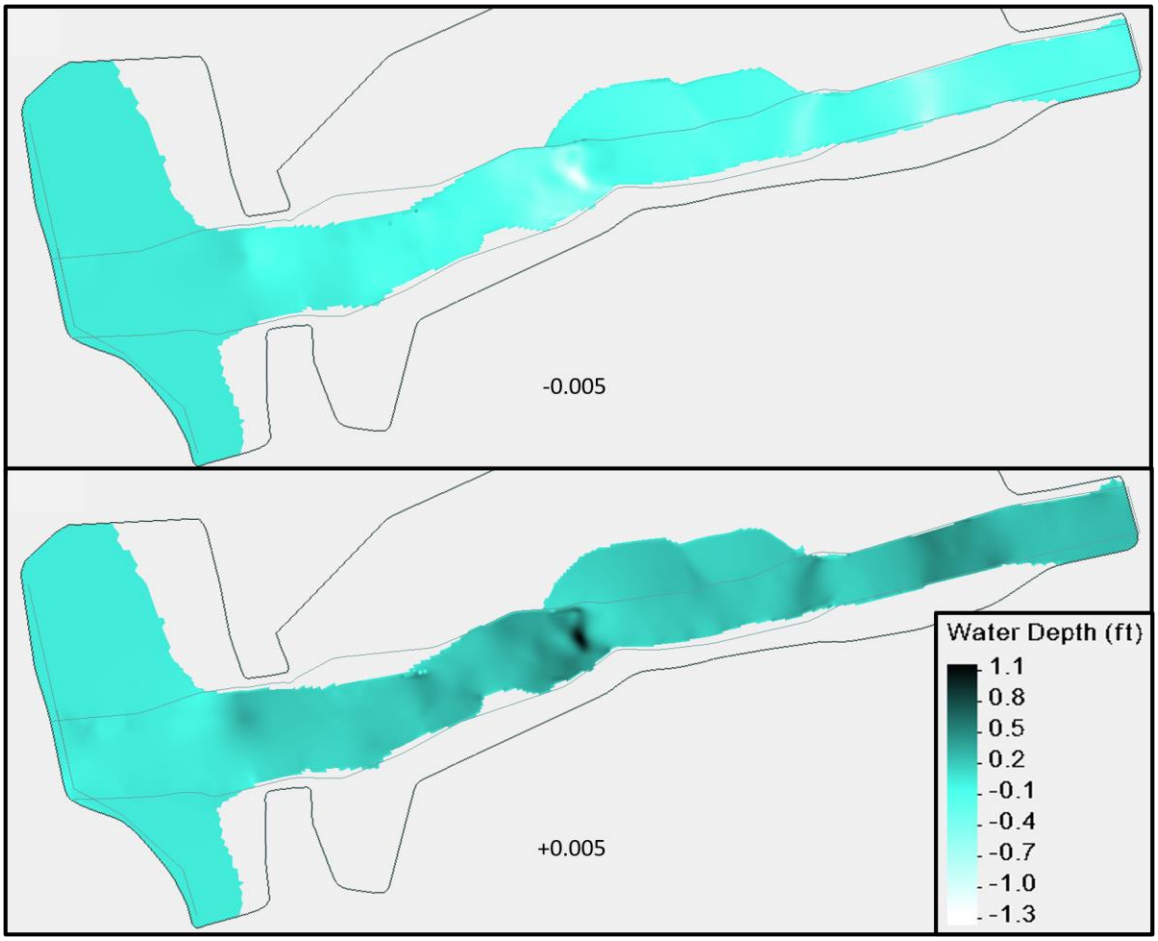

Figure C- 37. Little Mill Creek, Q100 flow with Smith River Q25 backwater event. Difference in water depth results between the base case and a sensitivity simulation with a decrease (top) and increase (bottom) of 0.005 in the entire model's materials roughness values (sensitivity case – base case).

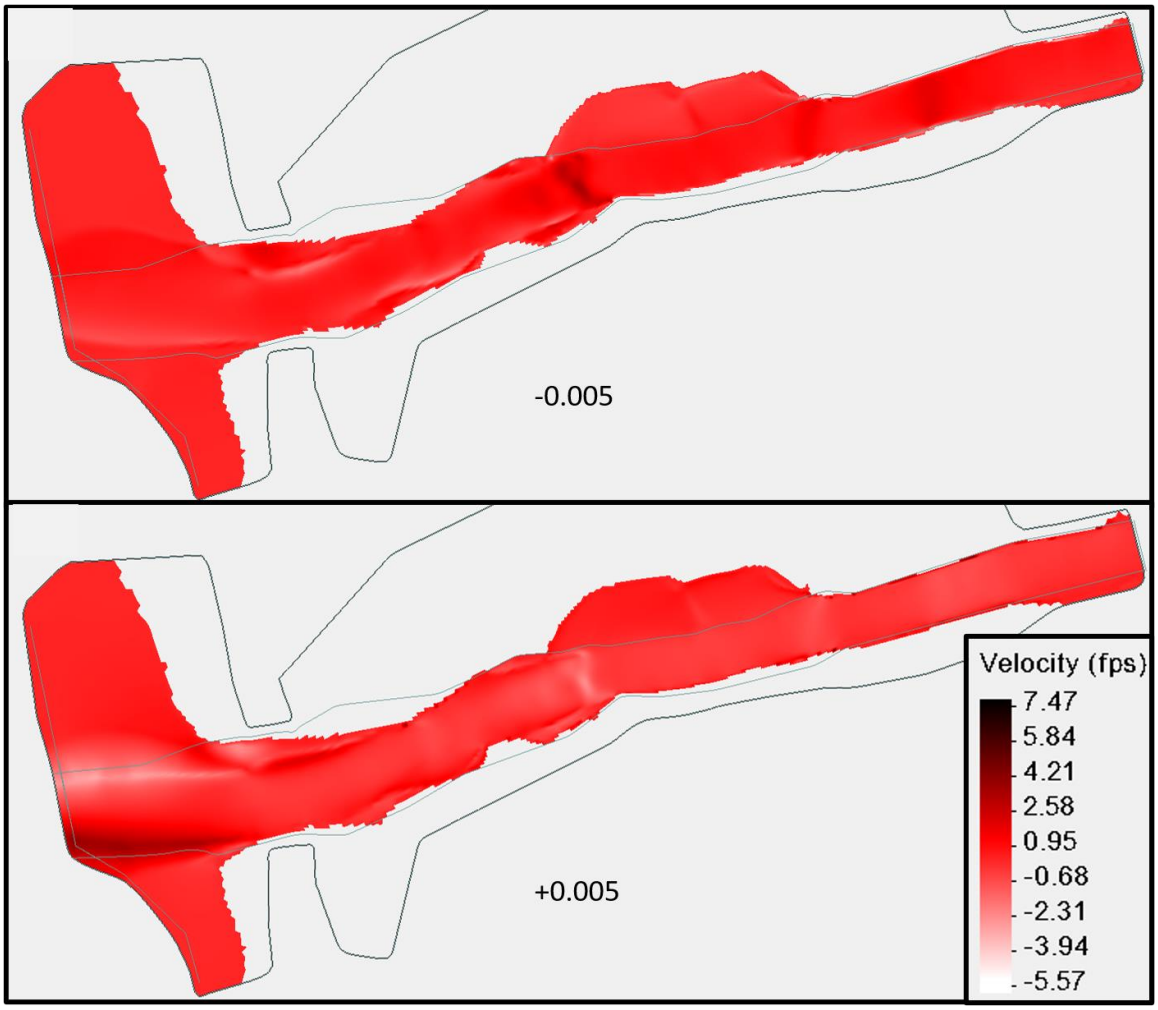

Figure C- 38. Little Mill Creek, Q100 flow with Smith River Q25 backwater event. Difference in velocity results between the base case and a sensitivity simulation with a decrease (top) and increase (bottom) of 0.005 in the entire model's materials roughness values (sensitivity case – base case).

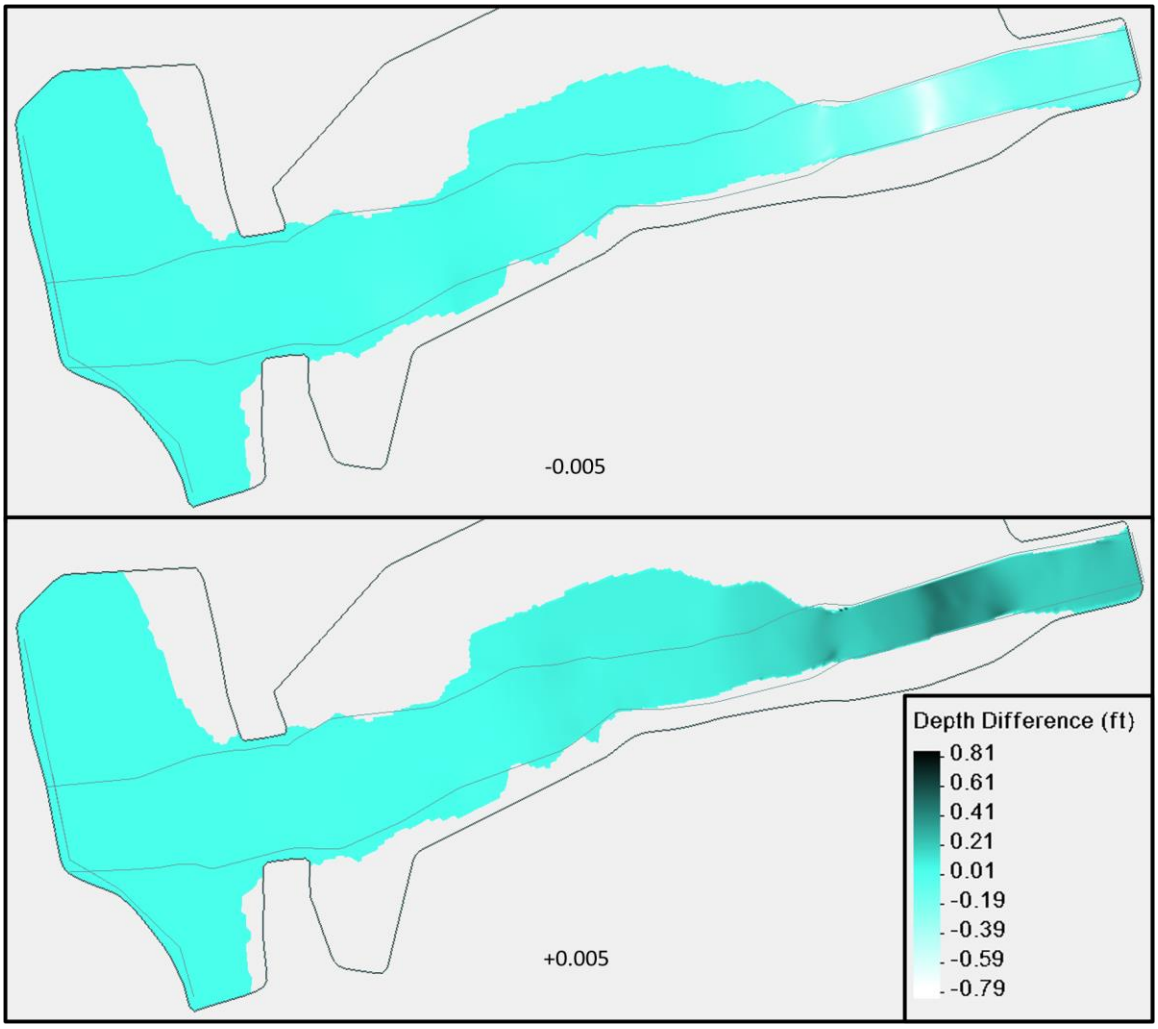

Figure C- 39. Little Mill Creek, Q25 with Smith River Q100 backwater. Difference in water depth results between the base case and a sensitivity simulation with a decrease (top) and increase (bottom) of 0.005 in the entire model's materials roughness values (sensitivity case – base case).

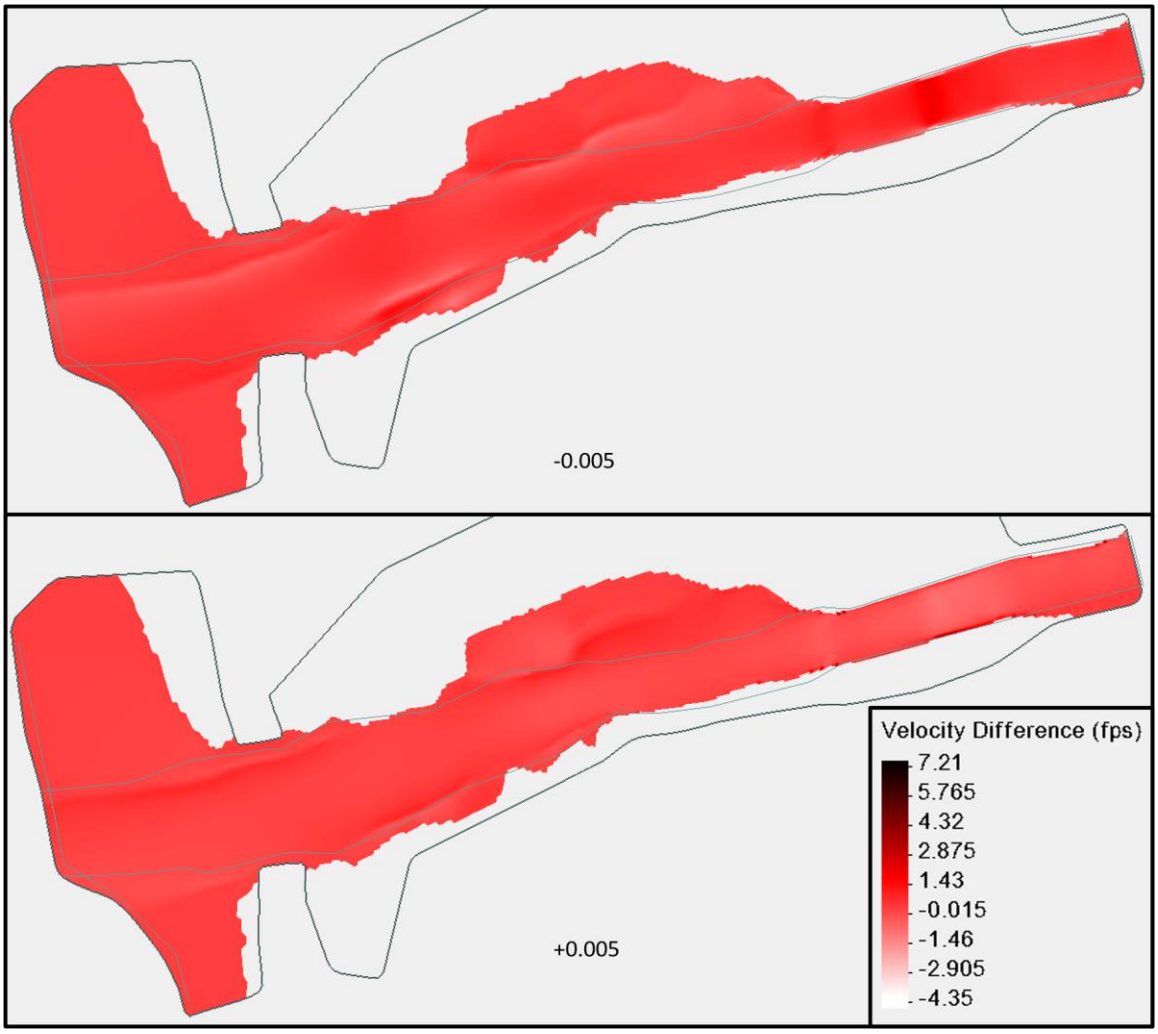

Figure C- 40. Little Mill Creek, Q25 with Smith River Q100 backwater. Difference in velocity results between the base case and a sensitivity simulation with a decrease (top) and increase (bottom) of 0.005 in the entire model's materials roughness values (sensitivity case – base case).

North Fork Ryan

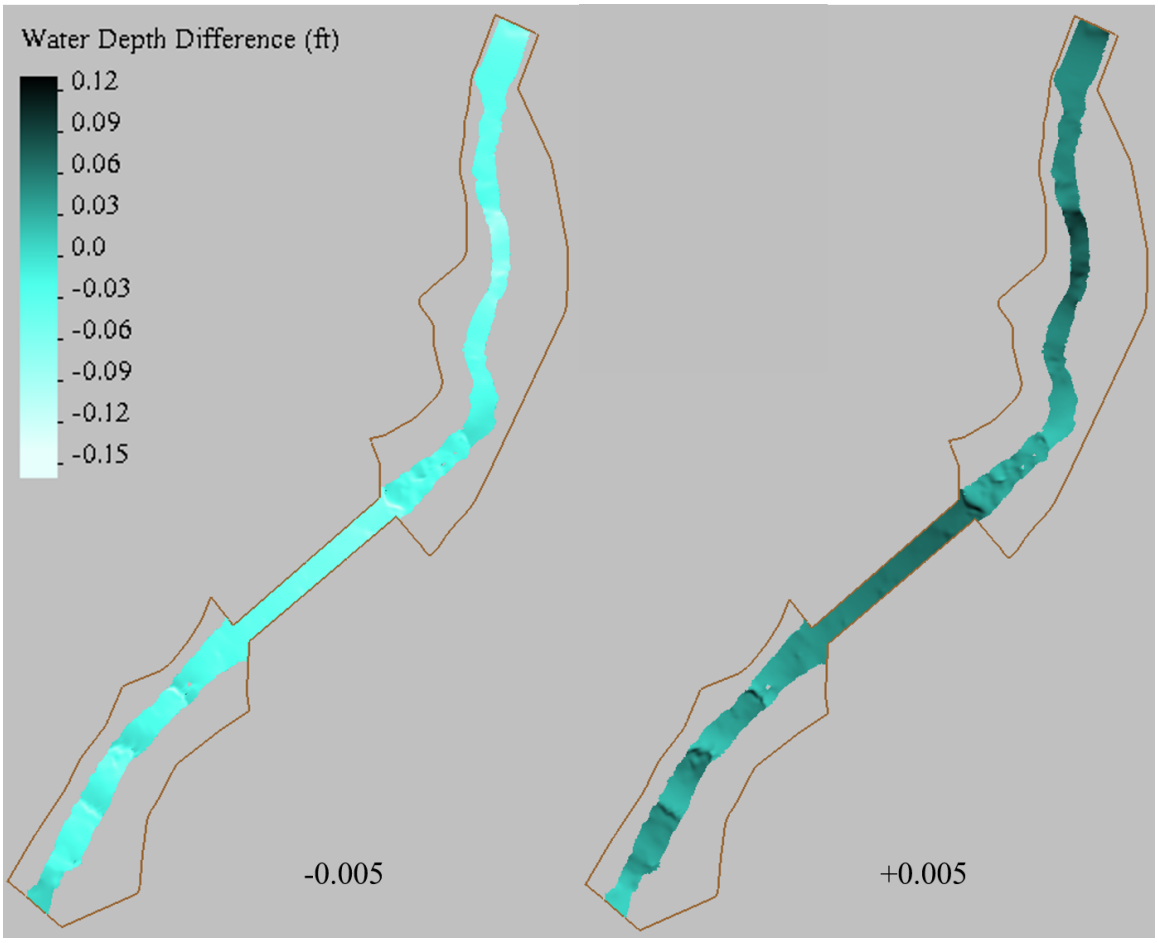

Figure C- 41. North Fork Ryan Creek, Q2. Difference in water depth results between the base case and a sensitivity simulation with a decrease (left) and increase (right) of 0.005 in the entire model's materials roughness values (sensitivity case – base case).

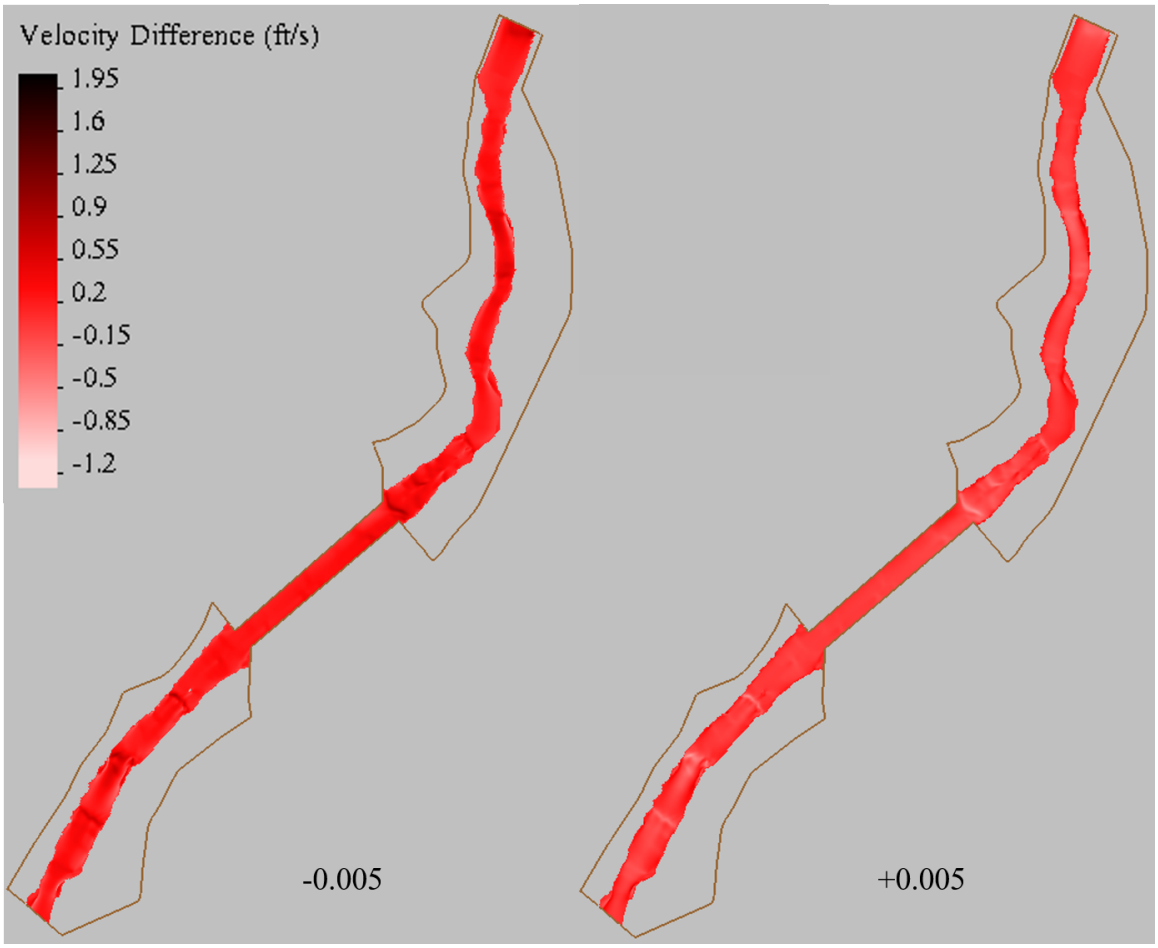

Figure C- 42. North Fork Ryan Creek, Q2. Difference in velocity magnitude results between the base case and a sensitivity simulation with a decrease (left) and increase (right) of 0.005 in the entire model's Manning's roughness values (sensitivity case – base case).

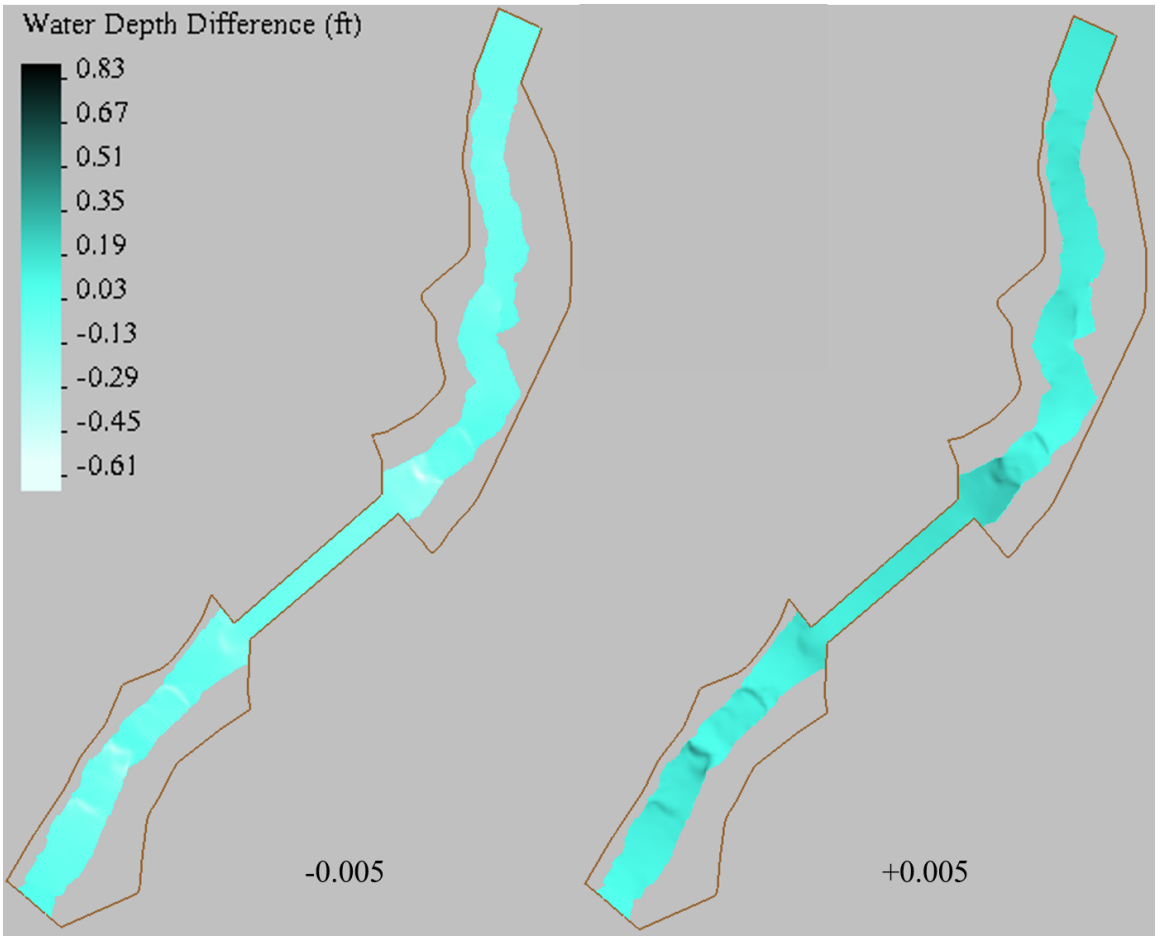

Figure C- 43. North Fork Ryan Creek, Q100. Difference in water depth results between the base case and a sensitivity simulation with a decrease (left) and increase (right) of 0.005 in the entire model's materials roughness values (sensitivity case – base case).

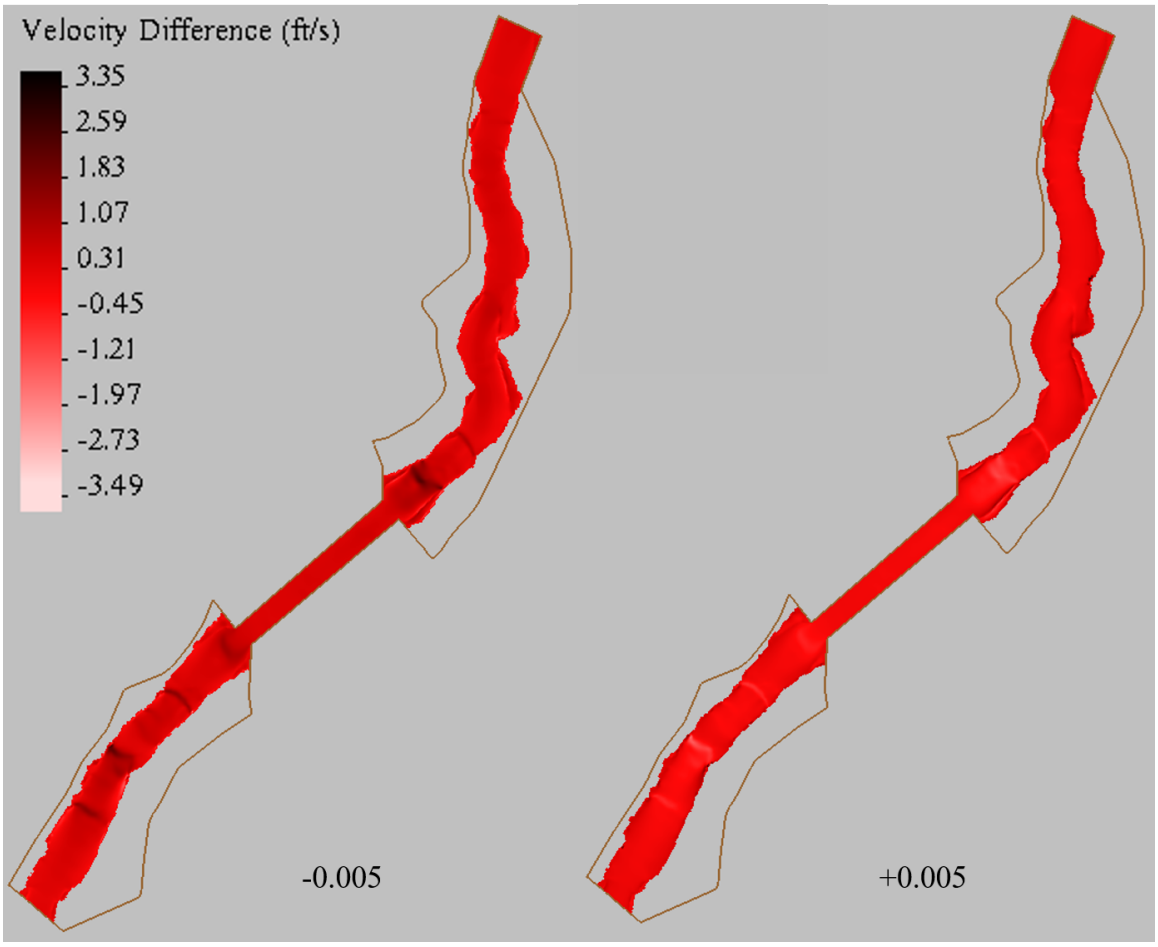

Figure C- 44. North Fork Ryan Creek, Q100. Difference in velocity magnitude results between the base case and a sensitivity simulation with a decrease of 0.005 in the entire model's materials roughness values (sensitivity case – base case).

Table C- 1. Differences in water depth and velocity results between full model material roughness change and streambed/RSP material roughness changes.

Roughness Change	Flow	Difference	Water Depth Differences	Velocity Differences
Full Model – Streambed	Q2	+0.005	Range: -0.01 to 0.02 ft	Range: -0.74 to 0.20 fps
Full Model – Streambed	Q100	+0.005	Range: -0.02 to 0.13 ft	Range: -0.64 to 2.60 fps
Full Model – RSP	Q2	+0.005	Range: -0.09 to 0.12 ft	Range: -0.81 to 1.04 fps
Full Model – RSP	Q100	+0.005	Range: -0.03 to 0.39 ft	Range: -1.41 to 3.31 fps

C.4 Previous 1-D Caltrans Analyses

North Fork Ryan

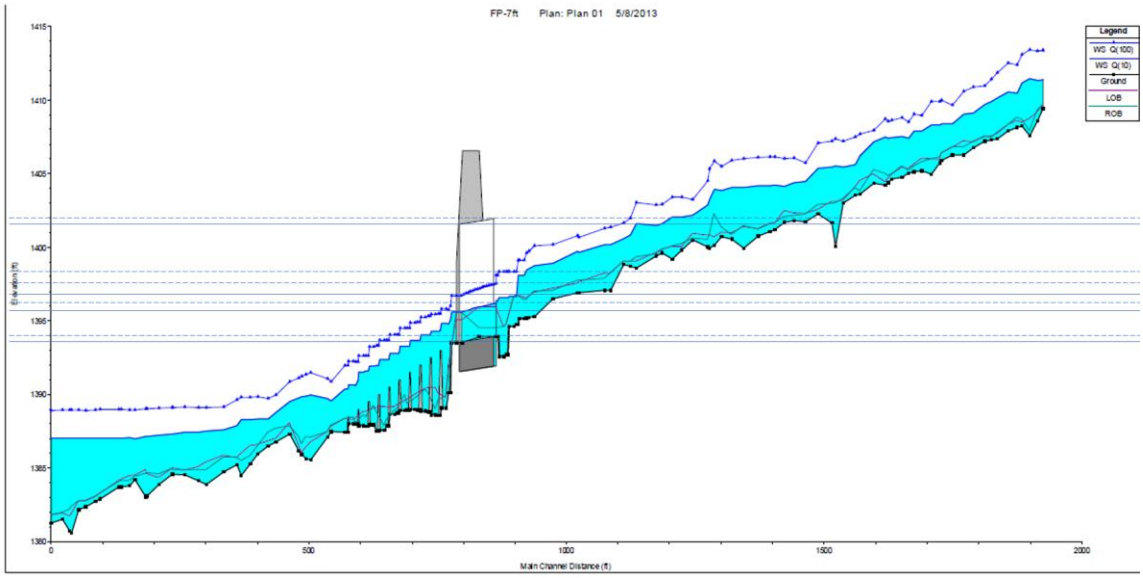

Figure C- 45. HEC-RAS water surface profile for North Fork Ryan Creek (adopted from Figure 21, Ryan Creek Project Report, AECOM 2014). Solid-shaded blue area represents water elevations during the 10-year flow. The North Fork Ryan Creek crossing structure is also represented as the vertical structure.

APPENDIX D – REFERENCE TABLES

D.1 RSP Standard Sizing Tables – New and Old

Table D- 1. Old RSP standard sizing based on weight from the California Bank and Shore (CABS) RSP Design Guide (adopted from Racin et al. 2000).

STANDARD Rock SIZE or Rock MASS or Rock WEIGHT		GRADING OF ROCK SLOPE PROTECTION **PERCENTAGE LARGER THAN**											
		RSP-Classes [A]											
		Method A Placement					Method B Placement						
		RSP-Classes other than Backing									Backing No.		
US unit		8 ton	4 ton	2 ton	1 ton	1/2 ton	1 ton	1/2 ton	1/4 ton	Light	1 [B]	2	3
	SI unit	8 T	4 T	2 T	1 T	1/2 T	1 T	1/2 T	1/4 T	Light	1 [B]	2	3
16 ton	14.5 tonne	0-5											
8 ton	7.25 tonne	50-100	0-5										
4 ton	3.6 tonne	95-100	50-100	0-5									
2 ton	1.8 tonne		95-100	50-100	0-5		0-5						
1 ton	900 kg			95-100	50-100	0-5	50-100	0-5					
1/2 ton	450 kg				95-100	50-100	-----	50-100	0-5				
1/4 ton	220 kg					95-100	95-100	-----	50-100	0-5			
200 lb	90 kg							95-100	-----	50-100	0-5		
75 lb	34 kg								95-100	-----	50-100	0-5	
25 lb	11 kg									95-100	90-100	25-75	0-5
5 lb	2.2 kg											90-100	25-75
1 lb	0.4 kg												90-100

[A] US customary names (units) of RSP-Classes listed above SI names, example US is "2 ton" metric is "2 T".
[B] "Facing" has same gradation as "Backing No. 1". To conserve space "Facing" is not shown .

Example for determining RSP-Class of outside layer. By using Equation 1, if the calculated W=135 kg (minimum stable rock size):
1. Enter table at left and select closest value of STANDARD Rock SIZE which is greater than calculated W, in this case 220 kg
2. Trace to right and locate "50-100" entry 3. Trace upward and read column heading "1/4 T", then 1/4 T is first trial RSP-Class.

Table 5-1. Guide for Determining RSP-Class of Outside Layer

Table D- 2. New RSP standard sizing based on median particle size from Highway Design Manual (adopted from Caltrans, 2020).

Table 873.3A

RSP Class by Median Particle Size[3]

Nominal RSP Class by Median Particle Size[3]		d_{15}		d_{50}		d_{100}	Placement
Class [1], [2]	Size (in)	Min	Max	Min	Max	Max	Method
I	6	3.7	5.2	5.7	6.9	12.0	B
II	9	5.5	7.8	8.5	10.5	18.0	B
III	12	7.3	10.5	11.5	14.0	24.0	B
IV	15	9.2	13.0	14.5	17.5	30.0	B
V	18	11.0	15.5	17.0	20.5	36.0	B
VI	21	13.0	18.5	20.0	24.0	42.0	A or B
VII	24	14.5	21.0	23.0	27.5	48.0	A or B
VIII	30	18.5	26.0	28.5	34.5	48.0	A or B
IX	36	22.0	31.5	34.0	41.5	52.8	A
X	42	25.5	36.5	40.0	48.5	60.5	A
XI	46	28.0	39.4	43.7	53.1	66.6	A

NOTES:

[1]Rock grading and quality requirements per Standard Specifications.

[2]RSP-fabric Type of geotextile and quality requirements per Section 96 Rock Slope Protection Fabric of the Standard Specifications. For RSP Classes I thru VIII, use Class 8 RSP-fabric which has lower weight per unit area and it also has lower toughness (tensile x elongation, both at break) than Class 10 RSP-fabric. For RSP Classes IX thru XI, use Class 10 RSP-fabric.

[3]Intermediate, or B dimension (i.e., width) where A dimension is length, and C dimension is thickness.

Table D- 3. New RSP standard sizing based on median particle weight from Highway Design Manual (adopted from Caltrans, 2020).

Table 873.3B

RSP Class by Median Particle Weight(3)

Nominal RSP Class by Median Particle Weight		W_{15}		W_{50}		W_{100}	Placement
Class (1), (2)	Weight	Min	Max	Min	Max	Max	Method
I	20 lb	4	11	15	27	140	B
II	60 lb	14	39	50	94	470	B
III	150 lb	32	94	120	220	1,100	B
IV	300 lb	63	180	250	440	2,200	B
V	1/4 ton	110	300	400	700	3,800	B
VI	3/8 ton	180	520	650	1,100	6,000	A or B
VII	1/2 ton	250	750	1000	1,700	9,000	A or B
VIII	1 ton	520	1,450	1,900	3,300	9,000	A or B
IX	2 ton	870	2,500	3,200	5,800	12,000	A
X	3 ton	1,350	4,000	5,200	9,300	18,000	A
XI	4 ton	1,800	5,000	6,800	12,200	24,000	A

NOTES:

*(1)*Rock grading and quality requirements per Standard Specifications.

*(2)*RSP-fabric Type of geotextile and quality requirements per Section 96 Rock Slope Protection Fabric of the Standard Specifications. For RSP Classes I thru VIII, use Class 8 RSP-fabric which has lower weight per unit area and it also has lower toughness (tensile x elongation, both at break) than Class 10 RSP-fabric. For RSP Classes IX thru XI, use Class 10 RSP-fabric.

*(3)*Values shown are based on Table 873.3A dimensions and an assumed specific gravity of 2.65. Weight will vary based on density of rock available for the project.

D.2 Agency Design Preferences

Table D- 4. Prioritized order of stream crossing design implementation for multiple state agencies.

State	Agency	Design Preference Order	Source
CA	Caltrans	(1) Bridge; (2) stream simulation; (3) active channel/low-slope culvert; (4) hydraulic design (not for anadromous salmonid spawning habitat); (5) existing culvert retrofit	(Caltrans et al., 2007)
CA	CDFW	(1) Bridge; (2) stream simulation; (3) low-slope culvert; (4) hydraulic design	(CDFW, 2009b, 2009a)
OR	OR DFW	(1) Bridge; (2) Streambed simulation with bottomless arch or embedded culvert; (3) Streambed simulation with embedded round box culvert; (4) Non-embedded culvert (<0.5% slope); (5) Baffled culvert (0.5-12% slope) or structure with fishway	(ODFW, n.d.)
WA	WDFW	(1) Bridge; (2) no slope culverts, only for simple installations on low-gradient streams and bankfull width < 10 feet; (3) stream simulation, for complex installation at any stream gradient.	(Barnard et al., 2013)
MN	MN DOT	(1) Bridge; (2) geomorphic/stream simulation; (3) embedded and recessed culverts	(Hernick et al., 2019)
MA	MA DOT	(1) Valley span or stream span; (2) stream simulation or no-slope culvert; (3) bridge span, open bottom, or embedded culvert span greater than 1.2 times bankfull width	(MassDOT, 2010)
VT		(1) Low-slope for low risk sites (low gradient or short, ‘where passage of weak aquatic species is required’); (2) Stream simulation (any channel slope); (3) hydraulic option	(Bates & Kirn, 2009)
NH		(1) Bridge or open bottom structure; (2) other designs based on stream characteristics*; (3) hydraulic design	(University of NH, 2009)

*No specific design ranking - appropriate design chosen based on stream characteristics and designers professional judgements (‘generally preferred’ structure characteristics: open-bottom, slope similar to

natural channel, similar streambed composition, spanning greater than bankfull width to allow for wildlife passage on banks)

Table D- 5. Prioritized order of stream crossing design implementation for multiple federal agencies.

Entity	Design Preference Order	Source
NMFS (U.S.)	(1) Nothing (2) Bridge (3) Streambed simulation (4) Non-embedded culvert (often referred to as hydraulic design) (5) Baffled culvert or fishway structure – for steeper slopes	(NMFS, 2001)
USFS	(1) Span valley with bridge or viaduct (2) Stream simulation with floodplain connectivity (3) Stream simulation (4) Hydraulic design for fish passage (5) Hydraulic design for flood capacity	(USFS Stream Simulation Working Group, 2008)
FHWA (U.S.)	(0) No impedance (1) Geomorphic simulation, Category 1 (2) Hydraulic simulation, Category 2 (3) Hydraulic design, Category 3	(Hotchkiss & Frei, 2007)
B.C. Canada	open-bottom structures and some embedded closed-bottom structures	(B.C. Ministry of Forests, Lands and Natural Resource Operations, B.C. Ministry of Environment, and Fisheries and Oceans Canada, 2012)

APPENDIX E – ADDITIONAL SITE INFORMATION AND DESIGN DRAWINGS

E.1 Little Mill Creek

Little Mill Creek Longitudinal Profile

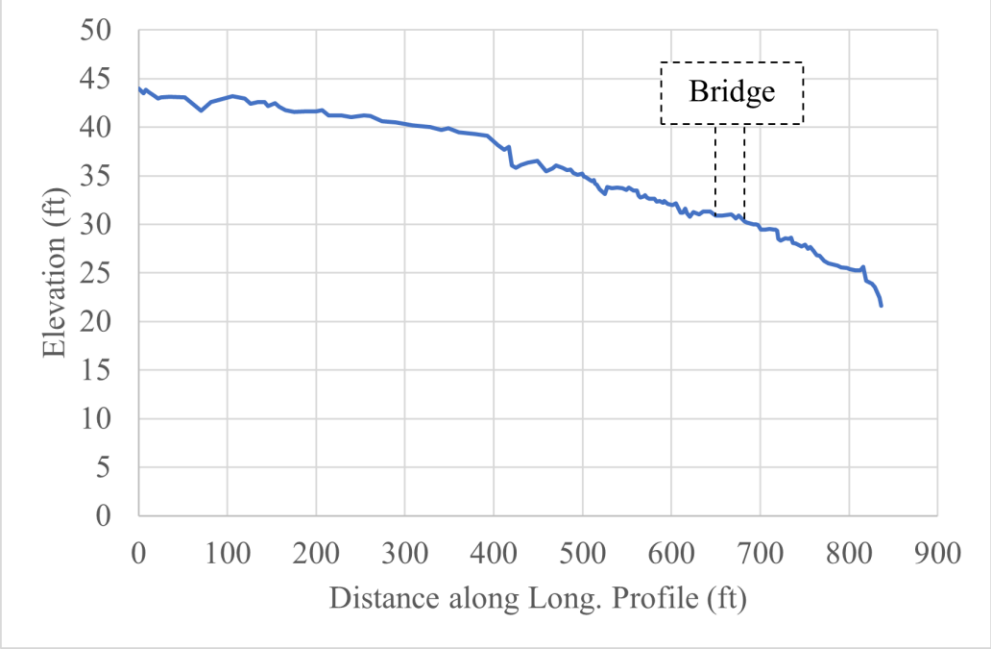

Figure E- 1. Longitudinal profile of Little Mill Creek at the thalweg. Distance along the longitudinal profile (x-axis) and elevation (y-axis) are shown. Elevation values are relative to the benchmarks taken during the stream survey and are not true elevations. The bridge face boundaries are shown on the profile. Flow is moving from left to right.

Little Mill Creek Design Drawings

The design drawings from the currently installed crossing design are presented on the following pages. The full-size drawings are available in Attachment 1.

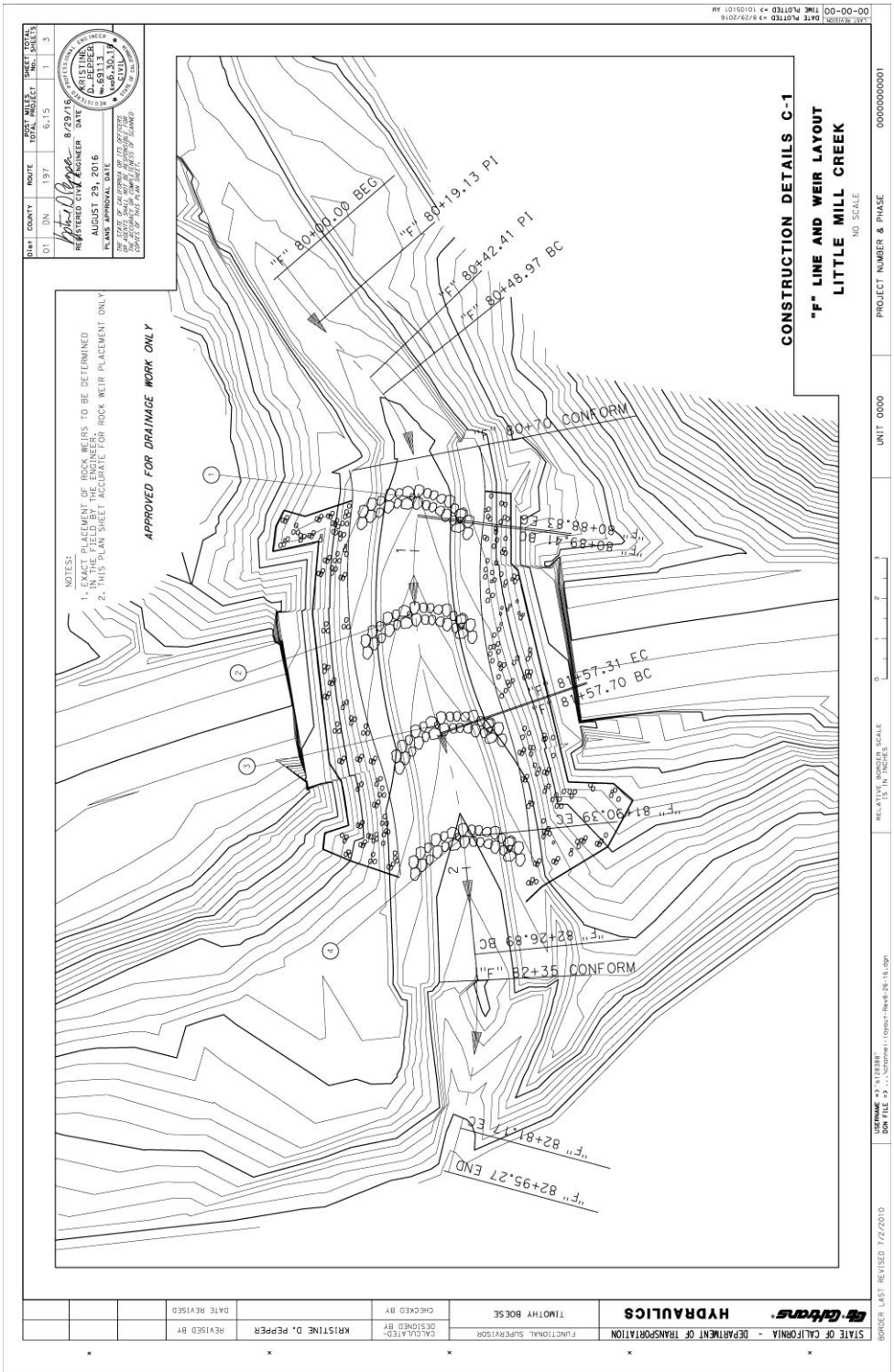

Figure E- 2. Caltrans design drawing of Little Mill Creek channel layout. Stations identified along flowline. See the first page (C-1) in Attachment 1 for full-size drawing.

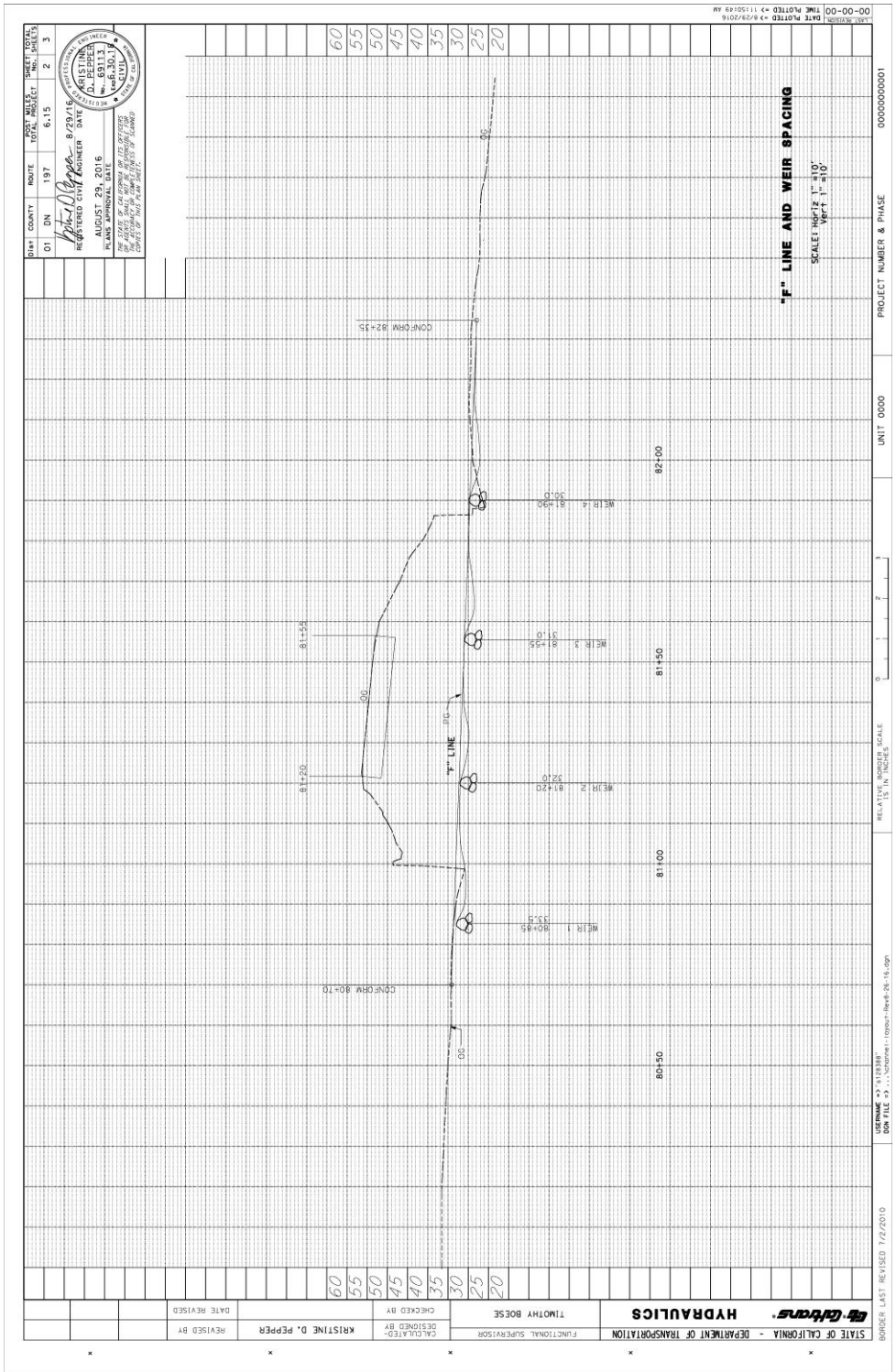

Figure E- 3. Caltrans design drawing of Little Mill Creek channel layout. Stations identified at rock weirs. See the second page in Attachment 1 for full-size drawing.

E.2 North Fork Ryan Creek

North Fork Ryan Creek Longitudinal Profile

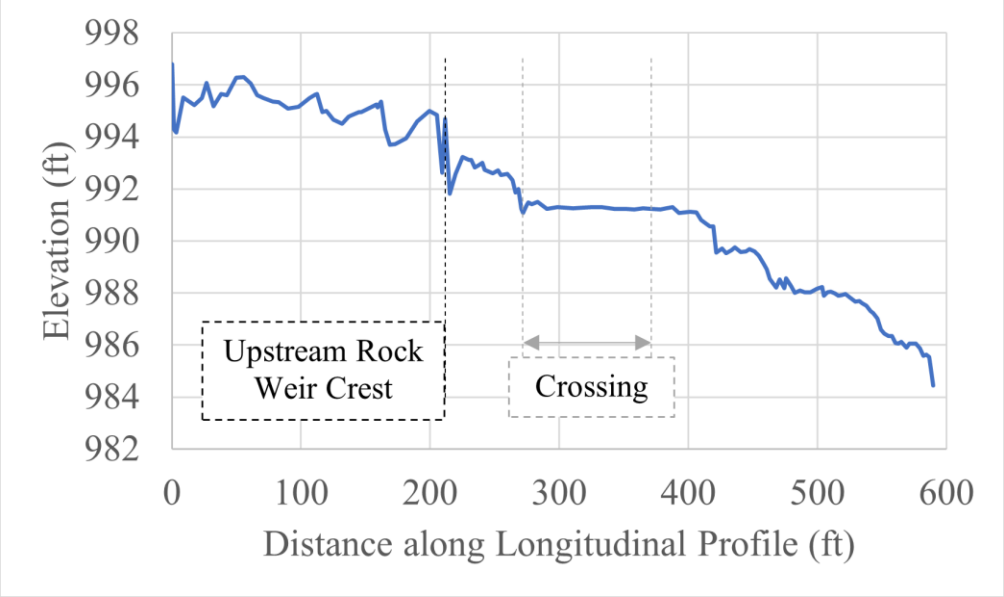

Figure E- 4. Longitudinal profile of North Fork Ryan Creek at the thalweg. Distance along the longitudinal profile (x-axis) and elevation (y-axis) are shown. Elevation values are relative to the benchmarks taken during the stream survey and are not true elevations. The upstream rock weir crest and the crossing boundaries are shown on the profile. Flow is moving from left to right.

North Fork Ryan Creek Design Drawings

The design drawings from the currently installed crossing design are presented on the following pages. The full-size drawings are available in Attachment 2.

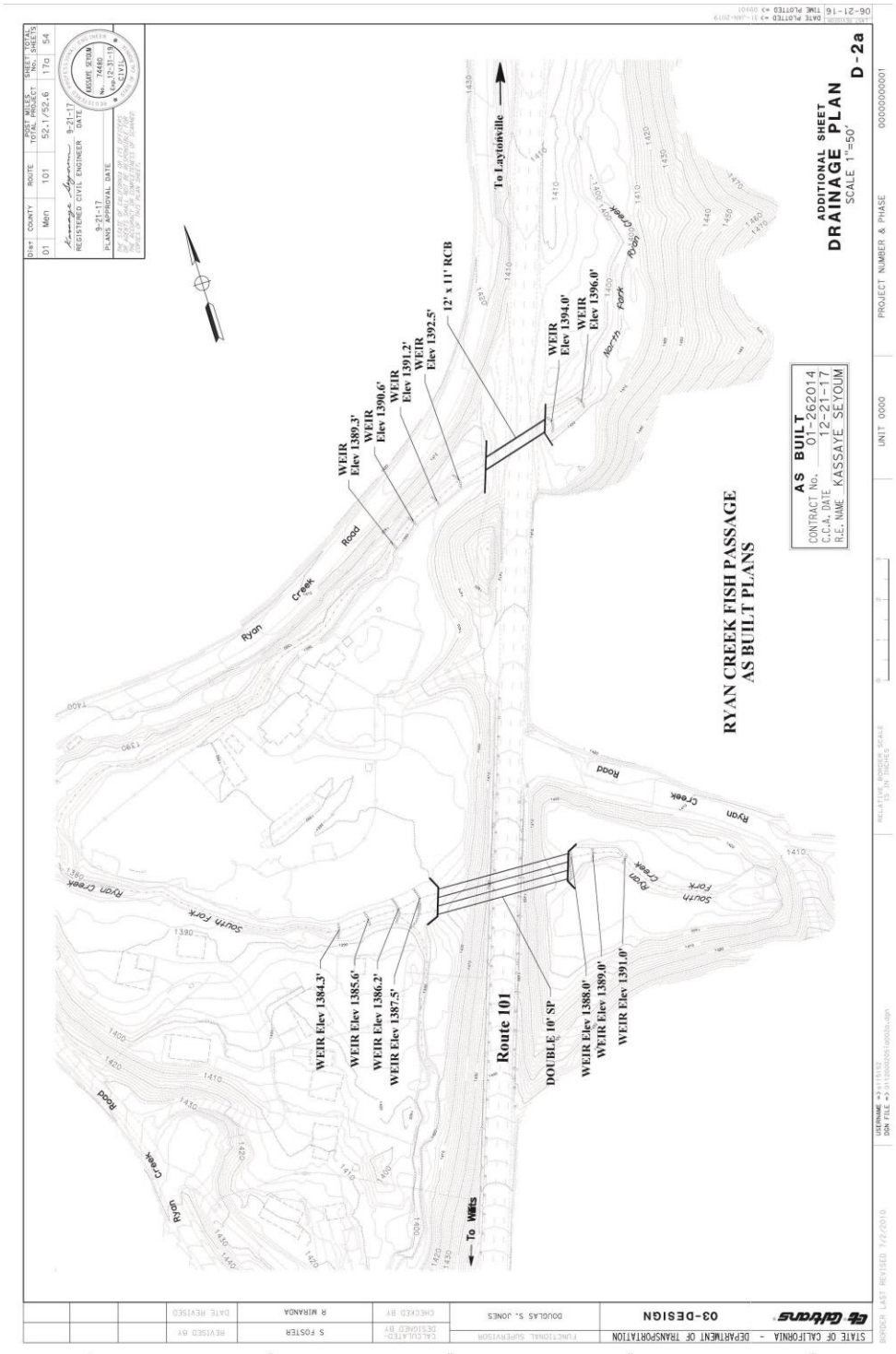

Figure E- 5. Caltrans design drawing of North Fork Ryan Creek channel layout in drainage plan. See the first page (D-2a) in Attachment 2 for full-size drawing.

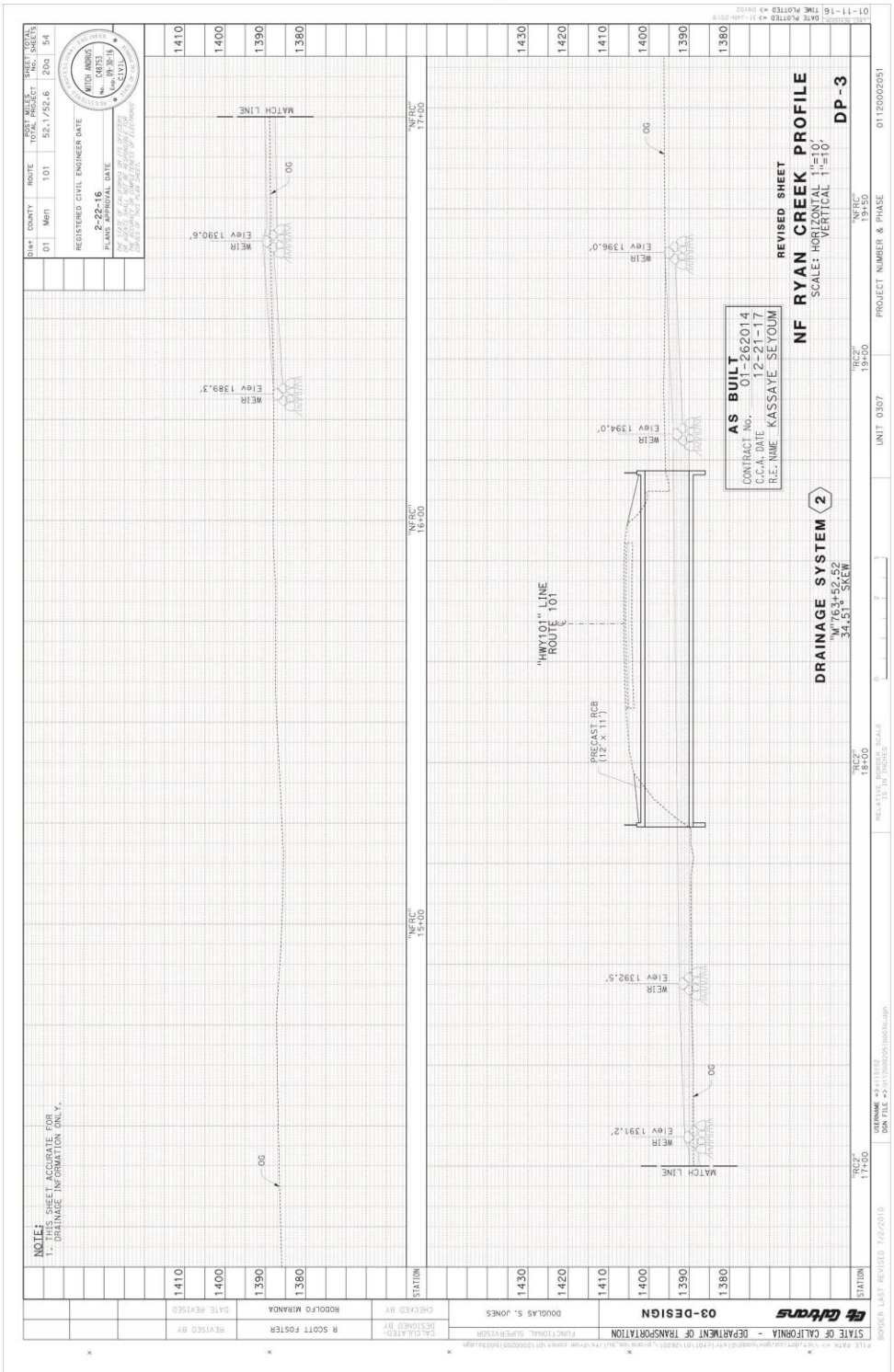

Figure E- 6. Caltrans design drawing of North Fork Ryan Creek profile. See the second page (DP-3) in Attachment 2 for full-size drawing.

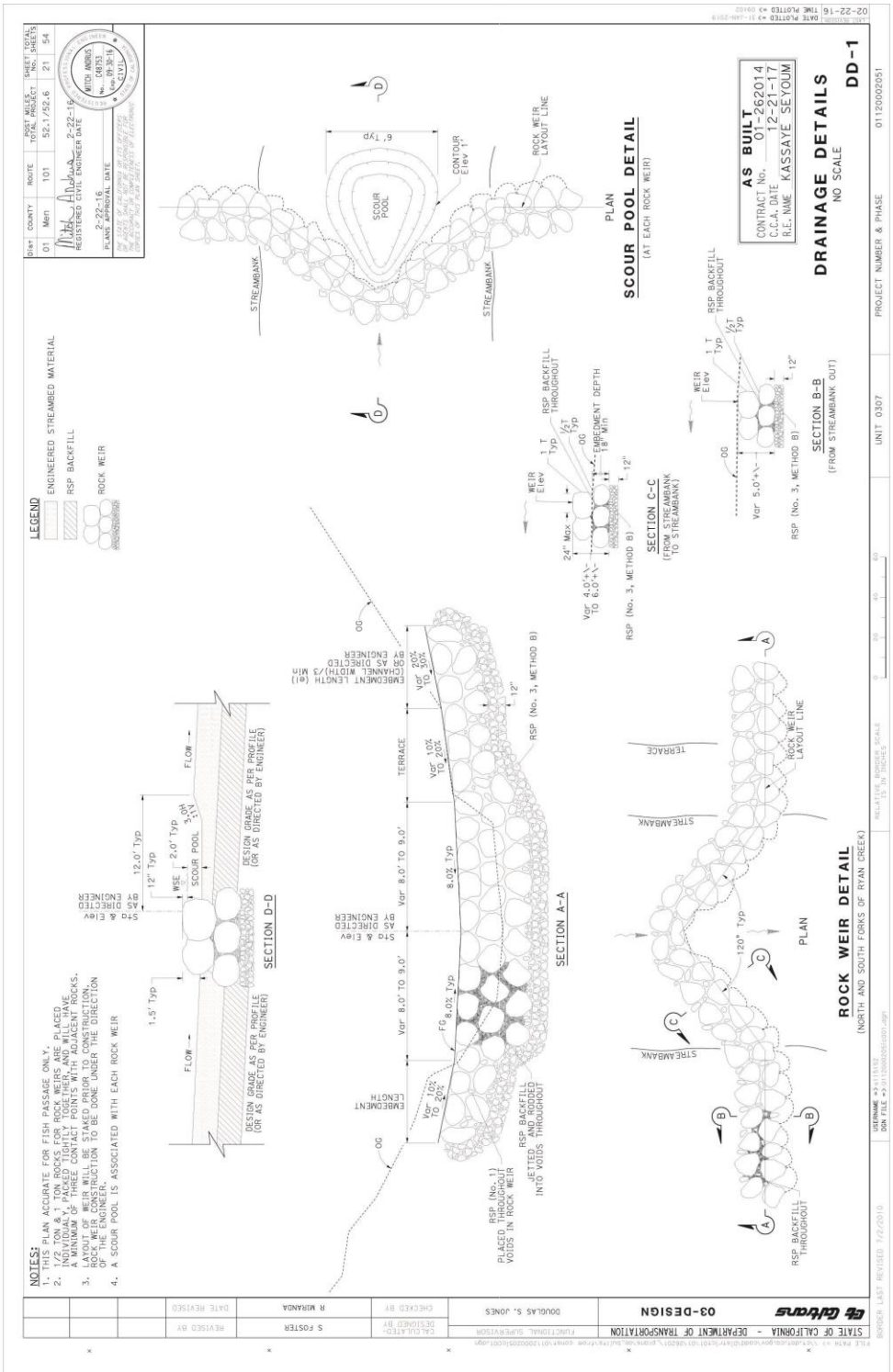

Figure E- 7. Caltrans design drawing details of North Fork Ryan Creek rock weirs. See the third page (DD-1) in Attachment 2 for full-size drawing.

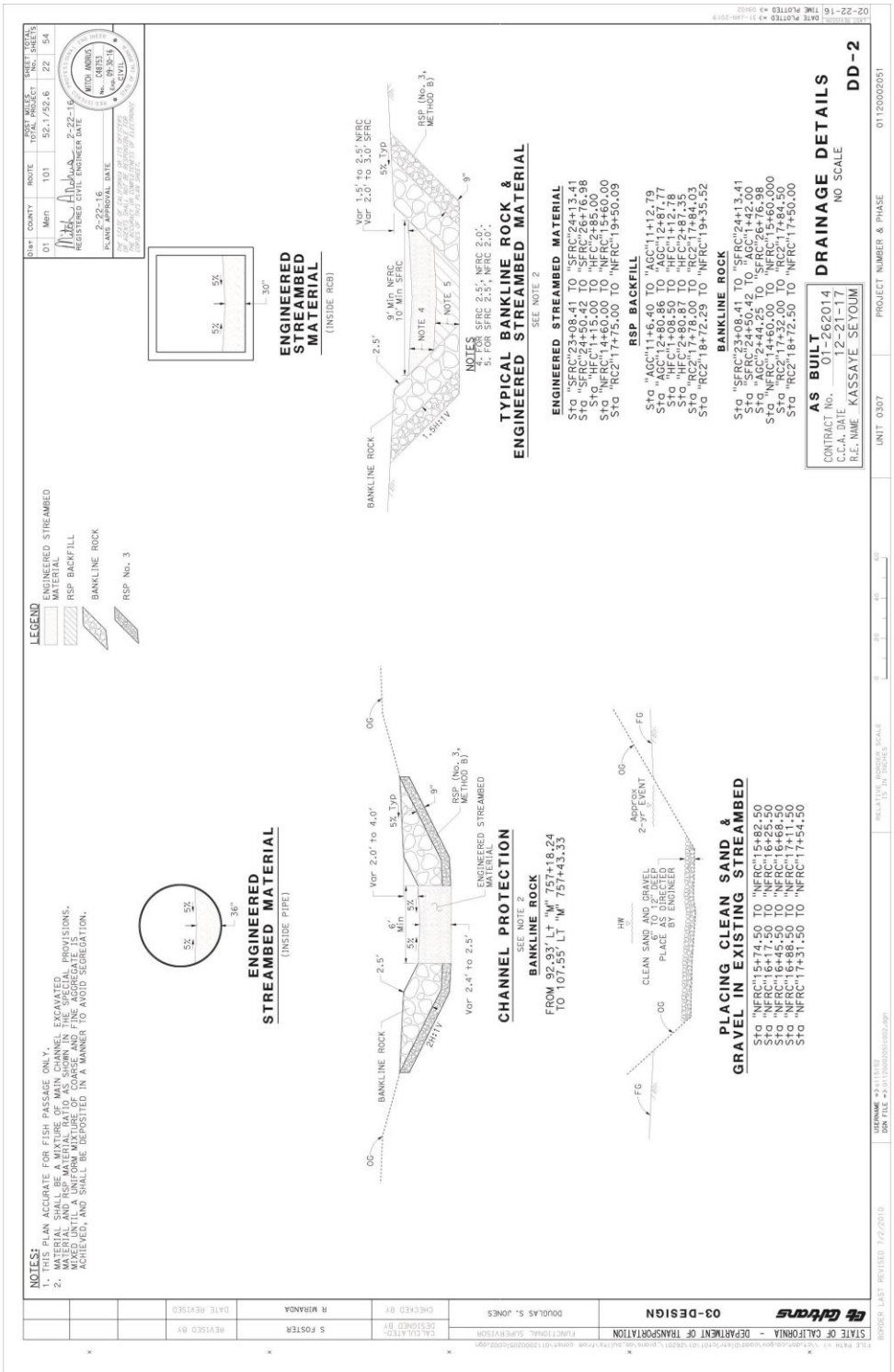

Figure E- 8. Caltrans design drawing details of North Fork Ryan Creek engineered streambed material. See the fourth page (DD-2) in Attachment 2 for full-size drawing.

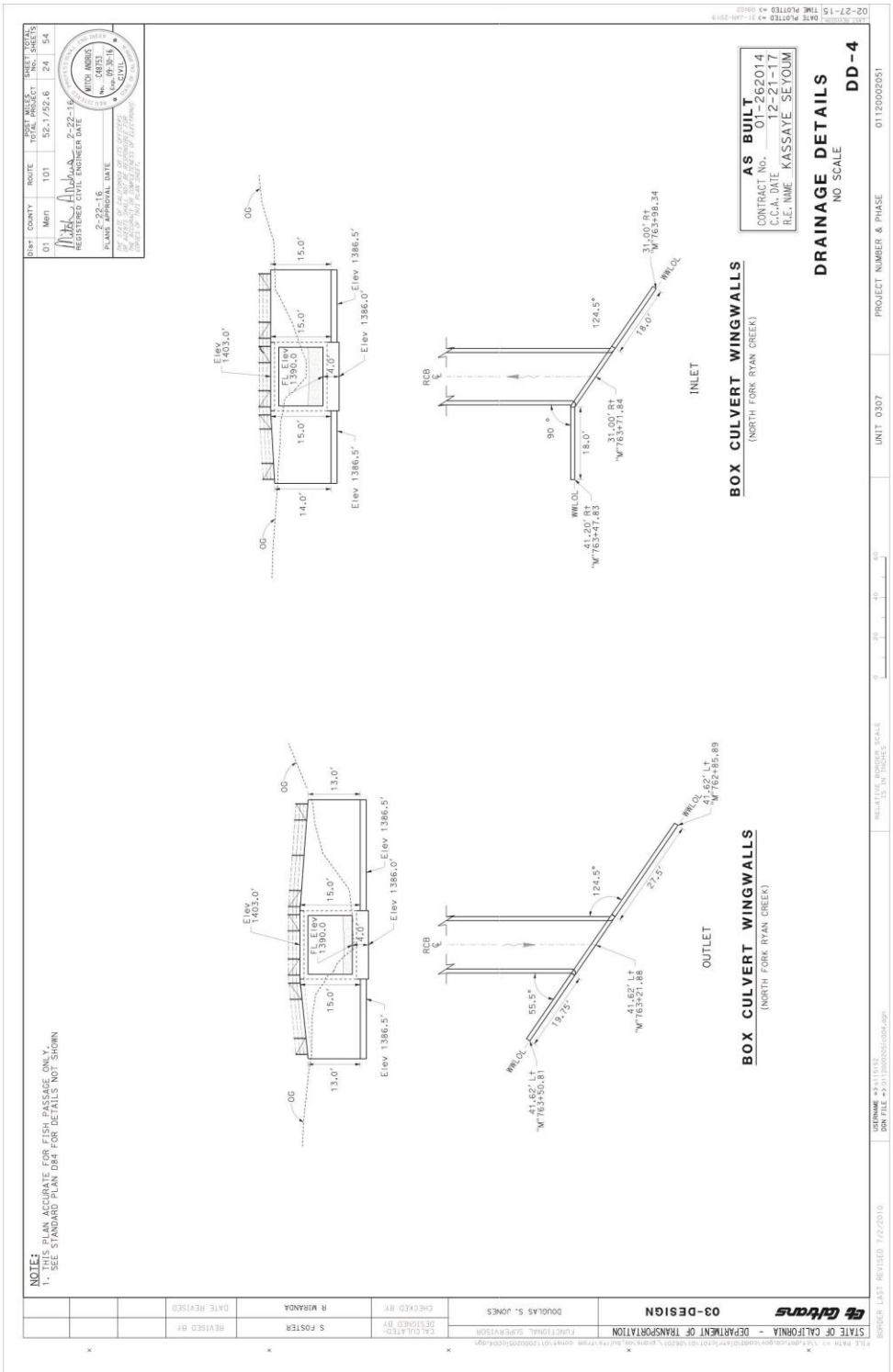

Figure E- 9. Caltrans design drawing details of North Fork Ryan Creek box culvert wingwalls. See the fifth page (DD-4) in Attachment 2 for full-size drawing.

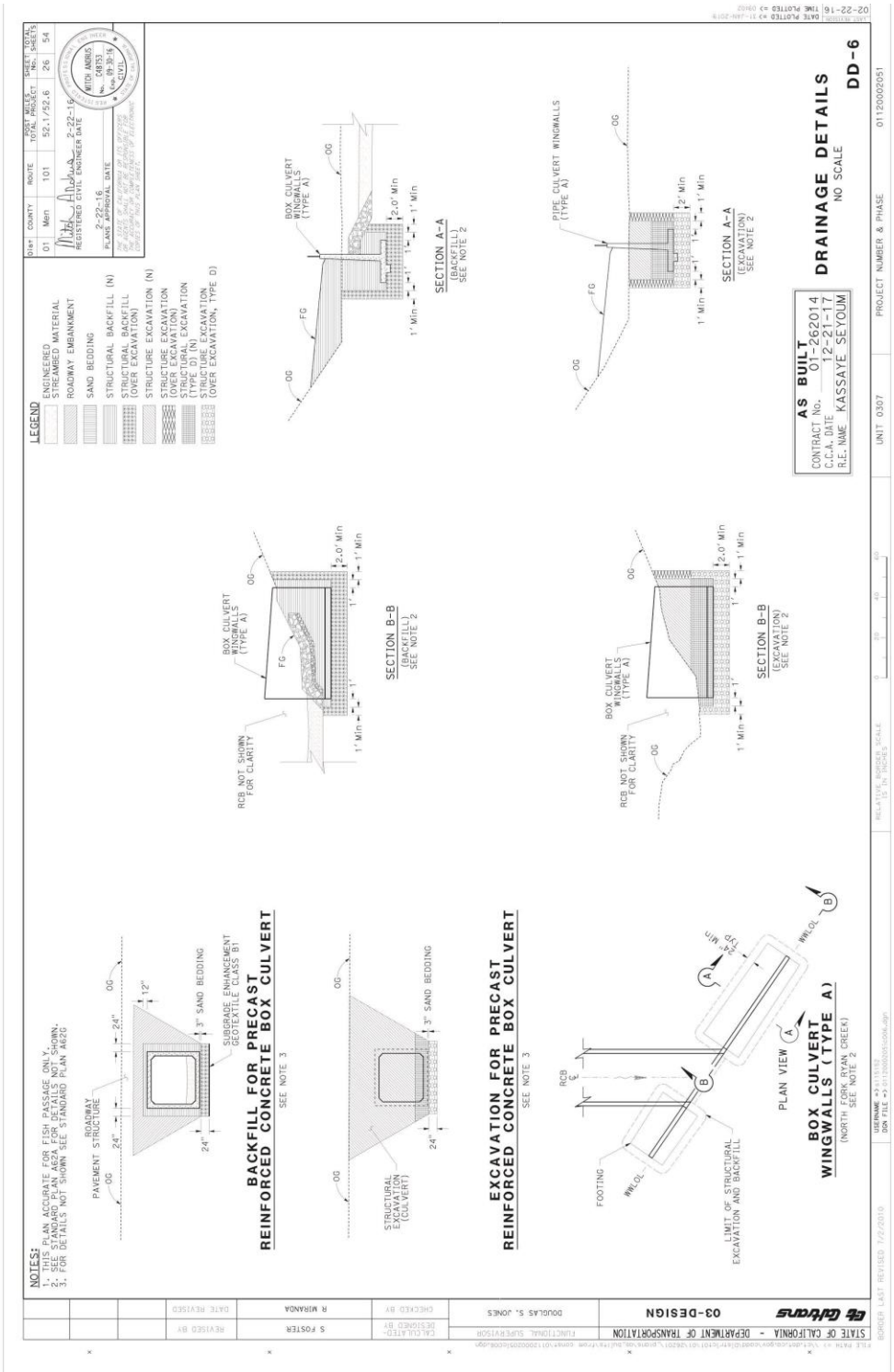

Figure E- 10. Caltrans design drawing details of North Fork Ryan Creek box culvert embedment. See the sixth page (DD-6) in Attachment 2 for full-size drawing.